Phospho-regulation of Lrg1 controls polarised growth in the human fungal pathogen *Candida albicans*

PhD research thesis

University of Sheffield

Department of Molecular Biology and Biotechnology

Simon Paul Watton

Submitted: February 2015

Thesis abstract

The small GTPase Rho1 is the positive regulatory subunit of β-1,3 glucan synthase, responsible for the main structural component of the cell wall. In turn Rho1 is negatively regulated by Lrg1, its GTPase activating protein (GAP).

Here it is shown that a *C. albicans lrg1ΔΔ* mutant constitutively forms highly elongated and invasive pseudohyphae. Using Rho1 and Exo84 as markers, it is shown that the extended polarised growth is in part due to a failure to relocate the polarity machinery from the bud tip to the bud neck. A GFP reporter that binds specifically to active Rho1 also shows this increase in polarised growth in *lrg1ΔΔ* is due to an increase in Rho1 activity. *Ca*Lrg1 contains 4 complete motifs and an additional 15 minimal sites for phosphorylation by Cdc28/Cdk1. These sites are clustered in an N-terminal extension missing from the *S. cerevisiae* Lrg1 homologue. Consistent with this, GST-Lrg1 is phosphorylated *in vitro* by Cdc28. Substitution of the putative Cdk1 targets with non-phosphorylatable alanine has little phenotypic effect. However, phosphomimetic glutamate substitutions results in highly polarised growth similar to, but milder than the *lrg1ΔΔ* phenotype.

*Ca*Lrg1 also contains 4 motifs for phosphorylation by the Cbk1 kinase, one of which is also within the N-terminal extension. Cbk1 phosphorylates GST-Lrg1 *in vitro* and replacement of the Cbk1 motifs with phospho-mimetic residues also produces a similar phenotype to the *lrg1ΔΔ* strain. Phosphomimetic mutations of Lrg1 in either Cdc28 or Cbk1 sites was also shown to increase the susceptibility of *C. albicans* to the echinocandin class of drug, a major tool in the treatment of *Candida albicans* infection. Taken together these results suggest that the regulation of polarised growth of the yeast bud is mediated by Rho1 whose activity and mobility is in turn controlled by the action of both Cdc28 and Cbk1 on Lrg1.

Acknowledgements

Firstly, I would like to thank Lucy for her constant support and patience with me over the last seven years. You always believed in me, even when times were hard, and I probably wouldn't be where I am today without you.
I would also like to thank my Mom, Dad and Gemma, for their continuous encouragement and support throughout my life and their unvarying belief that I would reach this point.

I would like to thank my supervisor, Prof. Pete Sudbery, for first of all giving me the opportunity to complete this PhD study. I would also like to thank him for his support and help that he has provided throughout it.

I would like to thank the current and past members of the Sudbery lab. Especially Dr David Caballero-Lima for his experimental knowledge and direction, Dr Lina Alaalm for her advice and tea breaks and, and Jamie Greig for his extensive cloning wisdom and banter. I would also like to thank Janet Trevithick, Laura Hunt, Hannah Regan and Iliyana Kaneva.

I would like to thank Dr Jeremy Craven for his design and production of various computer programmes, including the GFP-RID tracing programme.

I would also like to thank the BBSRC for funding the project.

Finally I would like to thank Abi, Sophie, Sarah and Katie for all those drunken Wednesday nights where we managed to forget about the rigours of science for an hour or two!

Declaration of collaboration

The majority of work undertaken in this study was performed by the author; however a number of experiments would not have been possible without help from collaborators.

1. The live cell images used for the localisation of GFP-RID in synchronised cells gained from elutriation used for Figure 4.21 were taken by Dr D. Caballero-Lima (University of Sheffield).
2. The Cbk1 kinase assay performed on Lrg1, shown in figure 5.3, was performed by I. Kaneva (University of Sheffield).

Abbreviations

AIDS	Acquired Immune Deficiency Syndrome
APC	Anaphase Promoting Complex
AP	Antarctic Phosphatase
ATP	Adenosine triphosphate
BLAST	Basic Local Alignment Search tool
BSA	Bovine Serum Albumin
CAK	CDK Activating Kinase
cAMP	Cyclic adenosine monophosphate
CDD	Conserved Domain Database
CDK	Cyclin Dependent Kinase
CGD	*Candida* Genome Database
CoIP	Co-Immunoprecipitation
CWI	Cell wall integrity pathway
DAPI	4',6-diamidino-2-phenylindole
DIC	Differential Interference Contrast
DMSO	Dimethyl sulfoxide
DTT	Dithiothreitol
ECL	Enhanced Chemiluminescence
EDTA	Ethylenediaminetetraacetic Acid
EGTA	ethylene glycol tetraacetic Acid
ELM	Eukaryotic Linear Motif
FITC	Fluorescein isothiocyanate
GAP	GTPase Activating Protein
GDI	GDP-dissociation inhibitor
GDP	Guanosine Diphosphate
GEF	Guanine Exchange Factor
GFP	Green Fluorescent Protein
GO	Gene Ontology
GPI	Glycosylphosphatidylinisotol
GS	Glucan synthase
GST	Glutathione-S-Transferase
GTP	Guanosine Triphosphate
HA	Hemagglutinin
IP	Immunoprecipitate
IPTG	Isopropyl β-D-1-thiogalactopyranoside
LiAc	Lithium Acetate
mA	milli-amp
MAPK	Mitogen Activated Protein Kinase
MBF	MluI Binding Factor

ORF	Open Reading Frame
OD	Optical Density
PAGE	Polyacrylamide Gel Electrophoresis
PBS	Phosphate Buffered Saline
PCR	Polymerase Chain reaction
PKA	Protein Kinase A
PVDF	Polyvinylidene Fluoride
RAM	Regulation of Ace2 and Morphogenesis Network
SAP	Secreted Aspartyl Protease
SBF	Swi4/Swi6 binding factor
SDE	Septum Degradation Enzyme
SDS	Sodium Dodecyl Sulphate
SDW	Sterilised Distilled Water
TAE	Tris-Acetate-EDTA
TBS	Tris Buffered Saline
TE	Tris-EDTA
TEMED	Tetramethylethylenediamine
w/v	Weight/Volume
YPD	Yeast Extract Peptone Dextrose
YPM	Yeast Extract Peptone Maltose
λppase	Lambda Phosphatase

Table of Contents

1 General Introduction

1.1 *Candida albicans* is a major human pathogen

Candida albicans (*C. albicans*) is a fungal pathogen which lives commensally in both the genito-urinary and gastro-intestinal tract of humans. Usually the organism does not cause a problem to its host, but can be the cause of opportunistic infections on mucosal surfaces such as candidiasis (thrush). However, in immuno-compromised patients such as those with AIDS or receiving cancer related chemo-therapy, the fungus can disseminate from the gut or in-dwelling devices and cause a serious infection in the blood stream -candidemia.
In a 10 year study of 30,000 patients with hospital acquired fungal infections in the U.S.A, it was shown that nearly 80 % of fungal nosocomial infections are caused by *Candida spp,* with three quarters of these due to *C. albicans* alone (Becksague and Jarvis, 1993). Another similar study of 24,000 patients in the U.S.A indicated that *C. albicans* is the 4th most common nosocomial infection, accounting for around 10 % of the total. In addition, mortality rates among those infections caused by *C. albicans* approached 40 %, the highest of any of the organism in the study. The same study also estimated the cost of *Candida* infections to be $1 billion a year (Wisplinghoff et al., 2004). It is for this reason, and the fact that most anti-fungal drugs also target human processes, that *C. albicans* requires rigorous study.

1.2 The genetics and evolution of *C.albicans*

Although *C. albicans* shares many processes with the budding yeast *Saccharomyces cerevisiae (S. cerevisiae)*- which has provided many insights into cellular processes- it is thought that the two organisms diverged as long as 840 million years ago (Heckman et al., 2001) and as such they differ in many ways. For example, *S. cerevisiae* interprets the codon CUG as the amino acid leucine as in the universal code, whereas some *Candida* species, including *C. albicans* read the same codon as the amino acid serine (Ohama et al., 1993). Another distinction between the *C. albicans* and *S. cerevisiae* is their growth morphology. *S.*

cerevisiae grows in ovoid, typical "budding yeast" form and as elongated pseudohyphae, while *C. albicans* can grow in three different morphologies, which will be discussed in more detail later. As a consequence of this divergence, although similarities can be drawn from the better studied model organism, it again emphasizes the importance of direct study on *C. albicans.*

In approaching research of *C. albicans*, there are many challenges and difficulties that must be faced. As mentioned above, problems with translation of the genetic code means that any popular research tools, such as the use of the Green Fluorescent Protein (GFP) and selectable markers used in *S. cerevisiae* research*,* need to be codon optimised. It also means that *C. albicans* proteins cannot be used in the *S. cerevisiae* two-hybrid system for interaction studies -although a similar system for direct use in *Candida* has recently been published (Stynen et al.). More significantly perhaps, is the fact that until recently no haploid stage has been identified in *C. albicans* and it was classed as an obligate diploid, ruling out mating of haploid forms to create new strains as a tool for research. Although *Candida* species do contain a mating-type loci (MTL) similar to that in *S. cerevisiae* (Hull and Johnson, 1999), and strains that are homozygous for either mating type a or α can mate, (Lockhart et al., 2002a) a meiotic system had never been found (Taylor et al., 1999) and diversity was thought to be brought about by the ability to maintain different karyotypes and random chromosome loss (Bennett and Johnson, 2003). This ability to maintain different karyotype number presented obvious difficulties in research. Recently however, research has indicated that *C. albicans* do exist in a haploid state of which opposite mating types are capable of mating (Hickman et al., 2013).

1.3 The different morphologies of *C. albicans*

As mentioned earlier, *C. albicans* is unusual as it is capable of growth in three different morphologies (Figure 1.1). In the yeast morphology, much the same as *S. cerevisiae,* cells grow in spherical/ovoid nature and once daughter cells reach a defined size, they undergo cytokinesis and separate easily from each other. Pseudohyphal cells on the other hand, grow as chains of elongated cells that have visible constrictions at the septum but remain joined together at this point. Highly polarised true hyphal cells grow with parallel sides and

do not branch like the pseudohyphal morphology. True hyphal cells do not appear to have any constrictions at the septum, despite the fact the septum is present on a molecular level, as seen by GFP-fused septin proteins which mark the site of septation (Berman and Sudbery, 2002). There are many hypotheses on why *C. albicans* is polymorphic. The highly branched nature of pseudohyphal cells could be seen perhaps, as a mechanism for foraging for nutrients away from the mother cell (Berman and Sudbery, 2002). Another hypothesis centres on the switch between yeast and true hyphal morphologies being an ideal mechanism for dissemination and invasion of the host tissues and cells. Although some evidence does point towards this hypothesis, such as invasion of agar by hyphal cells and mutants in hyphal growth being less virulent in mouse and human infection models (Dieterich et al., 2002; Lo et al., 1997), the idea is still controversial amongst the scientific community and is reviewed fully in: (Gow et al., 2002). The transition between the three different morphologies can be induced by changes in temperature, pH, concentration of CO_2 and serum etc (as shown in table 1.1), so it seems likely that transition between them is in some way related to interaction with the host.

C. albicans also has the ability to undergo White-Opaque switching. This involves switching from the more common white, domed colonies with round cells to the less common opaque, flat colonies that contain cells which are larger and more ovoid (Figure 1.2). The switch occurs roughly once in every one thousand cell divisions (Slutsky et al., 1987). It has been observed that homozygous strains at the MTL locus are capable of undergoing the white-opaque switch, whilst heterozygotes are not (Lockhart et al., 2002b) (Miller and Johnson, 2002). Interestingly, opaque cells are 10^6 times more efficient at mating than white cells (Miller and Johnson, 2002), suggesting that the mating-type locus is responsible for the switch.

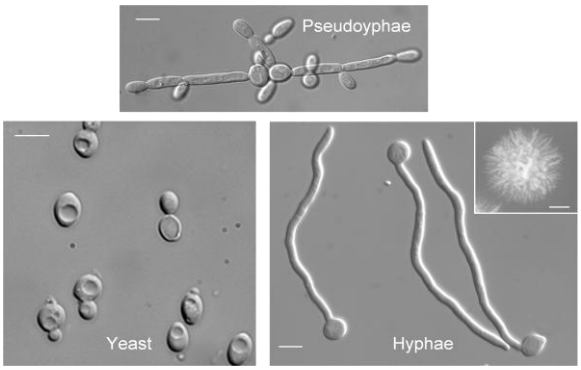

Images taken from (Sudbery et al., 2004)

Figure 1.1 The different growth morphologies of *Candida albicans*

C. albicans grow in three different morphologies that are induced by changes in temperature, pH and the presence of serum. The organism grows as budding yeast type growth with spherical to ovoid cells, pseudohyphae, which are long chains of elongated cells which remain joined at the constricted septum and as true hyphae. True hyphae posess parallel walls within the germ tube and lack of constrictions at the septum sites between each cell in the tube.

Yeast	Pseudohyphae	Hyphae
≤30 °C	35 °C	37° C
pH 4	pH 6	pH 7
	Nitrogen starvation	Serum
	High levels of phosphate	GlcNac
		CO_2

Table 1.1 *C. albicans* morphology is affected by environmental conditions

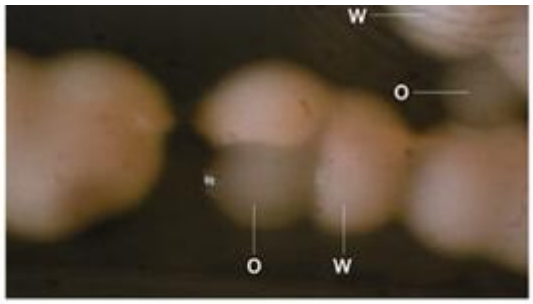

Taken from (Berman and Sudbery, 2002)

Figure 1.2 The White-Opaque switch in *C. albicans*
White (W) and opaque (O) cells can be seen here after 3 days growth at 23°C on synthetic complete medium. The White-Opaque switch is thought to be controlled by the mating type locus.

1.4 S. cerevisiae provides a model of polarised growth

The three different morphologies of *C. albicans* require either short (yeast) or sustained (hyphae/pseudohyphae) periods of polarised growth and polarised growth is an essential process for the majority of eukaryotes. In order for polarised growth to occur, secretory vesicles containing all the components for cell expansion must be directed to the correct site in the cell cortex. This process has been studied extensively in S*. cerevisiae* to provide a model which is mirrored in many cell types, such neurons and microvilli in higher organisms and hyphal growth in fungi.

1.4.1 Cdc42: the hub of cell polarisation

Cdc42 is a small GTPase that was first discovered in *S. cerevisiae* in a temperature sensitive mutant of cell growth and actin polarisation (Adams et al., 1990; Johnson and Pringle, 1990) and homologs across other species complement yeast *cdc42* mutants (Chen et al., 1993). Cdc42 cycles between its active GTP-bound state and its inactive GDP-bound state using its intrinsic GTPase activity. However, GTP hydrolysis is stimulated by the GTPase activating proteins (GAPs): Bem2, Bem3, Rga1 and Rga2 (Tong et al., 2007; Zheng et al., 1994; Zheng et al., 1993). Activation of Cdc42 is controlled by the guanine nucleotide exchange factor (GEF)

Cdc24 (Zheng et al., 1994). To initiate polarised growth, Cdc42 must localise towards a chosen site in the cell cortex, defined by bud-site selection markers. One such marker is the Ras-family GTPase, Rsr1. It is thought that upon conversion of Rsr1-GTP to Rsr1-GDP by its GAP Bud2, Rsr1 releases Cdc24, stimulating the formation of Cdc42-GTP which can then signal to the actin cytoskeleton for polarisation, reviewed in (Park and Bi, 2007). It is this link between the bud site selection marker Rsr1 and the centre of cell polarisation Cdc42, shown in figure 1.3, which dictates that a new bud will emerge in the correct place.

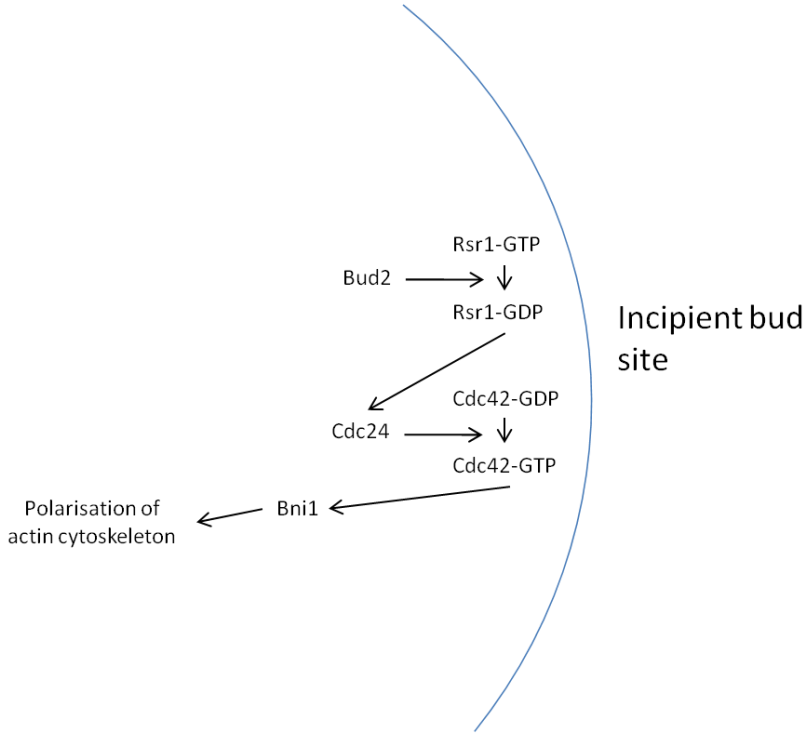

<u>Figure 1.3</u> Polarisation of the actin cytoskeleton to the incipient bud site in *S. cerevisiae* requires Rsr1 and Cdc42.

The bud site selection marker Rsr1 marks the site of bud emergence. Once converted to its GDP bound form it releases the guanine nucleotide exchange factor Cdc24 which in turn activates Cdc42. Cdc42 then acts to polarise the actin cytoskeleton to this site through the formin Bni1 (discussed below).

1.4.2 The polarisome

Once Cdc42 has been localised to the site of bud emergence, it must transduce a signal for the actin cytoskeleton to polarise towards this site. It is thought to do this through the formin protein Bni1, which physically interacts with Cdc42 and another Rho-GTPase, Rho1, and requires Cdc42 for its localisation (Evangelista et al., 1997; Kohno et al., 1996; Ozaki-Kuroda et al., 2001). Through its formin homology 1 (FH1) domain Bni1 binds profilin, which in turn adds actin monomers to actin cables, nucleating non-branched actin filaments and preventing "capping" of the elongated structure (Sagot et al., 2002b; Zigmond et al., 2003). Bni1 is a member of the polarisome, a multimeric protein complex localised at the site of polarised growth, which also contains the scaffold protein Spa2 and its localisation regulator Pea2, the Bni1 activator Bud6, and the Sec4 GAPs Msb3 and Msb4 involved in vesicle tethering (discussed later). Therefore the polarisome allows transduction of the Cdc42 signal to the actin cytoskeleton through Bni1 and links this with the subsequent delivery and tethering of vesicles to the plasma membrane.

1.4.3 The actin cytoskeleton

S. cerevisiae contains three distinct actin structures: actin cables for exocytosis, actin patches for endocytosis and actin rings for cytokinesis.

Actin cables consist of single linear actin filaments bundled together by actin binding proteins (Moseley and Goode, 2006). They are polarised towards sites of polarised growth and provide the major system for exocytosis (Pruyne et al., 1998; Sagot et al., 2002a). The formin Bni1 nucleates actin cables towards the bud cortex whilst a different formin Bnr1 nucleates them towards the mother bud neck (Imamura et al., 1997). The purpose of actin cables is to allow delivery of secretory vesicles from the Golgi to the sites of growth. This process is controlled by a number of Rab GTPases and is depicted in figure 1.4. Ypt31 allows vesicles to bud off the Golgi and then recruits the GEF (Sec2) for Sec4 (Ortiz et al., 2002). Sec2 and Sec4 then mediate vesicle transport along actin cables via the class-V myosin Myo2 and its light chain Mlc1, to the site of polarised growth (Goud et al., 1988; Walch-Solimena et al., 1997) (Schott et al., 2002).

Actin patches are focused at sites of polarised growth (Adams and Pringle, 1984) and possibly polarised by Cdc42 (Adams et al., 1990). They are short, branched actin filaments (Young et al., 2004) and are nucleated by the Arp2/3 complex (Winter et al., 1997). The role of actin patches is one in endocytosis. They are required for the uptake of excess membrane lipids and synthetic enzymes that were first delivered along the actin cables (Valdivia et al., 2002; Ziman et al., 1996).

1.4.4 The Exocyst

Upon reaching the plasma membrane vesicles must be tethered to it in order for fusion to take place. Tethering is mediated by a protein complex called the exocyst. This multimeric complex comprises eight subunits: Sec3, Sec15, Sec5, Sec6, Sec8, Sec10, Exo70 and Exo84 (TerBush et al., 1996). All subunits except Sec3 can associate with vesicles and a pool of Exo70 along with Sec3 can localise to the plasma membrane independently of the actin cytoskeleton (Boyd et al., 2004). Cdc42 has been shown to interact directly with both Exo70 and Sec3 (Wu and Brennwald, 2010; Zhang et al., 2001), with Sec3 localisation required for correct exocyst localisation (Finger et al., 1998). Thus Cdc42 is acting upon Sec3 to provide a spatial landmark for the exocyst to assemble at the site of polarised growth. Once vesicles reach the site of growth, a complete exocyst is formed and the vesicle is tethered at the plasma membrane before membrane fusion mediated by the T-SNARE and V-SNARE proteins (Rothman, 1996). A model of polarised growth in *S. cerevisiae* is shown in figure 1.4.

1.4.5 Polarised growth and the cell cycle

The cell cycle of *S. cerevisiae* contains 2 periods of polarised growth, interspersed with isotropic or uniform growth. During G1, growth is polarised towards the site of bud emergence and later on the bud tip before becoming isotropic during G2 to expand the daughter cell size (figure 1.5). Growth again becomes polarised during cytokinesis in order to produce the primary septum consisting of chitin and secondary septum of in-growing cell wall before cell division. These changes in growth require careful control of signalling

proteins, membrane proteins and other species to bring about the correct response of the processes discussed above to ensure secretory vesicles are targeted to the sites of growth.

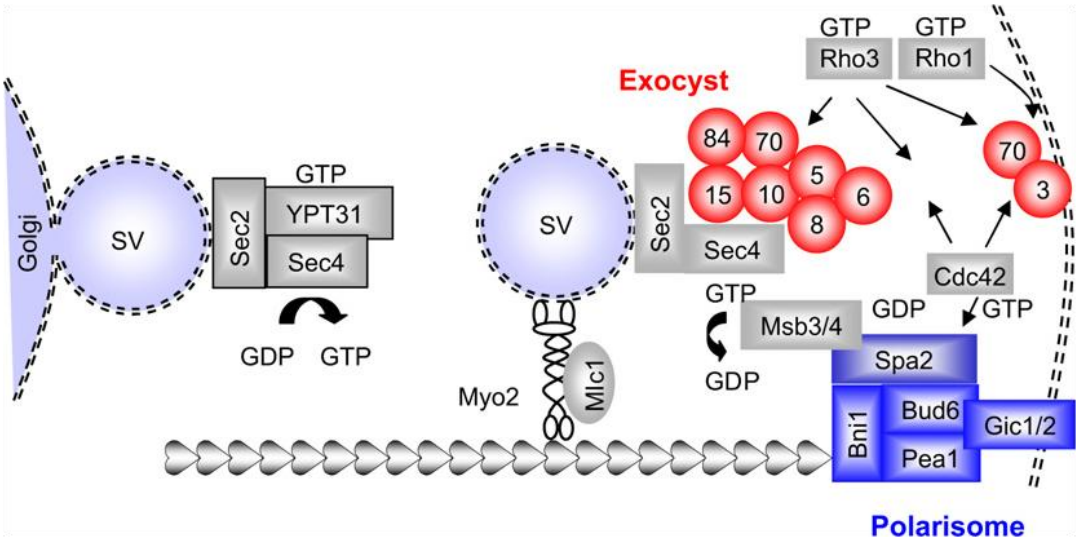

Figure 1.4 Polarised growth in *Saccharomyces cerevisiae*

Polarised secretion in *S. cerevisiae* requires Rab GTPases, actin cables, Myo2 and the Exocyst. The Rab GTPase, Ypt31, allows secretory vesicles to leave the Golgi before recruiting the Sec4 GEF Sec2. Sec2 and Sec4 license vesicle transport along actin cables (polarised via the polarisome complex at the bud tip), using the class V myosin Myo2 and its light chain Mlc1. Upon arriving at the growing bud tip, exocyst components on the vesicles combine with the independently localising exocyst components Exo70 and Sec3 to create a complete exocyst complex. Vesicles are now tethered at the bud tip membrane ready for fusion mediated by the SNARE proteins. Image taken from (Sudbery, 2008).

As polarised growth in *S. cerevisiae* is linked to the cell cycle, many of the cues for polarised growth are controlled by the master cell cycle regulator Cdk1 (Cyclin-Dependent Kinase 1), also known as Cdc28. Cdk1 requires different cyclins during stages of the cell cycle; three during G1 (Cln1-3) and six during G2 (Clb1-6)

During G1, Cdk1-G1 cyclins promote the activation the Rho-GTPase Cdc42 in a number of ways. Firstly Cdk1-Cln2 allows release of Cdc24, the Cdc42 exchange factor (positive

regulator), from its sequestering protein in the nucleus to the presumptive bud-site (Nern and Arkowitz, 2000). Cdk1-Cln2 also phosphorylates the negative regulators of Cdc42 Bem3 and Bem2 (Knaus et al., 2007) and Rga2 (Sopko et al., 2007). These events allow active Cdc42 to send signals that promote reorganisation of the actin cytoskeleton towards the bud site. Then, during G2, Cdc42 is required to re-distribute from the bud tip to the daughter cell cortex, a process requiring Cdk1-Clb2 (Pruyne and Bretscher, 2000). It has also been speculated that $Cdk1^{G2}$ may regulate phospholipid flippases that are required for Cdc42 re-localisation from the bud tip to the cortex (Enserink and Kolodner, 2010).

The morphogenesis checkpoint is mediated by Swe1 and Mih1 and serves to ensure that there is no disturbance to the actin cytoskeleton or septin ring before cells progress through the G2/M transition. Swe1 can phosphorylate Cdk1 on tyrosine 19, inhibiting the kinase and hence stalling the cell cycle (Booher et al., 1993). Whilst Mih1 is thought to reverse this phosphorylation so that mitosis can continue (Enserink and Kolodner, 2010). Further reinforcing the relationship between the cell cycle and polarised growth is the fact that *S. cerevisiae* can use the morphogenesis checkpoint through Swe1 to encourage pseudohyphal growth (La Valle and Wittenberg, 2001).

Finally, $Cdk1^{G2}$ is required for exit from mitosis through the anaphase promoting complex (APC). Cdk1 phosphorylates components of the APC resulting in binding of the APC to Cdc20 (Rudner and Murray, 2000) and subsequent degradation of the G2 cyclins.

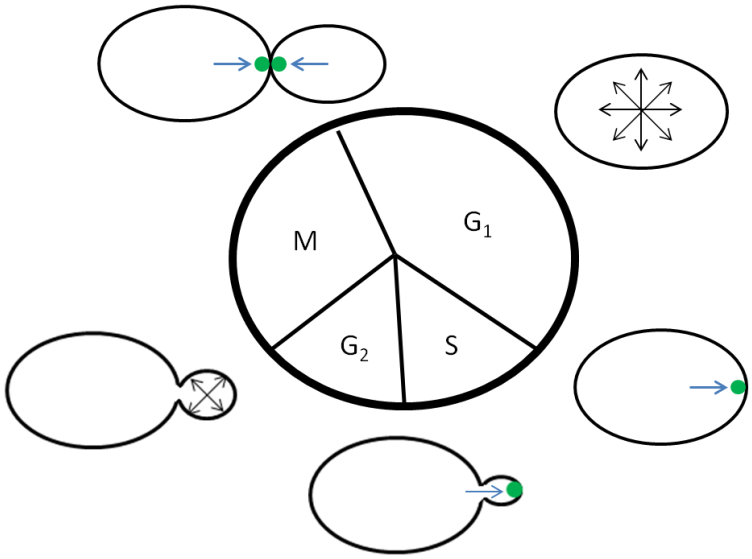

Figure 1.5 Polarised growth is linked to the cell cycle in *S. cerevisiae*

During the yeast cell cycle there are multiple periods of both isotropic and polarised growth mediated by localisation of Cdc42 (green). During the majority of G1, growth (indicated by arrows) is isotropic, leading to expansion of the mother cell. Then, late in G1 and near the S phase transition, growth becomes polarised towards the incipient bud site so that the daughter bud emerges. During G2/M phase, growth again becomes isotropic so that the whole of the daughter cell expands to two thirds the size of the mother. Growth is then directed at the mother bud neck during cytokinesis to provide the primary and secondary septum between the two cells ready for cell separation.

1.5 Polarised growth in *C. albicans* hyphae

S. cerevisiae provides a good model for polarised growth in yeast but does not provide any insight into the highly polarised nature of the *C. albicans* hyphal morphology. In this morphology, the polarisation machinery remains at the hyphal tip throughout the cell cycle instead of re-distributing to the daughter cell cortex to promote isotropic growth. What follows will be a discussion of the key differences in the molecular machinery of polarised growth in *C albicans.*

1.5.1 Selection and maintenance of the site of hyphal growth

The role of Rsr1 in marking the site of bud emergence in *S. cerevisiae* was discussed above. Deletions of the Rsr1 protein in *C. albicans* result in abnormal yeast and hyphal morphologies, with hyphae containing frequent bends and an increased amount of branching (Hausauer et al., 2005). Furthermore, the same study associated these defects in morphology with irregular actin patch polarisation and mis-localisation of the polarisome and septin rings. These pieces of evidence point to Rsr1 acting not only as a cortical marker for the establishment of the site of germ tube evagination, but also as a stabiliser of the polarity machinery later on in hyphal growth. It has also been shown that Rsr1 activity is localised to hyphal tips, which is necessary for the localisation of the Rho-GTPase Cdc42 (Pulver et al., 2013). This led to the proposal that in *C. albicans*, Rsr1 is required to "fine-tune" the distribution of Cdc42 at the hyphal tip and does not just act as a bud-site selector. The model of Cdc42 discussed earlier requires that the protein transduce its signal through the polarisome member, Bni1, to organise the actin network towards the site of polarised growth. Components of the polarisome of *C. albicans* have been shown to localise to a crescent at the hyphal tip surface along with Cdc42, signifying that the model may also be true here (Crampin et al., 2005; Jones and Sudbery, 2010). The exocyst also localises to a surface crescent in *C. albicans* and is thought to be controlled by Cdc42 in the same way as in *S. cerevisiae,* except not all vesicles are thought to be carrying exocyst components (Jones and Sudbery, 2010). Another role Cdc42 plays in hyphal growth is the induction of hyphal-specific genes (Bassilana et al., 2005) especially when localised at the tip (Pulver et al., 2013). Hyphal growth also requires a higher level of Cdc42 than yeast growth (Bassilana et al., 2005). The ability of Cdc42 to cycle between its GTP-bound and GDP-bound states has been shown to be important for hyphal growth, with mutants lacking the GAPs Rga2 and Bem3 being competent at growing as hyphae in pseudohyphal conditions whilst in strains with constitutively bound GTP-Cdc42, cells were swollen with stable septin bars (discussed later) indicating lack of progression of hyphal growth (Court and Sudbery, 2007).

1.5.2 Hyphal tips have a Spitzenkörper structure

When the myosin light chain Mlc1, which is associated with vesicles, is visualised with a GFP tag in *C. albicans* hyphae, it can be seen to localise to a spot just behind the hyphal tip (Crampin et al., 2005). This implies the presence of a Spitzenkörper structure. The Spitzenkörper has been known for some time in filamentous fungi to drive the growth and direction of hyphae (Virag and Harris, 2006). The Spitzenkörper is a very dynamic structure (Jones and Sudbery, 2010), with a stream of incoming vesicles being balanced exactly by an outward stream. *S. cerevisiae* and *C. albicans* yeast and pseudohyphal morphologies do not contain the Spitzenkörper (Crampin et al., 2005).

The vesicle supply centre model was first proposed in 1989 and suggested that the shape of a *C. albicans* hyphae was dictated by the equal diffusion in all directions of vesicles from a vesicle supply centre behind the hyphal tip (Bartnicki-Garcia et al., 1989). Taking the vesicle supply centre model, the molecular evidence of hyphal growth in *C.albicans* and polarised growth in *S. cerevisiae,* leads to a model of hyphal growth (Sudbery, 2011) (shown in figure 1.6). In this model, vesicles are licensed for exit from the Golgi by the GTPase Ypt31, recruiting Sec2 and hence Sec4. Vesicles then travel along actin cables thorough the hyphae until they accumulate in the Spitzenkörper before docking with the exocyst and fusion with the plasma membrane. However, this has recently been challenged with the idea that the hyphal shape is brought about by the density of exocyst components on the hyphal tip determining the rate of vesicle fusion, rather than their rate of diffusion from the Spitzenkörper (Caballero-Lima et al., 2013).

1.5.3 The septins localise differently in the three *C. albicans* morphologies.

In *S. cerevisiae,* the four septins (GTPases) Cdc3, Cdc10, Cdc11, and Cdc12, have been shown to make a ring around the bud neck composed of 10 nm filaments. The septins act as scaffolds, recruiting proteins required for cytokinesis later on in the cell cycle, and also acting as a diffusion barrier between the mother cell and the growing daughter bud. The septins are reviewed fully in (Oh and Bi, 2011).

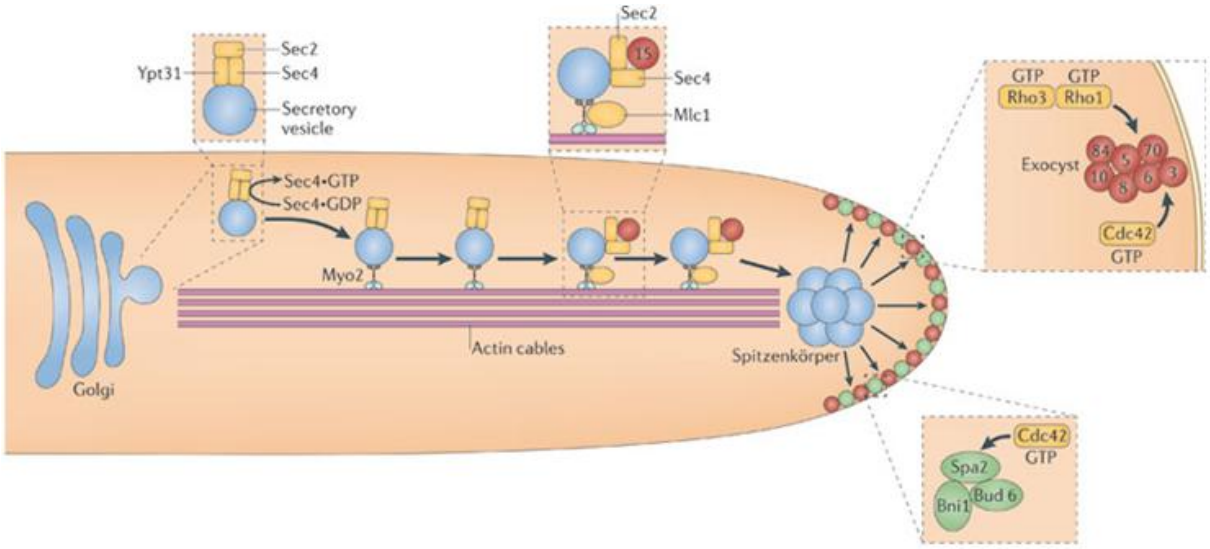

Image taken from (Sudbery, 2011).

<u>Figure 1.6</u> A model of hyphal growth in *C. albicans*

During hyphal growth in *C. albicans*, secretory vesicles are transported along actin cables to sites of polarised growth in a manner similar to that in *S. cerevisiae*, regulated by the Rab GTPases Ypt31, and Sec4 (Figure1.4). In *C. albicans*, vesicles accumulate at a structure just behind the growing tip called the Spitzenkörper before tethering to the membrane via the exocyst. In the vesicle supply centre model, the diffusion of vesicles from the Spitzenkörper dictates the shape of the hyphal tip, however recent research suggest the shape is more likely defined by the localisation of exocyst subunits on the plasma membrane.

In *C. albicans* there are two essential septins, Cdc3 and Cdc12 and non-essential septins Cdc10, Cdc11 and Sep7, which all play a role in septum formation and cytokinesis (Sudbery, 2007; Sudbery, 2001; Warenda and Konopka, 2002). The septins localise differently in yeast, pseudohyphal and hyphal morphologies of *C. albicans* (Sudbery, 2001). In the yeast morphology, septins first form a ring at the mother-bud neck before later splitting in two before cytokinesis for the primary and secondary septum to form in between. Pseudohyphae show a similar localisation pattern. During hyphal growth, septins first form bars at the neck of early germ tubes before later re-assembling into a ring structure in the hyphal tube that marks where the septum will form. Again this ring later splits in two before

cytokinesis. This different localisation of the septins provides a useful technique in distinguishing between the different *C. albicans* morphologies and is shown in figure 1.7.

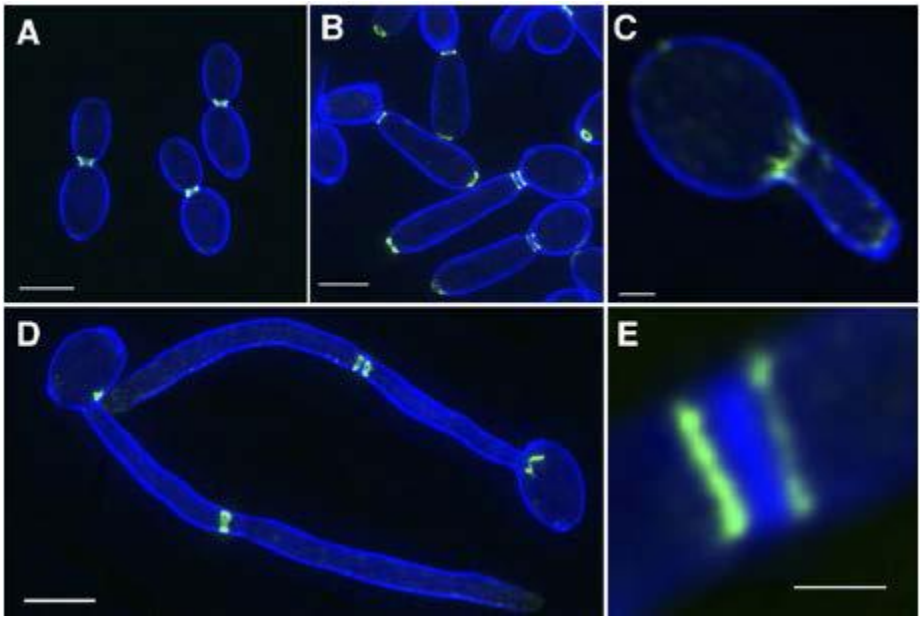

Image taken from (Sudbery, 2007)

Figure 1.7 The differential localisation of the septins in *C. albicans* morphologies
During growth as yeast (A) and pseudohyphae (B) the *C. albicans* septins localise to a ring around the mother-bud neck which later splits in two during cytokinesis. During hyphal growth, the septins first appear as bars at the base of the early hyphal germ tube (C). Later on they form a ring (D) along the length of the hyphae before splitting in two for the septum to form in between (E).

1.5.4 Hyphal growth and the cell cycle

As discussed above, in *S. cerevisiae*, the cell cycle is linked to morphogenesis by the master cell cycle regulator Cdc28/Cdk1. However, in *C. albicans* hyphae, polarised growth is not linked to the cell cycle. The Spitzenkörper drives emergence of the early germ tube before the cell cycle has started, before spindle pole body duplication and DNA replication (Hazan et al., 2002). However, the cell cycle and polarised growth in hyphae are both controlled by Cdc28 (Bishop et al., 2010).

As discussed earlier, Cdc28 activity is regulated in part by binding to cyclins. Three G1 cyclins control cell cycle progression and morphogenesis in *C. albicans:* Ccn1 (Sinha et al., 2007); Cln3 (Chapa y Lazo et al., 2005)and Hgc1 (Hyphal-specific G1 cyclin) (Zheng and Wang, 2004). Mutants of either of these cyclins are able to start hyphal growth but fail to maintain it. The *cln3* shut-down is lethal, with cells arresting in G1 with swollen tips and bends in the hyphae. The *ccn1ΔΔ* mutant fails to maintain hyphal growth after germ tube formation and *hgc1ΔΔ* mutants cease hyphal growth early after induction, producing only small protrusions. Deletion of *CCN1* and *HGC1* does not inhibit cell cycle progression, but does inhibit growth dramatically, suggesting that they play a bigger part in morphogenesis than the cell cycle (Biswas et al., 2007)

1.5.5 Targets of Cdc28 during polarised growth

The kinase Cdc28 regulates many of the proteins that are involved in polarised growth. Perhaps most interestingly, Cdc28-Hgc1 phosphorylates and inactivates Rga2, the Cdc42 GAP (Zheng et al., 2007). As Cdc42 is seen as the master regulator of polarised growth, this provides a mechanism for the highly polarised growth of hyphae in which inactivation of Rga2 allows continued activation of Cdc42 at the hyphal tip and hence continued polarised growth. Cdc28-Hgc1 and Cdc28-Ccn1 also phosphorylates Sec2, which is important for its localisation to the Spitzenkörper and normal hyphal growth (Bishop et al., 2010). An important part of the hyphal morphology is the lack of cell separation at the end of the cell cycle. This is regulated in two ways by Cdc28. Firstly, Cdc28-Hgc1 phosphorylates the transcription factor Efg1 leading to down regulation of the septum degradation enzymes (SDE's) (Wang et al., 2009). Secondly, Cdc28-Hgc1 phosphorylates the septin Sep7. This prevents Cdc14 localising to the septin ring and hence the kinase Cbk1 (discussed later in this chapter) licensing Ace2 to transcribe the SDE's (Gonzalez-Novo et al., 2008). Cbk1 itself and its regulator Mob2, is also a target of Cdc28 and will be discussed in due course. A model of the Cdc28 action to repress the SDE's is shown in figure 1.8.

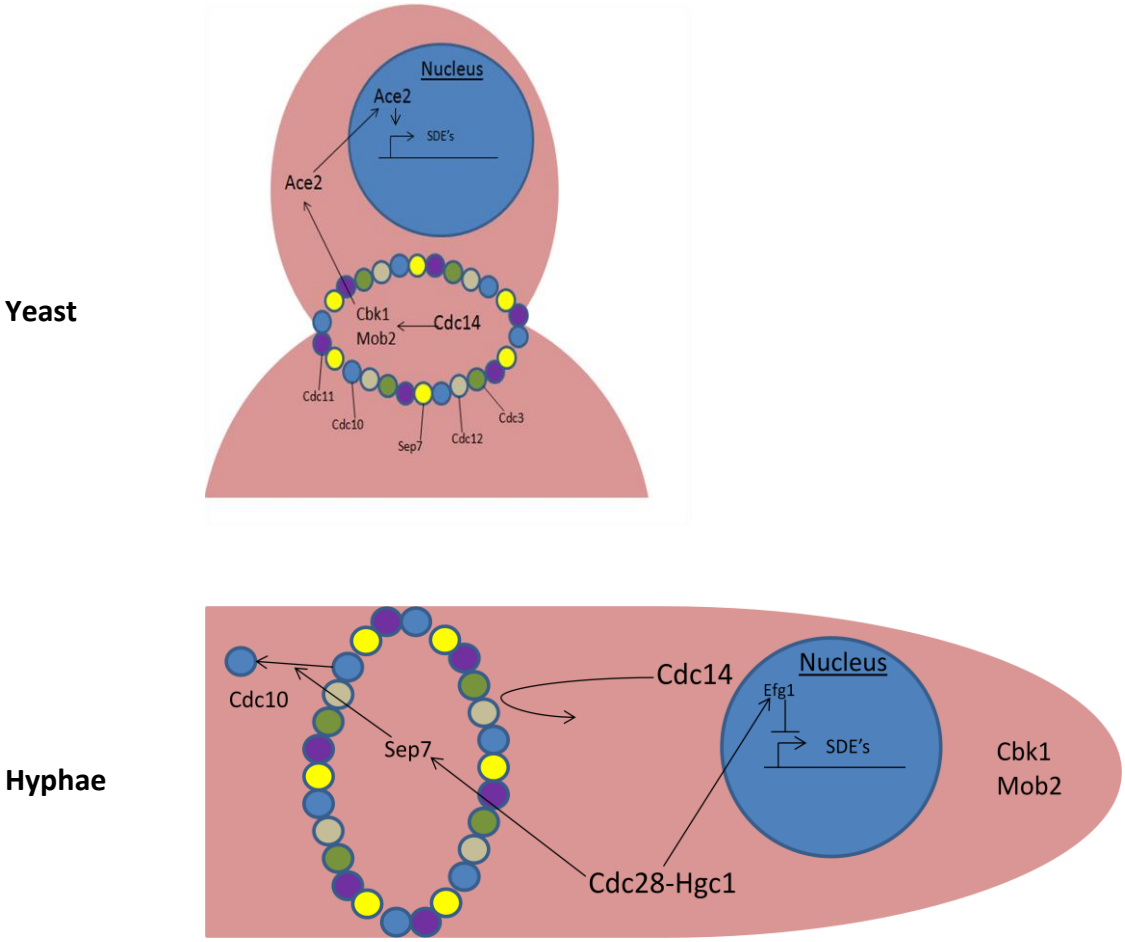

<u>Figure 1.8</u> Cdc28 represses cell separation in *C. albicans* hyphae

During yeast growth, Cdc14 is released from the nucleus upon activation of the mitotic exit network. This allows dephosphorylation of Cdc28 sites on Cbk1 by Cdc14 so that Cbk1 can licence Ace2 to the daughter nucleus for the transcription of the septum degrading enzymes (SDEs) and cell separation can occur.

During hyphal growth, Cdc28-Hgc1 represses cell separation in two ways. Firstly, it phosphorylates the transcription factor Efg1, which in turn represses expression of the SDEs. Secondly, it phosphorylates the septin Sep7, making the septin Cdc10 more dynamic and blocking Cdc14 from entering the septum. This allows Cbk1-Mob2 to remain at the hyphal tip so they don't licence Ace2 to enter the daughter nuclei and transcribe the SDEs. Image modified from (Sudbery, 2011).

1.6 Cell signalling pathways that control morphogenesis in *C. albicans*

Hyphal-specific genes that are induced upon environmental cues in *C. albicans* include those for proteins involved in cell wall reorganisation and adherence such as Hwp1 (Hyphal cell wall protein 1), Ece1 (Extent of cell elongation 1) and Als3 (Agglutinin-like synthase) (Biswas et al., 2007). Transcription of these genes is controlled by two major transcription factors Efg1 and Cph1 and others such as Rim101 and Czf1. *C. albicans* senses environmental cues such as temperature, pH, *N*-acetylglucosamine and CO_2 levels using membrane receptors and must transduce these signals to bring about a transcriptional response (Biswas et al., 2007). There are two well studied signal transduction pathways that lead to hyphal growth, the Cek1 pathway leads to stimulation of the Cph1 transcription factor, whilst the cAMP-PKA pathway stimulates the Efg1 transcription factor. Both pathways are reviewed in (Biswas et al., 2007) and are shown in figure 1.9.

The Cek1 pathway is a Mitogen-Activated Protein Kinase pathway (MAPK) consisting of Cst20, Ste11, Hst7, and Cek1. Deletion of any of these components results in defects in hyphal growth in response to many conditions except serum. This pathway can also be activated by Cdc42 binding to Cst20 (Su et al., 2005).

The cAMP-PKA pathway consists of Tpk1 and Tpk2- the catalytic subunits of the cAMP dependent protein kinase A (cAMP-PKA) - and their regulatory subunit Bcy1. Both Tpk1 and Tpk2 are needed for hyphal growth, although Tpk1 appears to be more important on solid medium and Tpk2 more so in liquid medium (Sonneborn et al., 2000).

Both the cAMP-PKA and MAPK pathway are regulated by the upstream component Ras1, most probably by increasing production of cAMP in the former and an unknown mechanism in the latter.

Hyphal-specific genes are negatively regulated by the transcription factor Tup1 in concert with any one of its co-repressors: Rfg1, Mig1 or Nrg1, deletion of which cause constitutive filamentation (Biswas et al., 2007). Interestingly, recent unpublished work showed that Cdc28 phosphorylates Nrg1 in order to repress it and allow hyphal morphogenesis to occur (Alaalm, LM, PhD thesis, Sheffield University).

1.6.1 The small GTPase Rac1 is required for embedded filamentous growth in *C. albicans*

This study has already discussed the importance of two small G-proteins, Cdc42 and Rho1 in cell polarity in both *S. cerevisiae* and *C. albicans*. The small G-protein Rac1 has been shown to be required for hyphal growth and invasiveness in other fungi (Mahlert et al., 2006; Vallim et al., 2005; Virag et al., 2007), whilst in mammals, Rac1 homologs regulate signalling pathways that also control cell polarity (Bosco et al., 2009). It has been shown that the *C. albicans* Rac1 and its GEF Dck1 are required for hyphal growth when the organism is embedded in a matrix but not when grown in liquid culture (Hope et al., 2008) (Bassilana and Arkowitz, 2006). Rac1 is not needed for organisation of the cytoskeleton and its role is independent of Cdc42, (Bassilana and Arkowitz, 2006). These results show that even though both Cdc42 and Rac1 are involved in cell polarity, they each perform different roles in *C. albicans*. Like human Rac1, it has been shown that *C. albicans* Rac1 shuttles between the plasma membrane and the nucleus (Vauchelles et al., 2010), although the purpose of this remains unknown. It has been shown that Rac1 functions upstream of the mitogen activated protein Cek1 and Mkc1 (Mpk1 in the *S. cerevisiae* CWI) (discussed above) (Hope et al., 2010) which links it to both hyphal growth and cell wall integrity.

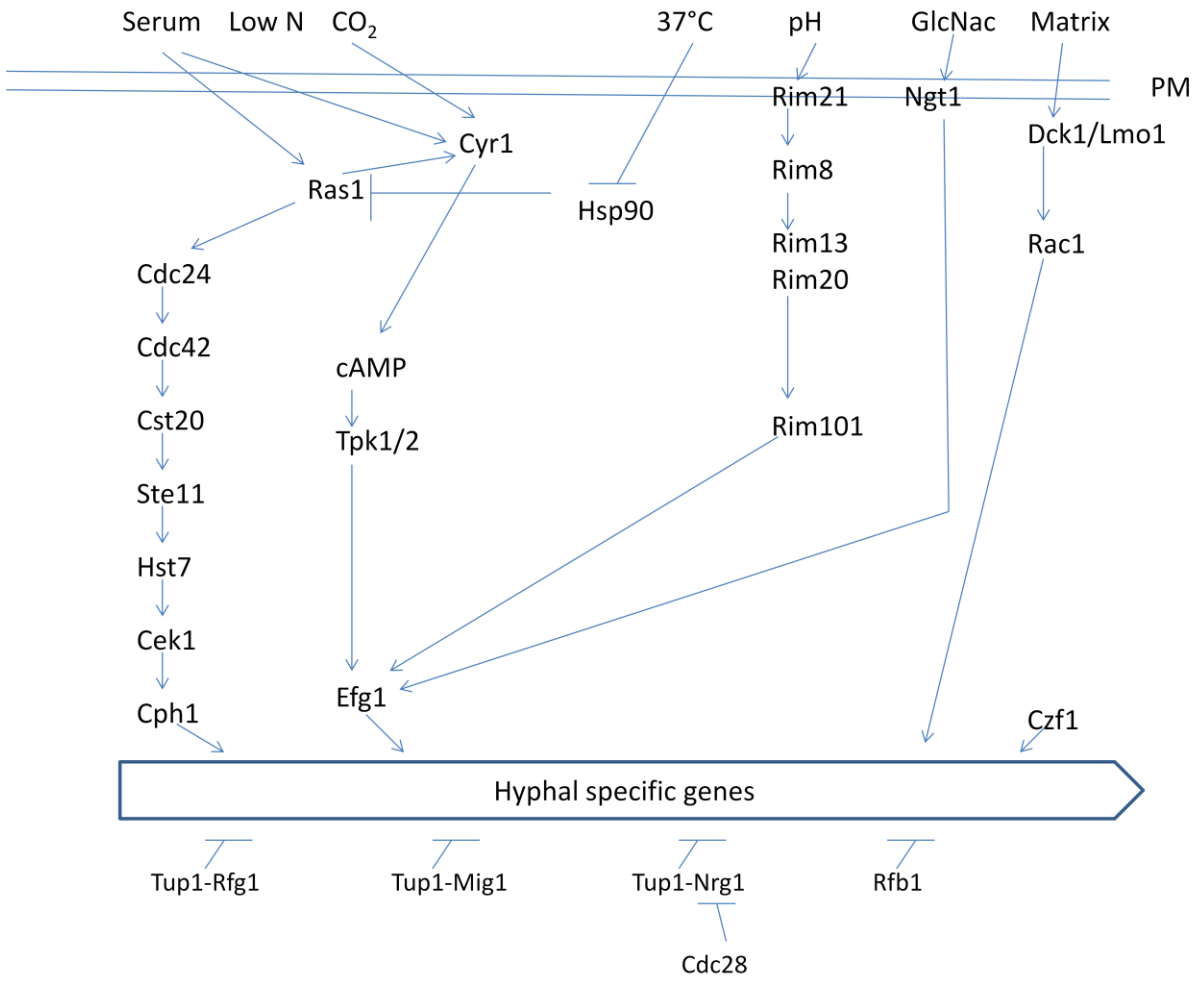

Figure 1.9 Numerous signalling pathways contribute to *C. albicans* hyphal morphogenesis

1.7 The *C. albicans* cell wall

The *Candida albicans* cell wall has two main functions: maintenance of the structural integrity of the cell and recognition/adhesion to either the human host or other surfaces such as catheters. The cell wall and its role in adhesion is reviewed fully in (Gow and Hube, 2012) and (Chaffin, 2008). Briefly, the cell wall is composed of two main layers which have been identified by differing electron densities. The outer cell wall is composed of *N*- and *O*-linked mannans and cell wall proteins such as adhesins and invasins. The inner layer is comprised of two different forms of polysaccharide: β-glucans (β-1,3 and β-1,6) and chitin. β-1,3-glucan provides a flexible branched network to which β-1,6-glucan and chitin are

attached. This inner layer provides structural rigidity to the cell whilst the outer layer is less permeable, preventing host molecules from entering (Gow and Hube, 2012). The majority of cell wall proteins (CWPs) are covalently attached to the β-1,6-glucan via a Glycosylphosphatidylinositol (GPI) anchor. *Pir* proteins are also covalently attached to the β-1,3-glucan, whilst some proteins do not use a covalent bond but remain cell wall associated (Chaffin, 2008). In *S. cerevisiae,* the glucan synthases are embedded in the plasma membrane and extrude glucan polymers into the cell wall by addition of UDP-glucose (Klis et al., 2006; Lesage and Bussey, 2006) which is also thought to be the case in *C. albicans.* The chitin synthases operate in a similar way (Lesage and Bussey, 2006).

1.8 Rho1 is a central member of the cell wall integrity pathway

In *S. cerevisiae,* Rho1 is a small GTPase that localises to sites of growth (Yamochi et al., 1994), which is anchored in the cell membrane via prenyl groups. *RHO1* is essential and temperature sensitive mutants show a failure to maintain growth of the daughter bud (Yamochi et al., 1994). Rho1 is a central member of the cell wall integrity pathway (CWI) shown in Figure 1.10. The CWI pathway has been well studied in *S. cerevisiae*, is mainly conserved in *C. albicans* (Blankenship et al., 2010) and is required to maintain the structure, shape and strength of the cell wall in response to both external stimuli and internal cues for cell wall remodelling. The CWI pathway consists of a series of membrane sensors (Wsc1-3, Mid2, Slt2) and a MAP kinase signalling cascade that are linked by Rho1-GTP.
The MAP kinase pathway consists of: Pkc1, Bck1, Mkk1/2 and Mpk1, with each one activating the next in turn by phosphorylation (Levin, 2011). The deletion of any kinase downstream of Pkc1 results in osmoremedial cell lysis at 37 °C, whereas loss of Pkc1 itself results in osmoremedial cell lysis at all temperatures (Levin and Bartlett-Heubusch, 1992; Paravicini et al., 1992). Interestingly, Mpk1 is mainly located in the nucleus but shuttles to the cytoplasm under cell wall stress (Kamada et al., 1995) and is also seen at sites of polarised growth (van Drogen and Peter, 2002) which requires the polarisome scaffold Spa2. The Mkk1-2 kinases are also localised to sites of polarised growth in a manner dependent on Spa2 (van Drogen and Peter, 2002). Perhaps this provides a link between sites of polarised

growth and the cell wall integrity machinery. The MAP kinase cascade in the CWI culminates on two transcription factors: Rlm1 and SBF (Swi4 and Swi6).

Rlm1 is phosphorylated by Mpk1 so that it remains nuclear (Jung et al., 2002) and is responsible for the majority of CWI mediated transcription and as such has been subjected to many genome-wide analyses (Jung and Levin, 1999) (Lagorce et al., 2003). Around 25 genes are differentially transcribed when Mkk1 is constitutively active (Jung and Levin, 1999), with the majority being suspected or known cell wall proteins. Another study used constitutively active Rho1 and Pkc1 to identify a set of genes common between the two (Roberts et al., 2000), which included Rlm1 itself, suggesting that a feedback loop exists.

SBF is composed of both Swi4 and Swi6, with the former being recruited to the promoters of cell wall stress genes first before the latter is recruited to allow binding of RNA polymerase II (Kim and Levin, 2011; Kim et al., 2008). This mechanism of activation is important so that SBF is not recruited to the promoters of cell cycle genes that it can control on its own during G1 instead of the CWI regulated genes. SBF is thought to regulate cell wall and morphogenesis genes, especially the β-1,3-glucan synthase component *FKS2* (discussed later) and *PLC1*, a cyclin (Baetz et al., 2001).

1.9 Targets of Rho1

Other than Pkc1 and the subsequent MAP kinase cascade discussed above, Rho1 targets: Bni1 and Bnr1, Sec3, Skn7 and β-1,3-glucan synthase, which are discussed in detail below.

1.9.1 Bni1 and Bnr1

As previously mentioned Bni1 and Bnr1 are both formins that nucleate and protect actin filaments from capping. Bni1, a member of the polarisome, polarises actin to the bud tip (Ozaki-Kuroda et al., 2001), whereas Bnr1 polarises actin to the mother-bud

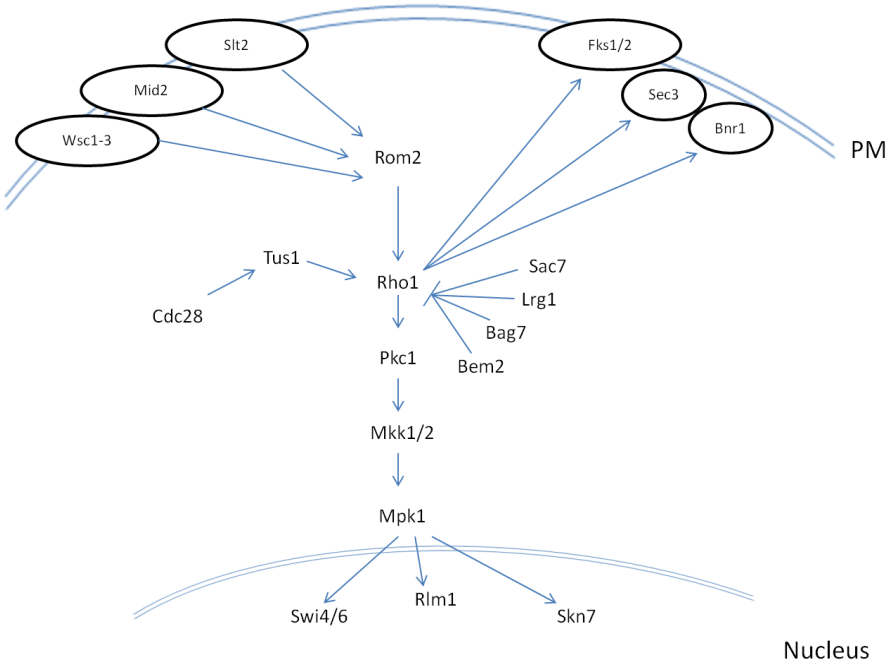

Figure 1.10 The yeast cell wall integrity (CWI) pathway

The CWI consists of a series of cell surface sensors linked to various output pathways via the GTPase Rho1, and serves to maintain cell wall integrity under external stresses and in response to cell wall growth needs. Regulation of transcription programmes and links to actin reorganisation, exocyst regulation and glucan synthesis are mechanisms through which the CWI achieves its goal and all are discussed in the text. Like all GTPases, Rho1 is regulated by numerous GEFs and GAPs that may be specific for each potential target.

neck (Buttery et al., 2007). Rho1-GTP (along with other Rho proteins) has been shown to interact with Bni1 (Kohno et al., 1996). This interaction prevents auto-inhibitory binding of the N-terminal Rho-binding domain (RBD) of Bni1 to its own C-terminal domain (Alberts, 2001). Furthermore, the localisation of Bni1 to the bud tip is dependent on its Rho1-binding domain (Fujiwara et al., 1998). This evidence points to Rho1 affecting polarisation of the actin cytoskeleton during cell wall remodelling.

1.9.2 Sec3

Discussed earlier, Sec3 is a member of the exocyst structure, acting as a landmark for exocyst assembly at sites of polarised growth. Rho1, Rho3 and Cdc42 all associate with Sec3 (Zhang et al., 2001; Zhang et al., 2008). Rho1-GTP interacts with Sec3, is required to establish and maintain Sec3 polarity (Guo et al., 2001) and Rho1 and Cdc42 actively compete *in vitro* for the N-terminal Domain of Sec3 (Zhang et al., 2001). This data suggests

that both Cdc42 and Rho1 are directing information for Sec3 to mark the site of polarisation and exocyst docking but at different times during polarised growth.

1.9.3 Skn7

Ssk1 and the transcription factor, Skn7, are the only currently identified yeast proteins that are related to the bacterial two-component signal transduction pathways (Li et al., 1998). Both are known to be regulated through the *HOG1-MAPK* signalling pathway and work antagonistically under changes in extracellular osmolarity, reviewed in (Levin, 2011). However, there have been numerous lines of evidence to suggest that Skn7 is also regulated by Rho1. Rho1-GTP has been shown to associate with Skn7 between the transcription factor's DNA-binding and response regulator domains (Alberts et al., 1998). Skn7 also contributes to cell wall integrity. Overexpression of the CWI sensor *MID2* stimulates a Skn7 transcriptional reporter (Ketela et al., 1999) and has been implicated in the function of Crz1, required for induced expression of *FKS2* (required for β-1,3-glucan synthesis) (Williams and Cyert, 2001). Growth defects of a *pkc1* mutant can also be overcome by overexpression of *SKN7* (Brown et al., 1994). These lines of evidence all point towards a role for Skn7 in cell wall integrity and biogenesis, although genes regulated by the transcription factor as a result of stimulation by the CWI pathways have yet to be elucidated.

1.9.4 β-1,3-glucan synthase

A major component of the yeast cell wall is β-1,3-glucan (Kollar et al., 1997). The polymer consists of chains of glucose linked by β-glycosidic bonds and provides the main structural support to the cell wall. The enzyme responsible for glucan synthesis, glucan synthase (GS), catalyses the glucan chains from monomers of UDP-glucose and is the major target of a large proportion of anti fungal drugs, the echinocandins, which interfere with GS activity (Beauvais et al., 1993; Perlin, 2007). GS is located in the plasma membrane and extrudes polymers onto the outside of the cell (Kopecka and Kreger, 1986). There are two alternative catalytic domains of the *S. cerevisiae* glucan synthase, encoded by the closely related genes *FKS1* and *FKS2* (Mazur et al., 1995). Fks1 and Fks2 have multiple transmembrane domains and a large cytoplasmic domain. Rho1 is an essential regulatory subunit of glucan synthase

and the GTPase stimulates activity of the GS in a manner dependent on GTP (Qadota et al., 1996). As would be expected, both proteins localise to sites of cell wall growth (Qadota et al., 1996). Further to this, glucan synthase co-localises and moves in concert with actin patches (Utsugi et al., 2002). As well as controlling GS directly, Rho1 plays a role in the transcription of the *FKS1* and *FKS2* genes.

FKS1 is the major gene expressed under normal growth conditions (Ram et al., 1995), and is regulated in a cell-cycle dependent manner by the transcription factor SBF (see above) (Igual et al., 1996; Spellman et al., 1998). *FKS1 is* also weakly regulated by the Rlm1 transcription factor after activation via the CWI MAPK pathway (Igual et al., 1996; Jung and Levin, 1999). *FKS2* is expressed at low levels under good growth conditions and is up-regulated in response to stresses on the cell wall, lack of carbon, mating pheromone or absence of *FKS1* (Mazur et al., 1995; Zhao et al., 1998). Cell wall stress causes an increase in *FKS2* expression in the short-term by the calcineurin-activated transcription factor Crz1 (Zhao et al., 1998). However, this high expression is maintained during prolonged cell wall stress by the activation of SBF through the CWI MAPK pathway (discussed earlier) (Zhao et al., 1998). It is important then to note that Rho1 controls β-1,3- glucan synthase production in multiple ways, not only through direct interaction with GS but also through regulation of the expression of *FKS1* and *FKS2*.

1.9.5 Rho1 is regulated by multiple GAPs and GEFs

As a GTPase, Rho1 must cycle between GTP and GDP bound states and there are multiple GEFs and GAPs that regulate Rho1 between these states, shown in figure 1.11

There are 3 GEFs that regulate Rho1: Tus1, Rom1 and Rom2 (Kono et al., 2008; Ozaki et al., 1996). Loss of either *TUS1* or *ROM2* causes temperature sensitive growth, whereas loss of both *ROM1* and *ROM2* is lethal. (Ozaki et al., 1996; Schmelzle et al., 2002). By binding to cell surface sensors Mid2 and Wsc1 with their N-terminal domain and to Rho1 via a RhoGEF domain, Rom1 and Rom2 transduce signals at the cell membrane to the CWI pathway (Philip and Levin, 2001). Tus1 however, does not contain the N-terminal domain to bind surface sensors as its role is mainly in cell cycle activation of Rho1. This activation occurs through Cdc28-Cln2 phosphorylation of Tus1, and recruits Tus1 to the growing bud (Kono et al.,

2008). Interestingly, it has been speculated that further phosphorylation of Tus1 by the polo-like kinase Cdc5 (Yoshida et al., 2006) serves to relocate Rho1 to the mother bud neck later on in the cell cycle (Levin, 2011). As expected by the localisation of Rho1, all three Rho1 GEFs require the actin cytoskeleton to localise to sites of polarised growth (Kono et al., 2008; Manning et al., 1997).

Four GTPase-activating proteins (GAPs) are known to act on Rho1; Bem2 (also a GAP of Cdc42), Sac7, Bag7 and Lrg1. These GAPs seem to stimulate Rho1 according to its different downstream targets. Bem2 and Sac7 are both involved in down-regulation of the MAPK signalling pathway through lack of Pkc1 stimulation by Rho1 (Martin et al., 2000; Schmidt et al., 2002). Sac7 is also involved in organisation of the actin cytoskeleton (Schmidt et al., 2002) along with Bag7. Lrg1 serves as the only GAP that negatively regulates the β-1,3-glucan synthase through its action on Rho1 (Watanabe et al., 2001). However, a study in *N. crassa* revealed that Lrg1 affected the PKC/MAK1 pathway and actin organisation, as well as GS activity. The study also showed that Lrg1 was required for hyphal tip extension and to prevent aberrant branch formation (Vogt and Seiler, 2008a). This then indicates that the function of Lrg1 may have diverged from *S. cerevisiae* in the highly polarised *N. crassa*.

As well as regulation by GAPs and GEFs, Rho1 can be regulated by guanine nucleotide exchange factors (GDIs). *S. cerevisiae* possess one GDI, Rdi1 which can extract both Rho1 and Cdc42 from the plasma membrane and hence inhibit their activity (Eitzen et al., 2001; Richman et al., 2004). Interestingly, the *C. albicans* ortholog of Rdi1 is regulated by the hyphal repressor Nrg1 (Kadosh and Johnson, 2005). Due to Rho1 being essential for growth and targeting multiple mechanisms such as cell wall signalling, the actin cytoskeleton, cell wall synthesis and the exocyst, Rho1 has been implicated in controlling cell polarity in *S. cerevisiae,* reviewed in (Madden and Snyder, 1998).

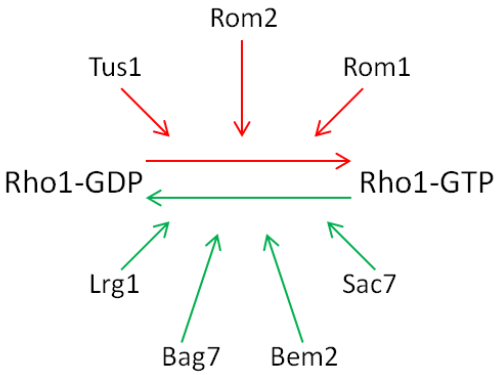

Figure 1.11 Multiple GAPs and GEFs regulate Rho1 GTP cycling
The GTP-bound state of Rho1 is regulated by multiple factors. The GEFs Tus1, Rom2 and Rom1 stimulate exchange of GDP for GTP on Rho1. However, the GAPs Lrg1, Bag7, Sac7 and Bem2 stimulate the inherent GTPase activity of Rho1 to hydrolyse GTP to GDP.

1.10 *Candida albicans* Cbk1 is a member of the NDR family kinases

The *Candida albicans CBK1* (cell wall biosynthesis kinase) gene was first identified due to its homology to a serine/threonine kinase, UKC1, in *Ustilago maydis* (McNemar and Fonzi, 2002). *Candida albicans* Cbk1 was noted as being required for maintaining cell morphology, differentiation of yeast cells into hyphae and cell separation. It was also shown that *cbk1* null mutants have an altered pattern of expression in genes associated with the cell wall and the transition from yeast to hyphal growth.

Candida albicans Cbk1 is a member of the NDR (nuclear dbf2-related) kinase group (a sub-class of AGC protein kinases) which is highly conserved amongst many organisms (Hergovich et al., 2006). Members of this group include: Trc in *Drosphila melanogaster,* SAX-1 in *Caenorhabditis elegans,* Sid2 and Orb6 in *Schizosaccharmyces pombe* and namesake of *Candida albicans* Cbk1 due to its high homology, Cbk1 in *S. cerevisiae*. The family of kinases are involved in important cellular processes such as morphological changes, proliferation, apoptosis and mitotic exit and are reviewed fully in (Hergovich et al., 2006). All members of the family share structural similarities. They contain a conserved serine/threonine residue within the activation domain which is auto-phosphorylated- (unlike other AGC kinases)- and a serine/threonine at a C-terminal hydrophobic region, phosphorylation of which is also

important in activation (Tamaskovic et al., 2003). Phosphorylation of this C-terminal site is often by a Ste-20 like kinase such as Mst3 in humans (Stegert et al., 2005). In contrast to other NDR kinases, yeast variants also have weakly conserved extensions at the N-Terminus (Hergovich et al., 2006).

1.11 Cbk1 is a member of the RAM network

The Cbk1 protein is a component of the yeast RAM (regulation of Ace2 transcription factor and polarised morphogenesis) network, shown in figure 1.12. In *S. cerevisiae,* the RAM network is understood well and it is comprised of at least 5 other proteins with varying functions: Mob2 forms a complex with Cbk1 and is required for its localisation and activation (Weiss et al., 2002); Kic1 (a Ste20-like kinase) acts upstream of Cbk1 and probably activates it through phosphorylation (see above); Hym1 interacts with both Cbk1 and Kic1 and is important for proper localisation of the complex; Pag1 is a large scaffold protein that may aid the action of Kic1 and Sog2 is an essential component of the network with as yet an unidentified function (Nelson et al., 2003). As the name suggests the role of the RAM network is two-fold: In the first instance it is responsible for maintaining polarised growth within the cell. Mob2 and Cbk1 both localise to the bud tip during polarised growth and the daughter nucleus and bud neck during late mitosis, with Cbk1 being activated throughout this time (Weiss et al., 2002). Furthermore, all components of the network are localised to sites of polarised growth and mutants of each fail to maintain polarised growth correctly, as shown by the following: more spherical cells, wider bud necks and an increase in the number of aborted mating projections (Nelson et al., 2003).

The second role of the RAM network is to maintain daughter cell-specific localisation of Ace2. As discussed above, Ace2 is a transcription factor that, when localised to the daughter cell by the Cbk1/Mob2 complex, activates the expression of daughter-specific genes, such as *CTS1* and *SCW11,* that encode chitinases or glucanases responsible for the cell wall degradation that separates the two cells (Colman-Lerner et al., 2001). This process of licensing Ace2 to the daughter nuclei is dependent on dephosphorylation of Cdc28 sites on Cbk1 by Cdc14 (Brace et al., 2011) (figure 1.8). Hence, any deletion in the RAM network leads to cell separation defects.

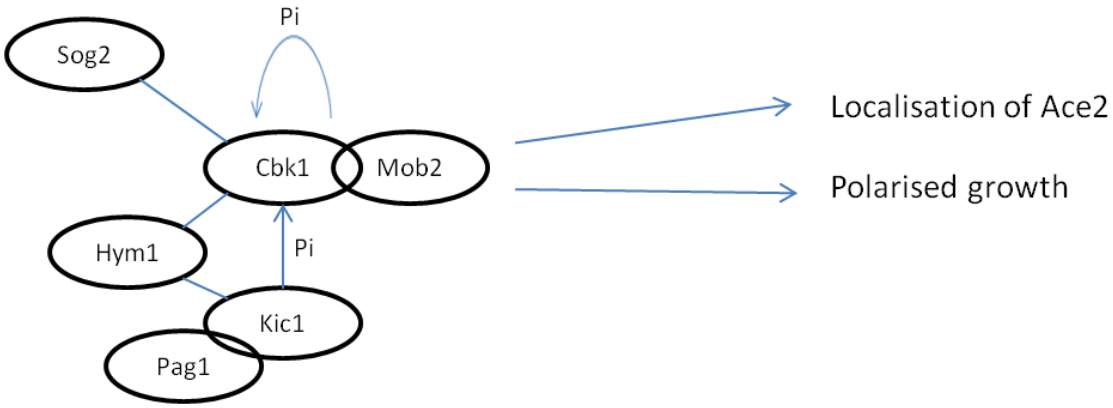

<u>Figure 1.12</u> The *S. cerevisiae* RAM network

The <u>R</u>egulation of <u>A</u>ce2 and <u>M</u>orphogenesis (RAM) network is responsible for localisation of the Ace2 transcription factor to the daughter nucleus and is essential for polarised growth. It is composed of at least six proteins of which Cbk1 is the key kinase. Cbk1 is activated in two ways: by phosphorylation by the upstream kinase Kic1 and auto-phosphorylation whilst bound to its partner Mob2.

Song *et al,* sought to investigate the role of the RAM network in *C. albicans* and its function in cell polarity and hyphal growth (Song et al., 2008). It was found that each of the *S. cerevisiae* orthologs in *C. albicans* were critical for the network to function properly. Mutants in any of the components result in cells that appear more spherical with a cell lysis phenotype. RAM network mutants also form large aggregates with mother and daughter cells failing to separate after mitosis. Furthermore, it was observed that RAM network mutants in *C. albicans* fail to form hyphae under all laboratory conditions that normally induce the morphology. In addition, it was found that expression of many genes required for hyphal growth is also RAM network dependent. These results show that although the *C. albicans* RAM network functions in much the same way as the *S. cerevisiae* model, it has diverged to include control of hyphal morphogenesis. Interestingly, homologs of Cbk1 in *N. crassa* and *A. nidulans* are also required for hyphal growth (Shi et al., 2008; Yarden et al., 1992). The *N. crassa CBK1* homolog *COT1* has also been shown to interact genetically with the Rho1 GAP *LRG1.* It is clear that the RAM network plays an important role in *C. albicans* and Cbk1 is a central member which requires further study. In 2010 Regan, H (Phd thesis,

University of Sheffield) sought to identify targets of the Cbk1 kinase in *C. albicans* by searching the proteome for targets with Cbk1 phosphorylation consensus motifs. A total of 1,445 potential targets were identified with varying numbers of internal motifs. Potential targets for investigation were then chosen based on those with the highest number of phosphorylation sites and their known/predicted role in polarised growth. The study identified the Rho1 GAP Lrg1 (above) as a potential target of Cbk1 but no further investigation was conducted.

1.12 Aims of this study

The critical role that Cdc28, Cbk1 and Rho1 all play in cell morphogenesis and polarised growth in *C. albicans* is discussed above. In *S. cerevisiae* it has been shown that Cdc28 regulates Rho1 activity through its action on the GEF Tus1. It has also been shown that in *N. crassa,* the Rho1 GAP Lrg1 is required for hyphal tip extension and maintenance of cell polarity. This study sought to investigate to what degree the as yet uncharacterised *C. albicans* Lrg1 protein played in the organism's morphogenesis and polarisation. It was also investigated whether Cdc28 regulates the cell wall integrity pathway through phosphorylation of Lrg1 and the potential cellular consequences resulting from this. Due to the joint action of Cdc28 and Cbk1 in bringing about hyphal growth, as well as genetic evidence linking *CBK1* and *LRG1* homologs, the regulation of Lrg1 by Cbk1 was also examined.

2 Materials and Methods

2.1 Culture Media

Media was prepared with deionised water and separated into 0.1 L aliquots before autoclaving at 121 °C, 15 psi for 20 minutes. Broth was stored at room temperature and plates were stored at 4 °C.

2.2 *Candida albicans* growth media

YPD

YPD contained 1 % w/v Bacto™-yeast extract, 2 % w/v Bacto™-peptone, 2 % w/v D-glucose (Fisher Scientific) and 80 mg L^{-1} uridine (Sigma Aldrich). For plates 2 % Bacto™-agar was added.

YPM

YPM is the same as YPD but contains 2 % w/v Maltose instead of glucose.

Minimal medium (YNB)

Minimal medium contained 2 % w/v D-glucose (Fisher Scientific), 0.67 % w/v yeast nitrogen base (without amino acids), 80 mg L^{-1} histidine (Sigma Aldrich), 80 mg L^{-1} arginine (Sigma Aldrich) and 80 mg L^{-1} uridine (Sigma Aldrich). For agar plates 2 % Bacto™-agar was added.

If the media was required to select for prototrophic strains, the appropriate amino acid was omitted from the media.

Met3-OFF media

Met3-Off media contained: 2 % w/v D-glucose (Fisher scientific), 0.67 % w/v yeast nitrogen base (without amino acids), 60.6 mg L^{-1} methionine, 373 mg L^{-1} cysteine, 770 mg L^{-1} complete supplement media lacking methionine, 80 mg L^{-1} uridine.

Met3-On media

Met3-On media contains the same ingredients as Met3-Off media but lacking both methionine and cysteine.

2.3 *Escherichia coli* growth media

2TY plus Ampicillin

2TY contained 1 % w/v Bacto™-yeast extract, 1.1 % w/v Bacto™-tryptone and 0.5 % w/v NaCl (Fisher Scientific). Media was then adjusted to pH 7.4 with NaOH. For plates, 1.5 % Bacto™-agar was then added.

If selection for resistance to ampicillin was required, the media was cooled after autoclaving to approximately 55°C before ampicillin was added to a final concentration of 100 µg ml^{-1}.

2.4 Growth conditions for *C. albicans* and *E. coli*

To induce the three different morphologies of *C. albicans*, the following conditions were used:

Morphology	pH of media	Temperature (°C)	New-born calf serum (v/v %)
Yeast	4.0	30	-
Pseudohyphae	5.5	36	-
Hyphae	7.0	37	20

Overnight cultures were grown in YPD media, unless otherwise stated, with shaking at 30 °C. For experimental cultures, after addition of serum if required and then pH adjustment, relevant media was pre-warmed at the required temperature for at least 30 minutes prior to inoculation.

Growth on Caspofungin

To analyse susceptibility to caspofungin, *C. albicans* strains were first inoculated into YPD and grown at 30°C overnight to stationary phase. Cultures were then sonicated for 5s to break up any clumps of cells and then adjusted with fresh YPD to read the same absorbance at OD_{600}. The cells were subjected to serial dilutions to $1x10^4$ and $1x0^6$ final concentrations. 1 µl of each dilution was then spotted onto YPD agar plates containing different concentrations of Caspofungin acetate (Sigma Aldrich).

Transformation of *Candida albicans*

Transformation of *C. albicans* was carried out using the lithium acetate method adapted from (Wilson et al., 1999).

A single *C. albicans* colony to be transformed was inoculated into 10 ml YEPD and left to incubate at 30 °C with shaking overnight. Using the overnight culture, 50 ml pre-warmed and aerated fresh YEPD was inoculated to an OD_{600} of 0.2 and incubated at 30 °C with shaking until the OD_{600} reached approximately 0.6. Cells were harvested by centrifugation at 3000 rpm for 5 minutes, re-suspended in wash buffer (10 mM Tris-HCL, pH 7.5, 1 mM EDTA and 100 mM LiAc) and centrifuged at 8,000 rpm for 15 seconds. The cell pellet was again re-suspended in 200 µl wash buffer. The cell re-suspension was then split in half, with each half added to the following: 300 µl 55 % w/v polyethylene glycol 4400 (PEG), 30 µl 10x TE buffer (100mM Tris-HCL, pH 7.5, 10mM EDTA), 36 µl of 1 M lithium acetate and 10 µl of 10 mg/ml denatured salmon sperm (boiled for 3 minutes, kept on ice thereafter) (Sigma Aldrich). To the experimental sample 100 µl of transforming DNA from a PCR reaction (see Polymerase chain reaction (PCR) for *C. albicans* transformation) or 8-10 mg linearised plasmid DNA was added whilst 100 µl of sterile, deionised water was added to the negative control. After gentle mixing using a pipette tip, the cells were incubated in a 30 °C water bath overnight. 40 µl of dimethyl sulfoxide (DMSO) was then added to each tube followed

by a gentle inversion and heat-shock at 42 °C for 15 minutes. Cells were then harvested by centrifugation at 8000 rpm for 15 seconds and gently re-suspended in 200 µl sterilised, distilled water. Cells were spread onto pre-warmed plates of the required selection media and left to incubate at 30 °C for 3-4 days before any colonies present were re-streaked onto selective media, incubated at 30 °C and then tested for correct integration by colony PCR.

Preparation of chemically competent *E. coli*

The *DH5α* strain of *E. coli* (Delta Biotechnology) was made chemically competent using the Rubidium chloride method. The strain was grown in one litre of 2TY media to an OD_{550} of 0.48. Cells were harvested and re-suspended in 40 ml ice cold TfbI buffer (30 mM KAc, 10 mM $RbCl_2$, 10 mM $CaCl_2$ 50 $MnCl_2$, 15 % glycerol, pH 5.8 (adjusted with acetic acid)) before incubation on ice for 10 minutes. Cells were again harvested and re-suspended in 5 ml ice cold TfbII buffer (10 mM MOPS, 75 mM $CaCl_2$, 10 mM $RbCl_2$, 15 % glycerol, pH 6.5 (adjusted with potassium hydroxide)) before being incubated on ice for 15 minutes. Cells were then dispensed into 100 µl aliquots and flash-frozen in liquid nitrogen before being stored at -80 °C.

Transformation of *E. coli*

Transformation of *E. coli* was carried out using *DH5α* chemically competent cells. Cells were taken from storage at -80 °C and thawed on ice. To 50 µl of cells, 200-300ng of DNA was added and left to incubate on ice for 10 minutes. The cells were then heat-shocked at 42 °C for 45 seconds before the addition of 450 µl of 2TY broth and incubation at 37 °C for 60-90 minutes. 50, 100 and 300 µl aliquots were spread onto 2TY plus ampicillin plates and incubated at 37 °C overnight. Colonies obtained were subjected to Miniprep procedure and restriction digest to test for presence of correct plasmid.

2.5 DNA techniques

Polymerase chain reaction (PCR) for *C. albicans* transformation

DNA for a *Candida albicans* transformation was prepared in the following PCR reaction: 20 µl 20 µM forward primer, 20 µl 20 µM reverse primer, ~200 ng DNA plasmid template, 6.5 µl Milli-Q filtered water, 12.5 µl Biomix Red ^{tm} (Bioline). Biomix Red^{tm} is a master-mix, ready to use, mixture of buffer, dNTP's, magnesium and Taq polymerase. The resulting mixture was then split into 10x 50 µl PCR reaction tubes before being amplified on the following PCR programme:

	Temperature (°C)	Time	Cycle
Initial denature	94	2 min	x1
Denature	94	30 sec	x30
Anneal	Dependent on Primer T_m	30 sec	
Extend	68	1 min/kb	
Final extension	68	8 min	x1

After the reaction 5 µl was run on a 1% agarose gel to check for correct amplification and precipitated into 100 µl sterilised distilled water (see below)

DNA precipitation

DNA was precipitated in the following manner. PCR reaction samples were pooled and 1/10th the volume 3M sodium acetate, pH 5.3, was added. Twice the volume of 100 % ethanol was then added before gentle mixing by inversion. The samples were incubated at -80°C for a minimum of 1hr before centrifugation at 13,000 rpm for 25 minutes. The resulting pellet was washed twice by addition of 70% ethanol and centrifugation for 2 minutes at 13,000 rpm. The final pellet was air dried in a sterile hood for 10 minutes before being re-suspended in 105 µl sterile, distilled water. 5 µl of the final solution was run on a 1 % agarose gel to ensure DNA was still present.

Agarose gel electrophoresis

In order to analyse a DNA sample, 5-10 µl was loaded onto a 1 % agarose gel made with 1X TAE buffer (0.4 M Tris, 0.2 M acetate, 0.01 M EDTA). Gels were submerged horizontally in 1X TAE buffer and 10 µl ethidium bromide added for visualisation of the DNA. Loading dye was added to samples to a concentration of 1X if needed and DNA Hyperladder 1 (Bioline) was used to indicate size of bands present. Gels were run at 70 V for 90 minutes before an image was taken using a UV transilluminator with CCD camera (UVItec Ltd).

Colony PCR

For each colony gained from a *C. albicans* transformation, a small amount of cells were added to 6 µl Milli-Q^{TM} water, boiled at 95°C for 6 minutes and incubated at -80°C for 45minutes. Once defrosted, 2 µl of the mixture was added to the following: 2 µl 20 µM forward primer, 2 µl 20 µM reverse primer, 12.5 µl Biomix^{TM} Red, 6.5 µl Milli-Q^{TM} water. For the *lrg1ΔΔ* strain 2 µl genomic DNA (see Genomic DNA extraction) was used in the reaction.

The 25 µl reaction was then run on the following PCR reaction:

	Temperature (°C)	Time	Cycle
Denature	94	3 min	X1
Anneal	Dependent on Primer T_m	1 min	
Extend	68	1 min/kb	
Denature	94	30 sec	X30
Anneal	Dependent on Primer T_m	30 sec	
Extend	68	1 min/kb	
Final extension	68	8 min	x1

After amplification, 15 µl the reaction was run on a 1 % agarose electrophoresis gel to check for presence of a product.

Genomic DNA extraction

Genomic DNA from *C. albicans* was extracted in the following way: 1.5 ml of a stationary phase overnight culture was pelleted and re-suspended in 250 µl extraction buffer (100 mM NaCl, 10 mM Tris pH 7.8, 1 mM EDTA, 0.1 % SDS), 300 µl phenol:chloroform:isoamylalcohol (24:24:1) was added followed by 200 µl acid washed 600 µm glass beads (Sigma Aldrich 425-600 µm diameter) before vortexing for 3 minutes. 200 µl TE buffer (10 mM Tris-HCL, pH 7.5, 1 mM EDTA) was added and the sample centrifuged at 13,000 rpm for 5 minutes. The top aqueous layer of the sample was removed and added to a fresh microfuge tube before addition of 1 ml 100 % ethanol and centrifugation at 13,000 rpm for 1 minute. The supernatant was then removed and the pellet re-suspended in 400 µl TE buffer before addition of RNAse to a final concentration of 75 µg/ml and incubation at 37°C for 14 minutes. $1/10^{th}$ volume of 3 M NaAc pH 5.3 and 2x volume 100 % ethanol was added and the sample incubated at -80°C for 2 hours. The sample was then centrifuged for 15 minutes at 4°C, 13,000 rpm, the pellet was washed in 70 % ethanol and centrifuged again for 5 minutes, 4°, 13,000 rpm. The final pellet was re-suspended in 50 µl sterilised, distilled water.

PCR Preparation of DNA for cloning and sequencing.

DNA fragments prepared from genomic DNA for sequencing or cloning were amplified with the proofreading Velocity™ Enzyme (Bioline). 500 ng genomic DNA was added to a reaction containing: 1 µl 20 µM forward primer, 1 µl 20 µM reverse primer, 10 µl Hi-Fi enzyme buffer, 0.5 µl 100mM dNTP mix, 1.5 µl DMSO, 1µl (2 units) velocity enzyme, plus the required amount of Milli-Q ™ water to make the reaction up to 50 µl. The reaction was then run on the following program:

	Temperature (°C)	Time	Cycle
Initial denature	98	5 min	x1
Denature	98	30 sec	x35
Anneal	Dependent on Primer T_m	30 sec	
Extend	72	1 min/kb	
Final extension	72	8 min	x1

1 µl of the reaction was run on an agarose gel to check amplification and the rest of the product was cleaned up (see Purification of DNA fragments from agarose gels and PCR products) before further analysis.

Sequencing of DNA fragments was carried out by Sheffield University's Core Genomic Facility.

Preparation of plasmid DNA

For first analysis of plasmids possibly containing ligated inserts, an alkaline extraction or dirty mini-prep was performed. 1.5ml of overnight *E. coli* culture from a single colony was pelleted for 1 minute at 13,000 rpm before re-suspension in 100 µl solution 1 (50 mM glucose, 25 mM tris-HCL pH 8, 10 mM EDTA). 200 µl solution 2 (0.2 M NaOH, 1 % SDS) was added and the sample inverted 4-5 times before addition of 150 µl solution 3 (5 M KOAC, 11.5 % acetic acid) and immediate inversion. The sample was incubated on ice for 10 minutes, centrifuged for 5 minutes at 13,000 rpm and the supernatant extracted to a fresh tube. 400 µl phenol:chloroform:isoamylalcohol (24:24:1) was added and vortexed for 5 seconds before centrifugation at 13,000 rpm for 5 minutes. The top aqueous layer was then extracted and transferred to a fresh tube before addition of 1 ml 100% ethanol and precipitation at -20°C for 30 minutes. The DNA was pelleted at 13,000 rpm for 15 minutes at 4°C, washed with 70% ethanol and pelleted again at 4°C for 5 minutes. The final pellet was re-suspended in 50 µl sterilised, distilled water. 1 µl 10mg/ml RNase was added per 2 µl DNA in a restriction endonuclease digest (described below) to check for correct presence of ligated inserts.

Pure plasmid DNA for transformation, sequencing, etc, was isolated from single colonies of *E. coli* by either a Qiaprep Spin Miniprep Kit (Qiagen®) or PureYield™ Plasmid Midiprep system (Promega). A single colony was grown in 5 ml (Miniprep) or 100 ml (Midiprep) 2TY plus ampicillin (100 µg ml^{-1}) overnight at 37 °C before performing isolation of DNA according to manufacturer's instructions. After each procedure, presence of the correct plasmid was checked by restriction endonuclease digestion and visualisation on a 1 % agarose gel.

Restriction endonuclease digestion

Restriction endonuclease enzymes were obtained from New England Biolabs (NEB) and typically used in 20 µl reactions according to manufacturer's instructions. Plasmids used to transform into *C. albicans* were used in 30 µl reactions for higher transformation efficiency. Enzyme reactions were incubated at 37 °C for a minimum of 2 hours with gentle agitation before visualisation on a 1 % agarose gel to check if restriction had proceeded to completion and estimate concentration. For downstream reactions other than transformations, the enzyme was inactivated at 65 °C for 20 minutes.

Dephosphorylation of Vector DNA

To reduce re-ligation of linearised plasmid vector, 5' phosphate groups were removed using Antarctic Phosphatase (AP) enzyme (NEB). 1-5 µg of linearised vector was used along with AP buffer (NEB) to a final concentration of 1X and 2 µl (10 units) of AP enzyme. The reaction mixture was incubated at 37 °C for 30 minutes before inactivation of the enzyme at 65 °C for 15 minutes. After inactivation, the mixture was subjected to a Qiagen© PCR purification kit according to manufacturer's instructions to yield pure, linearised DNA.

Purification of DNA fragments from agarose gels and PCR products

DNA to be purified from restriction endonuclease reactions was separated on a 1 % agarose gel before being cut out and purified by QIAquick Gel Extraction Kit (Qiagen©) according to manufacturer's instructions.

DNA from PCR reactions to be sequenced was purified by Qiagen© PCR purification kit according to manufacturer's instructions.

Ligation of DNA fragments

After preparation of vector (de-phosphorylation) and insert fragments, they were mixed together in molar ratios of 1:1, 1:3 and 1:5 respectively, with 30 ng of vector being used. Each ligation was performed in a final volume of 10 µl with 1 µl (400 units) of T4 DNA ligase (NEB) and 1 µl 10X T4 Buffer. Reactions were left at room temperature overnight before 1 µl and 5 µl of each was transformed into *E. coli.* Plasmids were recovered from single colonies

via dirty miniprep (see Preparation of plasmid DNA) nd subjected to an endonuclease reaction to test for correct orientation of insert.

Site directed mutagenesis

Site directed mutagenesis was carried out using the Agilent QuickChange Multi Site-Directed Mutagenesis kit. Primers were designed with the Stratagene primer design program (Agilent technologies: www.genomics.agilent.com/primerDesignProgram). 50 ng of plasmid DNA to be mutated was subjected to a PCR reaction and Dpn1 treatment according to manufacturer's instructions before transformation into the XL10-Gold Ultracompetent cells provided.

Mutated plasmids we recovered from single colonies by Mini-prep kit (see Preparation of plasmid DNA) and sent to be sequenced by Sheffield University's Core Genomic Facility.

2.6 Protein techniques

RIPA buffer

RIPA buffer used for protein extractions contains: 50 mM Tris-HCl pH 7.2, 0.1 % TritonX-100, 0.1 % sodium deoxycholate, 150 mM NaCl. EDTA-free protease inhibitor cocktail (Roche) was added to RIPA buffer according to manufacturer's instructions. When protein extractions were used to look for phosphorylation, phosphatase inhibitor cocktail III (Roche) was also added to the buffer according to manufacturer's instructions.

Protein extraction of *C. albicans*

From an overnight culture of *C. albicans,* 2.5 ml was inoculated into 47.5 ml pre-warmed YEPD (or Met3 ON-OFF media if required) prepared to induce the relevant morphology and incubated at the relevant temperature for the required amount of time. After incubation, cells were harvested by centrifugation at 4,000 rpm for 1 minute. Supernatant was discarded and the pellet re-suspended in 1 ml of chilled, sterilised distilled water before being transferred to a 1.5 ml screw-top microfuge tube. Cells were pelleted again at 13,000 rpm for 15 seconds, supernatant was discarded and the pellet kept on ice. The pellet was re-

suspended in up to 250 µl of the relevant RIPA buffer (chilled) depending on pellet size and roughly the same amount of chilled, sterilised glass beads was added. Proteins were extracted using a Mini-Beadbeater-16 (Biospec) or FastPrep®24 cell disrupter (MP Biomedical). For the FastPrep® cell disrupter, the machine head was pre-cooled by using 50g of dry-ice and setting the machine to 6.0 m/s for 10 seconds. Samples were then subjected to 3 x 4.0 m/s for 30 seconds with 10 seconds on ice in between. Alternatively, samples were subjected to 3x 30 second bursts with 1 minute on ice in between on the Mini-Beadbeater-16 machine. Samples were then subjected to centrifugation at 4°C, 11,000 rpm for 6 minutes to separate cell lysate from debris. The lysate was transferred to a fresh tube and centrifuged again at 11,000 rpm for 15 seconds before supernatant was again transferred to a fresh tube. Protein concentration was calculated using a Bradford assay (see below). If the total cell lysate was to be analysed, 5X protein loading dye (250mM Tris pH 6.8, 10% SDS, 30% glycerol, 20% β-mercaptoethanol, 0.02% Bromo Phenol Blue,) was added to the sample to a final concentration of 1X and samples boiled for 5 minutes before storage at -80°C if not being used immediately. Otherwise samples were subjected to purification by immuno-precipitation.

Measurement of Protein concentration using the Bradford Assay

Protein samples were diluted 1/50 in RIPA buffer and 20 µl of the resulting solution added to 1 ml Protein Assay Dye (Biorad), vortexed and left to equilibrate for 5 minutes. Optical density (OD) of the sample was measure at OD_{595}. Similarly, solutions with known concentrations of bovine serum albumin (BSA) were also measured in the same manner to provide a standard curve of protein concentration versus optical density. Protein concentrations of samples could then be estimated from this standard curve.

Inhibition of Cdc28-as1 by 1NM-PP1

An overnight culture of the Cdc28-as1 strain was re-inoculated 1/20 into fresh media with a final concentration of 25 µM 1NM-PP1 (Merck Calbiocehm®) and grown for two hours.

De-phosphorylation of protein samples by Lambda phosphatase

Protein samples were prepared with RIPA buffer in the absence of phosphatase inhibitors. 10 µl $MgCl_2$, 10 µl PMP buffer (NEB) and 1 µl (400 units) lambda phosphatase (NEB) was added to 2 mg protein sample in a final volume of 100 µl and incubated at 37°C for 1 hour.

Immuno-precipitation of epitope tagged proteins using Novex ® Protein G magnetic Dynabeads®

Dynabeads® were prepared and bound with 7.5 µg of the relevant antibody according to manufacturer's instructions. A total cell lysate with 2 mg ml^{-1} of protein and 50 µl magnetic beads were incubated at 4 °C, rolling, for 1 hour. Beads and lysate were then separated with a magnet and the beads washed 3 times with 200 µl RIPA buffer. Antibody and bound target proteins were eluted in 50 µl 1X protein loading dye by boiling for 5 minutes and the supernatant stored at -80 °C.

Purification of GST tagged proteins from *E. coli*

An overnight culture of GST plasmid containing strain was diluted 1:100 into 400ml fresh LB media plus ampicillin and incubated at 37°C until an OD_{600} of 0.6 was reached. Isopropyl β-D-1-thiogalactopyranoside (IPTG) was then added to a final concentration of 1mM to induce protein expression and further incubated for 3 hours at 37°C. Cells were pelleted at 4,500 rpm for 10 minutes, resuspended in ice-cold PBS (137 mM NaCl, 2.7 mM KCl, 10 mM Na_2HPO_4, 1.8 mM KH_2PO_4), pelleted again at 4,000 rpm for 10 minutes and placed at -80°C for 1 hour. The cell pellet was re-suspended in 15 ml lysis buffer (50 ml PBS plus 1 protease inhibitor tablet (Roche)) and sonicated for 5x 30 seconds with 1 minute on ice in between. Triton X-100 (Sigma) was added to a final concentration of 1% and incubated at 4°C, rolling for 30 minutes before centrifugation at 15,000 rpm for 30 minutes. The supernatant was added to a fresh tube with 400 µl Glutathione sepharose 4B beads (GE Healthcare) and incubated at 4°C, rolling, for 2 hours. The whole sample was then applied to a poly-prep chromatography column (Biorad) and lysate allowed to run through before washing with 2 ml PBS 3 times. Protein was eluted by sealing the column, addition of 500 µl elution buffer (20 mM reduced glutathione (Sigma), 20 mM Tris-HCl pH 8, 100 mM NaCl, 10 % glycerol)

and incubating at 4°C, rolling, for 30 minutes before allowing the elution to run through the column. The elution step was repeated twice.

Cdc28 *in-vitro* kinase assay using phospho(Ser)-CDK antibodies

Kinase assay was carried out as described in (Bishop et al., 2010). Cdc28-HA was immuno-precipitated as stated above from total cell lysates as using modified RIPA buffer (50mM Tris HCl pH 7.2, 0.1% sodium deoxycholate, 0.1% Triton X-100, 50mM sodium fluoride, 0.2 mM Sodium orthophosphate, 0.2mM β-glycerol phosphate and 1x complete protease inhibitor cocktail (Roche)) and the protein left bound to the magnetic beads. The beads were then washed twice with 750 mM NaCl, once with 150 mM NaCl and once with 50 mM Tris-HCl pH 7.5. A *BWP17* lysate was also used as a negative control. 10 µg substrate polypeptide, prepared as (see Purification of GST tagged proteins from E. coli), were added to the beads along with 5X kinase buffer (50 mM Tris-HCl pH 7.5, 10mM EGTA pH 8, 0.1 % tween, 1 mM DTT, 1mM β-Glycerol phosphate, 200 µm ATP) to a final concentration of 1X. One control was carried out without ATP. The final mix of beads, substrate and buffer were incubated for 1 hour at 37 °C, shaking, before boiling in 1X Protein loading Dye for elution. Samples were run on an SDS-PAGE gel, transferred to PVDF membrane (GE Healthcare) and probed with rabbit anti-phospho(Ser)-CDK (Cell-Signalling) antibody. Membranes were then stripped (see Stripping of PVDF membrane) and re-probed with anti-GST antibody.

Cbk1 *In-vitro* kinase assay using ^{32}P-ATP

Radioactive kinase assay was performed using a modified protocol from (Jansen et al., 2006). Total cell lysate was prepared using lysis buffer (40 mM Tris [pH 8.0], 150 mM NaCl, 25 mM NaF, 1 mM PMSF and 1x protease inhibitor cocktail III (Roche)) and a cell disrupter (Constant Systems). Cbk1-Myc was immuno-precipitated using EZview agarose beads (Sigma Aldrich) according to manufacturer's instructions before being washed once with lysis buffer, 3 times with wash buffer (40 mM Tris pH 8.0, 500 mM NaCl) and once with kinase buffer (20 mM Tris pH 8.0, 150 mM NaCl and 5 mM $MnCl_2$). Beads were then incubated with 30 µl kinase buffer, 10 µg substrate polypeptide, 20 µm ATP and 10 µCi γ-^{32}P-ATP for one hour at room temperature. The reaction was stopped by adding 7 µl 5x loading buffer and boiling for 3 minutes. Samples were then separated by SDS-PAGE, the gel then stained with Instant Blue Coomassie (Expedeon) and dried on blotting paper.

Phosphorylation was then visualised using Kodak Phosphor screens which were scanned using a Personal FX phosphoimager (Bio-Rad)

Sodium-dodecyl sulphate polyacrylamide gel electrophoresis (SDS-PAGE)

Percentage of acrylamide in gel	Range of separation (kDa)
15	10-43
12	12-60
10	20-80
7.5	36-94
5.0	57-212

Resolving gel	6 %	8 %	10 %	12 %	14 %
SDW (ml)	6.1	5.7	5.3	4.9	4.5
Prosieve 50 (acrylamide) (ml)	1.2	1.6	2.0	2.4	2.8
1.5 M Tris-HCl, pH 8.8 (ml)	2.5	2.5	2.5	2.5	2.5
10% SDS (ml)	0.1	0.1	0.1	0.1	0.1
10% Ammonium persulphate (ml)	0.1	0.1	0.1	0.1	0.1
TEMED (µl)	4	4	4	4	4

Stacking gel (5%)	Volume
SDW (ml)	3.1
Prosieve 50 (acrylamide) (ml)	0.5
0.5 M Tris-HCl, pH 6.8 (ml)	1.3
10% SDS (µl)	50
10% Ammonium persulphate (µl)	50
TEMED (µl)	5

Once the gel had set, the comb was removed, wells washed out and tank filled with 1X running buffer: 125 mM Tris-base, 460 mM glycine, 0.5 % SDS. Once samples were loaded, empty lanes were loaded with 1X protein loading dye to prevent smiling of the gel. Gels were run first at 90 V for around 15 minutes until samples were pulled through the stacking gel into the resolving one. The voltage was then increased to 140 V and gels run until the relevant size standards were resolved.

Proteins were transferred from the gel to a nitrocellulose membrane (Hybond-C) using the Mini-Trans blot cell (BioRad). Transfer Buffer (125 mM Tris-base, 460 mM glycine, 20 % methanol) was cooled at -80°C briefly and 4 pieces of Whatman filter paper, 1 piece of membrane and 2 fibre pads were soaked in it. A sandwich was then prepared, consisting of 1 fibre pad laid on the black side of a transfer cassette, followed by 2x Whatman paper and then the smoothed protein gel. The membrane was then laid on top, air bubbles removed and 2x Whatman paper laid on top followed by the last fibre pad. The cassette was closed and immersed in cooled transfer buffer in the tank system with the gel to the anode, before being run at 150 mA for 90 minutes per gel.

After, protein transfer was checked by staining the membrane with Ponceau S solution (Sigma-Aldrich) and then washing with distilled water.

For the In-Vitro kinase assay, proteins were transferred to PVDF membrane (GE Healthcare) which requires activation in 100 % methanol for 30 seconds and equilibration in transfer buffer for 15 minutes before transfer takes place.

Western blotting

Western blotting block buffer consists of 2.5 g of milk powder (Sigma-Aldrich) dissolved in 50ml Tris-buffered saline with Tween20-TBS-T (2.44 % Tris-HCl, 8 % NaCl, pH7.6, 0.1% Tween-20). After protein transfer, membranes were blocked in a falcon tube with 10 ml milk and incubated at 4°C, rolling for 90 minutes to overnight. The blocking milk was discarded before 10 ml of milk with a 1:3000 dilution of primary antibody was added and incubated at 4°C, rolling for 90 minutes to overnight. This milk was then discarded and the blot washed in 10ml TBS-T for 15 minutes and then twice more for 5 minutes, rolling all the time. 10 ml of milk with a 1:3000 dilution of secondary antibody with HRP conjugated was then added and incubated at 4°C, rolling for no longer than 1 hour. The membrane was again washed with TBS-T, once for 15 minutes then four more times for 5 minutes each, rolling all the time. Western blots were visualised using Amersham^{TM} ECL Advance (GE Healthcare) or laboratory- made ECL, depending on strength of signal required. For the commercial ECL, 200 µl solution A was mixed with 200 µl solution B, pipetted onto a glass plate and the blot laid protein side down on top of the solution for 4 minutes, being turned 90° halfway through. For laboratory made ECL, 1 ml solution 1 (100 mM Tris-HCl pH 8.5, 2.5 mM Luminol, 0.4 mM p-coumaric acid) and 1ml solution 2 (100 mM Tris-HCl pH 8.5, 0.0006 % H_2O_2) was incubated with the membrane at 4 °C, rolling for 4 minutes. Blots were imaged using a GenGnome (Syngene) western blot visualiser.

Stripping of PVDF membrane

The PVDF membrane was incubated in stripping buffer (20 ml SDS 10%, 12.5 ml Tris HCl pH 6.8 0.5M, 67.5 ml MilliQ water, 0.8 ml β-mercaptoethanol) for 1 hour at 37 °C, rolling. The membrane was then washed 5 times in distilled water, 4 times in TBS-T for 15 minutes rolling, before re-probing.

Elutriation of *C. albicans* cells

Elutriation of *C. albicans* cells was carried out using a Beckman JE 5.0 elutriation rotor. The strain in question was grown to stationary phase in liquid YPD before re-inoculation into 1 L fresh YPD to a dilution of 1:10,000. Cells were then grown overnight at 30 °C and the OD_{600} read to ensure that cells were still in logarithmic growth phase (between 0.4-0.6). The culture was then sonicated briefly to aid separation of daughter cells.

The rotor was set up in a centrifuge and all air bubbles removed via flow through of SDW (sterilised deionised water) at 200 ml/min and centrifugation at 1000 rpm. Once set up the rpm was increased to 4200 and flow-rate set to 60 ml/min. The culture was added to the elutriator via the input pipe until the chamber had filled with cells at which point the input was switched back to SDW. The rotor was left to spin at 4200 rpm for 5-10 minutes in order that the cells form a density gradient. The rotor was then lowered to 4100 rpm so that cells could migrate towards the output pipe. 100ml fractions were collected and checked to ensure only small, unbudded cells were being collected. The centrifuge was slowed at 100 rpm at a time down to 3800 rpm to ensure all un-budded cells were extracted. The collected cells were then concentrated and re-inoculated into fresh YPD for time-course experiments.

2.7 Microscopy

Formaldehyde fixing of cells.

To fix cells for differential interference contrast (DIC) microscopy, 40 µl 37% formalydehyde (Sigma-Aldrich) was added to 1ml of cell culture and mixed gently by inversion before incubation at room temperature for 15 minutes. Cells were pelleted by centrifugation for 15 seconds, 13,000 rpm, washed in PBS (137 mM NaCl, 2.7 mM KCl, 10 mM Na_2HPO_4, 1.8 mM KH_2PO_4), pelleted again and re-suspended in PBS and kept at 4°C until visualised on a Leica DIC microscope.

Ethanol fixing of cells

Cultured cells were first pelleted by centrifugation for 15 seconds, 13,000 rpm, before being fixed in 70% ethanol. The cells were then kept at 4°C until they were visualised, when they were pelleted and re-suspended in PBS.

Staining cells with Aniline Blue

An overnight culture of *C. albicans* was diluted 1/20 into fresh YPD media and grown for the required length of time. 1 ml of the resulting culture was then pelleted and washed twice in PBS (137 mM NaCl, 2.7 mM KCl, 10 mM Na_2HPO_4, 1.8 mM KH_2PO_4) before re-suspension in PBS plus aniline blue stain to a final concentration of 0.05%. Cells were visualised as described below with the CFP filter.

DAPI staining

Fixed cell were suspended in PBS and mixed with 4',6-diamidino-2-phenylindole (DAPI) to a final concentration of 0.002 mg/ml and incubated for 5 minutes at room temperature. They were then visualised as described below with the DAPI filter.

Florescence microscopy

Fluorescence microscopy imaging was performed on a Delta Vision Spectris 4.0 microscope with Softworx™ 3.2.2 software (Applied Precision Instruments). The microscope had a hood that was heated to the relevant temperature for the morphology being examined. The FITC filter (ex 494 nm, em 518 nm) was used to visualise YFP or GFP, CFP (ex 436 nm, em 465 nm) filter for Aniline blue and DAPI filter (ex 358 nm, em 461 nm) for DAPI stained cells. Z-stack images were taken of cells and deconvolved using the Softworx™ programme; sum projections of multiple Z-planes are used in the text.

DIC microscopy

DIC microscopy was performed on a Leica microscope (model; 0202-519-508L). Images were captured using HC Image live software (Hamamatsu).

2.8 *C. albicans* strains used in this study

Strain name	Genotype	Reference
BWP17	*ura3::λimm434/ ura3::λimm434his1::hisG/ his1::hisG arg4::hisG/arg4::hisG*	(Wilson et al., 1999)
lrg1ΔΔ	*BWP17 lrg1::URA3/ lrg1::HIS1*	This study
pMAL2-GFP-RHO1	*BWP17* HIS1:pMAL2-GFP-RHO1	(Caballero-Lima et al., 2013)
pMAL2-GFP-RHO1/lrg1ΔΔ	*BWP17* HIS1:pMAL2-GFP-RHO1/ *lrg1::URA3/ lrg1::HIS1*	This study
lrg1Δ/pMET3-LRG1/EXO84-GFP	*BWP17 lrg1::ARG4/ URA3:pMet3-LRG1/EXO84-GFP-HIS1*	This study
lrg1Δ/pMAL2-GFP-LRG1(993-4404)	*BWP17 lrg1::ARG4/ HIS1:pMAL2-GFP-LRG1(993-4404)*	This study
lrg1Δ/pMAL2-GFP-LRG1	*BWP17 lrg1::ARG4/ HIS1:pMAL2-GFP-LRG1*	This study
GFP-RID	*BWP17 RP10::ARG4-pACT1GFPRID*	This study- produced with plasmid from: (Corvest et al., 2013)
lrg1ΔΔ/GFP-RID	*BWP17 lrg1::URA3/ lrg1::HIS1/RP10::ARG4-pACT1GFPRID*	This study- produced with plasmid from:(Corvest et al., 2013)
LRG1-MYC	*BWP17 LRG1-5xMYC-URA3*	This study
CDC28-1as	*BWP17 CDC28-1as:URA3/ cdc28::HIS1*	(Bishop et al., 2010)
LRG1-MYC/CDC28-1as	*BWP17 LRG1-5xMYC-ARG4 CDC28-1as:URA3/ cdc28::HIS1*	This study
CDC28-HA/CDC28-HA	*BWP17 CDC28-HA-URA3/CDC28-HA-ARG4*	(Caballero-Lima et al., 2013)
pMET3-CLN3	*BWP17 cln*3Δ::*ARG4/URA3-MET3*	(Chapa y Lazo et al., 2005)
pMET3-CLB2	*clb2::HIS1/*P_{MET3}*-CLB2:URA3*	(Bensen et al., 2005)
pMET3-CLB4	*clb4::ARG4/*P_{MET3}*-CLB4:URA3*	(Bensen et al., 2005)

pMET3-CLN3/LRG1-MYC	*BWP17 cln*3Δ*::ARG4/URA3-MET3/LRG1-MYC-HIS1*	This study
pMET3-CLB2/LRG1-MYC	*clb2::HIS1/*P_{MET3}*-CLB2:URA3/LRG1-MYC-ARG4*	This study
pMET3-CLB4/LRG1-MYC	*clb4::ARG4/*P_{MET3}*-CLB4:URA3/LRG1-MYC-HIS1*	This study
lrg1ΔΔ/LRG1-MYC	*BWP17 lrg1::ARG4/ lrg1::HIS1/LRG1-6xMYC-URA3*	This study
lrg1ΔΔ/LRG1(2E2D$_{CDC28}$*)-MYC*	*BWP17 lrg1::ARG4/ lrg1::HIS1/LRG1(*T7E, S65D, T273E, S319D*)-6xMYC-URA3*	This study
lrg1ΔΔ/LRG1(4A$_{CDC28}$*)-MYC*	*BWP17 lrg1::ARG4/ lrg1::HIS1/LRG1(*T7A, S65A, T273A, S319A*)-6xMYC-URA3*	This study
lrg1ΔΔ (URA$^-$*, ARG*$^-$*)*	*BWP17 lrg1::FRT / lrg1::HIS1*	This study
lrg1ΔΔ/LRG1(2E2D$_{CDC28}$*)-MYC/GFP-RID*	*BWP17 lrg1::ARG4/ lrg1::HIS1/LRG1(*T7E, S65D, T273E, S319D*)-6xMYC-URA3/RP10::ARG4-pACT1GFPRID*	This study- produced with plasmid from:(Corvest et al., 2013)
lrg1ΔΔ/LRG1(4A$_{CDC28}$*)-MYC/GFP-RID*	*BWP17 lrg1::ARG4/ lrg1::HIS1/LRG1(*T7A, S65A, T273A, S319A*)-6xMYC-URA3/ RP10::ARG4-pACT1GFPRID*	This study- produced with plasmid from:(Corvest et al., 2013)
CBK1-MYC	*BWP17 CBK1-MYC-URA3*	Caballero-Lima, D. University of Sheffield
cbk1ΔΔ	*BWP17 cbk1::HIS1/cbk1::ARG4*	This study
Cbk1ΔΔ/LRG1-MYC	*BWP17 cbk1::HIS1/cbk1::ARG4/LRG1-MYC-URA3*	This study
lrg1ΔΔ/LRG1(2E2D$_{CBK1}$*)-MYC*	*BWP17 lrg1::ARG4/ lrg1::HIS1/LRG1(S80D, T623E, S1009D, 1059E)-6xMYC-URA3*	This study
lrg1ΔΔ/LRG1(4A$_{CBK1}$*)-MYC*	*BWP17 lrg1::ARG4/ lrg1::HIS1/LRG1(S80A, T623A, S1009A, 1059A)-6xMYC-URA3*	This study
lrg1ΔΔ/LRG1(15E$_{CDC28}$*)-MYC*	*BWP17 lrg1::ARG4/ lrg1::HIS1/LRG1* (T7E, S65D, T273E, S319D, S36D, S50D, S120D, S125D, T127E, T129E, S173D, S195D, S271D, T503E,T1067E)*-6xMYC-URA3*	This study

2.9 *E. coli* strains used in this study

Strain Name	Genotype	Reference
BL-21	*E. coli* B F-, ompT, hsdS (rB-, mB-), gal, dcm	G.E. Life Sciences
DH5α	F-, *supE*44, ΔlacU169 (80lacZΔM15), hsdR17, recA1, endA1, gyrA96, thi-1, relA1	Delta Biotechnology

2.10 Plasmids used in this study

Plasmid	Description	Reference
pCIP10-LRG1-MYC-URA	Contains *CaLRG1* tagged with *6xMYC* flanked by 600 bp *LRG1* promoter and 300 bp *LRG1 3'* UTR. Used for re-integration of *LRG1* into its native promoter.	Greig, J. University of Sheffield
pCIP10-LRG1(2E2D$_{CDC28}$)-MYC-URA	As *pCIP10-LRG1-MYC-URA,* with mutations to produce phospho-mimetic residues in the four full Cdc28 motifs	This study
pCIP10-LRG1(2E2D$_{CBK1}$)-MYC-URA	As *pCIP10-LRG1-MYC-URA,* with mutations to produce phospho-mimetic residues in the four Cbk1 motifs.	This study
pCIP10-LRG1(4A$_{CDC28}$)-MYC-URA	As *pCIP10-LRG1-MYC-URA,* with mutations to produce non-phosphorylatable residues in the four full Cdc28 motifs.	This study
pCIP10-LRG1(4A$_{CBK1}$)-MYC-URA	As *pCIP10-LRG1-MYC-URA,* with mutations to produce non-phosphorylatable residues in the four Cbk1 motifs	This study
pExpArg-pACT1GFPRID	Contains the *GFP-RID* reporter under control of the *ACT1* promoter. Integrates into the *CIP10* locus.	(Corvest et al., 2013)
pBKs-FKH2-URAF	*C. albicans* Ura Flipper selectable marker flanked by 5' and 3' *FKH2* fragments.	Greig, J. PhD thesis, University of Sheffield, 2014
pBKs-LRG1-URAF	As *pBKs-FKH2-URAF* with *FKH2* fragments replaced with *KpnI-LRG1(5')-XhoI* and *NotI- LRG1(3')-SacII.*	This study
pGEX-4T1	N-terminal GST tagging and expression vector.	G.E. Life Sciences

GST-LRG1(NT)	Contains the first 990 bp of *C. albicans LRG1* cloned into the multiple cloning site of *pGEX-4T1* with *BamHI* and *XhoI*.	This study
GST-LRG1-4A(NT)	As *GST-LRG1(NT)* with mutations to produce non-phosphorylatable residues in the four full Cdc28 motifs.	This study
pFa-URA3	Used to produce a deletion cassette with the *URA3* gene.	(Gola et al., 2003)
pFa-HIS1	Used to produce a deletion cassette with the *HIS1* gene.	(Gola et al., 2003)
pFa-ARG4	Used to produce a deletion cassette with the *ARG4* gene.	(Gola et al., 2003)
pFA-HIS1-MAL2p-GFP	Produces a transformation cassette for N-terminal tagging of *LRG1(* full length and N-terminal deletion) with GFP and under the control of the regulatable *MAL2* promoter.	(Schaub et al., 2006)
pFA-URA3-MET3p	Generates a PCR product in order to place *LRG1* under the control of the *MET3* promoter.	(Gola et al., 2003)
pFa-MYC-URA3	Produced a C-terminal tagging cassette to tag *LRG1* with 5x*MYC.*	(Lavoie et al., 2008)

2.11 Oligonucleotides used in this study

Purpose	Name	Sequence
LRG1 deletion	Lrg1-del-F	TTTGATTTTGTTTATTATTTGTTTTACTGGGTTT TGTTTTGTGATTTTGATTTTTGACAGTTTAATA ACGAAGCTTCGTACGCTGCAGGTC
	Lrg1-del-R	TATACATATAAAAGAAAAGAATACGGGGGAA AAAAAAGGAATGATTGGCAATTCTTTATTAAT TTCTGTTCTGATATCATCGATGAATTCGAG
LRG1 deletion check	Lrg1-del-F-Check	GTCTTCCTCCTCCTAACTAA
ARG4 check	R-Arg4	AATGGATCAGTGGACCGGTG
HIS1 check	Reverse His1	
LRG1 internal check	Lrg1-F1	GCAGTTTCCCCGACCCCGG

	Lrg1-R1	AGACACCAAATGGAACCCGGT
Placing *LRG1* under the *MET3* promoter	Lrg1-Met3-S1	TTGCCAAGAAGTATCTTTAAGAGGTATATTGA TTCTAACCCTGTATTGATCAAAACAAACATCTA GATCGAAGCTTCGTACGCTGCAGGTC
	Lrg1-Met3-S2	TGCATTAGGGTTGCCAAATGAATGGTGTATACT ATTACCTCGTTGAGGGGTATCAAACGAATGCT TCATCATGTTTTCTGGGGAGGGTATTTAC
Checking *MET3* promoter	Met3-F	TATGCGATTGTGGCTCATAGTAACG
	Lrg1-R2	ATTGAGTTGCTGAATCTTGT
C-terminal tagging of Exo84 with GFP	S1-Exo84-XFP	ACAATTGGAAGAATTAAAACTGGTGGGATTAAA TGTTGATTATATATTTGAGTCTATATTAAATCTT GAAGGTCGACGGATCCCCGGGTT
	S2-Exo84-XFP	GATTGGAGCAGGTGTTTTATTTAGTATTATTGC TGGGATATTATTGGTTTCTTCATTGGTTTTGTTA TATTCGATGAATTCGAGCTCGTT
Checking *EXO84-GFP*	G1-Exo84	CGTCATGGTGATGTTGATTC
	GFP-R1	ATTTGTGCCCATTAACATCA
N-terminal Lrg1 tagging with *GFP*	Lrg1-Nterm-GFP-F	TTGCCAAGAAGTATCTTTAAGAGGTATATTGAT TCTAACCCTGTATTGATCAAAACAAACATCTAG ATCAGCACCTGCGCCAGCCCCTGCGC
	Lrg1-Nterm-GFP-R	TGCATTAGGGTTGCCAAATGAATGGTGTATACT ATTACCTCGTTGAGGGGTATCAAACGAATGCTT CATAGCACCTGCGCCAGCCCCTGCGC
Deleting the first 990 bp of *LRG1*	Lrg1-Nterm-del- F	TTTGATTTTGTTTATTATTTGTTTTACTGGGTTTT GTTTTGTGATTTTGATTTTTGACAGTTTAATAAC GAAGCTTCGTACGCTGCAGGTC
	Lrg1-Nterm-del-R	ATTTAAAGCTCGAACAAACTGACTGGTGATTTCC AATCCACATTTGGCACAAACTTTACGACTTTTCT TAGCACCTGCGCCAGCCCCTGCGC
Checking *GFP-LRG1*	GFP-seq3	AATACTCCAATTGGCGATGGCCCTG
	Lrg1-R1	AGACACCAAATGGAACCCGGT
Checking *GFP-LRG1(991-4404)*	Lrg1-R3	GTTTTCGTGCCATCTTGTTC
C-terminal tagging Lrg1 with Myc	Lrg1-TAP-MYC-F	AAACGAAACTCTGTTTCTCGAATTGAATCCAAA ATCCAAAATAGAGAATTAAATGGTATTAGTGA GAGAGGTCGACGGATCCCCGGGTTAGAACAGA

		AGCTTATATCCGAA
	Lrg1-TAP-HA-MYC-R	GCTTGAAAAAAAATTAGTCGTGTGGTGTTTAAC ACTATTGATGGTTTAGATTAAGCAGAGTTTTGC TTC TCGATGAATTCGAGCTCGTT
Checking *LRG1-MYC*	Myc-R	GTATACATGCATTTACTTATAATGGCGCGC
	Lrg1-F3	AGCTGACAAGGCAAGAAAGG
Amplification of *LRG1* 1-330 for cloning into GST vector	L GST BamHI Fwd	CGCGGATCC ATGAAGCATTCGTTTGATACC
	L GST XhoI Rev	CCG CTCGAGCTTACGACCTGG TTTCCTTTC
Amplification of *LRG1 5'* and 3' fragments for the *URAF* plasmid	Lrg1-UraF-s1-KpnI	CGGGGTACCAACCAAGAAAAGAAAAACAAT
	Lrg1-UraF-s2-XhoI	CCGCTCGAGGTTATTAAACTGTCAAAAAT
	Lrg1-UraF-s3-NotI	AAGGAAAAAAGCGGCCGCACAGAAATTAATAA AGAATT
	Lrg1-UraF-s4-SacII	TCCCCGCGGTAAACCCCTTTTGAGTAAAT
Deletion of *CBK1*	Cbk1-del-F	CTCAATTCAACAAGTTTGAACTTTTGTATCA ATCAAAAAGAAACGATTCATTTTTTGACAA GTGTGTCCTGAAGCTTCGTACGCTGCAGGTC
	Cbk1-del-R	TGGCAACTATCAAAGATAATGCATAAACAAT AACATCATCCGGCTGTACTACCATTCCAAATG ACCACCTTCTGATATCATCGATGAATTCGAG
Checking *CBK1* deletion	Cbk1-del-check-F	CAACACACTCAAAATCAACACG
CBK1 internal primers	Cbk1-F1	CCAGTTCAACAACATCCACA
	Pfa-cbk1-seq-r1	GGAACCTTCAAACACTCATT
Deletion of *CBK1* via 500 bp homology	Cbk1-s1	GAAGCTTCGTACGCTGCAGGTCAAGATCTATAA AACTCTATT
	Cbk1-s2	TCTGATATCATCGATGAATTCGAGTAGTGTGG TACGAGTAGAAC
	Cbk1-s3	GACATTTTCTCAAAACAGGC
	Cbk1-s4	TTCTACACTTCAAAGCAATT
Checking *CBK1* deletion with 500bp	Cbk1-pst1-F	ATTAGCCTGCAGAAGCTTTACAATTTTAATAG

Mutagenesis of Cdc28 motifs	T7A	AACATGAAGCATTCGTTTGATGCCCCTCAACG AGGTAATAGTA
	T7E	AACATGAAGCATTCGTTTGATGAACCTCAACG AGGTAATAGTATA
	S65A	CCCCTCAAAGACTCAGGTTCAGCTCCTAGACGA AAATTCAATCCA
	S65D	CCCCTCAAAGACTCAGGTTCAGATCCTAGACGA AAATTCAATCCA
	T273A	CATTCAATAGCAGTTTCCCCGGCCCCGGAAAA ACAAGATTCAGCA
	T273E	CATTCAATAGCAGTTTCCCCGGAACCGGAAAA ACAAGATTCAGCA
	S319A	CAACAACAACAAGAACCATCAGCACCTTCAAA ACTGGAAAGGAAA
	S319D	CAACAACAACAAGAACCATCAGATCCTTCAAA ACTGGAAAGGAAA
	S36A	ATCGACAATAAATATTGTTGAAGCTCCCGACA ATAGAGGATCAATAA
	S36D	ATCGACA ATAAATATTG TTGAAGATCCCGACAATAGAGGATC AATAA
	S50A	TAGCTACAACTGAACCATCA GCACCGCCGCCA CCACAACA ACCCC
	S50D	TAGCTACAACTGAACCATCAGATCCGCCGCCA CCACAACA ACCCC
	S120A,S125A,T127A,T129A	TTCACAATCAATGCATCCATCTGCGCCAGTTC CTT CTGCACCTGCACCTGCACCAGCACCAGCA CCTACAACCA
	S120D,S125D,T127E,T129E	TTCACAATCAATGCATCCATCTGATCCAGTTCC TT CTGATCCTGAACCTGAACCAGCACCAGCAC CTACAACCA
	T156A,T160A,S173A	GCTAAGATACTATATACCCCGAGATGCCCCACC ACAAGCC CCACCAATGAGTCAACTTCCGAAAC CTGTG GGGAAAGCGC CCCAACCTAATTGGAC AAACT
	T156E,T160E,S173D	GCTAAGATACTATATACCCCGAGATGAGCCACCA

		CAAGAG CCACCAATGAGTCAACTTCCGAAACCTG TGGGGAAAGATC CCCAACCTAATTGGACAAACT
	S195A	CCATCATATAATGCTCCTGATAGTTTTCAGCAACA GA
	S195D	CCATCATATAATGATCCTGATAGTTTTCAGCAACA GA
	S223A	ATTTTGGCACTGAACCAATA ATATCGGCACCAGA ACTGTC GTCAAGGCAAC
	S223D	ATTTTGGCACTGAACCAATAATATCGGATCCAGA ACTGTC GTCAAGGCAAC
	S271A	GACCCTTCTCAAAGACATTCAATAGCAGTTGCCCCG GCCC CGGAAAAACAAGATTCAGCAACTC
	S271D	GACCCTTCTCAAAGACATTCAATAGCAGTTGACCC GGAAC CGGAAAAACAAGATTCAGCAACTC
	T503A	TAAATTTTGGAACGTTTGTATTGCTCCAGATTCAGT TGGTCTCCAAA
	T503E	GGT CATACTTCTACTGTTATTGAACCAACTGGTGT ATTGGATA ATA
	T1067A	GGTCATACTTCTACTGTTATTGCCCCAACTGGTGT ATTGGATA ATA
	T1067E	GGTCATACTTCTACTGTTATTGAACCAACTGGTGT ATTGGATA ATA
	S1230A	CAAATCA ATAAAAATCC CTTGAAAGCACCTGAT TTTA GTATTCAGAATGCTG
	S1230D	CAAATCAATAAAAATCCCTTGAAAGATCCTGATT TTAGTATTCAGAATGCTG
Mutagenesis of Cbk1 motifs	S80A	TTGGACATTCTCGTTCCCATGCTCATACTTCTAAT AACGG
	S80D	CCATTTGGACATTCTCGTTCCCATGATCATACTTC TAATAACGGCAAACGA
	T623A	GTTATTGCATAAAAAGTTTGGTGCTCCTCCTAATA AGGATGACCT
	T623E	AAAAGTTCACATGAGTTATTGCATAAAAAGTTTG GTGAGCCTCCTAATAAGGATGACC
	S1009A	CACAAATACTCATCTTGATAGAACAGCTGATTTGT TAAAGAATGAGAAATC
	S1009E	GGCAAACCACAAATACTCATCTTGATAGAACAGA TGATTTGTTAAAGAATGAGAAATCATTAACTTT

	T1059A	CTCACCGACTCAAAGCTGCTGGTCATACTTCTACT
	T1059E	CTGCTCCTCACCGACTCAAAGCTGAGGGTCATA CTTCTACTGTTAT
Sequencing of Lrg1	FS1	GCATCAAATACAACTCGATCG
	FS2	CAGCAACAGAAACAGAATAAACTAATC
	FS3	CAAGTGGCATTATGTGAATATG
	FS4	GTGCAAAAGTTCACATGAGTT
	FS5	GTAATTCATCAATCGATTGTTTG
	FS6	GATGAGAACCTTTCGGTAACC
	FS7	GGTATTGATTCAGATTTAGGTGTAGG
	FS8	GCACCTAACATATTAATTTCCAA
	Lrg1-F6	GGATATTCTTGAGTTTTACG
	Lrg1-R2	ATTGAGTTGCTGAATCTTGT

3 Lrg1 controls polarised growth in *C. albicans*

3.1 Introduction

3.1.1 The Lrg1 protein

The *S. cerevisiae* Lrg1 protein is a GTPase activating protein (GAP) for the GTPase Rho1. Rho1 is the central member of the cell wall integrity pathway (CWI), responsible for transducing signals based on external or internal stress cues to gene expression and cell wall remodelling proteins. The CWI pathway's main outputs are: the formins Bni1 and Bnr1, the exocyst component responsible for vesicle tethering at the plasma membrane Sec3, Skn7 and the β-1,3-glucan synthase (see chapter 1 and (Levin, 2011)). *S. cerevisiae* Lrg1 contains 3 LIM (protein-protein interaction) domains and a RhoGAP domain (Muller et al., 1994) and is required for cell fusion (Fitch et al., 2004). Lrg1 is also required for efficient cell separation and deletion mutants show increased invasiveness (Svarovsky and Palecek, 2005). The main role of the Lrg1 GAP is to negatively regulate the activity of Rho1 on the β1,3-glucan synthase, preventing new cell wall material from being made (Watanabe et al., 2001), although negative effects on the Pkc1 pathway have also been reported (Lorberg et al., 2001a). The CWI is largely conserved in *C. albicans* and on the Candida Genome Database (CGD), the open reading frame, orf19.7489, is annotated as *LRG1* based on its homology to the *S. cerevisiae* gene (61%), with 35.5% identity at the amino acid level. A detailed study of the hypothetical *C.albicans* Lrg1 protein will be discussed later in this chapter. Furthermore, in the filamentous fungi *Neurospora crassa,* Lrg1 is required for hyphal tip extension and prevention of excessive branch formation, indicating a divergence in function from that in *S. cerevisiae* (Vogt and Seiler, 2008b).

3.1.2 The exocyst is responsible for secretory vesicle docking

The exocyst is a multimeric protein complex comprised of eight subunits in S. *cerevisiae*: Sec3, Sec15, Sec5, Sec6, Sec8, Sec 19, Exo70 and Exo84 (TerBush et al., 1996). Sec3 and a pool of Exo70 localise to the plasma membrane independently of the actin cytoskeleton, whilst the remaining subunits are delivered to the plasma membrane on vesicles along actin

cables (Boyd et al., 2004). The role of the exocyst is to tether secretory vesicles containing the materials for cell growth to the plasma membrane when they arrive at sites of polarised growth. Once tethered, the vesicle and plasma membrane fuse.

Jones and Sudbery, 2010, localised the components of the exocyst in C*. albicans* and characterised their dynamics (Jones and Sudbery, 2010). They identified the *C. albicans* orthologues of *S. cerevisiae* Sec3, Sec6, Sec8, Exo70, and Exo84 proteins and showed that they localise to a surface crescent at the growing hyphal tip. Furthermore, in contrast to *S. cerevisiae*, they identified that exocyst components were not present on each vesicle arriving at the hyphal tip due to their moderate fluorescence recovery rates after photobleaching. Multiple members of the *C. albicans* exocyst have also been identified as being required for hyphal growth. Sec3 has been shown to be required for maintenance of hyphal growth after the formation of the first septin ring (Li et al., 2007). *S cerevisiae* Exo84 has been shown to be phosphorylated by Cdc28 and its cyclin Clb2*,* causing disassembly of the exocyst complex and hence inhibition of cell growth at the metaphase-anaphase transition (Luo et al., 2013). However, recent research has shown that during *C. albicans* hyphal growth, Exo84 is instead phosphorylated by Cdc28-Hgc1 (a hyphal-specific cyclin) and growth continues to occur throughout mitosis (Caballero-Lima and Sudbery, 2014). These observations suggest that the *C. albicans exocyst* has a large part to play in the highly polarised growth required during hyphal growth.

A recent study attempted to model the 3-dimensional characteristics of hyphal growth based on the localisation of key components (Caballero-Lima et al., 2013). The localisation of members of the exocyst, Rho1 and its positive regulator Rom2 were all determined and this data was used to model how a hyphal germ tube would grow based on the fact that β-1,3-glucan was being added in these locations. Interestingly, the study assumed that Rho1, and therefore the β-1,3-glucan synthase was always active at the hyphal tip because the crescent of its positive regulator Rom2 was broader than the crescent of Rho1. It has also been shown that active Rho1 is localised to sites of growth such as the yeast bud or hyphal tip and the eventual sites of septum formation in *C. albicans* (Corvest et al., 2013). However, it is still not known what regulation lies behind this re-localisation of Rho1 from the growing tip to the sites of septum formation and whether it is the location or activity of Rho1 that denotes where cell wall growth occurs.

3.1.3 The echinocandins forms a group of drugs targeting the β-1,3-glucan synthase

As described above, one target of the Rho1 GTPase in *C.albicans*, and for which it is a regulatory subunit, is the β-1,3-glucan synthase, encoded by *FKS1* or *FKS2*. The enzyme produces β-1,3-glucan chains from monomers of UDP-glucose (Beauvais et al., 1993) and is thought to extrude them out of the cell and into the cell wall structure (Kopecka and Kreger, 1986). Glucan polymers make up a large component of the cell wall and as such provide major structural integrity to the organism (Kollar et al., 1997). Due to the high structural integrity provided by this cell wall component, the glucan synthase is a major target for a group of anti-fungal drugs, the echinocandins, of which caspofungin is a synthetically produced member. This family of drugs work by non-competitive inhibition of the glucan synthase (Perlin, 2007), resulting in a lack of glucan production, a decrease in cell wall integrity and ultimately cell death. Due to this family of drugs being so important for clinical treatment of *C. albicans,* it is perhaps not surprising that mutations in the *FKS1* and *FKS2* genes (both naturally occurring and acquired) produce major resistance to drug therapy (Beyda et al., 2012).

3.1.4 Activity of Rho proteins can be measured with reporters containing the Rho-binding domain

As discussed earlier, Rho1 has many cellular targets. In mammalian cells, the serine/threonine kinase Rock1 is a target protein of the Rho1 homolog, RhoA, and has been shown to bind through a Rho-binding domain (Dvorsky et al., 2004; Fujisawa et al., 1996). This domain is known to only bind Rho1 when the GTPase itself is already bound to GTP and therefore active, which has been useful in detecting levels of active cellular RhoA via pull down-assays (Kimura et al., 2000). Similarly, in *S. cerevisiae,* the Pkc1 protein has also been shown to bind to Rho1-GTP through a domain also named Rho1-binding domain (Nonaka et al., 1995a) which has been used in pull-down assays to estimate the level of active Rho1 in the cell (Kono et al., 2008). The *S. cerevisiae* domain has been used to map the Rho1 binding domain on the *C. albicans* Pkc1 protein (Corvest et al., 2013) to a 265 amino acid region of the protein, assigned the Rho1 Interaction Domain (RID). Corvest *et al*, cloned this region into a plasmid with a promoter and C-terminal green fluorescent protein (GFP) tag.

Once integrated into the *C. albicans* genome, the GFP-RID construct would bind to active Rho1 (Rho1-GTP) and provide an *in vivo* reporter on the level and location of active-Rho1 that could be visualised via fluorescence microscopy. GFP-RID was confirmed as being a reporter of active Rho1 and had no deleterious effects on the growth of cells, despite effectively acting as a competitive inhibitor to other Rho1 binding proteins.

3.1.5 Aims of this chapter

This study sets out to try and characterise the *C. albicans* putative Rho1 GAP, Lrg1, and its role during polarised growth in *C. albicans*. The theoretical sequence of the protein will be analysed before phenotypic analysis of *LRG1* gene deletion. The effect on the localisation and activity of Rho1 will be analysed in cells lacking Lrg1 in an attempt to elucidate the regulatory role of the protein on Rho1. The localisation of other polarity components will also be examined in an *lrg1ΔΔ* strain. An *lrg1ΔΔ* strain will also be tested for sensitivity to the echinocandin, caspofungin.

3.2 Strain construction

3.2.1 Construction of an *lrg1ΔΔ* null strain

To determine the role of Lrg1 in *C. albicans* it was first decided to delete both copies of *LRG1* and assess the resulting cellular phenotype. Deletion of the two copies of the *LRG1* gene was performed in the *BWP17 (Wilson et al., 1999)* strain. The *BWP17* strain is auxotrophic for three amino acids: Arginine, Uridine and Histidine, and is made prototrophic for these markers by the addition of the *ARG4, URA3* or *HIS1* genes, respectively. All strains in this study use *BWP17* as the parental strain unless otherwise stated. *LRG1* was deleted via transformation of a PCR product containing the *ARG4* or *HIS1* marker and flanked by fragments of identity to the regions 5' and 3' of the *CaLRG1* gene. (figure3.1a). Transformants showing prototrophy for the relevant marker were tested for correct integration of the cassette with a PCR reaction (figure 3.1b). Once both markers had been shown to be integrated, forward and reverse *LRG1* internal primers were used to ensure no copy of the gene remained elsewhere in the genome (figure 3.1c) and an *lrg1ΔΔ* strain had been created.

3.2.2 Construction of a *MAL2-GFP-RHO1/lrg1ΔΔ* strain

During growth as yeast in wild-type *C. albicans*, active Rho1 has been shown to localise to sites of growth, i.e. the bud tip, cell cortex and the bud neck (Corvest et al., 2013). To assess whether Rho1 has a different localisation pattern in the absence of its regulator Lrg1, both copies of *LRG1* were deleted (as shown in figure 3.1) in a strain where Rho1 was already N-terminally epitope tagged with GFP (*HIS1- P_{MAL2}-GFP-RHO1) (Caballero-Lima et al., 2013)* to create a *P_{MAL2}-GFP-RHO1/lrg1ΔΔ* strain**.** As a GTPase, Rho1 must be N-terminally tagged in order not to disturb the CAAX box at the C-terminus required for prenylation. In performing the N-terminal tagging, the *RHO1* promoter would be disturbed, so the whole *GFP-RHO1* construct was placed under the control of the maltose regulatable *MAL2* promoter to ensure expression of the gene.

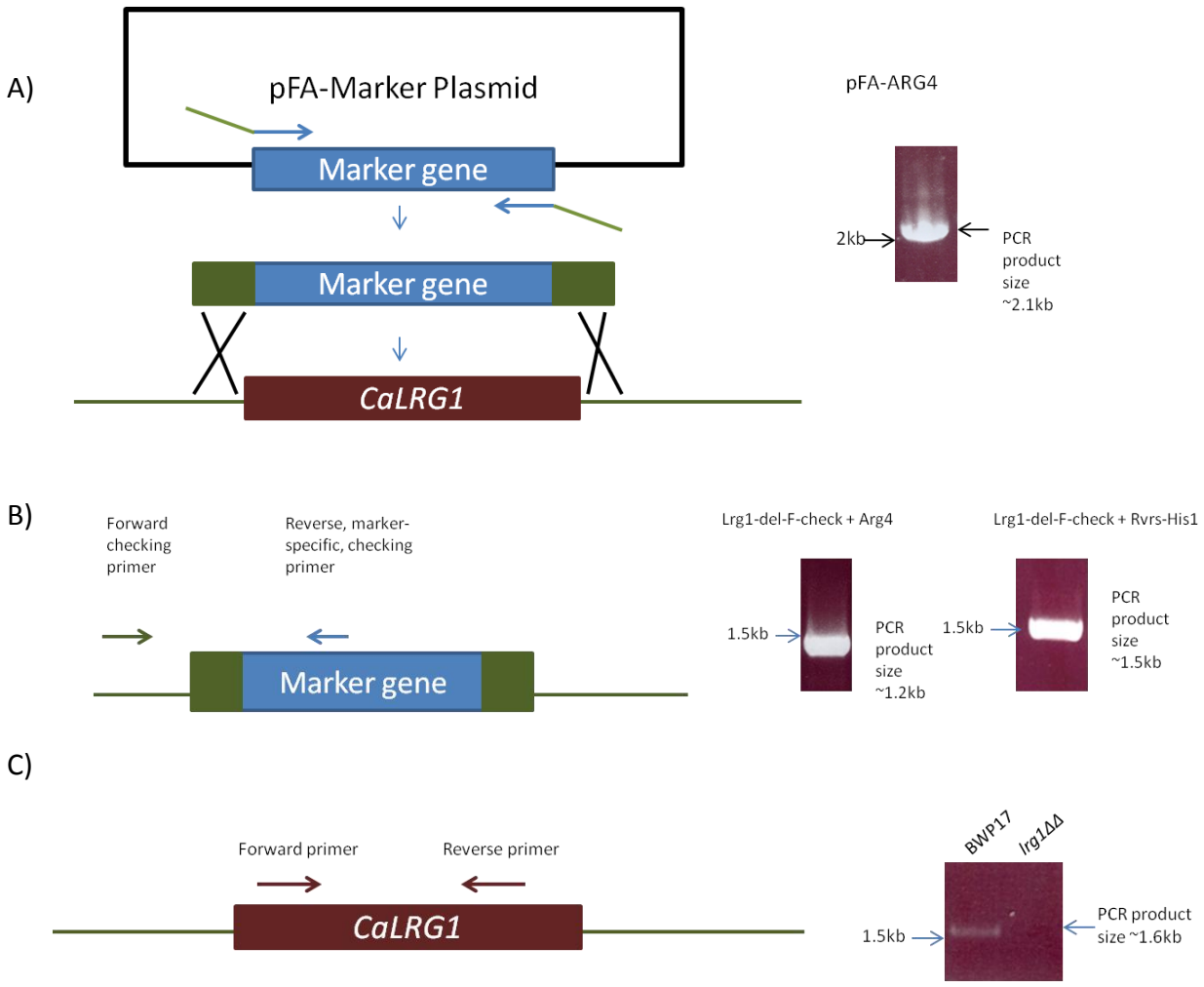

Figure 3.1 Strategy for deletion of the *LRG1* ORF in *C. albicans*

(A) The *lrg1-del-F* and *lrg1-del-R* primers amplify the pFA-ARG4/HIS1 plasmid to produce a cassette with a 5' segment identical to a region upstream of *LRG1* and a 3' segment identical to a region downstream of *LRG1*. Transformation of either cassette results in homologous recombination and therefore deletion of the ORF and prototrophy for that particular marker. 5 µl of each PCR reaction was visualised on a 1% agarose gel before transformation to ensure correct amplification. (B) Correct integration of the cassette into the genome was checked by PCR using a forward primer upstream of *LRG1*and a reverse primer in the marker gene sequence, followed by visualisation of the product on a 1% agarose gel. (C) Once both copies of *LRG1* had been deleted with two separate selectable markers, primers with homology to a sequence inside *LRG1* were used in PCR to ensure no copy of the gene remained elsewhere in the *C. albicans* genome.

3.2.3 Construction of P_{MET3} driven *LRG1* in an *EXO84-GFP* strain

Exo84 is a member of a multi-subunit complex known as the exocyst, responsible for tethering of secretory vesicles to the plasma membrane during polarised growth. It was of interest to investigate whether Rho1 regulates the relocation of the exocyst from the bud tip to the mother-bud neck. In order to investigate this issue, it was necessary to tag *EXO84* with a GFP epitope in a strain where *LRG1* was not present. One copy of *LRG1* was deleted in the *BWP17* parental strain whilst the other copy was placed under the control of the regulatable *MET3* promoter.

A regulatable promoter was used in order to follow the localisation of Exo84-GFP as the cells were depleted of Lrg1, instead of visualising cells that were already growing in the *lrg1ΔΔ* phenotype. However, in reality the Lrg1 protein was too stable and cells did not grow as the correct phenotype until around twenty hours after repression by methionine, therefore it was not possible to follow Exo84-GFP as Lrg1 was depleted. Instead the strain was used to view the localisation of Exo84 in cells that which P_{MET3}-*LRG1* was already fully repressed.

The first copy of *LRG1* was deleted as is shown in figure 3.1. To place the remaining copy of *LRG1* under a regulatable promoter, PCR was used to create a *URA3*- P_{MET3} cassette with identical regions at either end to the region directly upstream of *C. albicans LRG1* so that the *LRG1* promoter was replaced as shown in figure 3.2. This strain was then used to tag *EXO84* with *GFP* via a PCR generated *GFP-HIS1* cassette with identity at either end to the region directly downstream of *EXO84* as shown in 3.3. The resulting strain was named *lrg1Δ/* P_{MET3}*-LRG1/EXO84-GFP.*

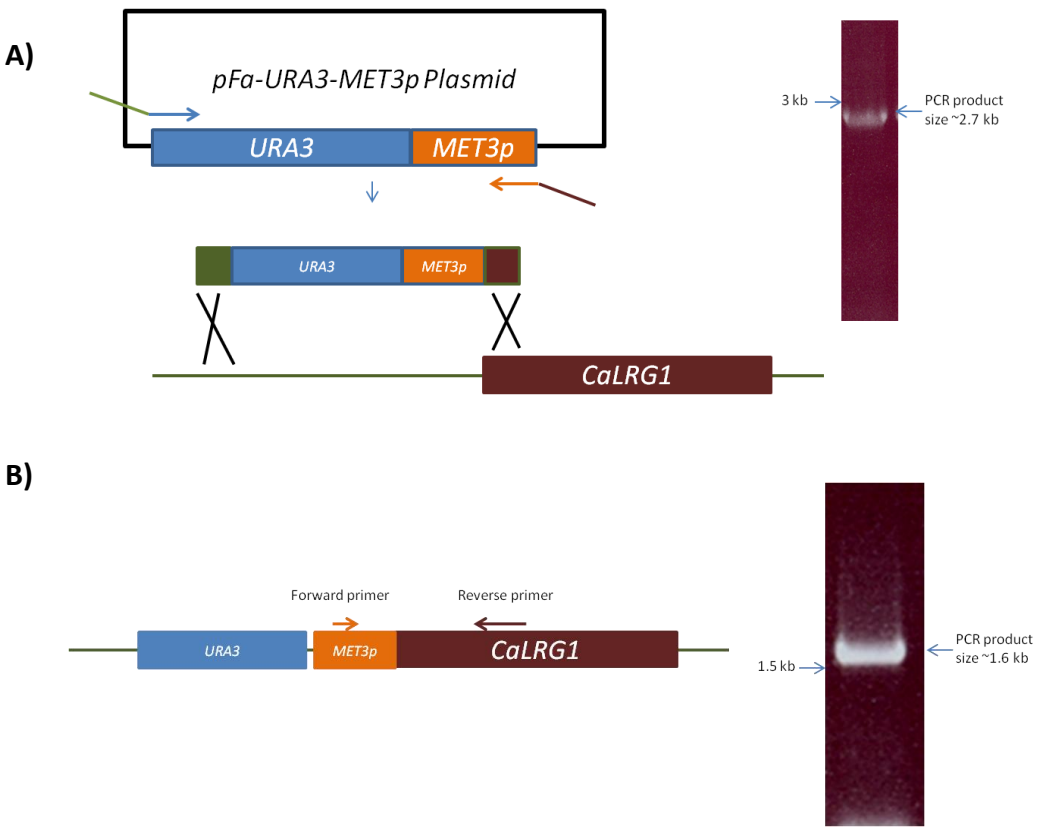

Figure 3.2 Construction of a P_{MET3} driven *LRG1*

(A) The *lrg1-Met3-F* and *lrg1-Met3-R* primers amplify *URA3*- P_{MET3} cassette with a 5' segment homologous to a region upstream of *LRG1* and a 3' segment homologous to the region at the start of *LRG1*, minus the ATG start codon. Transformation of either cassette results in homologous recombination to place a copy of the gene under control of the P_{MET3} promoter and autotrophy for uridine. A small amount of each cassette was visualised on a 1% agarose gel before transformation to ensure correct amplification. (B) Correct integration of the cassette into the genome was checked by PCR using a forward primer within P_{MET3} and a reverse primer in *LRG1* before visualisation on a 1% agarose gel.

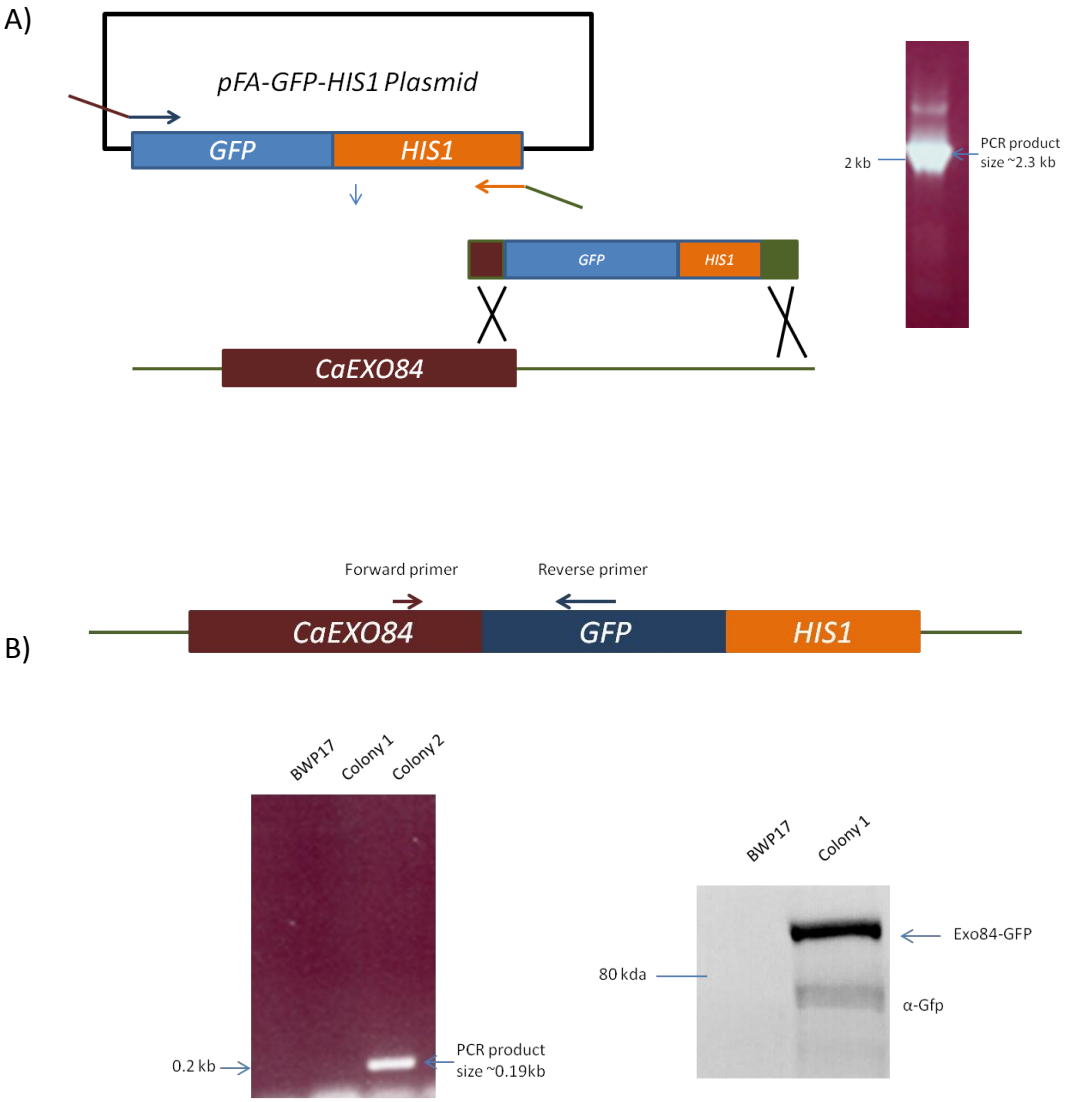

<u>Figure 3.3</u> C-terminal tagging of *EXO84* with *GFP-HIS1*

(A) The *pFA-GFP-HIS1* plasmid was used to amplify a cassette with 5' identity to the end of *EXO84* minus a stop codon and 3' identity to a region downstream of *EXO84.* Correct amplification was checked by visualisation of 1% agarose gel, followed by transformation in *C. albicans.* (B) Integration of the cassette was checked using a forward primer in *EXO84* and a reverse primer in *GFP*, before protein expression was detected by western blot.

3.2.4 Deletion of the *C. albicans* Lrg1 N-terminus

To further explore the role of the Lrg1 N-terminal extension seen in *Ca*Lrg1, the region of the gene encoding this part of the protein was deleted and the resulting phenotype assessed. It was necessary to replace the first 990 bp of *LRG1* with a prototrophic marker; however in doing so, the promoter region would be separated from the remainder of *LRG1.* This problem was overcome by replacing the region of the gene with a *HIS1-MAL2p-GFP* cassette as shown in figure 3.4, providing both a regulatable maltose promoter for gene expression and a GFP tag to visualise the truncated protein. To ensure that any phenotype seen was a result of the truncated protein only, the part gene deletion was performed in an *LRG1/lrg1Δ* heterozygote, meaning this was the only copy of *CaLRG1* present. To also make sure that the N-Terminal GFP tag on the Lrg1 protein did not cause any deleterious effects, the *HIS1-MAL2p-GFP* cassette was also placed in front of the full length *LRG1.* The resulting strains were named *lrg1Δ/* P_{MAL2}*-GFP-LRG1(993-4404)* and *lrg1Δ/*P_{MAL2}*-GFP-LRG1*.

A)

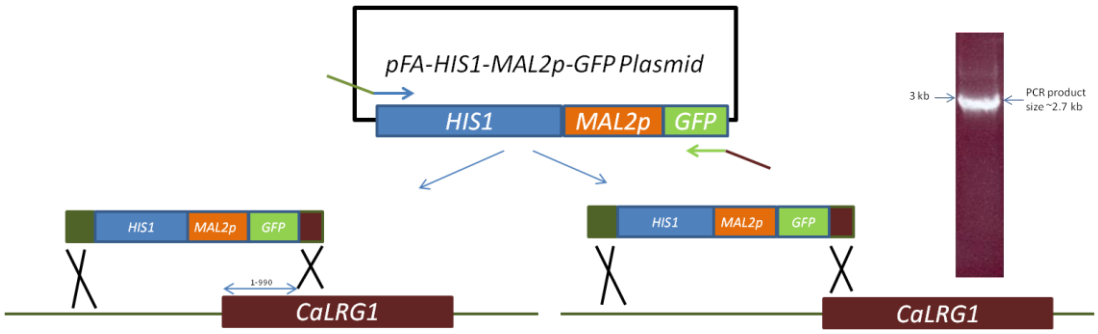

B)

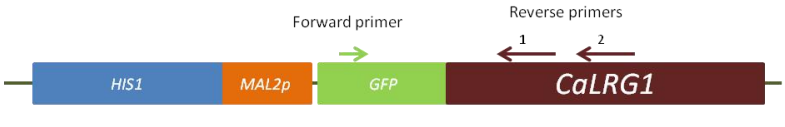

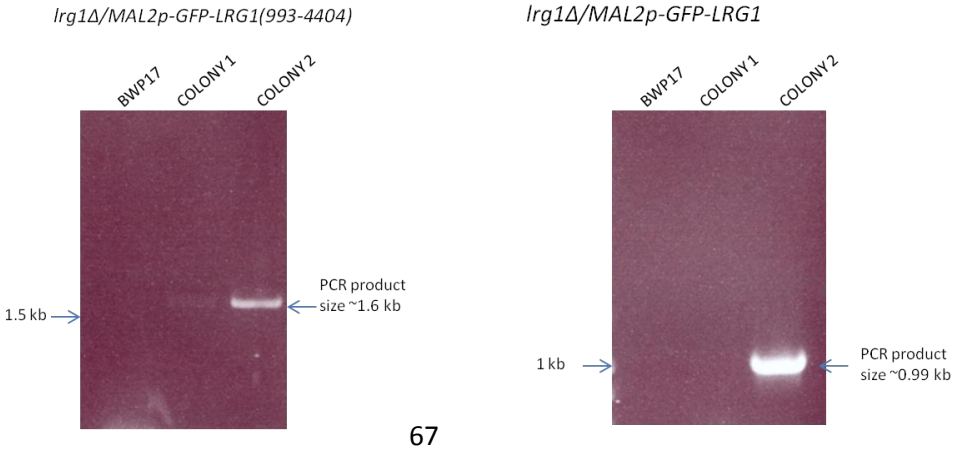

C)

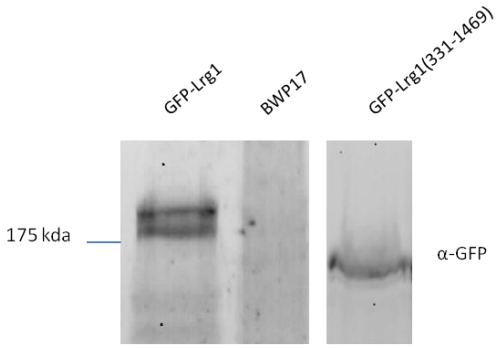

<u>Figure 3.4</u> Construction of N-terminally *GFP* tagged *LRG1* and an N-terminally *GFP* tagged *LRG1* lacking its N-terminal extension

A) The *pFA-HIS1- MAL2p-GFP* plasmid was used as a backbone to produce two separate transformation cassettes. Both had a 5' region homologous to a sequence upstream of *LRG1*, with one cassette having a 3' region homologous to the start of *LRG1* minus the ATG start codon, producing an N-terminally GFP-tagged *LRG1* under the control of the *MAL2* promoter after transformation and integration. The other cassette had 3' identity to a region of *LRG1* starting at 990 bases; this also produced an N-terminally *GFP*-tagged *LRG1* under the control of the *MAL2* promoter, but excluded the N-terminal extension. (B) Correct integration of either cassette was confirmed in a PCR reaction using forward primers in *GFP* and reverse primers in *LRG1*. The differing size products are attributed to differing primers being used. (C) Both the wild-type GFP-Lrg1 and GFP-Lrg1 N-terminal deletion were checked for correct protein expression by western blot.

3.3 Results

3.3.1 C. albicans Lrg1 contains an N-terminal extension that is absent from *S. cerevisiae* Lrg1.

A search of multiple protein databases using the NCBI Conserved Domain Database (CDD) (Marchler-Bauer et al., 2013) was performed on the *C. albicans* protein sequence, with results shown in (figure 3.5 top). The CDD search shows 4 major domains in the Lrg1 protein; 3 LIM domains (Zinc-finger domains responsible for protein-protein interactions (Dawid et al., 1998) and the RhoGAP domain at the C-terminus that provides the main function of the protein. These four domains are the same as those seen in the *S. cerevisiae* homolog of the Lrg1 protein. Interestingly, when the C*. albicans* Lrg1 homolog is aligned with the *S. cerevisiae* Lrg1 protein using the ExPASy SIM alignment tool (Huang and Miller, 1991) (figure 3.5 middle) the two align over almost the whole length of *Sc*Lrg1 with an identity of 41.54%. The LIM domains are highlighted in yellow with ~40% homology, and the RhoGAP domain at the C-terminus has ~50% homology. However, there is an N-terminal extension of 330 amino acids in *Ca*Lrg1 that is not present in *Sc*Lrg1. This N-terminal extension is only seen in the *Candida spp* and is not present in other fungi such as, *S. pombe, A. gossypii, A. nidulans, N.crassa, U. maydis* or *C. neoformans.* Furthermore, the CDD search of *Ca*Lrg1 does not identify any known domains in this N-terminal extension (figure 3.5 top). Additionally, using the IUPred web server (Dosztanyi et al., 2005) to predict regions of disorder of a protein based on free energy, it can be seen that the N-terminal extension seen in *C. albicans* Lrg1 is highly disordered up until the start of the first two LIM domains where the protein becomes globular (figure 3.5 bottom). Regions of disorder in a protein are potential areas for its regulation as they are free for other proteins to interact with. Due to this N-terminal extension gained by the *C. albicans* protein we speculated that Lrg1 had gained both extra function and regulation of function compared to the *S. cerevisiae* homolog.

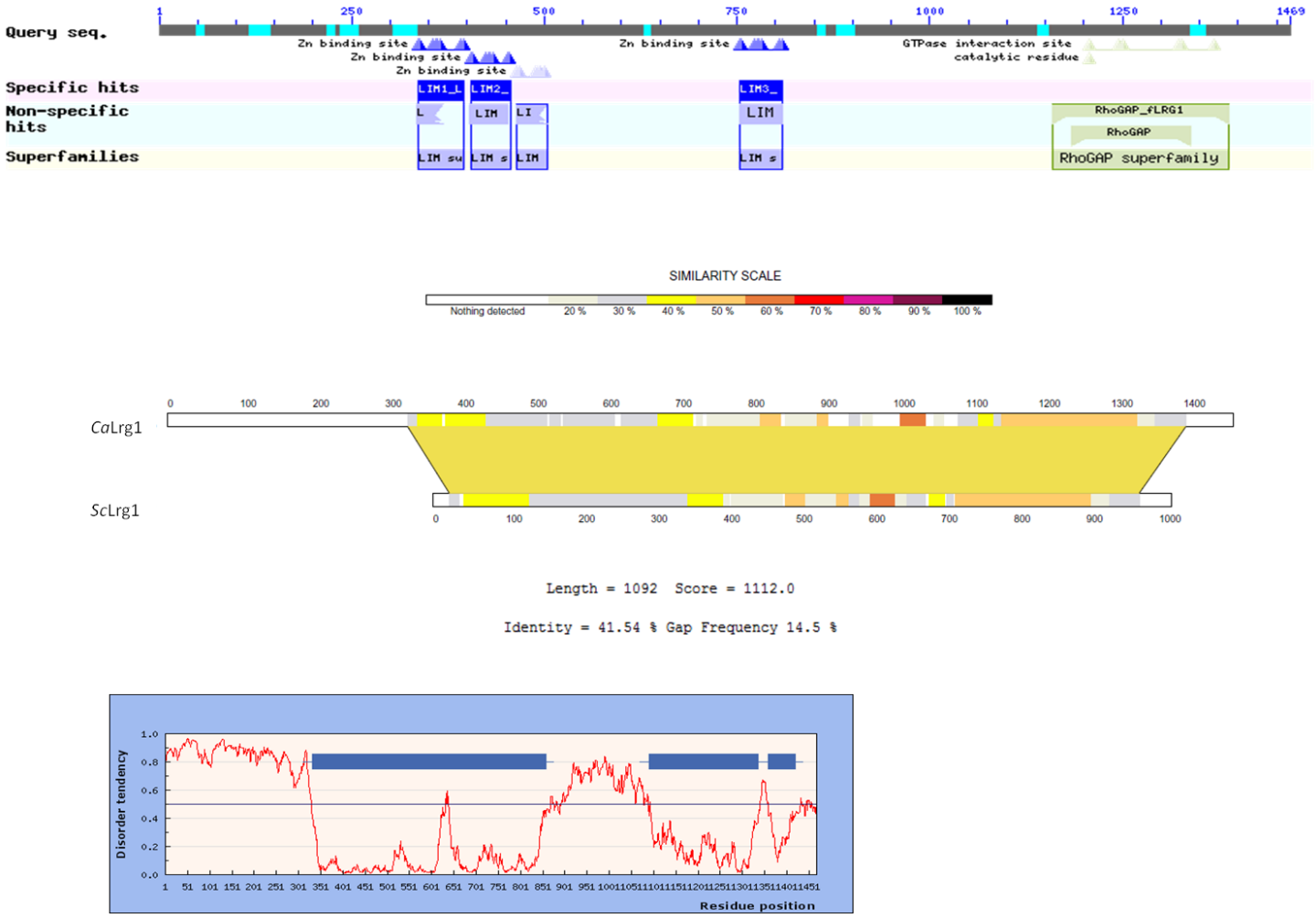

Figure 3.5 *Ca*Lrg1 contains a non-conserved N-terminal extension not seen in *S. cerevisiae* Lrg1

Top: An NCBI Conserved Domain Database (CDD) (Marchler-Bauer et al., 2013) analysis of *C. albicans* Lrg1 reveals conserved LIM and RhoGAP domains.

Middle: *Ca*Lrg1 and *Sc*Lrg1 were aligned using SIM from ExPASy (Huang and Miller, 1991), and visualised using the graphical viewer LALNVIEW (Duret et al., 1996), identifying a non-conserved N-terminal extension in *C. albicans* Lrg1. LIM domains are yellow, the RhoGAP domain is grey.

Bottom: Free energy prediction of *Ca*Lrg1 using IUPred (Dosztanyi et al., 2005) shows the N-terminal extension as highly disordered. Red line depicts disorder tendency and Blue boxes show predicted domains.

3.3.2 LRG1 is a negative regulator of polarised growth

In order to deduce the phenotype of the *lrg1ΔΔ* strain, an overnight culture was re-inoculated into both yeast (30°C, pH4) and hyphal (37°C, pH7, 20% calf serum) inducing conditions and grown for 3 hours and 90 minutes respectively. Cells were then fixed with formaldehyde before visualisation (figure 3.6). This was also performed with the parent strain- *BWP17*- as a control. When grown under yeast inducing conditions, the *lrg1ΔΔ* strain is highly polarised, growing with extremely elongated cells that fail to separate and show branching similar to the pseudohyphal morphology. To quantify the *lrg1ΔΔ* phenotype when grown as yeast, images of this and the *BWP17* strain were used to calculate the average length: width ratios of cells (figure 3.6). The calculated length: width ratios clearly show that the cells lacking *LRG1* are longer (4.884± .37) in comparison to the wild-type strain (1.384± .032), which is seen as statically significant when an un-paired t-test is performed.

When grown under hyphal-inducing conditions, cells still appear highly branched; however this could be a consequence of the overnight growth as yeast. In order to test whether the branched cells seen in cells grown as hyphae are actually from before the strain was induced, *lrg1ΔΔ* was induced to form hyphae and individual cells visualised every 30 minutes over a period of 210 minutes from stationary phase. An example of cells followed like this is shown in (figure 7.-top). Cell "A" has already formed the start of a yeast bud at the time of induction, however it goes on to form a germ tube and then a mature hyphal cell with parallel sides, showing that cells can grow as hyphae even when they lack *LRG1*. However, a germ tube emerges from cell "B" after 30 minutes and this continues to grow as normal hyphae with parallel sides up until around 150 minutes. At this point the cell wall appears to become increasingly thick and what appears to be a pointed tip forms within the cell a considerable distance from the outer hyphal tip. As time passes, growth appears to continue at the "inside" tip causing the hyphae to swell at this point. To further analyse this strange thick cell wall seen in cell "B", the *lrg1ΔΔ* strain was grown in hyphal-inducing conditions for 2 hours and then stained with aniline blue to visualise whether it is composed of β-1,3-glucan. Cells were then visualised by fluorescence microscopy and images are shown in figure 3.7 (bottom). It can be seen that in the cells that exhibit this "double" tip

phenotype, each tip shows a crescent of aniline blue corresponding to β-1,3-glucan but the space in between is not stained. This could indicate that the thick cell wall seen is not glucan and is chitin. However, there is also a possibility that the dye is unable to penetrate the thick cell wall.

The *lrg1ΔΔ* hyphal cells shown in the above time-course also appear to be extending slower than one would expect from a wild-type strain. To investigate this, fifteen cells of both the *BWP17* and *lrg1ΔΔ* strain were induced to form hyphae and visualised every 20 minutes for 140 minutes to follow germ tube extension. The average length of hyphae at each time point was calculated for each strain and is shown in figure 3.8. It can be seen that after 140 minutes, the average hyphal length for the *BWP17* strain is 27.1 ±2.3 µm, whilst the average length for the *lrg1ΔΔ* mutant is 7.8 ±2.3 µm, indicating a much slower rate of hyphal extension in this strain.

In conclusion, it can be said that cells lacking *LRG1* show unregulated polarised growth when grown in yeast-inducing conditions. When grown under hyphal-inducing conditions, *lrg1ΔΔ* hyphae grow at a much slower rate than would be expected in wild-type cells. However, in a small proportion of hyphae, growth appears to become un-regulated, resulting in a thick cell wall which isn't composed of glucan and swelling of the hyphal tube.

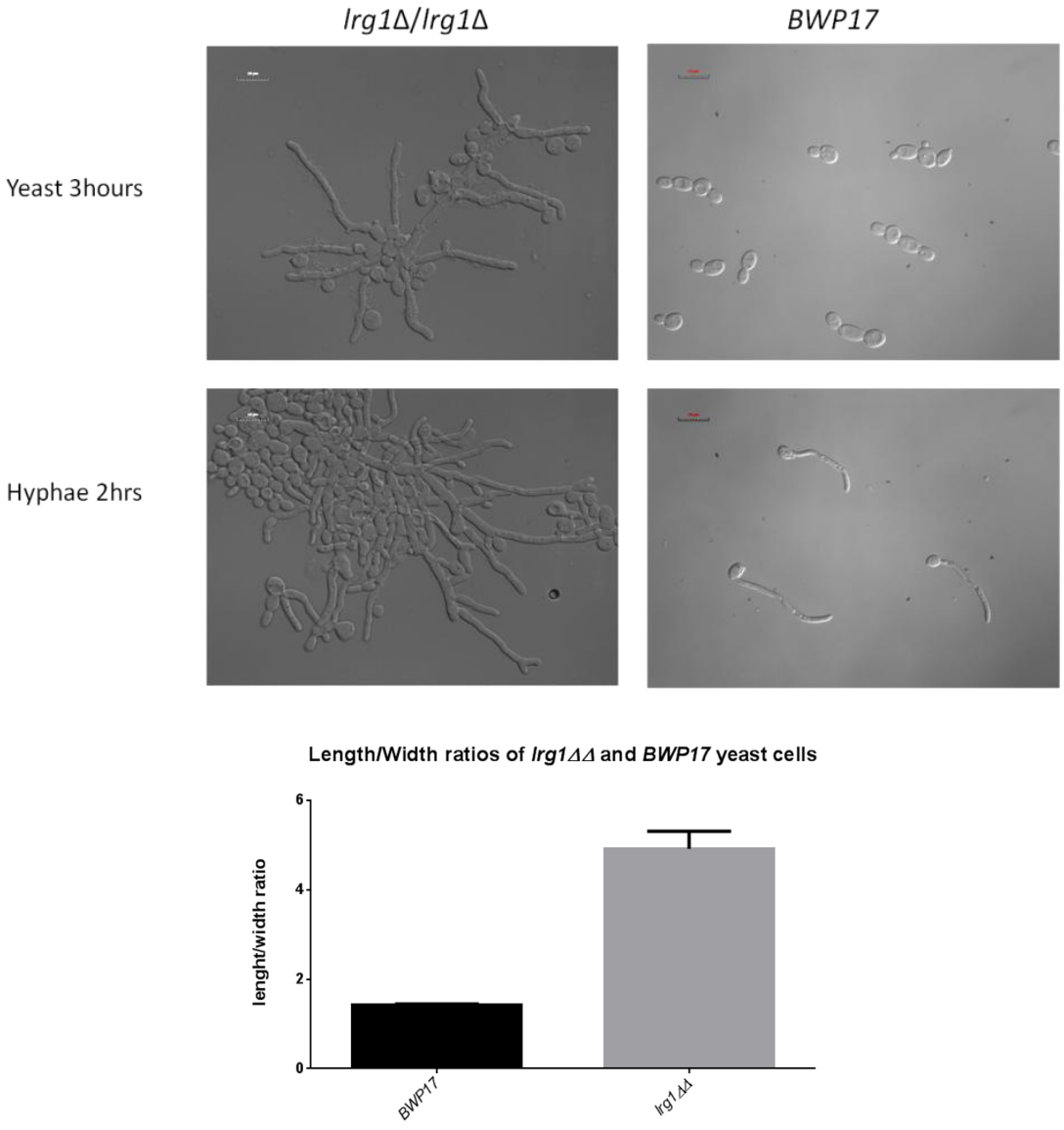

Figure 3.6 Lrg1 is required to negatively regulate polarised growth in *C. albicans*

Top: Overnight cultures of a wild-type *BWP17* (right panel) strain and the *lrg1ΔΔ* null strain (left panel) were re-inoculated into media to induce either the yeast (top) or hyphal (bottom) morphologies. Yeast were grown for 3 hours, Hyphae for 2 hours, before being fixed with formaldehyde and visualised on a Leica Differential Interference Contrast (DIC) Microscope. Scale bars represent 10 µm.

Bottom: The above images of cells grown as yeast were used to calculate the average length: width ratio of each strain. N=100 (*BWP17*), 60 (*lrg1ΔΔ*).

lrg1ΔΔ hyphal time-course

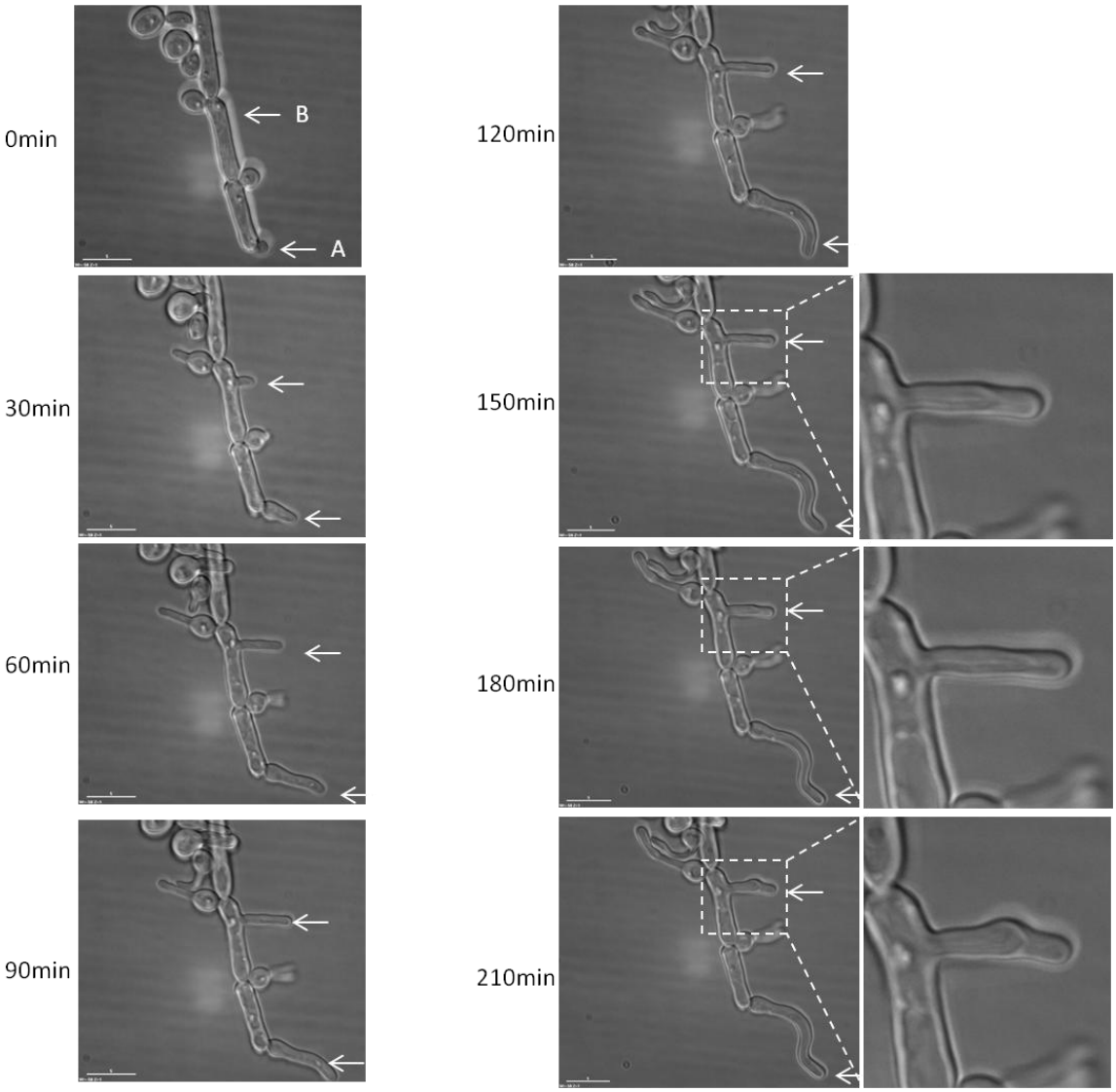

lrg1ΔΔ aniline stain, 2 hours after hyphal induction

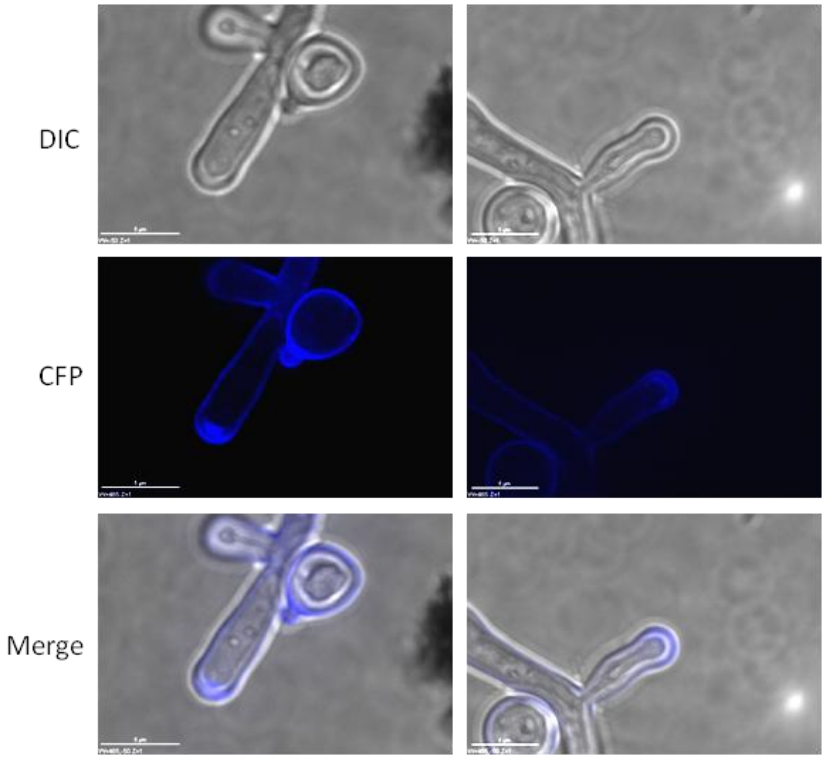

Figure 3.7 Growth of *lrg1ΔΔ* as hyphae

Top: *lrg1ΔΔ* cells were induced to form hyphae on agar pads embedded on microscope slides. Cells were imaged every 20 minutes from induction up until 210 minutes on a Delta Vision Spectris 4.0 microscope with Softworx™ 3.2.2 software (Applied Precision Instruments). Two cells can be seen, one that grows as a normal hyphae (A), albeit slower than one would expect, and one (B) that shows an unusual phenotype of a "double" tip with a thick cell wall. Scale bars represent 5 µm.

Bottom: *lrg1ΔΔ* cells were induced to form hyphae and grown for 2 hours before staining with aniline blue and hyphae with a "double tip" and thick cell wall imaged as above using the CFP filter.

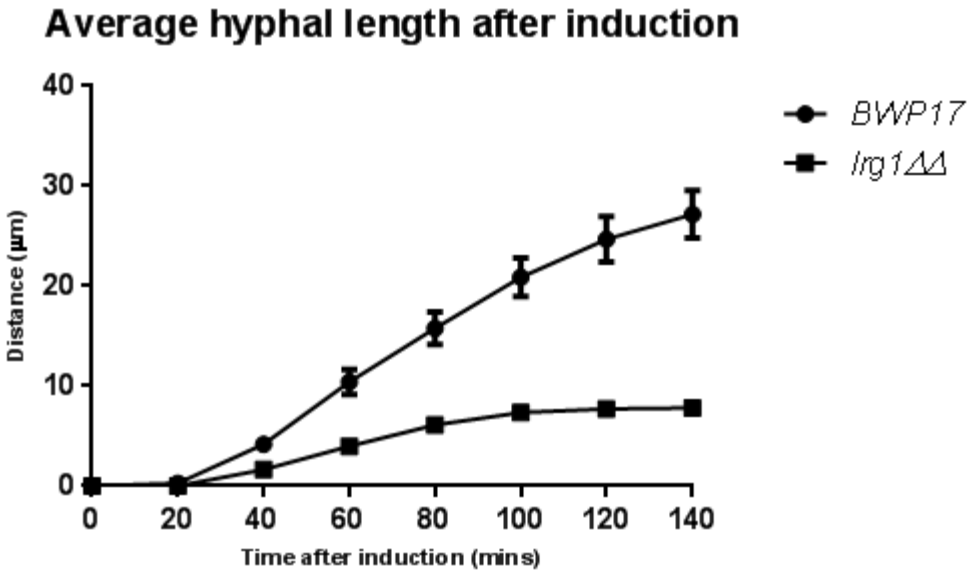

Figure 3.8 lrg1ΔΔ shows slower hyphal extension than the wild-type strain

BWP17 and *lrg1ΔΔ* cells were induced to form hyphae on agar pads and individual cells were visualised every 20 minutes for 140 minutes on a Delta Vision Spectris 4.0 microscope with Softworx™ 3.2.2 software (Applied Precision Instruments). The average hyphal length for each strain was then calculated at each time point. Error bars represent SEM and N=20.

3.3.3 Loss of *LRG1* results in an increase in invasiveness

Both the pseudohyphal and hyphal morphologies of *C. albicans* are known to be more invasive than the yeast morphology (Sudbery et al., 2004). To test whether the highly polarised nature of the *lrg1ΔΔ* strain is correlated with an increase in invasiveness of the cells, the strain was streaked onto YPD agar plates and incubated at 30 °C for 3 days. The resulting colonies were washed of the plate with water and gentle agitation, whilst any invasive cells would remain embedded in the matrix. As seen in figure 3.9, the majority of the cells in the *BWP17* control strain are washed off the agar matrix, with a small amount of cells, if any, observed where single colonies once grew. However, on the *lrg1ΔΔ* plate, a large majority of even the single colonies remain in the agar after washing. This shows that deletion of *LRG1* is associated with an increase in cell invasiveness.

3.3.4 Lrg1 localises to sites of polarised growth

It has been shown above that Lrg1 is a negative regulator of polarised growth, so it was of interest to deduce the cellular location of the protein to gain further insights into its function. A strain in which *LRG1* was C-terminally tagged with the green fluorescent protein (GFP) (Regan, H. Unpublished) was used. The *LRG1-GFP* strain was grown for 3 hours in yeast inducing conditions before visualisation on a fluorescence microscope. Images are shown in figure 3.10. It can be seen that in small buds, Lrg1-GFP localises to a crescent at the tip, whereas in larger cells, Lrg1-GFP localises to the site of septum formation. These are both sites of polarised growth and match the localisation pattern of Rho1 as one would expect due to its putative regulatory role on Rho1 in *C. albicans*.

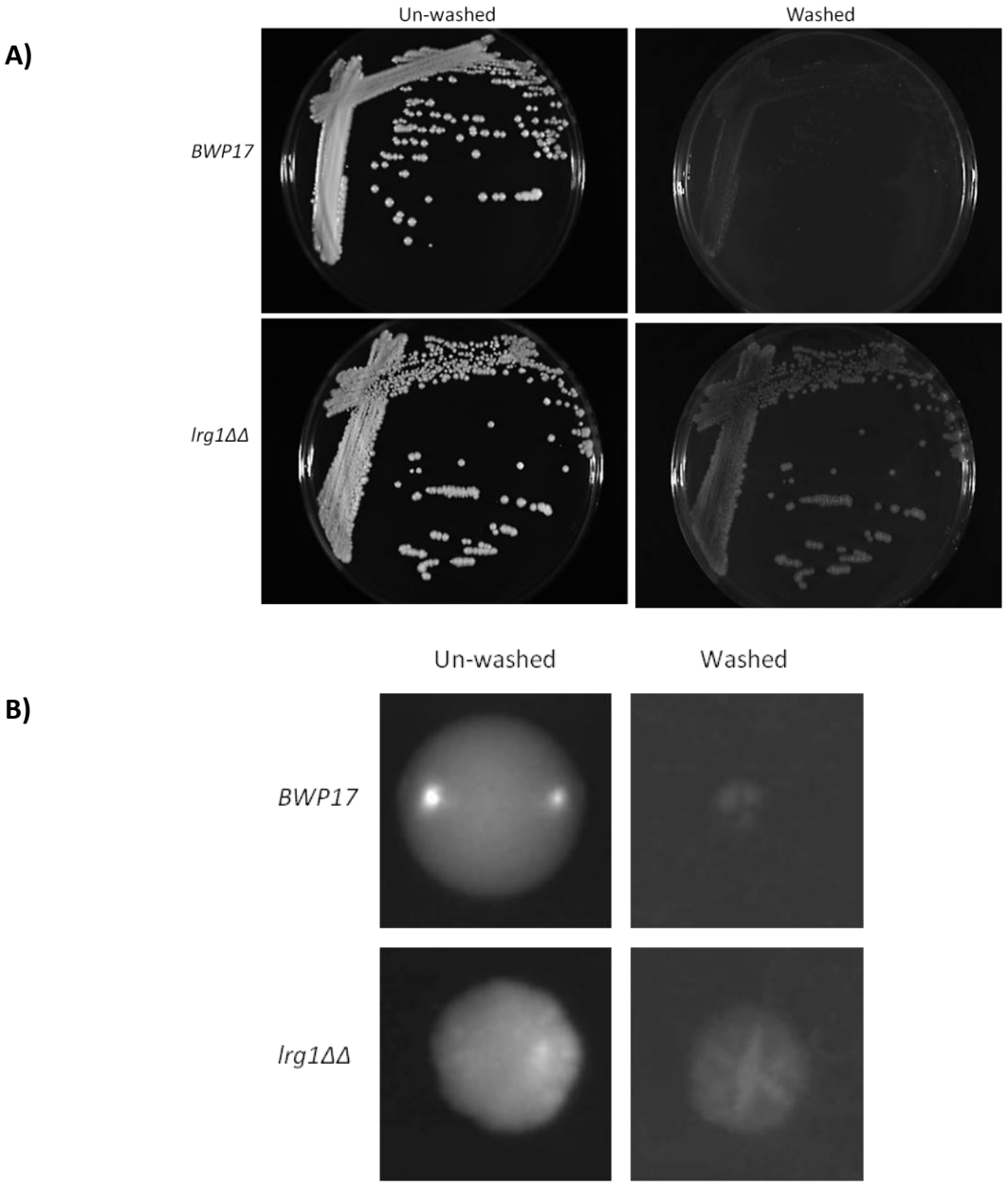

Figure 3.9 Loss of *LRG1* results in an increase in invasiveness

A) *BWP17(top)* and *lrg1ΔΔ (bottom)* cells were plated onto YPD agar plates to obtain single colonies. Plates after incubation for 3 days at 30°C are shown on the left panel. The plates were then washed using water and gentle agitation to remove any non-attached cell matter (right panel).

B) Zoomed images of single colonies from (A).

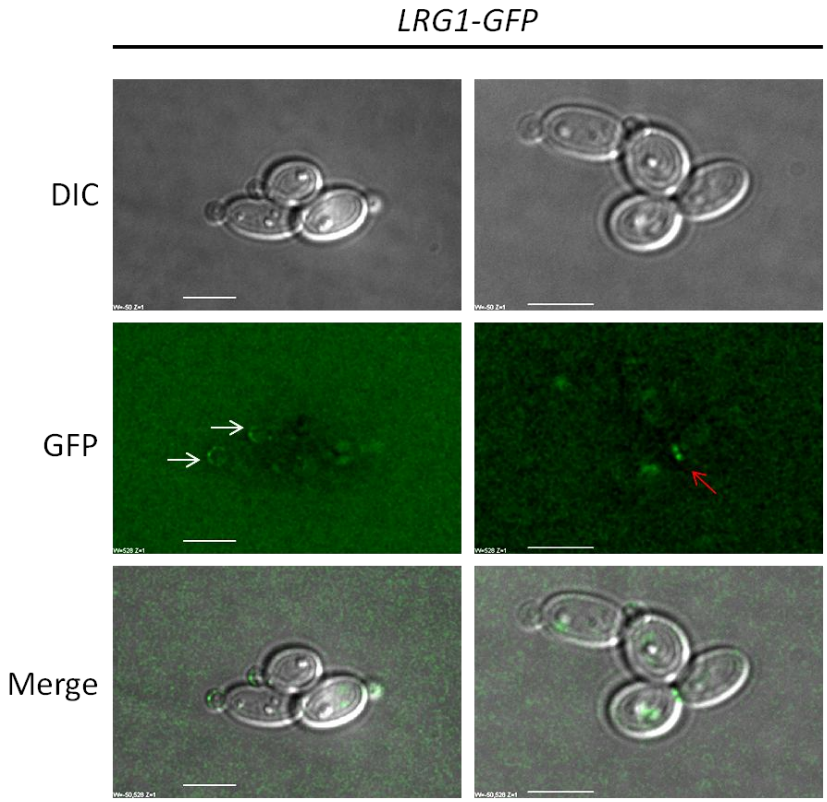

<u>Figure 3.10</u> Lrg1 localises to sites of polarised growth in *C. albicans*

LRG1-GFP was grown in yeast inducing conditions for three hours before visualisation on a Delta Vision Spectris 4.0 microscope with Softworx^{TM} 3.2.2 software (Applied Precision Instruments). Images taken using the DIC and FITC filters are shown along with a merged image of the two. White arrows show small buds with Lrg1 located at the tip, whilst red arrows depict large buds where Lrg1 has re-localised to the site of septum formation.

3.3.5 Re-localisation of GFP-Rho1 in an *lrg1ΔΔ* background during yeast growth is delayed

To investigate the location of Rho1 as the yeast bud forms in the absence of Lrg1, the P_{MAL2}-*GFP-RHO1/lrg1ΔΔ* and P_{MAL2}-*GFP-RHO1* strain were grown on maltose containing agar microscopy pads to induce expression of Rho1 under yeast inducing conditions. As can be seen in figure 3.11 (left panel), in the strain with two copies of *LRG1* present, GFP-Rho1 localises first to the apical tip of the growing bud. Once the bud becomes larger, GFP-Rho1 relocates to the mother-bud neck, presumably to direct the cell wall remodelling apparatus for formation of the primary and secondary septa and cytokinesis. On the other hand, in the *lrg1ΔΔ* background, whilst GFP-Rho1 does re-locate to the mother-bud neck, it does so when the bud is markedly more elongated than in a wild-type background (figure 3.11, right panel). To confirm this observation, the length of cells that showed GFP-Rho1 at either the bud tip or bud-neck was measured so as to give an indication of when Rho1 re-localised from one to the other. Results are shown in figure 3.12a.

It can be seen that the average length of wild-type cells with GFP-Rho1 at the tip is less than in the average length of cells lacking *LRG1*. Likewise this pattern is seen when the lengths of cells with GFP-Rho1 at the forming bud-neck are compared. Furthermore, an unpaired t-test on this data by GraphPad Prism (GraphPad Software 6, San Diego California USA, www.graphpad.com) shows that the difference between the wild-type strain and *lrg1ΔΔ* strain of both Tip and Bud-neck data sets are significantly different, with a p-value of 0.05. This shows that in the absence of *LRG1*, there is a delay in relocation of Rho1 from the apical tip to the mother-bud neck.

Further evidence for this delay in re-localisation is the fact that during growth as yeast, the wild type cells shows GFP-Rho1 at either the tip or the mother-bud neck, never both, but in cells lacking *LRG1,* 22% of cells show GFP-Rho1 at both locations at the same time (figure 3.12b) This indicates not only a delay in the re-localisation of Rho1 but also an incomplete re-localisation in the *lrg1ΔΔ* strain. The maintenance of Rho1 at the bud tip could result in continuous cell wall growth and provide a mechanistic explanation for the highly polarised nature of the *lrg1ΔΔ* mutant.

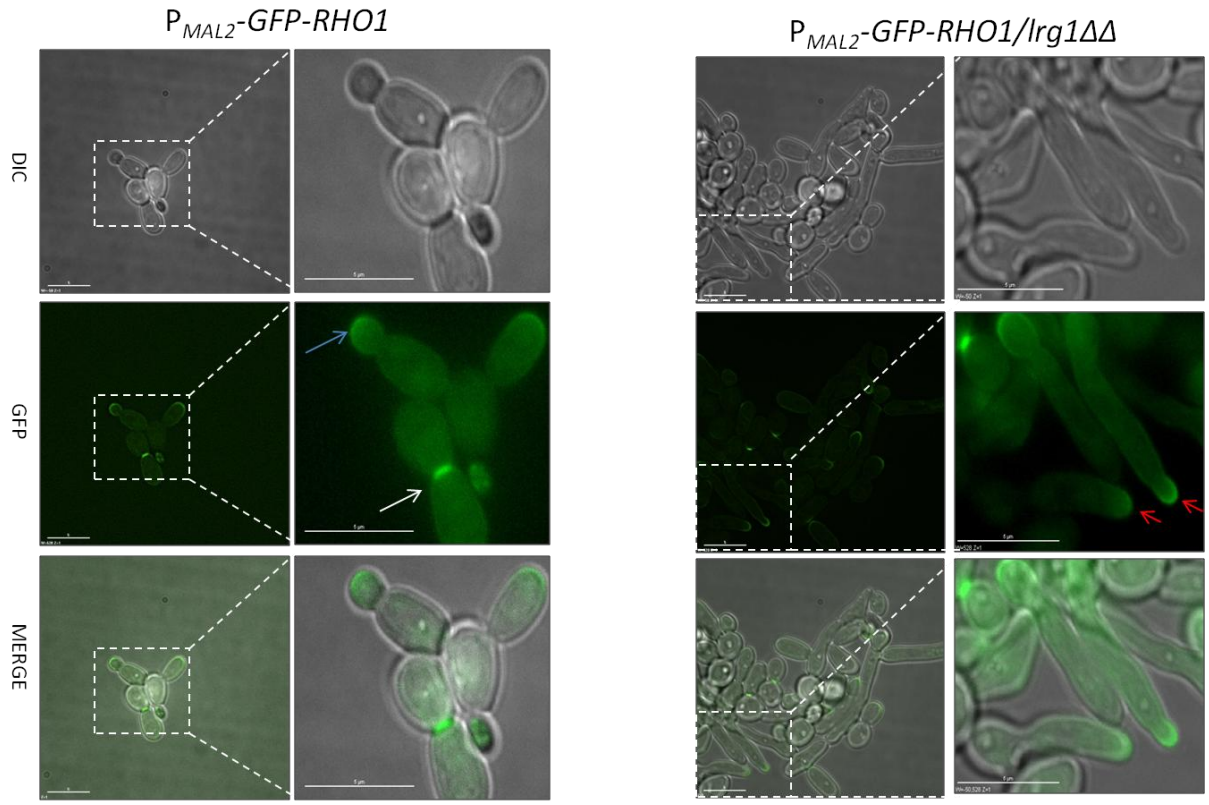

Figure 3.11 The localisation during yeast growth of GFP-Rho1 in an *lrg1ΔΔ* background

Overnight cultures of P_{MAL2}-*GFP-RHO1* and P_{MAL2}-*GFP-RHO1/lrg1ΔΔ* were re-inoculated onto minimal media agar pads grown at 30°C for 3 hours. Cells were visualised on a Delta Vision Spectris 4.0 microscope with Softworx™ 3.2.2 software (Applied Precision Instruments) using DIC and FITC filters. In wild type cells (left), GFP-Rho1 can be seen at the tip of small buds (blue arrow) and then the bud-neck of larger cells (white arrow). However, in cells lacking *LRG1*, cells where GFP-Rho1 can be seen at the tip have an increased length compared to the wild-type strain (red arrow). Scale bars represent 5 µm.

A)

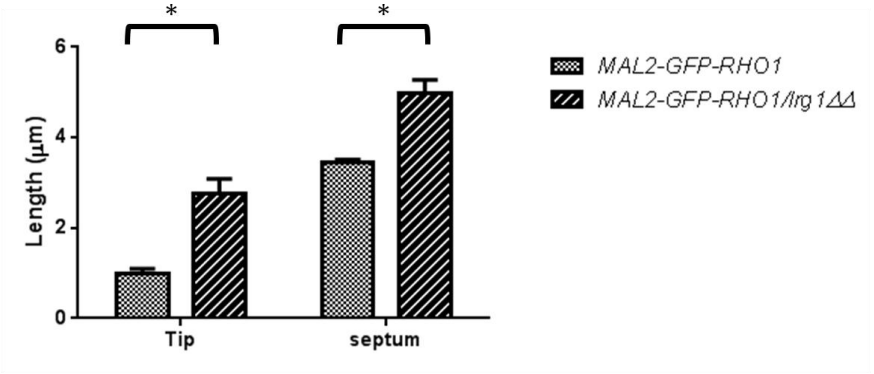

	Length of cells when GFP-Rho1 is seen at each location (µm)	
	TIP	Bud neck
BWP17	0.98± 0.118	3.45± 0.062
lrg1ΔΔ	2.76± 0.319	4.96 ± 0.307

B)

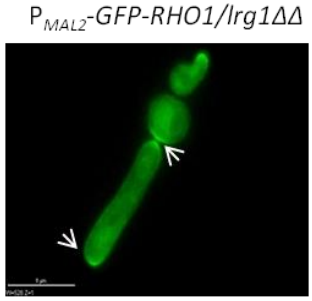

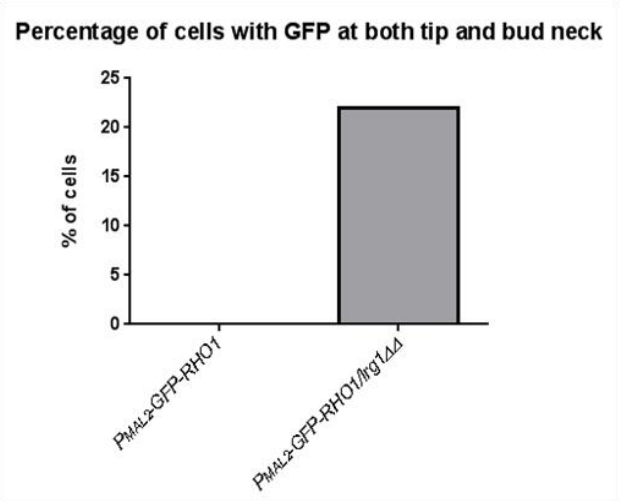

<u>Figure 3.12</u> Re-localisation of Rho1 from apical tip to mother-bud neck is delayed in an *lrg1ΔΔ* background during yeast growth

A) P_{MAL2}*-GFP-RHO1* and P_{MAL2}*-GFP-RHO1/lrg1ΔΔ* strains were grown as yeast as depicted in figure 3.11 and cells were analysed to measure their length when GFP-Rho1 could be seen at either the tip or mother-bud neck. The average lengths of cells ± SEM is depicted. N=60. A t-Test was performed using GraphPad Prism, with connecting bars above data sets showing a statistical difference, with a p-value of 0.05.

B) Cells were counted in P_{MAL2}*-GFP-RHO1* and P_{MAL2}*-GFP-RHO1/lrg1ΔΔ* strains to record the percentage of cells where GFP-Rho1 could be seen at both the tip and mother-bud neck. N=50

3.3.6 GFP-Rho1 becomes less focused at the hyphal tip in an *lrg1ΔΔ* background

To examine the distribution of GFP-Rho1 at the hyphal tip in wild-type and *lrg1ΔΔ* cells, P_{MAL2}-*GFP-RHO1/lrg1ΔΔ* and P_{MAL2}-*GFP-RHO1* cells were induced to form hyphae on maltose-based media, grown for 90 minutes and then visualised by fluorescence microscopy. In the wild-type strain it can be seen that GFP-Rho1 is localised to a relatively small cap around the hyphal tip (figure 3.13, left panel). In an *lrg1ΔΔ* mutant, Rho1 is still localised to a cap at the hyphal tip. However, the cap appears to be broader around the tip than in the wild-type strain (figure 3.13, right panel). To quantify this, the distance around the hyphal tip ("A" in figure 3.14) that GFP-Rho1 extends and the distance along the hyphae ("B" in figure 3.14) from the tip that GFP-Rho1 can be seen, was measured (figure 3.13). The average distance that GFP-Rho1 extends around the tip-measurement "A"-in wild-type cells is 1.80 µm ± 0.58, compared to 3.43 µm ± 0.41 in the absence of Lrg1. Similarly, the distance that Rho1 extends down the walls of the hyphae-measurement "B"-is 0.66 µm ± 0.24 in the wild-type strain but 1.39 µm ± 0.41 in *lrg1ΔΔ*. This suggests that Lrg1 is required to focus the localisation of Rho1 to a very precise region at the apical tips of hyphae. One could also speculate that an increased spread of Rho1 further around the hyphal tip could produce wider hyphae due to increased spread in deposition of cell wall material. However, when the widths of the hyphae of wild-type and *lrg1ΔΔ* mutants are compared (figure 3.14) - 1.00 µm ± 0.18 and 1.06 µm ± 0.29 respectively- no significant difference can be seen.

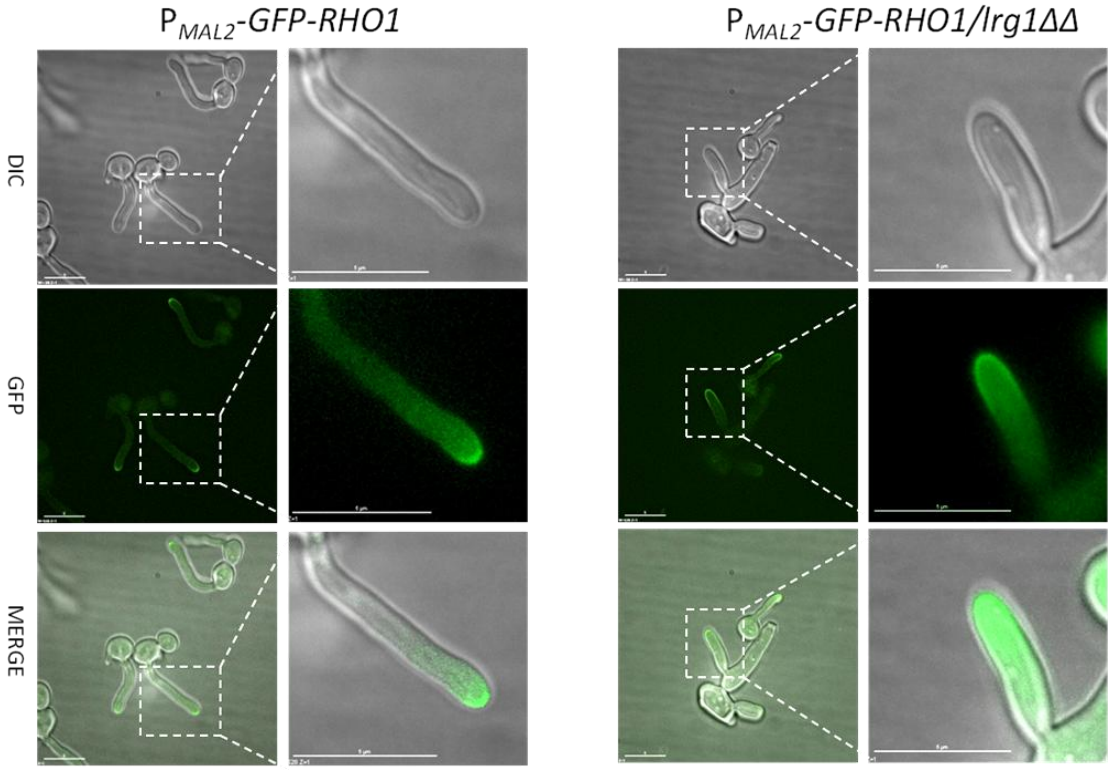

<u>Figure 3.13</u> The localisation during hyphal growth of GFP-Rho1 in an *lrg1ΔΔ* background

Overnight cultures of P_{MAL2}-*GFP-RHO1* and P_{MAL2}-*GFP-RHO1/lrg1ΔΔ* were re-inoculated onto minimal media agar pads and grown at 37°C for 90 minutes to induce the hyphal morphology. Cells were visualised on a Delta Vision Spectris 4.0 microscope with SoftworxTM 3.2.2 software (Applied Precision Instruments). GFP-Rho1 appears to form a broader cap around hyphae in cells lacking *LRG1* than in hyphae from wild-type cells. Scale bars represent 5 µm.

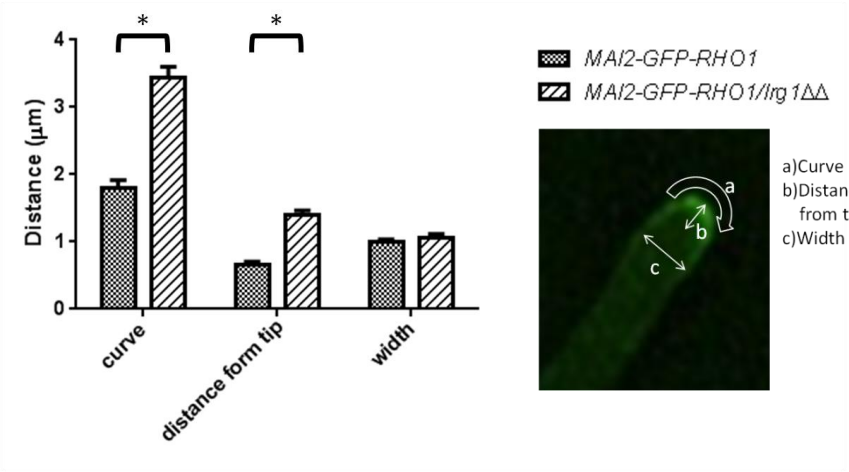

Figure 3.14 Rho1 is less precisely focused at the hyphal tip in an *lrg1ΔΔ* background
P_{MAL2}*-GFP-RHO1* and P_{MAL2}*-GFP-RHO1/lrg1ΔΔ* were grown as hyphae as depicted in figure 3.13 and cells were analysed to measure A) the length that GFP-Rho1 can be seen curving around the tip of the hyphae, B) the distance from the tip that GFP-Rho1 can be seen and C) their width. The average of each measurement ± SEM is depicted on the graph. N=45. A t-Test was performed using GraphPad Prism, with connecting bars above data sets showing a statistical difference, with a p-value of 0.05.

3.3.7 GFP-RID localises to sites where Rho1 is active

The above data uses an N-terminally GFP tagged Rho1 protein to try and assess the effects of deletion of the *LRG1* gene in *C. albicans*. However there are a number of problems with this strategy. Firstly, there are concerns that GFP tagged Rho1 is non-functional due to the inability to construct a strain in which this was the only copy of *RHO1* present and the fact that it is unable to complement a P_{TET}*-RHO1* strain (Caballero-Lima et al., 2013; Corvest et al., 2013). Furthermore, even if GFP-Rho1 is functional, the fluorescence that it emits only reports on the location of the protein, regardless of whether it is in the GTP-bound active form or not. To try and analyse the effects of *LRG1* deletion on active Rho1, a GFP-RID fluorescent reporter construct was used. The *pExpArg-pACT1GFPRID* plasmid (figure 3.15a), (Corvest et al., 2013) contains a 265 amino acid region from *C. albicans* Pkc1, homologous to the mapped region of *S. cerevisiae* Pkc1 that is known to interact with Rho1 bound to GTP only (Nonaka et al., 1995b) that is called the Rho1 Interaction Domain (RID). The RID domain is fused to GFP and placed in front of an *ACT1* promoter for cell-cycle independent expression, whilst the plasmid contains part of the RP10 locus for integration and the *ARG4*

gene for selection of transformants. Thus when transformed into *C. albicans* GFP-RID should bind to and be seen at sites where active Rho1 is localised.

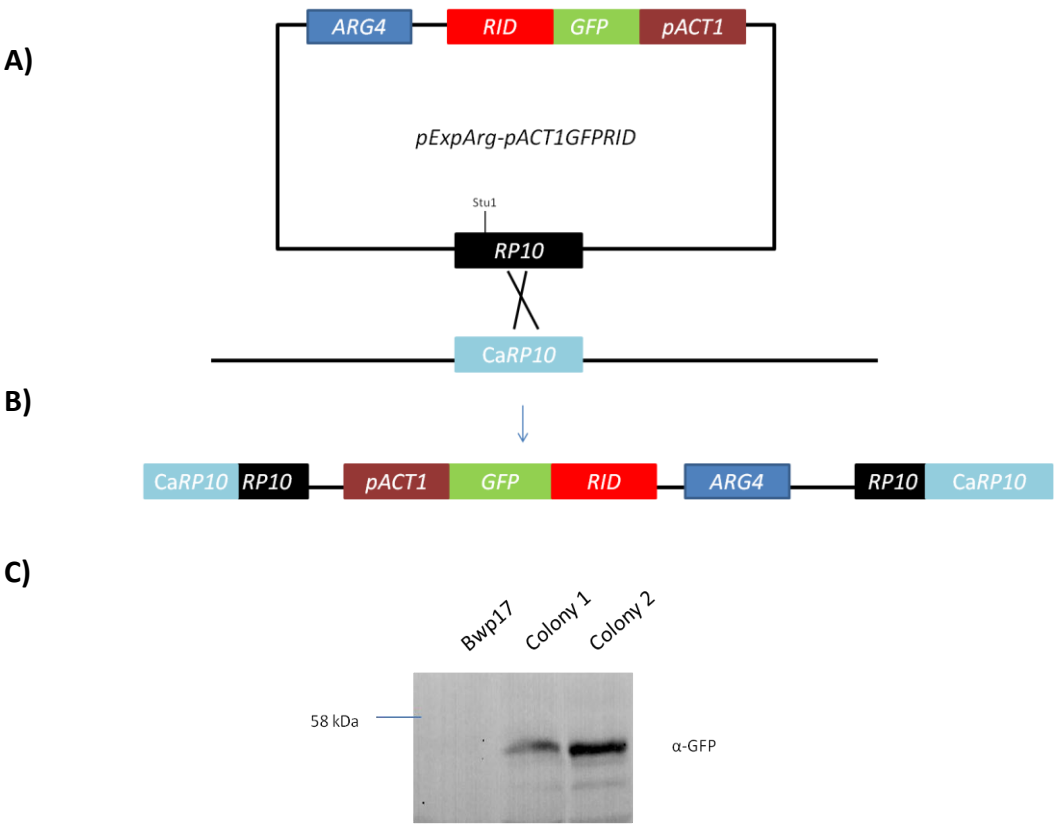

Figure 3.15 Transforming the *pExpArg-pACT1GFPRID* plasmid into *C. albicans*
The *pExpArg-pACT1GFPRID* plasmid is represented in (A) and contains a Stu1 restriction site in its RP10 locus used to linearise the plasmid. Once linearised, the plasmid goes through homologous recombination with the *C. albicans* genome at this locus, resulting in integration (B). Correct expression of the integrated GFP-RID construct was confirmed via SDS-PAGE, western blot and detection with antibodies to GFP (C)

3.3.8 The localisation of active Rho1 in the wild-type and *lrg1ΔΔ* strains.

To analyse the distribution of active Rho1 in yeast cells, the *pExpArg-pACT1GFPRID* plasmid was linearised and transformed into both the *BWP17* wild-type strain and the *lrg1ΔΔ* mutant. Correct integration (figure 3.15b) and expression of GFP-RID was confirmed by protein extraction, SDS-PAGE and western blot figure (3.15c). The resulting strains were named *GFP-RID* and *lrg1ΔΔ/GFP-RID*. These two strains were then grown on agar microscopy pads to induce the yeast morphology for 3 hours before visualisation via a DeltaVision fluorescence microscope. The images are shown in figure 3.16 (top-left). As with the GFP-Rho1 construct, GFP-RID can be seen localising to both the tips of small buds and the bud neck of large buds indicating that Rho1 is active at those locations in wild-type cells. In medium sized buds, active Rho1 can also be seen around the whole cell cortex, most probably indicating that growth has switched from a polarised to an isotropic state. To analyse the location of active Rho1 further, the lengths of wild-type cells with active Rho1 at the tip, cortex or bud neck was measured. The average lengths with SEM are shown i**n** figure 3.16 (centre-left panel). It can be seen that the cells with active Rho1 at the tip have an average length in microns of 2.249± 0.214 µm, whilst in cells with active Rho1 at the cortex the length is 3.228± 0.158 µm, and when re-localised to the bud neck the cells are 4.165± 0.163 µm long. This demonstrates that active Rho1 is first localised to the tip of small buds, then as they grow in size it is re-localised to the cortex for a period of isotropic growth, before again re-localising to the mother-bud neck once the cells reach a defined size in order to form the primary and secondary septa and go through cytokinesis.

It can also be seen that active Rho1 is present at the tip, cortex and septum of *lrg1ΔΔ/GFP-RID* cells. Unlike in wild-type cells, active Rho1 can also be seen at both the tip and the septum of cells simultaneously (figure 3.16, top-right, yellow arrow), similar to the result from visualisation of GFP-Rho1, with 30% of cells displaying this phenotype compared to 8% of wild-type cells (figure 3.16, bottom panel). This again indicates that the protein is failing to show appropriate re-localisation from the tip in large buds, providing a mechanism for the highly polarised phenotype the *lrg1ΔΔ* strain displays. In addition, GFP-RID can be seen at the tips of cells that are extremely long (figure 3.16, top-right, white arrow), indicating that active Rho1 has failed to re-localise to the cortex. It can be seen that the relevant

lengths of *lrg1ΔΔ* cells where active Rho1 is at the tip, cortex and bud neck are; 8.38± 1.496 µm, 4.707± 0.694 µm and 6.278± 0.497 µm respectively. A number of observations can be made here. Firstly, it can be noted that under all three active Rho1 locations, the average bud length of the mutant are greater than in wild-type cells, which are statistically different in an unpaired t-test, with a confidence interval of 0.01. This confirms that there is a delay in re-localisation of the growth machinery from the tip to the cortex and then subsequently the mother-bud neck in cells lacking Lrg1. Secondly, when the average lengths of the *lrg1ΔΔ* mutant cells analysed, it can be seen that those with active Rho1 at the tip are, on average, longer than those with the active GTPase at either the cortex or bud neck. This is counter intuitive, as one would expect the average bud length to increase and to be longest when Rho1 is at the bud neck, as is the case in the wild-type cells. However, one possible explanation for this is that there are effectively two populations of *lrg1ΔΔ* cells:

1. Cells where there is a complete failure of Rho1 re-localisation from the bud tip
    - Rho1 and the growth machinery become locked at the bud tip, growth remains polarised towards this location and the cells continue to increase in length.
2. Cells that only show a delay or incomplete re-localisation of Rho1 from the bud tip
    - The increase in time that growth remains polarised at the tip results in cells becoming longer
    - Rho1 eventually re-localises to the cell cortex and then the mother-bud neck to form the primary and secondary septum.
    - Resulting cells are longer than the average wild-type cell but not as long as cells where Rho1 remains fixed at the bud tip.

In the *lrg1ΔΔ* strain, the range of bud length with active Rho1 at the tip is from 1.293 µm to 36.616 µm, whereas at the cortex the range is from 2.19 µm to 12.98 µm and the septum 2.45 µm to 10.209 µm, showing that a proportion of buds with active Rho1 at the tip are much longer than any seen with active Rho1 at either the cortex or septum (figure 3.12, centre-right panel).

Overall, it can be concluded that lack of Lrg1 results in a delay in active Rho1 leaving the tip of buds, resulting in lengthening of buds compared to a wild-type strain. Furthermore, it can

be noted that in some cells active Rho1 fails to leave the tip at all giving rise to hyperpolarised long daughter cells.

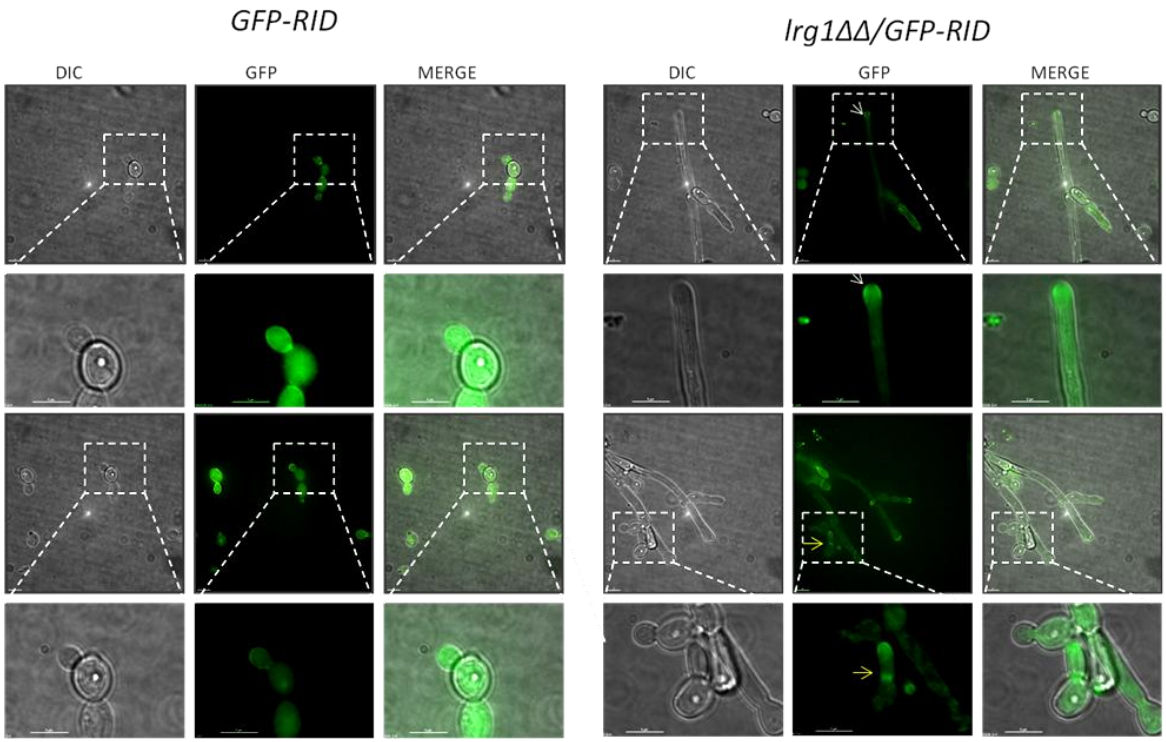

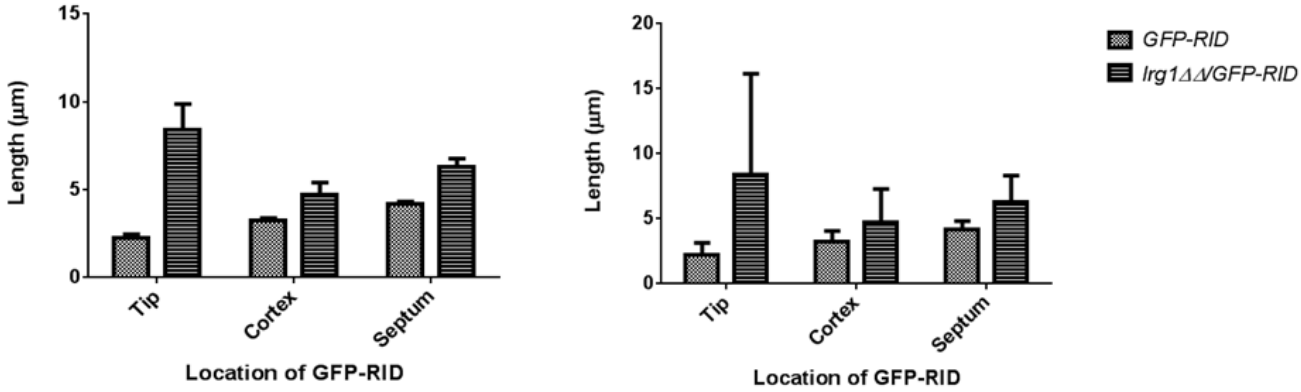

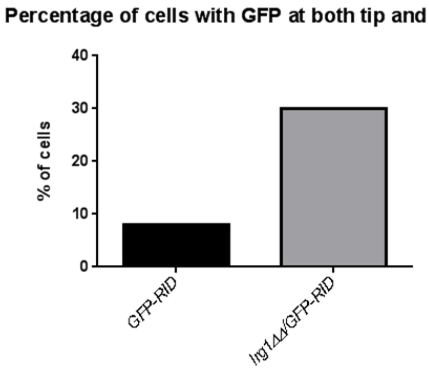

Figure 3.16 Re-localisation of GFP-RID is delayed in the *lrg1ΔΔ* strain

Top: The *GFP-RID* and *lrg1ΔΔ/GFP-RID* strains were grown for 3 hours in yeast inducing conditions on agar pads, before visualisation on a DeltaVision fluorescence microscope using DIC and FITC filters. White arrows indicate long cells with active Rho1 still localised to the septum, whilst yellow arrows indicate cells that possess active Rho1 at both the tip and septum. Scale bars represent 5 µm.

Centre left: The images of each strain were used to determine the average length (plus SEM) of cells when GFP-RID could be seen at the bud tip, cortex or septum. N=50

Centre right: Displays the same data as the bottom left panel but with the range of the data shown instead of SEM.

Bottom: The percentage of cell displaying GFP signal at both the tip and septum, concurrently.

**= statistically different with a confidence interval of ≤ 0.01

***= ≤ 0.001

3.3.9 Activity of Rho1 is increased in *C. albicans* cells lacking *LRG1*

To further investigate the activity of Rho1, the images of *GFP-RID* and *lrg1ΔΔ/GFP-RID* taken above were used in additional analyses. An image processing programme, FIJI (Schindelin et al., 2012), was first used to trace around cells expressing GFP-RID, with the line starting in the middle of the septum then bisecting the growing bud to the middle of the tip before tracing around the whole circumference of the buds cell wall. An example of this is seen in figure 3.17 (top panel). An in-house programme (Craven, J. University of Sheffield), then used the coordinates of this line to project the fluorescence intensity signal around the circumference of the cell wall onto the straight line from the mother-bud neck to the bud tip. In total, 52 cells of the *GFP-RID* strain and 64 cells of the *lrg1ΔΔ* strain were analysed this way and the plots from a selection of cells shown in figure 3.17 (bottom panel). This figure shows fluorescence intensity on the Y-axis, whilst the X-axis shows increasing distance from the bud tip from left to the septum on the right. Two lines of data are shown to represent each side of the daughter bud. The *BWP17* cells appear to show fluorescence from around 700 to 2000 units, whilst the graphs of cells lacking *LRG1* show fluorescence much higher, anything from 1000 to 4000 units, with the majority appearing to average between 2000

and 3000 units. To confirm this observation, the tracing of each cell was used to calculate its average fluorescence intensity, and then each value utilised to produce an overall average intensity for the *BWP17* and *lrg1ΔΔ* strains (Figure 3.18-left). The average (± SEM) intensity value for the wild-type strain is 1101± 5.80, whilst for the cells lacking *LRG1* the average is 1833± 84.96 and an unpaired t-test reveals that there is a significant difference between the two values with a p-value of 0.0001.

Next, to investigate the distribution of active Rho1 in the cell, the co-ordinates of the cell traces were used to take 3 individual fluorescence readings for each cell corresponding to the centre of the tip, centre of the septum and also halfway along the bud. Cells were then sorted as to which of the three measurements had the highest reading so that three groups were gained, each having cells which contained the majority of GFP-RID at the tip, septum or cortex. The average fluorescence intensity was then calculated for the relevant location of each of the 3 categories and is shown in figure 3.18 (right panel). Similar to the overall average GFP-RID fluorescence above, the average intensity seen in either the tip, septum and cortex of cells is around 2-fold higher in the strain lacking *LRG1* to that detected in wild-type cells. This difference is shown as significant when using an un-paired t-test. Also, in both strains the fluorescence seen in all three locations shows no significant difference between each other meaning that the tip, cortex and septum receive the same amount of active Rho1 at different stages of cell growth.

As the localisation and therefore level of fluorescence directly related to the level of active Rho1 in the cell, through binding of GFP-RID, these results indicate that lack of Lrg1 in *C. albicans* produces an increase in active Rho1 at the cell wall, which is independent of cellular location.

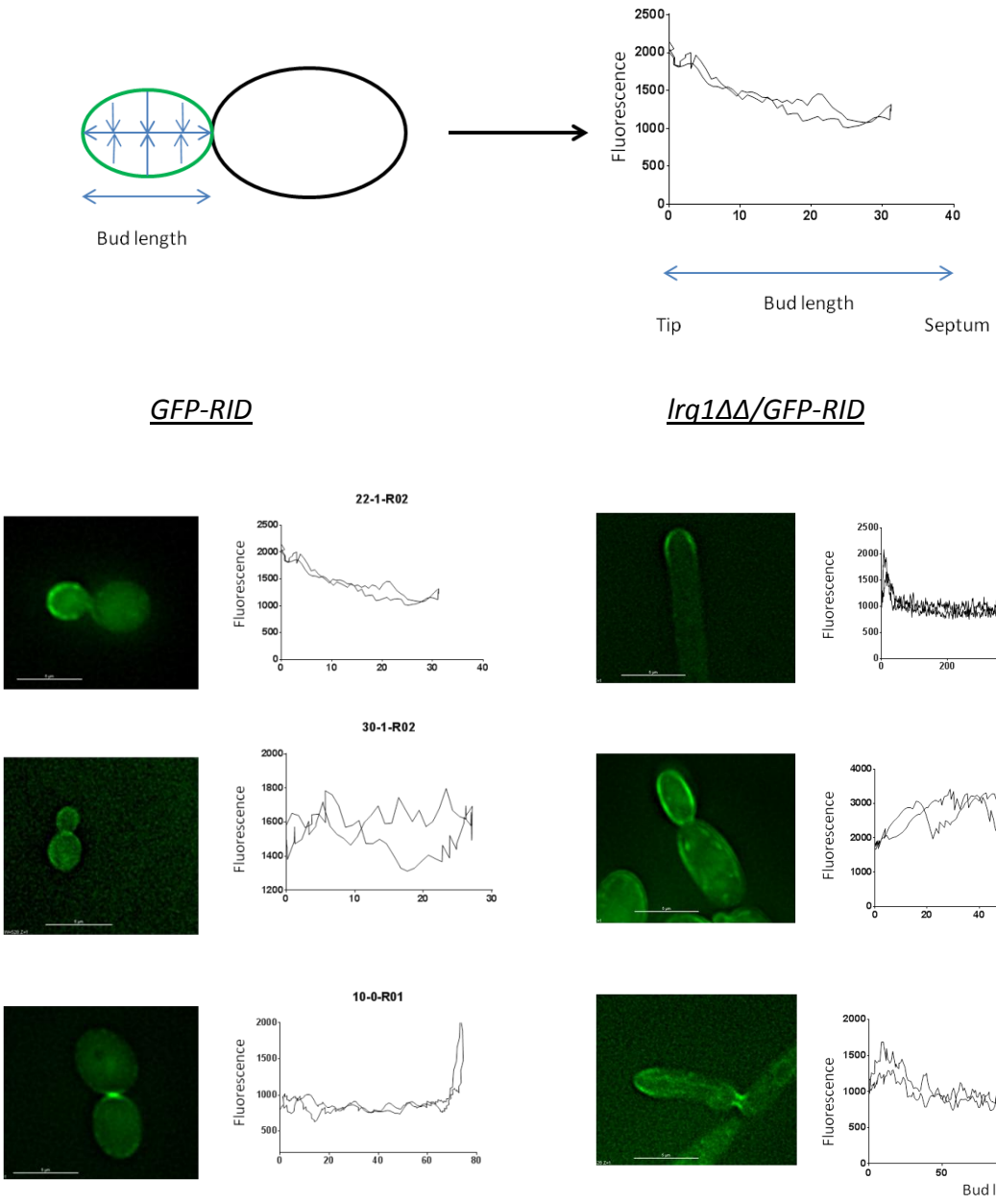

Figure 3.17 Projecting the intensity of GFP-RID onto bud length

Top: In order to analyse the GFP-RID strains, the wall of individual cells was traced around and the fluorescence intensity measured using the image processing programme FIJI (Schindelin et al., 2012) . Using an in house programme (Craven, J. University of Sheffield), this fluorescence intensity was projected onto the length of the bud to produce a graphical representation of fluorescence intensity (y-axis) vs. bud length (x-axis), with the tip of buds on the left and the septum on the right. Both units are arbitrary.

Bottom: A selection of GFP-Rid projections from both wild-type and *lrg1ΔΔ* cells. Scale bars represent 5 µm.

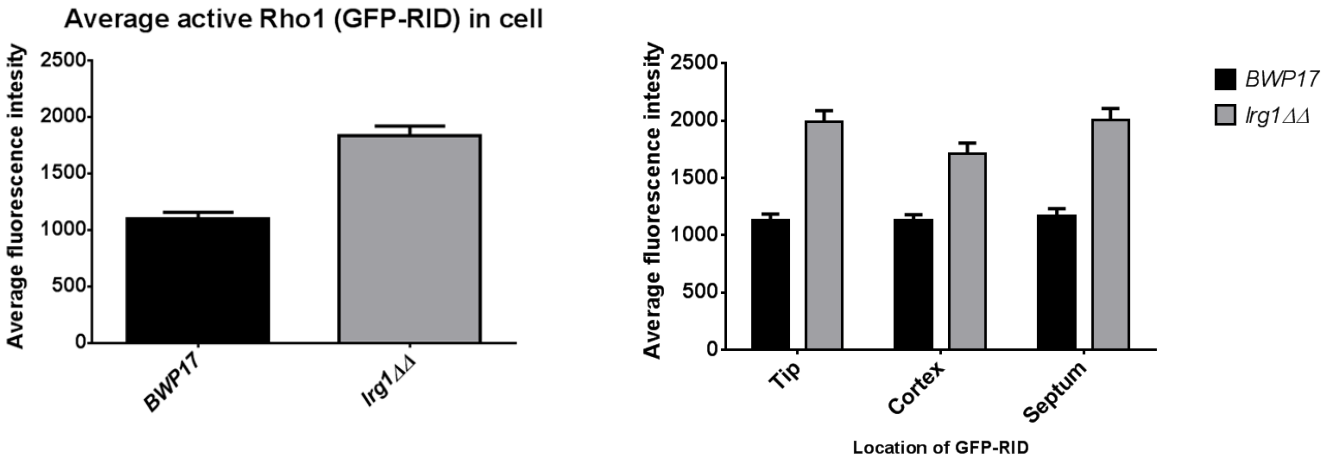

Figure 3.18 Rho1 activity is increased in cells lacking LRG1

Left: Using the fluorescence intensity plots above, the average GFP-RID signal from each cell was used to calculate an overall cell average for the wild type *GFP-RID* strain (*BWP17)* and the *lrg1ΔΔ/GFP-RID* strain. The values were significantly different to a p-value of 0.0001 in an unpaired t-test. *GFP-RID* n=52, *lrg1ΔΔ/GFP-RID* n=64

Right: Cell traces were categorised into group's dependent on whether their highest intensity reading was at the tip, cortex or septum. Each group was then used to calculate an average fluorescence reading for that particular location. 4 stars indicate a p-value of 0.0001 whilst 3 stars indicate a p-value of 0.001 in an unpaired t-test.

3.3.10 Deletion of *LRG1* causes hyper-susceptibility to caspofungin

Due to the increase in Rho1 activity seen in the *lrg1ΔΔ* strain via the GFP-RID construct, an increase in activity of the β-1,3-glucan synthase and hence an increased resistance to the echinocandin family of drugs that target this enzyme would be expected. This is indeed the case seen in other fungi such as *N. crassa* (Vogt and Seiler, 2008b). To test this hypothesis, overnight cultures of *BWP17* and *lrg1ΔΔ* were sonicated briefly to disturb clumps of cells, adjusted to read the same absorbance at OD_{600}, and then diluted to $1x10^{-4}$ and $1x10^{-6}$. The dilutions were then spotted onto agar plates containing increasing concentrations of caspofungin and incubated for three days at 30 °C. The results are shown in figure 3.19. In both dilutions of *BWP17*, it can be seen that as the concentration of caspofungin increases, the level of growth decreases as expected showing that drug is having the desired effect. With no caspofungin present the *lrg1ΔΔ* strain already grows slower than the wild-type, which must be taken into account when analysing the effect growth on caspofungin. Even at

the lowest concentration of caspofungin, growth of *lrg1ΔΔ* is highly inhibited when compared to that of the wild-type. This increased inhibition of growth continues to be observed at all drug concentrations tested with only a few small colonies seen at the highest concentration of 1 µg/ml of caspofungin. This is in contrast to what was first expected.

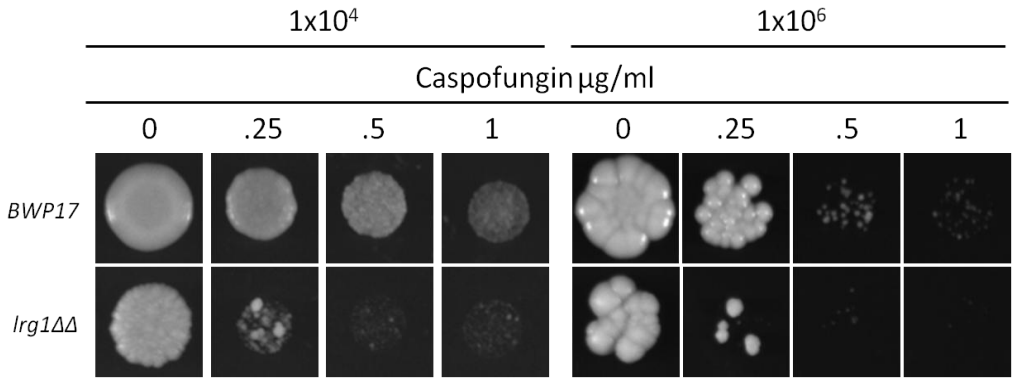

Figure 3.19 Lack of *LRG1* leads to hyper-susceptibility to caspofungin in *C. albicans*
BWP17 and *lrg1ΔΔ* strains were grown in YPD overnight, sonicated briefly and then adjusted so that they both read the same absorbance at OD_{600}. Cultures were then diluted to the indicated dilutions and spotted onto YPD agar plates with increasing concentrations of caspofungin.

3.3.11 Exo84 shows an incomplete re-localisation from the apical tip to mother-bud neck upon repression of *LRG1*

To investigate the localisation of Exo84 in the *lrg1Δ/ P_{MET3}-LRG1/EXO84-GFP* strain, cells were grown in yeast inducing conditions in either the presence or absence of methionine to repress and derepress the *MET3* promoter, respectively. As shown in figure 3.20, whilst *LRG1* is being expressed under the *MET3* promoter in the absence of methionine, Exo84-GFP localises first to the growing bud tip, resulting in polarised growth. There is then a period where Exo84-GFP is absent from the bud tip and is spread throughout the cell cortex (data not shown), before Exo84 then localises to the mother-bud neck resulting in the polarised growth required for cytokinesis. During yeast growth, Exo84 is only seen at both the tip and mother-bud neck in 2% of cells (figure 3.20, bottom). In contrast, when expression of *LRG1* is shut down by the addition of methionine, 24 % of cells show Exo84-

GFP at the apical tip of the highly polarised bud, but can also be seen at the site of the septum at the same time. This indicates that the exocyst is failing to properly relocate to the mother-bud neck in the same manner that Rho1 fails to re-localise. Therefore exocytosis and growth is continuing to occur at the apical tip as well as at the site of septum production. This is the pattern of Exo84 localisation seen in true hyphae (Caballero-Lima and Sudbery, 2014) and thus provides a reason for the increase in polarisation of *lrg1ΔΔ* cells. The observation also suggests that it is not only active Rho1 that fails to re-localise from the tip of buds when Lrg1 is absent, but that a large proportion of the whole cell growth machinery is also showing a delay in re-localisation.

3.3.12 Deletion of the *Ca*Lrg1 N-terminal extension has no deleterious effects during yeast or hyphal growth

To discover the effects of the Lrg1 N-terminal deletion, the *lrg1Δ/ P_{MAL2}-GFP-LRG1 (993-4404)* strain along with *BWP17* and *lrg1Δ/ P_{MAL2}-GFP-LRG1*, were induced to form both yeast and hyphae on maltose containing media. As shown in figure 3.21**,** the *lrg1Δ/ P_{MAL2}-GFP-LRG1* strain grows as both yeast and hyphae in a similar fashion to the *BWP17* wild-type control. Thus, it can be concluded that N-terminal GFP tagging of Lrg1 does not negatively affect the function of the protein. The strain with N-terminal deletion, *lrg1Δ/ P_{MAL2}-GFP-LRG1 (993-4404)*, also grows in a wild-type fashion as both yeast and hyphae. Consequently, it can be concluded that loss of the Lrg1 N-terminal extension does not have any deleterious effects. Nevertheless, as shown later in chapter 4, this part of the protein does have a role in regulating Lrg1 activity.

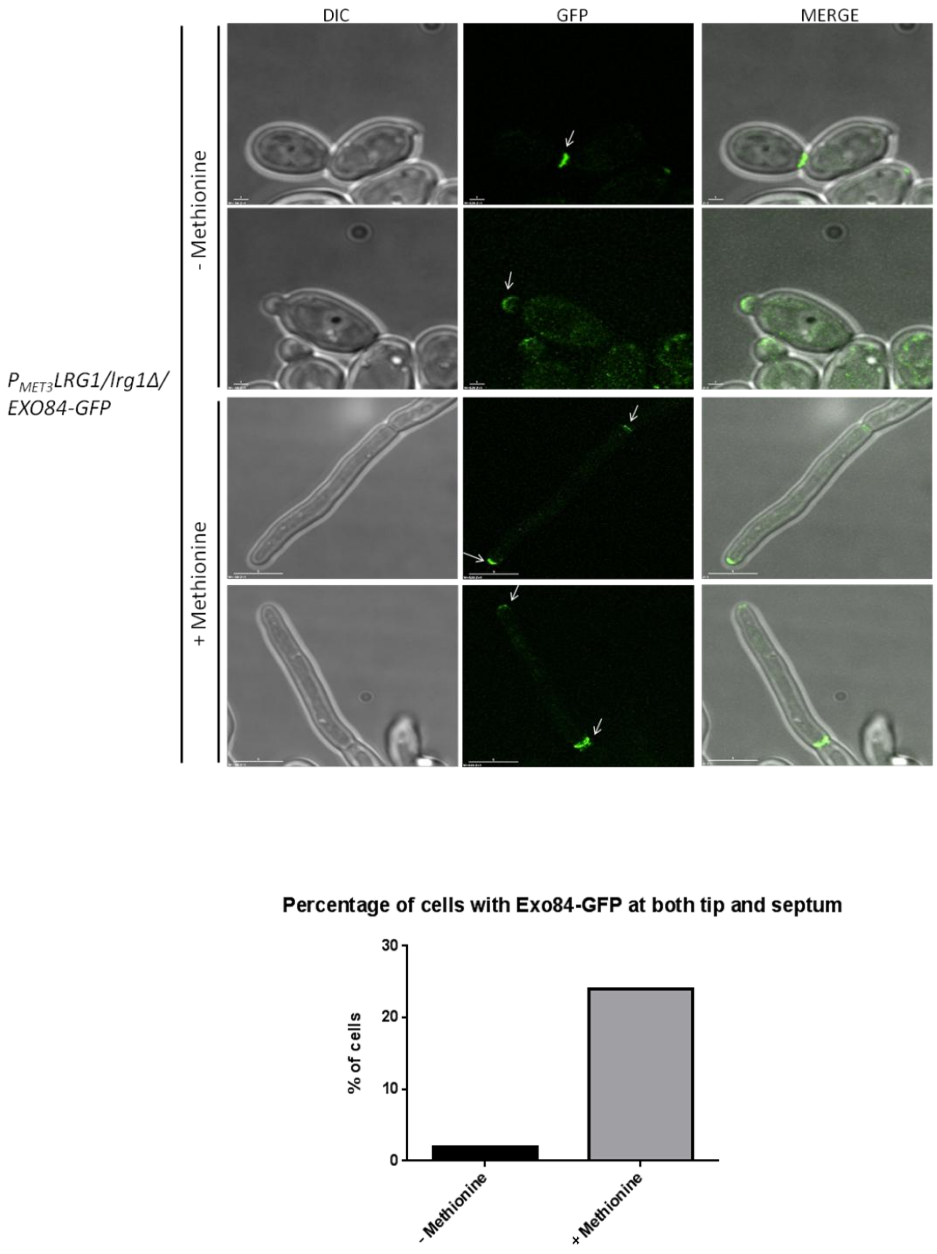

<u>Figure 3.20</u> Re-location of Exo84 from apical tip to mother-bud neck is delayed in the absence of *LRG1*

Top: The *P_{MET3}LRG1/lrg1Δ/EXO84-GFP* strain was grown in the presence/absence of methionine to either derepress/induce the *MET3* promoter respectively. Cells were re-inoculated onto required synthetic media from an overnight culture and induced to grow as yeast for 3 hours. Samples were then visualised using on a Delta Vision Spectris 4.0 microscope. Scale bars represent 1 µm.

Bottom: Images were analysed to count the percentage of cells that possessed Exo84-GFP at both the tip and septum. N=50.

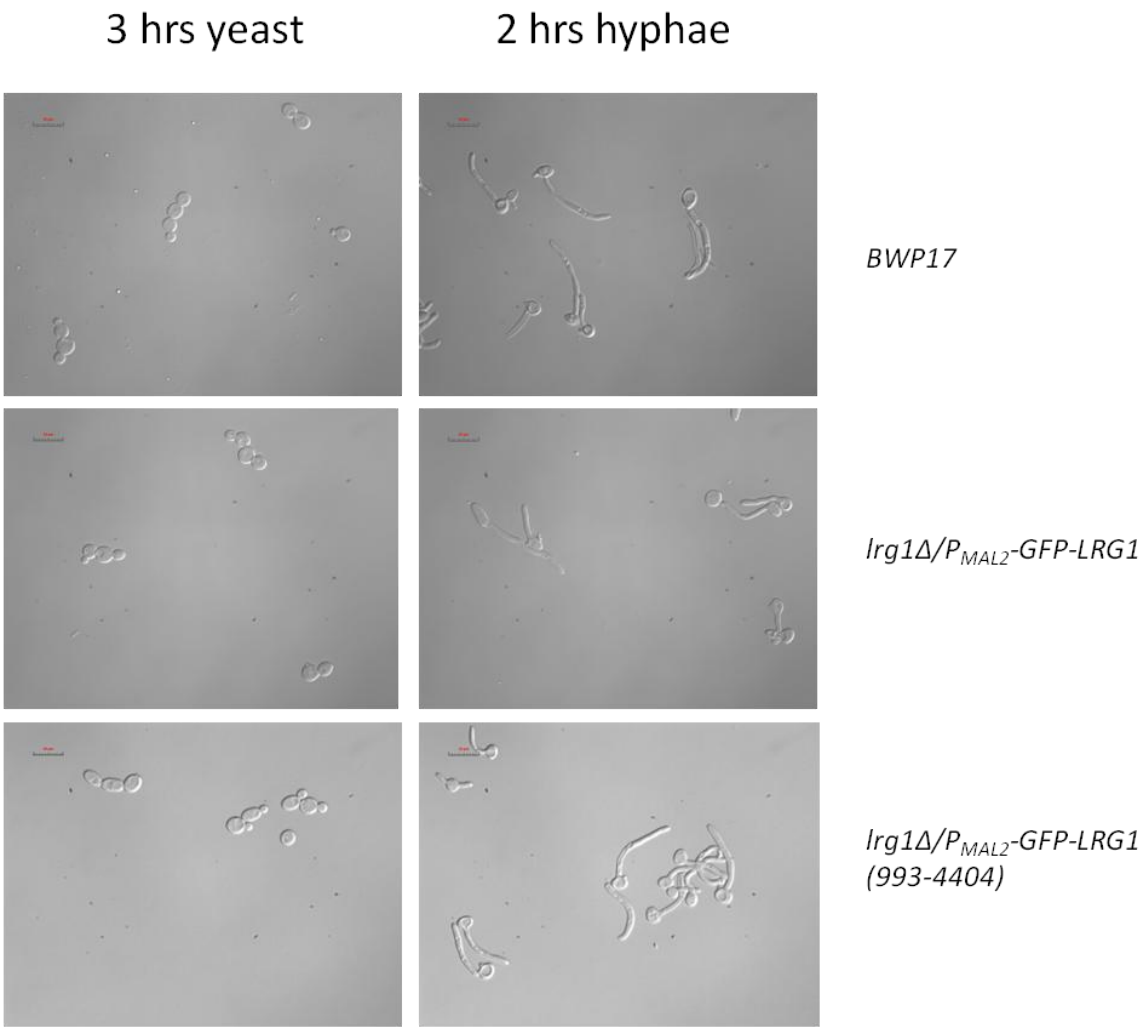

Figure 3.21 The Lrg1 N-terminal extension is not required for yeast or hyphal growth

BWP17, *lrg1Δ/ P$_{MAL2}$-GFP-LRG1* and *lrg1Δ/ P$_{MAL2}$-GFP-LRG1(993-4404)*, were re-inoculated from an overnight culture of YPM, to fresh YPM prepared to induce either yeast or hyphal growth. Cells were then grown for 2 hours as hyphae or 3 hours as yeast before formaldehyde fixing and visualisation using differential interference microscopy (DIC).

3.4 Discussion

3.4.1 *C. albicans* Lrg1 has an N-terminal extension not present in *S. cerevisiae*

Alignment of the hypothetical *C. albicans* Lrg1 sequence against the sequence of its *S.cerevisiae* ortholog revealed a 330 amino acid N-terminal extension in the *C. albicans* protein. Further analysis of *Ca*Lrg1 via IUPRED and the NCBI conserved domain database shows that this N-terminal domain is both highly disordered and does not contain any predicted domains. These pieces of data suggest an ideal region for the regulation of Lrg1. However, when the N-terminal extension of Lrg1 was deleted from the only copy of *LRG1* present in an *LRG1/lrg1Δ* heterozygote, no severe deleterious effect was detected during either yeast or hyphal growth. Hence the role of the N-terminal extension remains unclear.

3.4.2 Lrg1 is a negative regulator of polarised growth in *C. albicans*

To assess the cellular role of Lrg1 in *C. albicans,* both copies of *LRG1* were deleted in a *BWP17* parental strain and the resulting phenotype observed. During yeast growth, the *lrg1ΔΔ* strain shows extremely polarised, long cells that fail to separate, similar to pseudohyphal growth. The length: width ratio of these cells is 3.5 times larger than that of the wild type strain, demonstrating this elongated phenotype. During growth as hyphae, cells lacking *LRG1* also appear to grow as pseudohyphae due to the cells growth before hyphal induction. However, when hyphal growth is followed in the same cell from induction, hyphae appear to form correctly but extend at a rate greatly slower than wild-type cells. A number of cells also display a strange “double” tip as described above.
C. albicans pseudohyphal and hyphal cells are known to invade an agar matrix to a greater extent than cells grown as yeast. Therefore it is no surprise that the elongated, highly polarised cells of the *lrg1ΔΔ* strain also show an increased invasiveness into an agar plate when compared to the parental wild-type strain. This study showed that in the same manner as Rho1, Lrg1 localises to sites of polarised growth, raising the possibility that it has a regulatory role on the GTPase during this time.

3.4.3 *Ca*Lrg1 regulates the distribution of Rho1 during yeast growth

This study investigated the cellular distribution of Rho1 in cells lacking its negative regulator Lrg1 via visualisation of a GFP tagged version of the GTPase. In wild-type cells it is known that active Rho1 localises to sites of cell growth such as the growing tip and the site of septum formation during both yeast and hyphal growth (Corvest et al., 2013). This was also shown in this study. It was also shown that Lrg1 is required in *C. albicans* hyphal growth to focus the distribution of Rho1 to a small cap at the hyphal tip, rather than a broader area seen in the *lrg1ΔΔ* strain. Perhaps this lack of focus is the reason behind the "double" tip seen during hyphal growth as Rho1 produces unsolicited growth other than at the very tip of hyphae.

During growth as yeast, Rho1 was seen to delay its re-localisation from the growing bud tip to the mother-bud neck in cells lacking *LRG1.* The *lrg1ΔΔ* cells are on average longer when GFP-Rho1 is seen at either the tip or bud neck indicating the delay. Moreover, Rho1 re-localisation is not only delayed in *lrg1ΔΔ*, but in a substantial proportion of cells it is incomplete, shown by cells displaying GFP-Rho1 at both the tip and bud neck simultaneously. Indeed some cells exhibit a complete lack of re-localisation where Rho1 remains fixed at the growing tip and the bud becomes extremely long. This delayed, incomplete or non-existent re-localisation of Rho1 in *lrg1ΔΔ* is also seen when the GFP-RID reporter is used. This construct reports on the distribution and levels of GTP-bound active Rho1. Its use has both pros and cons. Firstly; the reporter allows both the levels of activity of Rho1 and its localisation simultaneously. The reporter also allows quantification of active Rho1 under physiological conditions. However, as GFP-RID binds to Rho1-GTP, the reporter will act as a competitor of Rho1 targets, so care must be taken to ensure this causes no deleterious effects. The observation of a defect in Rho1 distribution where no copy of *LRG1* is present, suggests that Rho1, through its regulator Lrg1, is a key protein in driving the re-location of the polarity complex, and therefore polarised growth from the bud tip to the site of septum formation. Further evidence for this is that the exocyst component Exo84 also shows this re-localisation defect in *lrg1ΔΔ*, proving other polarity components are also reliant on Rho1 and Lrg1 for their re-localisation. This has implications for growth as hyphae as one would assume Lrg1 may also delay Rho1 re-localisation during the highly polarised growth seen in this morphology.

*3.4.4 Ca*Lrg1 regulates the activity of Rho1 during yeast growth

The GFP-RID reporter construct was used to quantify the level of active Rho1 in wild-type and *lrg1ΔΔ* cells. The fluorescence emitted from the cell wall of growing yeast buds expressing GFP-RID was first projected onto the axis length of the bud itself. This data was then used to calculate an average active Rho1 content for the wild-type and *lrg1ΔΔ* strains. It was shown that in cells lacking Lrg1, average active Rho1 at the cell wall was almost double that of the parental strain. Furthermore, average active Rho1 at each site of growth- the tip, cortex or bud neck- was increased to the same extent. This shows that Lrg1 is required to regulate Rho1 activity to the same level at each location. One could also speculate that this lack of Rho1 inhibition in *lrg1ΔΔ* is responsible for the delay in its localisation.

An increase in Rho1 activity in cells lacking *LRG1* would lead to an increase in the production of β-1,3-glucan through the regulatory role of Rho1 on the glucan synthase. As mutants in the β-1,3-glucan synthase genes *FKS1* and *FKS2* lead to resistance to echinocandins, it was expected that an *lrg1ΔΔ* strain would also show a decreased sensitivity to these drugs as has been shown in *N. crassa* (Vogt and Seiler, 2008b). However, when grown on caspofungin, the strain lacking *LRG1* is shown to be more sensitive to the drug than the wild-type strain. The reason behind this is not known. Perhaps an increase in glucan synthase activity through Rho1 provides an increased number of targets for the drug to act upon rather than the limited number of active Rho1 molecules in the wild-type strain. Nonetheless, this result provides Lrg1 as interesting focal point for drug research.

4 Phospho-regulation of Lrg1 by Cdc28

4.1 Introduction

4.1.1 The Cdc28 kinase and the cell cycle

Eukaryotic cells use cyclin dependent kinases (CDKs) to control their cell cycle, with *S. cerevisiae* possessing 6 such kinases; Cdc28, Pho85, Kin28, Ssn3, Ctk1 and Bur1 (Enserink and Kolodner, 2010). Hartwell first discovered the Cdc28 kinase in *S. cerevisiae* in an important genetic screen for regulators of the cell cycle (Hartwell, 1974; Hartwell et al., 1973). The kinase phosphorylates either serine or threonine residues, but is proline directed, utilising the full consensus sequence S/T-P-x-K/R or the minimal consensus site S/T-P (Nigg, 1993). These consensus sites appear to be clustered in Cdc28 substrates (Moses et al., 2007). The Cdc28 kinase is necessary and adequate to drive the cell cycle but is supported in some early cell cycle functions by Pho85 (Huang et al., 2007), whilst the remaining CDKs are thought to be involved mainly in transcriptional processes (Meinhart et al., 2005).

To provide functional diversity, each CDK binds to multiple cyclins in order to phosphorylate different substrates. *S. cerevisiae* Cdc28 uses 9 such cyclins throughout the cell to alter its functionality; three G1 cyclins (Cln1-3) and six B-type cyclins (Clb1-6). Cln3 regulates the SBF (Swi4 cell-cycle box binding factor) and MBF (Mlu1 cell-cycle box binding factor) transcription factors that control transcription profiles for entry into S-Phase (START), including transcription of Cln1 and 2 (Dirick et al., 1995). Cln1 and Cln2 are required for the spindle pole body duplication (Haase et al., 2001) and bud morphogenesis (Cvrckova and Nasmyth, 1993) (discussed later). Clb5 and Clb6 are expressed later in G1 to regulate the initiation of S-phase (Schwob et al., 1994) and origin of replication firing (Dahmann et al., 1995), with Clb5 staying stable until mitosis, but Clb6 being degraded at the G1/S phase transition. Thus Clb5 is also responsible for efficient DNA replication (Donaldson et al., 1998). Clb3 and Clb4 are expressed from S phase until anaphase and required for DNA replication, spindle assembly and the transition from G2 to M phase (Richardson et al.,

1992). Clb1 and Clb2, involved in regulation of mitosis and bud morphogenesis (Lew and Reed, 1993), are expressed during G2-M phase of the cycle.

The kinase activating kinase Cak1, phosphorylates CDKs at residue T169, resulting in movement of the proteins T-loop which normally blocks the active site and PSTAIRE cyclin-binding helix, thus increasing the affinity of CDKs for cyclins (Kaldis et al., 1996; Ross et al., 2000). Far1 inhibits Cdc28 in response to mating pheromone and arrest cells at START (Chang and Herskowitz, 1990).

As well as regulation by differential cyclin utilisation, CDKs are also controlled by the cyclin dependent kinase inhibitors (CKIs) Far1 and Sic1 during G1, which bind to cyclin-CDK complexes and prevent substrate interaction (Peter and Herskowitz, 1994), (Nugroho and Mendenhall, 1994).

Cdc28 is further regulated at the morphogenesis checkpoint by the tyrosine kinase Swe1 and phosphatase Mih1. Swe1 delays the transition from G2 to M phase via the phosphorylation of tyrosine 19-resulting in inhibition of kinase activity and cyclin binding-on Cdc28 in response to actin and cytoskeleton stresses (Booher et al., 1993). The exact role of this checkpoint is controversial, possibly thought to be ensuring that the cells reach a critical size or shape before going through mitosis, reviewed in (Keaton and Lew, 2006), as deletion of Swe1 results in cells with a smaller size (Harvey and Kellogg, 2003). Conversely, the Mih1 phosphatase reverses the phosphorylation of tyrosine 19 on Cdc28 when all the conditions for cell cycle progression are met (Russell et al., 1989).

At the end of the cell cycle, Cdc28 substrates are de-phosphorylated by the phosphatase Cdc14 which is released from the nucleolus during late mitosis through the FEAR and MEN network, reviewed in (Enserink and Kolodner, 2010). This de-phosphorylation of substrates effectively resets the state of the cell ready for the next cell cycle.

4.1.2 The role of Cdc28 in morphogenesis in the model yeast *S. cerevisiae*

As discussed earlier, Cdc28 regulates morphogenesis of *S. cerevisiae* in multiple ways throughout the cell cycle. Firstly, once the site for bud emergence has been marked by the bud site selection pathway, and the levels of Cln2 have reached a critical stage, Cdc28-Cln2 marks Far1 for degradation which in turn releases Cdc24 from the nucleus (Henchoz et al., 1997). Cdc24 is the GEF for the GTPase Cdc42 and hence this action stimulates Cdc42

activity (Nern and Arkowitz, 2000). At the same time, Cdc28-Cln2 and Pho85 also phosphorylates the Cdc42 GAPs, preventing them from negatively regulating the GTPase (Sopko et al., 2007). Cdc42 is thought to be the key player in polarisation of the actin cytoskeleton toward the presumptive bud site so that the necessary material for growth can be delivered there. It has also been shown that as well as regulation of the vesicle delivery machinery, Cdc28 may also regulate the proteins that are required for regulation of vesicle transport itself, such as Sec2, Sec3 and Myo2 (McCusker et al., 2007) and also members of the exocyst required for fusion of the vesicle with the membrane (Luo et al., 2013).
Polarised growth requires both cell wall material- consisting of chitin and β-1,3-glucan- and phospholipids for the cell membrane. Cdc28 is thought to regulate all 3 of these components. Cdc28 phosphorylates the Tgl4 lipase, which then breaks down triglycerols into the precursors for membrane lipids (Kurat et al., 2009). Cdc28 is also known to phosphorylate the Chs2 chitin synthase, thus retaining it in the endoplasmic reticulum until it is required for formation of the septum at the end of mitosis (Teh et al., 2009).
Perhaps most interestingly for this study, Cdc28 has been shown to regulate the Rho1 GTPase (discussed earlier). One of the GEFs for Rho1, Tus1, has been shown to be directly phosphorylated by Cdc28-Cln2 at the G1/S phase (Kono et al., 2008). This phosphorylation activates Rho1 at the G1/S transition through Tus1 GEF activity and is also required for normal actin patch organisation. This indicates that Cdc28 is positively regulating cell wall remodelling through the CWI pathway via Rho1. Could Cdc28 also negatively regulate this process through Rho1 GAPs?
Cdc28 is also required for the switch from polarised to isotropic growth, although the direct target for this process is not known. It has however, been observed that redistribution of Cdc42 from the bud tip to the bud cortex is dependent on Cdc28-Clb2 and inhibited by Swe1 (Pruyne and Bretscher, 2000), giving rise to the possibility that Cdc28-Clb2 inhibit polar growth by turning off transcription of the G1 cyclins (Enserink and Kolodner, 2010). Enserink and Kolodner also raise the possibility that $Cdc28^{G2}$ regulation of phospholipid flippases is required for Cdc42 redistribution.

4.1.3 C. albicans morphogenesis and the Cdc28 kinase

Unlike *S. cerevisiae, C. albicans* possesses only 5 cyclins; two G1 cyclins Ccn1 and Cln3, two G2 cyclins Clb2 and Clb4, and a hyphal-specific cyclin Hgc1. Cln3 is essential, required for yeast and hyphal growth (Chapa y Lazo et al., 2005), depletion of which causes formation of non- budded hyphal-like filamented cells in yeast inducing conditions and bent hyphae with swollen tips in hyphal inducing conditions. The second G1 cyclin Ccn1 is not essential, however it is required for maintenance of hyphal growth once germ-tubes have formed (Loeb et al., 1999). Clb2 is essential, required for mitotic exit and regulates pseudohyphal growth with the 2nd G2 cyclin Clb4 (Bensen et al., 2005). During hyphal growth, the accumulation of the G2 cyclins is delayed (Bensen et al., 2005). The last cyclin, Hgc1 is hyphal-specific and expression is not dependent on the cell cycle, perhaps explaining why hyphal formation is also cell cycle stage independent (Zheng and Wang, 2004).
Given the presence of a hyphal-specific cyclin, it would be reasonable to assume that Cdc28-Hgc1 has a role in *C. albicans* morphogenesis. There have been a number of papers that have sought to investigate the role that Cdc28-Hgc1 plays in hyphal growth, summarised figure 4.1. The Cdc28-Hgc1 complex is known to phosphorylate and inactivate the Cdc42 GAP Rga2, allowing persistent Cdc42 activation at the hyphal tip (Zheng et al., 2007). The kinase-cyclin complex also phosphorylates Sec2, the GEF for Sec4 (Bishop et al., 2010) which is required for delivery of post-Golgi vesicles to the hyphal tip. As well as a direct involvement in polarised growth in hyphae, Cdc28-Hgc1 is required to inhibit cell separation at the end of the hyphal cell cycle. It regulates this in two main ways: firstly, the complex phosphorylates the transcription factor Efg1 leading to down regulation of the septum degradation enzymes (SDE's) (Wang et al., 2009); secondly, Cdc28-Hgc1 phosphorylates the septin Sep7 preventing Cdc14 and hence the kinase Cbk1 localising to the septin ring and licensing Ace2 to transcribe the SDE's (Gonzalez-Novo et al., 2008).

A recurring theme amongst the information above is that numerous cellular-growth processes are regulated via post-translational phosphorylation, of which many are reliant on Cdc28 kinase activity. Considering that: (i) Cdc28 is known to regulate Rho1 via phosphorylation of one of its GEFs Tus1 in *S. cerevisiae*; (ii) Cdc28 has diverged to play an extensive role in cell morphogenesis, including highly polarised growth in *C. albicans* and (iii)

deletion of Lrg1 in *C. albicans* results in highly polarised growth, we sought to investigate whether Cdc28 regulated *C. albicans* Lrg1 through phosphorylation and if so, what was the effect on growth at a cellular level.

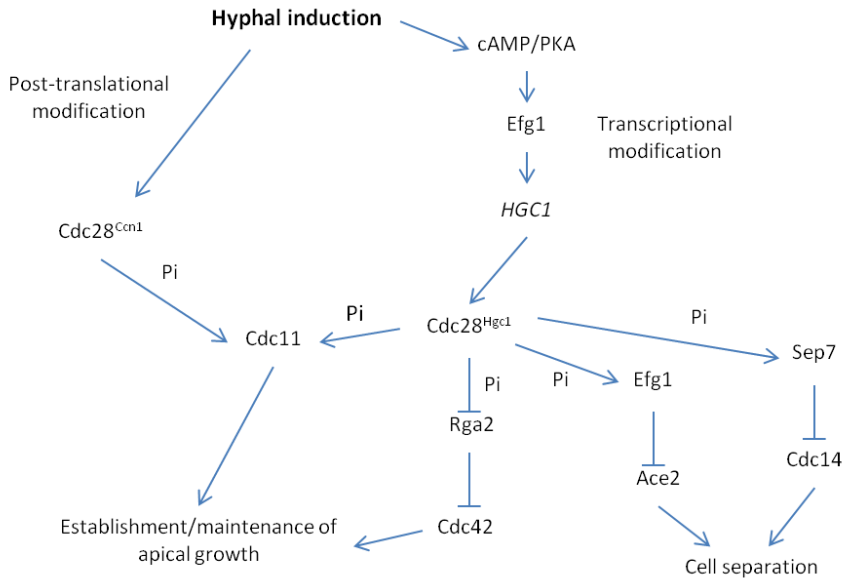

<u>Figure 4.1</u> The role of Cdc28p in hyphal growth and cell separation in *C. albicans*
The master cell cycle regulator has many roles within *C. albicans* hyphal morphogenesis and cell separation. It acts to maintain polarised growth at the hyphal tip by negatively regulating the Cdc42 GAP Rga2. It also represses cell separation during hyphal growth by activating the inhibitor of SDE transcription, Efg1 and preventing Cdc14 dephosphorylation which would eventually lead to the transcription factor responsible for SDE expression from entering the daughter nucleus. "Pi" represents phosphorylation taking place. Image adapted from (Wang, 2009).

4.1.4 Aims of this chapter

This chapter aims to understand the underlying regulation of the *C. albicans* Lrg1 protein and how this relates to the phenotype seen in an *lrg1ΔΔ* strain. Bioinformatics is used to analyse the protein, identifying potential regulatory phosphorylation sites. Evidence is then presented to provide Cdc28 as the potential regulatory partner. The relationship between Lrg1 and the master cell cycle regulator Cdc28 is discussed, as is the physiological role of Cdc28 action on Lrg1.

4.2 Strain construction

4.2.1 C-Terminal tagging of *C. albicans* Lrg1 with Myc

To investigate the phosphorylation state of the Lrg1 protein, it was first tagged at its C-terminus with a MYC epitope in a *BWP17* laboratory strain. A *PFA-MYC-URA* plasmid was used to produce a transformation cassette with 5' identity to the 3' end of *LRG1* (minus stop codon) and 3' identity to region downstream of *LRG1* (figure 4.2a) Correct transformants were confirmed using diagnostic PCR primers in *LRG1* and *MYC* (figure 4.2b) Colonies showing the correct PCR product were checked for protein expression by SDS-PAGE and western blot (figure 4.2b). The resulting strain will be referred to as *LRG1-MYC.*

4.2.2 Construction of a *GST-LRG1* expression vector

To investigate whether Cdc28 is capable of directly phosphorylating Lrg1 *in vitro,* an *in vitro* kinase assay was performed. To perform the assay, it was first necessary to obtain purified Lrg1. As Lrg1 is a large protein of 1468 amino acids, it was decided to purify only the N-terminal extension of Lrg1 corresponding to the first 330 amino acids to help aid protein folding when expressed in *E. coli.*

The pGEX-4T1 plasmid (GE Healthcare) contains the glutathione S-transferase gene under the control of an Isopropyl β-D-1-thiogalactopyranoside (IPTG)-inducible promoter, followed by multiple cloning site containing XhoI and BamHI. Cloning of the Lrg1 N-terminal region, shown in figure 4.3, into these sites created an N-terminally tagged *GST-LRG1(NT)* construct that can be induced for expression in *E. coli* by addition of IPTG. After expression, the GST tag then allows relatively clean and simple purification of the GST-Lrg1(NT) protein. The *GST-LRG1(NT)* plasmid was also then treated to multi-site directed mutagenesis in order to mutate the 4 codons that correspond to the full predicted Cdc28 consensus sites at positions T7, S65, T273 and S319 to codons that code for alanine. This residue is unable to be phosphorylated so will act as a negative control when assessing phosphorylation of *GST-LRG1(NT)* by Cdc28. The *GST-LRG1-4A(NT)* plasmid was sequenced in full to ensure no other mutations had been introduced.

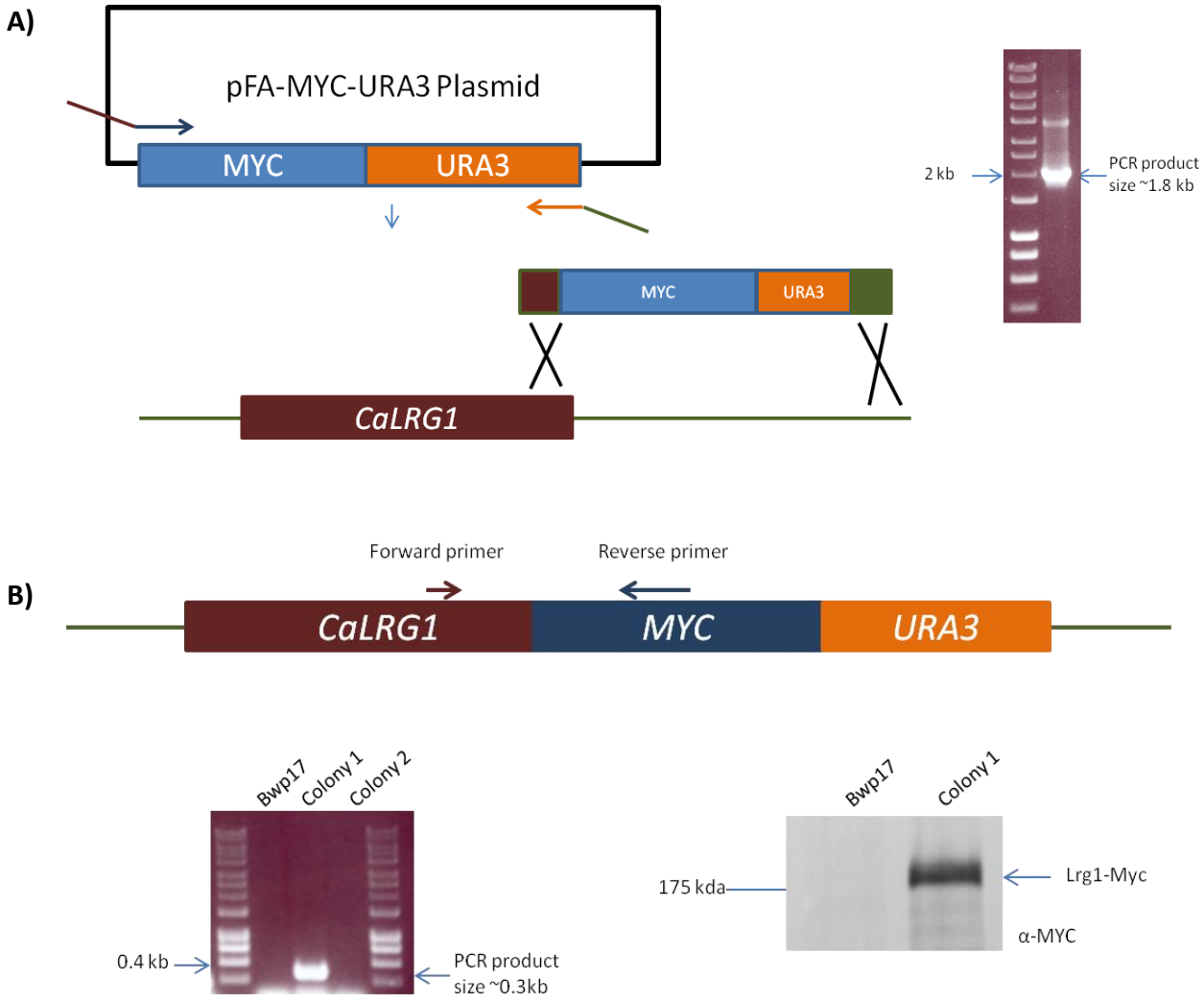

<u>Figure 4.2</u> Tagging of *Ca*Lrg1 with the MYC epitope

A) A *PFA-MYC-URA* plasmid was used to amplify a *MYC-URA3* cassette that possessed 5'identity to the end of *C. albicans LRG1* open reading frame (minus stop codon) and 3' identity to a region downstream of *LRG1*. Amplification was visualised via agarose gel electrophoresis and then transformed into *C. albicans.*

B) Correct integration of the cassette was confirmed via diagnostic PCR with a forward primer in *LRG1* and a reverse one in the MYC epitope, whilst correct expression of the fusion protein was detected by SDS-PAGE and anti-Myc western blot.

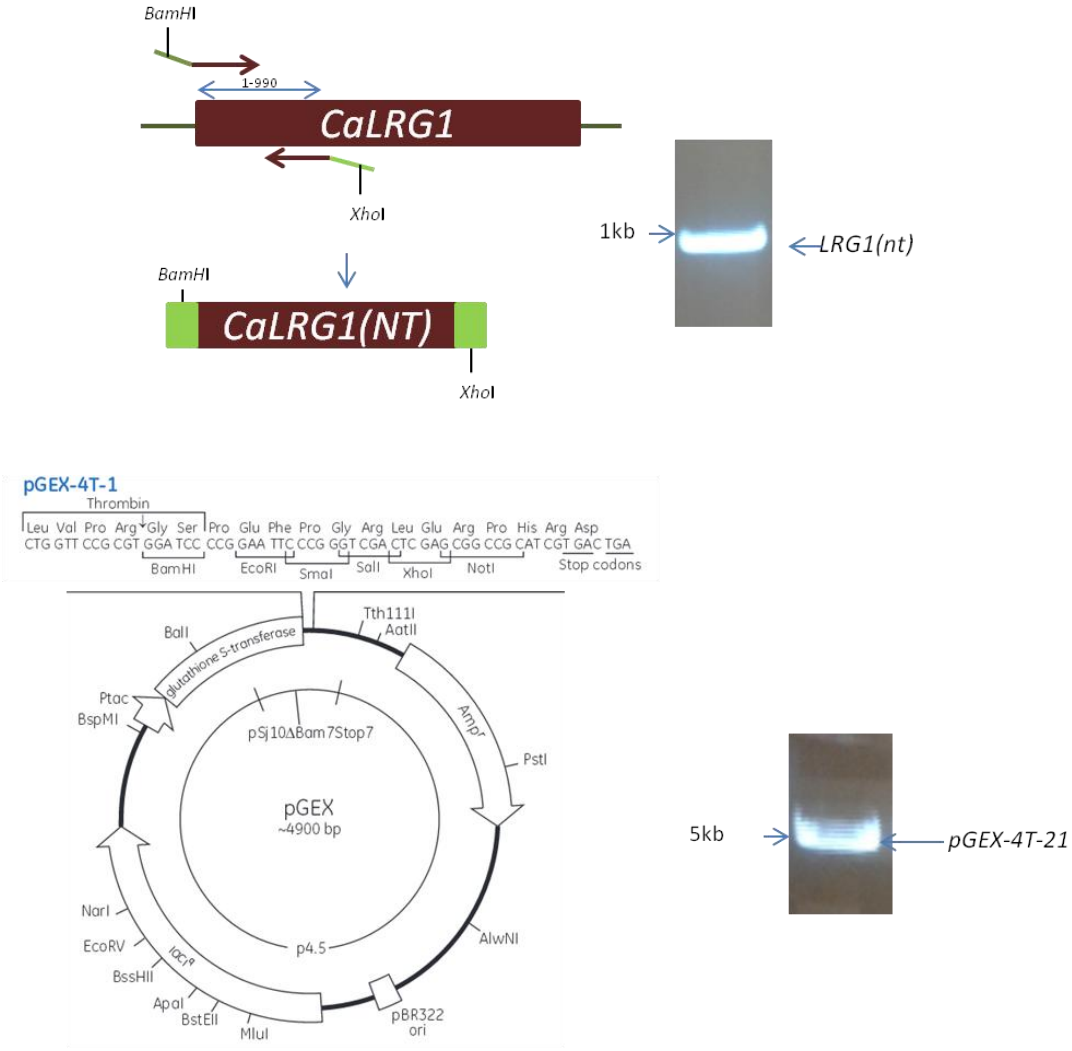

<u>Figure 4.3</u> Construction of a *GST-LRG1* expression vector

Top: The first 990 bps of the *CaLRG1* ORF was amplified with primers that incorporated a 5' BamHI and 3' Xho1 restriction endonuclease site.

Bottom: The *pGEX-4T1* plasmid (GE Healthcare) was linearised with *Xho*1 and *Bam*HI endonucleases and used in ligation reaction with the amplified *LRG1(NT).* Correct ligations were sequenced to ensure that the correct fragment was present. The resulting plasmid was then subjected to site-directed mutagenesis to mutate the four full Cdc28 consensus sites to non-phosphorylatable alanine. Two expression vectors were hence created: *GST-LRG1(NT)* and *GST-LRG1-4A(NT).*

4.2.3 The cloned *LRG1-MYC* construct

The physiological role of phosphorylation can be investigated by generating mutants in which the target residues are either substituted with non-phosphorylatable or phosphomimetic amino acids. Residues that are suspected of being phosphorylated can be mutated to phosphomimetic residues such as aspartic or glutamic acid, which will mimic the charge of a phosphate group so that the residue appears continually phosphorylated within the cell. Conversely, residues can be mutated to alanine which is unable to be phosphorylated within the cell. Using these two opposing mutations can give clues as to the cellular role of protein phosphorylation. It was of interest to see what were the effects of phosphomimetic and non-phosphorylatable mutations of the Cdc28 consensus sites in the N-terminus of Lrg1.

Previously, the standard strategy for introducing gene mutations would be to produce a transformation cassette with the mutated region of *LRG1* and selectable marker into a *LRG1/lrg1Δ* heterozygote. Homologous recombination would then take place and the mutated region would be introduced into the remaining copy of *LRG1.* However, problems have been identified using this method. Principally, it has been found that homologous recombination actually selects against deleterious mutations to produce integration of the selectable marker but not the mutated codons. For this reason, a different method of introducing a mutated version of *LRG1* was used. A MYC-tagged full length, mutated *LRG1* would be re-integrated into an *lrg1ΔΔ* strain via recombination in the *LRG1* promoter region to ensure this is the only copy of *LRG1* present. This strategy is shown in figure 4.4. The resulting strain was named *lrg1ΔΔ/LRG1-MYC.* The plasmid was used then used to mutate potential phosphorylation sites as depicted below in section 4.3.12

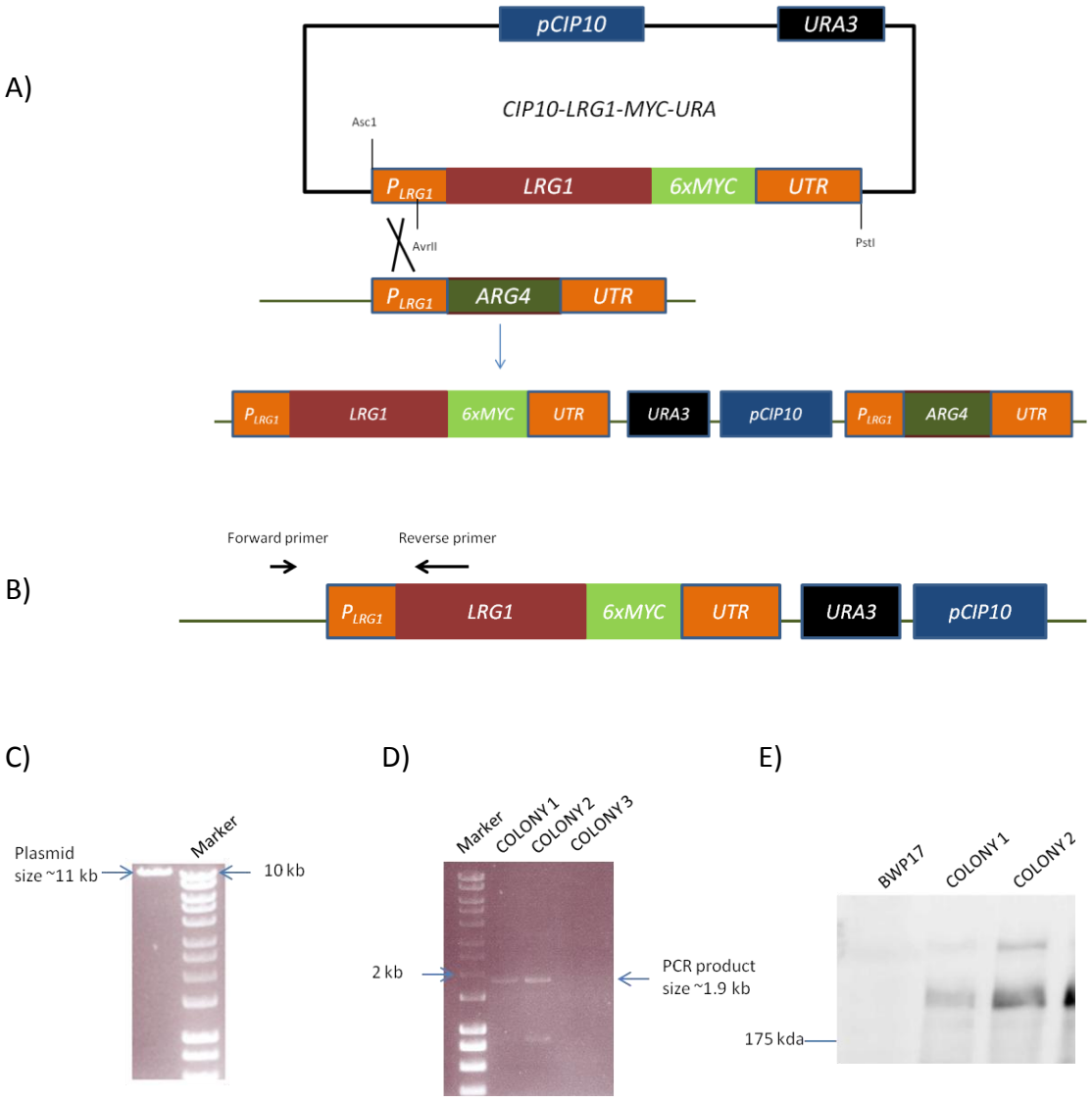

<u>Figure 4.4</u> Integration of the *pCIP10-LRG1-MYC-URA* plasmid into the lrg1ΔΔ strain

A) The *pCIP10-LRG1-MYC-URA* (Greig, J. University of Sheffield) plasmid contains a cloned, full length copy of *CaLRG1*, preceded by its own promoter. The 6xMYC tag, 3' *LRG1 UTR* and *URA3* gene are placed after the *LRG1* ORF. The plasmid is linearised via the *Avr*II site placed in the promoter region (C) and transformed into *lrg1ΔΔ*. Homologous recombination between promoter regions results in *LRG1-MYC-URA3* re-integrating at its native locus, whilst the selectable marker from the original gene deletion is retained within the genome.

B) and D) Correct integration of the plasmid was confirmed via diagnostic PCR with a forward primer upstream of P_{LRG1} and a reverse primer inside *LRG1*. Product was visualised by agarose gel electrophoresis

E) Correct expression of Lrg1-6xMYC was confirmed via SDS-PAGE and anti-MYC western blot.

4.2.4 Construction of the *pBKs-LRG1-URAF* plasmid

The *BWP17* lab strain contains only 3 selectable markers; Arginine, Uridine and Histidine. Therefore, to be able to visualise GFP-RID in the *lrg1ΔΔ/LRG1-MYC* phospho-site mutants, a recyclable marker was needed to provide an extra marker for the *pExpArg-pACT1GFPRID* plasmid. A plasmid was used (Greig, J. PhD thesis, University of Sheffield 2014) which contained a *URA3* selectable marker flanked by *FRT* sequences. In between the *FRT* sequences, the plasmid also contained the *FLP* recombinase gene (Morschhauser et al., 1999) under the control of the *SAP2* promoter. The *FKH2* regions either side of the *FRT* sequences were replaced with the regions 5' and 3' of *C. albicans LRG1* as depicted in figure 4.5. The resulting cassette was then cut from the plasmid and transformed into a *LRG1/lrg1Δ* homozygote. Homologous recombination resulted in replacement of the remaining *LRG1* with *FRT-P_{SAP2}-FLP-URA3-FRT*. Positive *LRG1ΔHIS1/LRG1ΔURAF* colonies were then grown in yeast carbon base-BSA (YCB-BSA) overnight before being plated onto 5-FOA (5-Fluoroorotic acid) media. Growth on YCB-BSA uses protein as the sole carbon source which activates the *SAP2* promoter, in turn expressing the *FLP* recombinase which utilises the *FRT* sequences either side of the *URA3* gene to excise it (Morschhauser et al., 1999). Growth on 5-FOA then selects for colonies which have consequently lost the *URA3* gene as 5-Fluoroorotic acid is converted to a suicide inhibitor by the gene product. The resulting strain; *lrg1ΔHIS1/lrg1Δ (URA^-, ARG^-)* displays only histidine prototrophy.

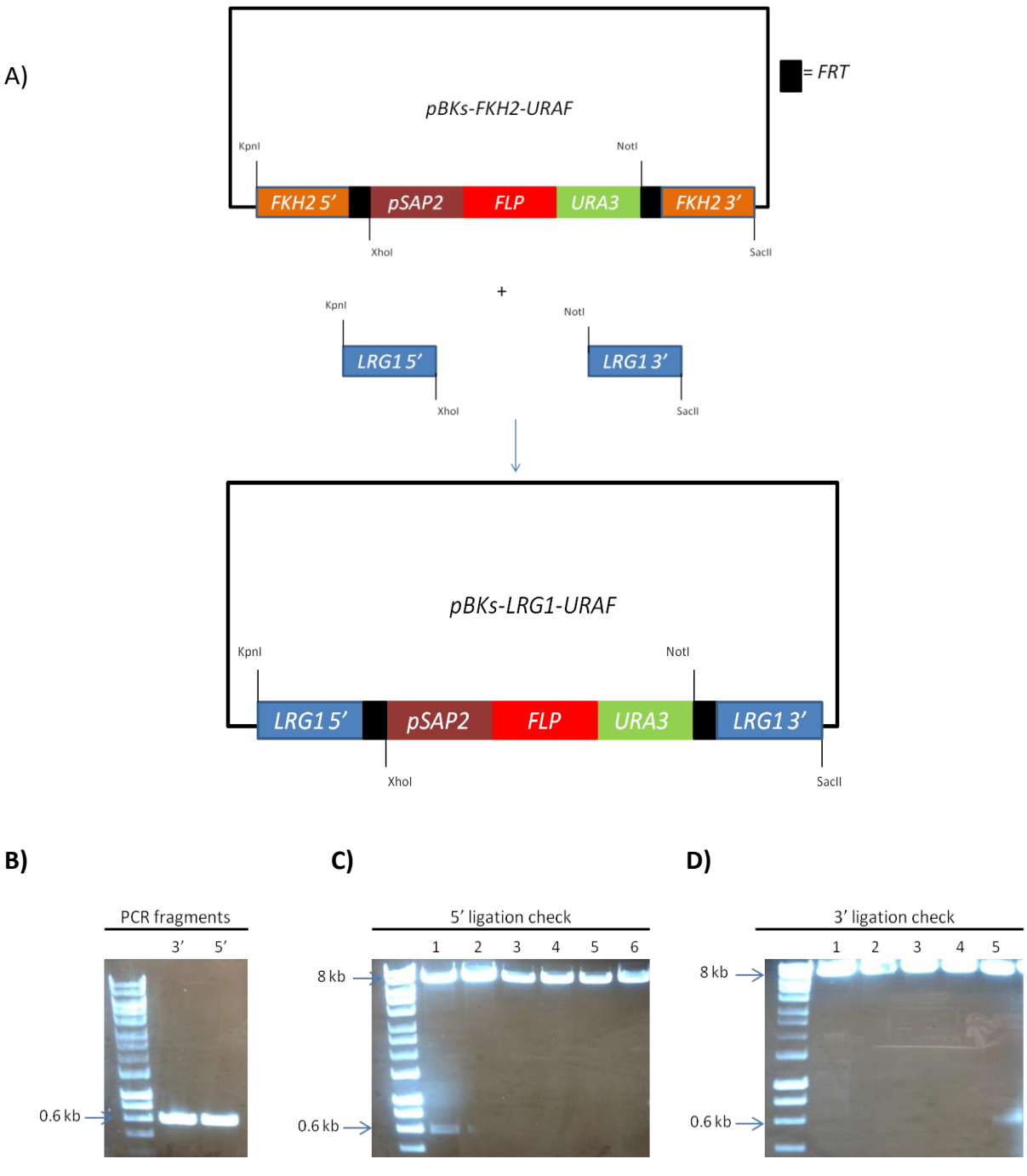

<u>Figure 4.5</u> Construction of the *pBKs-LRG1-URAF* plasmid

A) Schematic of the *pBKs-FKH2-URAF* plasmid being converted into *pBKs-LRG1-URAF*, with the *SAP2* promoter (*pSAP2) FRT* sequences, *FLP* recombinase and *URA3* gene shown.

B) 600 bp fragments of DNA from the 5' and 3' regions either side of *C. albicans LRG1* were cloned into the unique *Kpn*I-*Xho*I and *Not*I-*Sac*II sites of *pBKs-FKH2-URAF* in order to replace the *FKH2 5'* and *3'* fragments.

C) and D) Confirmation of fragment insertion via digestion with the enzymes used for insertion.

4.2.5 Construction of *lrg1ΔΔ/LRG1-MYC/GFP-RID* phospho-mutants

In order to investigate the activity of Rho1 in the Lrg1 phospho-mutants, the *pCIP10-LRG1-MYC-URA* wild-type, *2E2D* and *4A* plasmids were linearised and transformed into the *lrg1ΔΔ (URA$^-$, ARG$^-$)* strain made with the recyclable URA marker. Transformants were selected for on the grounds of histidine and uridine prototrophy and were checked via diagnostic PCR and western blot to ensure protein expression as shown in figure 4.4.

The three resulting strains were then used to transform the *pExpArg-pACT1GFPRID* (Corvest et al., 2013) plasmid into before selection on Uridine, Histidine and Arginine minus media. Correct expression of the GFP-RID protein was checked via SDS-PAGE and anti-GFP western blot as shown in chapter 3. The three strains produced were named *lrg1ΔΔ/LRG1-MYC/GFP-RID, lrg1ΔΔ/LRG1(2E2D$_{CDC28}$)-MYC/GFP-RID* and *lrg1ΔΔ/LRG1(4A$_{CDC28}$)-MYC/GFP-RID.*

4.3 Results

4.3.1 Analysis of *C. albicans* Lrg1 reveals multiple putative phosphorylation sites

The Eukaryotic Linear Motif resource predicts functional sites and motifs in Eukaryotic proteins (Dinkel et al., 2014). Analysis of *C. albicans* Lrg1 with ELM reveals four consensus phosphorylation motifs for the Cdk1/Cdc28 kinase (figure 4.6, red), characterised as S/T-P-X-K/R (Songyang et al., 1994). The four putative phosphorylation residues in these motifs are: threonine 7, serine 65, threonine 273 and serine 319. Furthermore, these motifs are located in the N-terminal extension identified as not being present in *S.cerevisiae* and one can speculate that these residues may provide a regulatory role in this protein extension. The Cdc28 kinase is also known to phosphorylate the minimal consensus site S/T-P, and a search of *Ca*Lrg1 reveals 15 of these minimal sites, 12 of which are located in the N-terminal extension (figure 4.26, brown). It has been shown that confirmed substrates for Cdc28 *in vivo* often frequently contain clusters of phosphorylation motifs (Moses et al., 2007) giving further evidence for Lrg1 as a candidate substrate for Cdc28 in *C. albicans*. Given that the N-terminal extension of *Ca*Lrg1 contains 16 of the possible 19 consensus sites adds to the evidence of a role in this region of the protein.

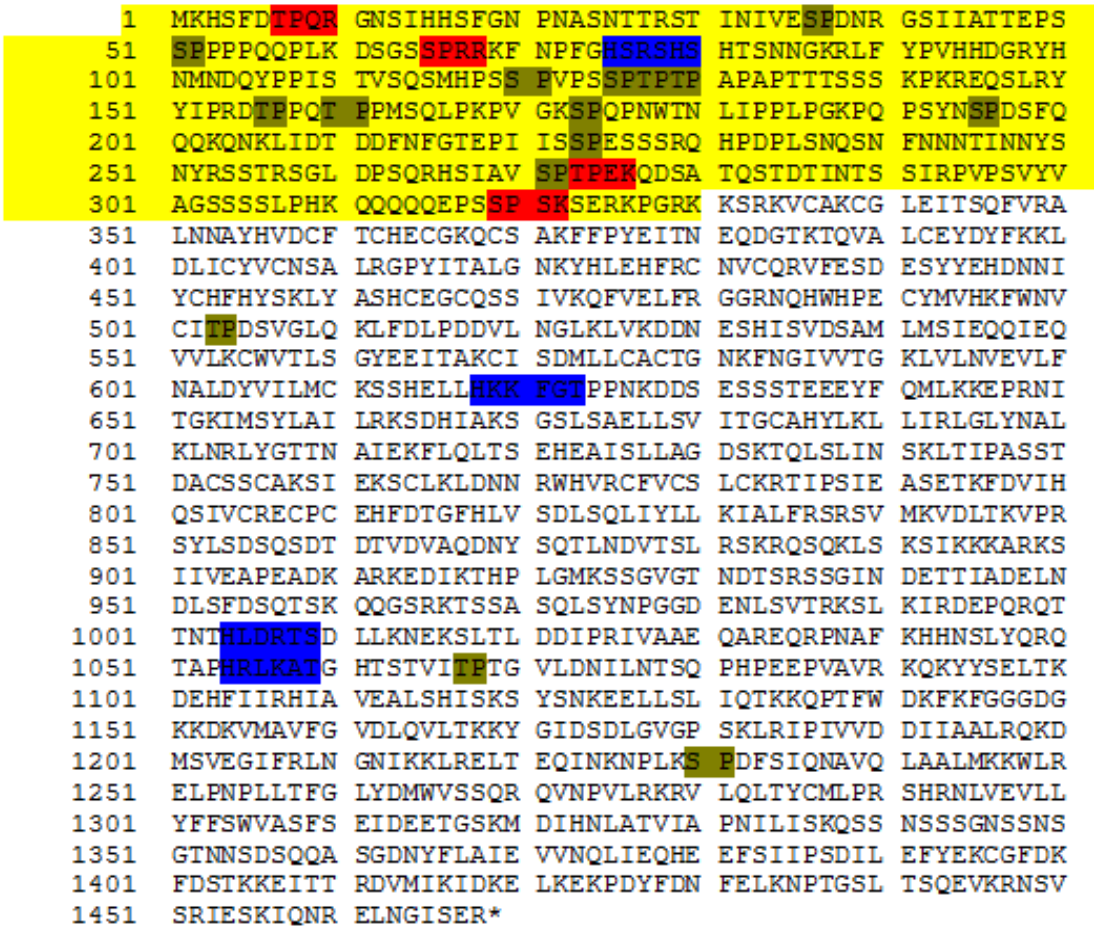

Figure 4.6 ***C. albicans*** **Lrg1 contains multiple putative Cdc28 phosphorylation sites**

Analysis of *Candida albicans* Lrg1 via the ELM database (Dinkel et al., 2014), reveals four full Cdc28 phosphorylation consensus motifs (S/T-P-X-K/R) highlighted in red. Further examination of the protein using a protein pattern search tool (Stothard, 2000) for minimal Cdc28 phosphorylation sites of either TP or SP reveals 15 such sites, highlighted in brown. The N-terminal extension of the *C. albicans* protein not seen in *S. cerevisiae* is highlighted in yellow. Phosphorylation consensus sites for the Cbk1 kinase (discussed in chapter 5) are highlighted in blue.

4.3.2 *C. albicans* Lrg1 is a phospho-protein

Phosphorylation of a protein can be detected via visualisation on a Western Blot (Wegener and Jones, 1984) where proteins with phosphate groups produce a slower migrating band than non-phosphorylated proteins, seen as a band shift. In order to analyse the phosphorylation state of Lrg1 in *C. albicans,* the *LRG1-MYC* strain was grown under yeast inducing conditions for 3 hours then subjected to protein extraction with phosphatase inhibitors. The cell lysate was run on SDS-PAGE and a western blot with anti-MYC antibody was performed. A separate lysate was also prepared without phosphatase inhibitors and treated with Lambda phosphatase and run alongside. A separate identical gel was also run and treated to an anti-PSTAIRE western blot, which recognises the PSTAIRE motif of cyclin dependent kinases, to show equal protein loading. The Results are shown in figure 4.7. In the lane with the untreated sample, two bands of Lrg1-Myc can clearly be seen, indicating a slower migrating form of the protein. The lane with the phosphatase treated sample however, shows a collapse of this doublet with only one concise band being observed. This indicates that the slower migrating band is indeed due to phosphorylation of Lrg1 during yeast growth.

4.3.3 Phosphorylation of *Ca*Lrg1 is lost upon deletion of its N-terminal region

If the phosphorylation of Lrg1 seen above is due to the cluster of Cdc28 motifs in the N-terminal extension, it follows that a version of Lrg1 lacking this region will not display any phosphorylation. To test this hypothesis, the *lrg1Δ/*P_{MAL2}*-GFP-LRG1* and *lrg1Δ/* P_{MAL2}*-GFP-LRG1 (993-4404)* strains were grown as yeast for three hours before protein extraction. A sample from each strain was then treated with lambda phosphatase treatment before being run on SDS-PAGE and subsequent western blot. The results are shown in figure 4.8. The untreated *lrg1Δ/* P_{MAL2}*-GFP-LRG1* sample shows two differentially migrating bands as before, which collapse to a single band upon phosphatase treatment, indicating that the protein is phosphorylated at this time point.

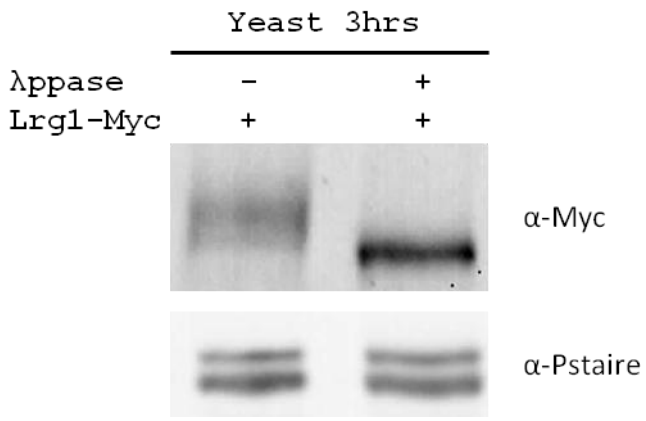

Figure 4.7 ***C. albicans*** **Lrg1 is a phospho-protein**

An overnight culture of the *LRG1-MYC* strain was re-inoculated into yeast inducing conditions for three hours. Total cell protein was then extracted in two separate samples, one with phosphatase inhibitors and one without, which was also subjected to lambda phosphatase treatment. The lysates were then run on a SDS-PAGE, followed by western blot and probing with anti-Myc antibodies. An identical gel was also run and probed with anti-PSTAIRE antibodies to show equal loading.

However, in the untreated *lrg1Δ/ P_{MAL2}-GFP-LRG1 (993-4404)* sample, the majority of the signal is in one lower band and the upper band seen in the full length protein has disappeared. However this band is actually migrating slightly faster than the phosphatase-treated sample, possibly caused by a change in the truncated protein's physical or chemical properties. There is still some slight band retardation of the protein, most probably due to phosphorylation at other sites along the protein. From this data, it can be concluded that a large amount of the phosphorylation seen on the *C. albicans* Lrg1 protein is located on the N-terminal extension, suggesting a possible role for the Cdc28 consensus motifs earlier identified.

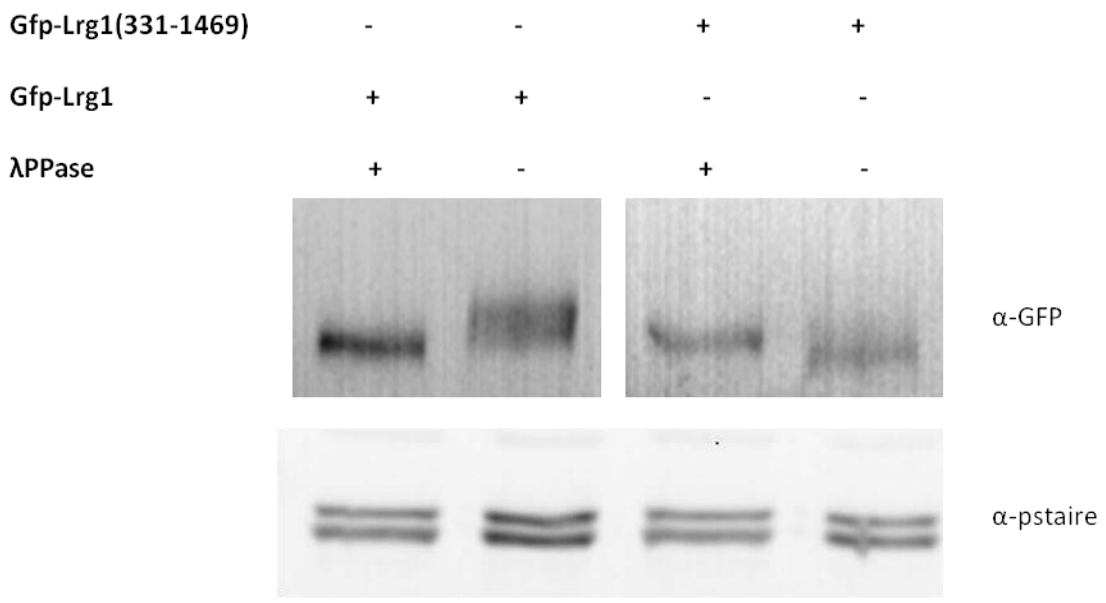

Figure 4.8 Phosphorylation of *C. albicans* Lrg1 is lost upon deletion of its N-terminal extension

The *lrg1Δ/P$_{MAL2}$-GFP-LRG1* and *lrg1Δ/P$_{MAL2}$-GFP-LRG1 (993-4404)* strains were grown in yeast-inducing conditions for 3 hours before being subjected to protein extraction. A sample of each was subjected to Lambda (λ) Phosphatase treatment before being run on SDS-PAGE and western blot with anti-GFP antibodies (top) to detect the protein. A separate gel was also run and treated to an anti-PSTAIRE western blot (bottom) to ensure that the samples were loaded equally.

4.3.4 The quantity and phosphorylation state of *Ca*Lrg1 changes upon inhibition of Cdc28

To further investigate the relationship between Cdc28 and Lrg1 *in vivo,* the phosphorylation state of Lrg1 upon inhibition of Cdc28 was explored. For this, Lrg1 was C-terminally tagged with the Myc epitope (described above) in *a CDC28-1as/cdc28Δ* strain (Bishop et al., 2010). The Cdc28-1as protein is an analogue-sensitive mutant which binds the ATP analogue 1NM-PP1, which then cannot be hydrolysed, hence locking the kinase in an inactive form (Bishop et al., 2000). The resulting strain was *LRG1-MYC/CDC28-1as/cdc28Δ.* This strain was then grown in yeast- and hyphal-inducing conditions both in the presence of 1NM-PP1 and DMSO as a negative control, respectively, before inhibition was checked by visualisation of the correct phenotype under the microscope. Cells induced to form hyphae whilst the Cdc28-

1as protein is inhibited fail to maintain polarisation of germ tubes, resulting in kinked hyphae (Bishop et al., 2010) whilst undergo elongation and swelling when grown as yeast (figure 4.9a). Cells were then treated to protein extraction, SDS-PAGE and western blot. As seen in (figure 4.9b), there is considerably less Lrg1-Myc in the samples that were subjected to 1NM-PP1 treatment compared to the control sample, even though the same amount of total cell lysate was loaded as shown with the anti-PSTAIRE blot. This indicates either less Lrg1 protein is being produced, or the protein is less stable or degraded quicker upon inhibition of Cdc28. When around 4 times more of the analogue treated sample is run than the control (figure 4.9c), it can be seen that in both yeast and hyphae, the 1NM-PP1 sample shows only the slower migrating top band of the two seen in the control samples. This indicates a hyper-phosphorylated form of the protein being present. Although at first it may seem counterintuitive that upon deletion of a kinase a protein becomes hyperphosphorylated, it has been previously reported that phosphorylation at one site is required for dephosphorylation at another, giving rise to this result (Jansen et al., 2006). However, there are other possibilities in this scenario; for example, Cdc28 may be required to act upon a phosphatase which then de-phosphorylates Lrg1. Either way, the phosphorylation state of Lrg1 changes upon inhibition of Cdc28.

4.3.5 Expression of GST-Lrg1(NT)

In order to express the recombinant GST-Lrg1(NT) wild-type and 4A phospho-mutant mutant proteins to use in an *in vitro* kinase assay, the relevant GST constructs were transformed into the BL21 *E. coli* strain. Protein expression was induced by addition of IPTG for 3 hours before protein extraction and purification via glutathione sepharose chromatography. The lysates from both induced and non-induced cells and the purified sample can be seen in figure 4.10. Induction of the Lrg1 fragment can be seen when IPTG is added at around 60 kDa (25 kDa for GST and 36 kDa for the Lrg1 fragment). It can also be seen that purification has resulted in only the GST-Lrg1 fragment and a fragment of GST alone being present.

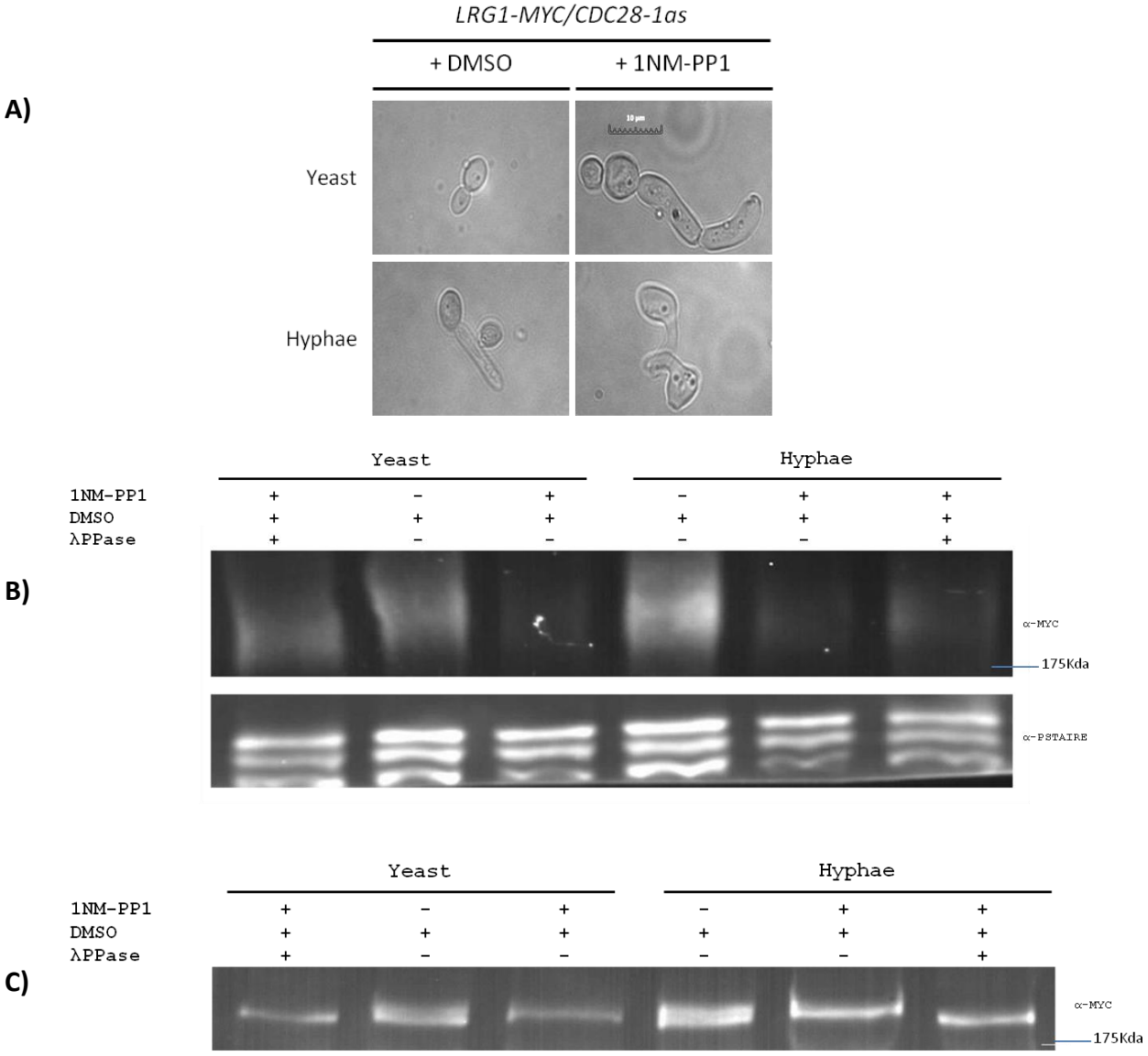

Figure 4.9 ***C. albicans*** **Lrg1 is less abundant and more phosphorylated upon inhibition of Cdc28-1as**

A) Images of *LRG1-MYC/CDC28-1as* with and without 1NM-PP1. Scale bar represents 10 µm.

B) The *LRG1-MYC/CDC28-1as* strain was grown in either the presence or absence of 1NM-PP1 for 90 minutes as both yeast and hyphae before protein extraction. A small sample was treated with λ phosphatase before 30 µg of each sample was run on SDS-PAGE and analysed by anti-MYC western blot. An identical gel was also treated to anti-PSTAIRE as a loading control.

C) The samples from (B) were re-run but adjusted so that 4 times the amount of lysate present in the 1NM-PP1 samples was present to compensate for the lower levels of Lrg1-MYC seen.

Images have been colour inverted to better visualise separate bands.

4.3.6 Cdc28 phosphorylates *C. albicans* Lrg1 *in vitro*

A strain where both copies of Cdc28 were C-terminally tagged with HA (*CDC28-HA/CDC28-HA*) (Caballero-Lima et al., 2013), was grown in yeast inducing conditions for three hours, before a protein extraction was performed. A lysate containing 2mg ml^{-1} was treated to an anti-HA immuno-precipitation (IP) to isolate the Cdc28-HA protein. To the isolated protein, 20 µg GST-Lrg1(NT) wild-type or 4A fragment was added with ATP before incubation at 37 °C. A kinase assay with the wild type fragment minus ATP and the wild-type fragment with an IP of a *BWP17* lysate was also performed as controls. After the kinase assay, reactions were run on SDS-PAGE and a western blot performed with an antibody that detects phosphorylated serine residues in the S/T-P-X-K/R CDK consensus motif.

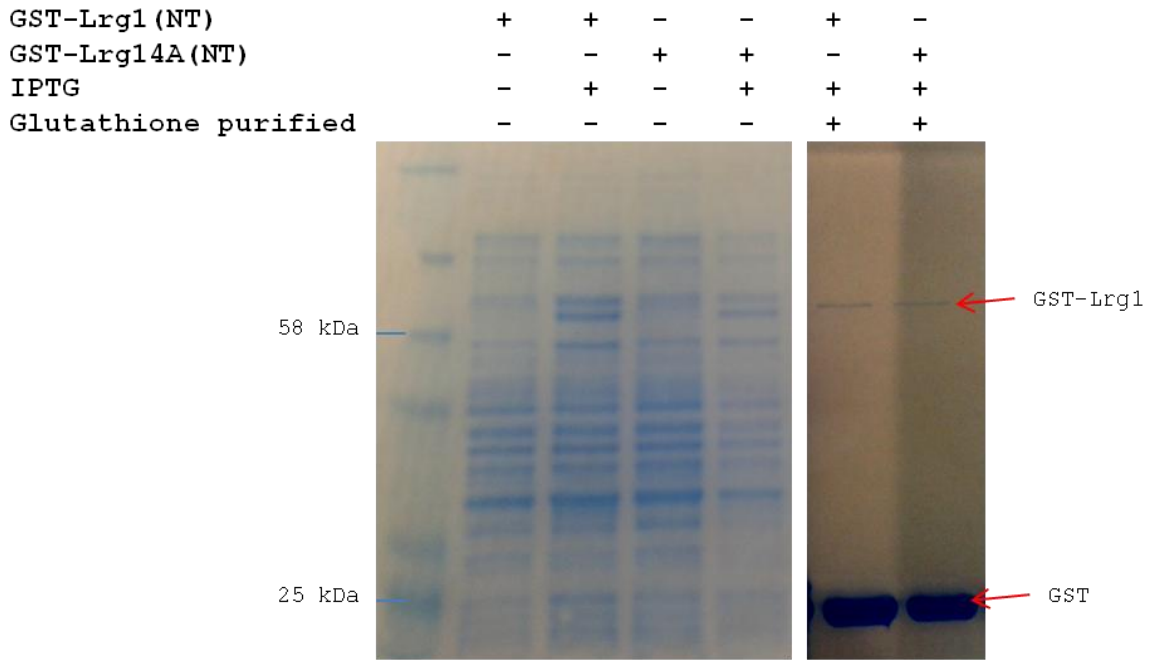

Figure 4.10 Purification of GST-Lrg1 from *E. coli* BL21 lysate

Expression of GST-Lrg1(NT) wild-type (WT) and 4A fragments was induced in *E.coli* BL21 cells by addition of IPTG to a log phase culture for 3 hours before protein extraction, glutathione sepharose chromatography and SDS-PAGE. Gels were stained with Expedeon Instant Blue protein stain. The difference between induced and non-induced cell lysates can be seen in the left panel whilst the purified fragment is seen in the right panel. The GST-Lrg1(NT) protein can be seen at around 60 kDa.

The results are shown in figure 4.11. The control lanes lacking either ATP or Cdc8-HA shows no signal as one would expect, indicating that both the IP is not contaminated with a different kinase that is capable of phosphorylating the fragment and that the reaction is dependent on ATP. The experimental lanes with the GST-Lrg1(NT) and GST-Lrg1-4A(NT) fragments each show two bands on the anti-P(S_{CDK}) blot, indicating that Cdc28 has phosphorylated each fragment during the assay. The signal from these lanes also shows two clear bands, migrating at different speeds, also confirming phosphorylation has taken place. One would however expect the 4A fragment to show no phosphorylation due the antibody only recognising full Cdc28 consensus sites, which have been mutated on this fragment. This anomaly could therefore be due to the anti-P(S_{CDK}) antibody recognising sites other than perfect Cdc28 consensus sites indicated by the manufacturer. Nonetheless, when the signal from lanes of the wild-type and 4A fragments are quantified using Syngene GeneTools gel analysis software and normalised against the amount of signal in the anti-GST and anti-HA blot, it can be seen that the wild-type fragment has a higher level of phosphorylation than the 4A mutant. It can be concluded from this that: 1) Cdc28 is capable of phosphorylating Lrg1 *in vitro* and 2) at least some of this phosphorylation occurs at the four full Cdc28 consensus sites in Lrg1 identified above.

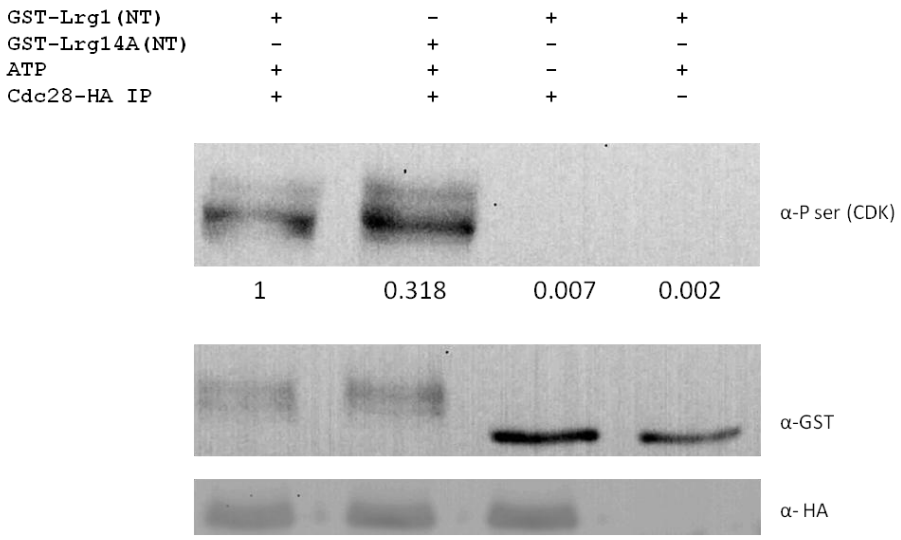

Figure 4.11 Cdc28 is capable of phosphorylating GST-Lrg1(NT) *in vitro.*
Cdc28-HA was purified from a 2 mg ml^{-1} cell lysate and used in an *in vitro* kinase assay with 20 µg of both the GST-Lrg1(NT) and GST-Lrg14A(NT) fragments. An assay with the wild-type fragment minus ATP was also carried out as a control, as was an assay lacking Cdc28-HA. After incubation, the samples were run on SDS-PAGE and treated to a western blot with anti-P(S_{CDK}) antibody (top) or probed with anti-GST (middle) antibodies. After the kinase assay, the beads used for the IP of Cdc28-HA were boiled and the lysate treated to SDS-PAGE and western blot with anti-HA anti-bodies (bottom). Lanes on each blot were quantified using Syngene GeneTools gel analysis software and the anti-P(S_{CDK}) blot normalised against the anti-GST and anti-HA images. The left lane was arbitrarily assigned a quantity of one, with other lanes shown as a proportion of this.

4.3.7 No direct interaction can be found between Cdc28 and Lrg1

In order to provide further evidence for a direct interaction between Lrg1 and Cdc28, a co-immunoprecipitation (Co-IP) was carried out. The *LRG1-MYC* strain was treated to an immuno-precipitation (IP) with anti-MYC magnetic beads to purify Lrg1-Myc. The eluted protein was then run on SDS-PAGE, western blot and probed with anti-PSTAIRE antibody to test for the presence of Cdc28. In this way, presence of Cdc28 indicates a direct interaction between the two proteins during the IP. A *BWP17* lysate was also subjected to an anti-MYC IP to ensure Cdc28 is not pulled-down non-specifically. Also due to the very transient interactions seen in kinase reactions, 4 separate IP's were performed, each with a different number of washes before elution to maximise the chances of detecting an interaction. The

results are shown in figure 4.12. It can be seen that none of the Co-IP's show any presence of Cdc28 when compared to the *BWP17* IP. This would indicate that Cdc28 and Lrg1 do not interact, however it is known that it is extremely difficult to show an interaction between a kinase and substrate using a Co-IP. Hence lack of a result does not necessarily mean no interaction takes place.

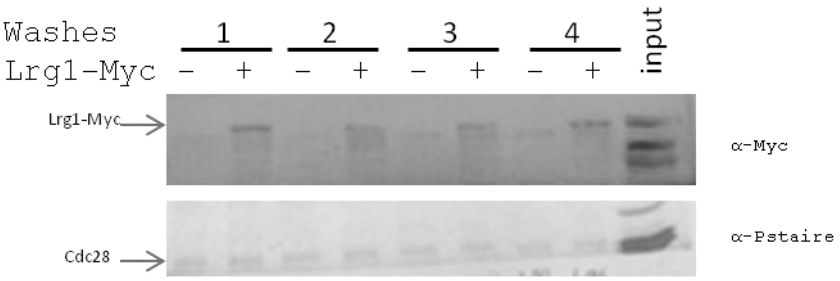

Figure 4.12 Cdc28 and Lrg1 show no interaction in a co-immunoprecipitation
The *LRG1-MYC* (+) and *BWP17* (-) strains were grown for 3 hours as yeast and then total cell lysate extracted. Lysates were adjusted to contain 2mg ml^{-1} protein and used for an IP with anti-MYC magnetic beads. To increase the chances of detecting an interaction, 4 IP's were performed, each with different amount of washes before protein elution. Eluted protein was then run on SDS-PAGE, western blot and probed with either anti-MYC or anti-PSTAIRE antibody. The input of the IP is also shown.

4.3.8 Analysis of Lrg1 phosphorylation in cyclin mutants

As discussed previously, Cdc28 requires a regulatory cyclin in order to maintain full kinase activity and phosphorylate specific substrates. The cyclin specificity of Cdc28 changes throughout the cell cycle. To try and assess which cyclin is responsible for the Cdc28 phosphorylation of Lrg1, the Lrg1 protein was epitope tagged with MYC as shown in figure 4.2, in different cyclin mutants. Strains with one copy of either the G1 cyclin Cln3 (Chapa y Lazo et al., 2005) or the mitotic cyclins Clb2 and Clb4 (Bensen et al., 2005) deleted, and the other copy placed under the control of the regulatable *MET3* promoter (Care et al., 1999) were used in order to create the following strains: P_{MET3}*-CLN3/LRG1-MYC,* P_{MET3}*-CLB2/LRG1-MYC* and P_{MET3}*-CLB4/LRG1-MYC.*

4.3.9 The phosphorylation state of Lrg1 is altered when the G1-cyclin Cln3 is depleted

To examine if the Cdc28 dependent phosphorylation of *C. albicans* requires the Cln3 cyclin, the P_{MET3}-*CLN3/LRG1-MYC* strain was grown as yeast in both the presence and absence of methionine overnight (Chapa y Lazo et al., 2005) to either induce or repress expression of the only copy of *CLN3* present, respectively. Correct repression of the gene was confirmed by visualisation of the phenotype, seen as swollen unbudded cells that form filaments (Chapa y Lazo et al., 2005), under a light microscope (figure 4.13a). Total cell protein was then extracted followed by SDS-PAGE and anti-MYC and anti-PSTAIRE western blot as a loading control. The results in figure 4.13b show that in the sample where expression of *CLN3 is* repressed by methionine, presence of Lrg1-Myc is almost undetectable. This is a similar situation to when Cdc28 is inhibited and points to either enhanced degradation of the protein or reduced expression when *CLN3* expression is repressed.

However, when the levels of the lysate with *CLN3* repressed are increased by a factor of 4 (figure 4.13c), the signal present shows a darker collapsed band compared to the de-repressed strain that has two bands present. This indicates that there is a loss of phosphorylation of Lrg1 upon repression of *CLN3* expression. However, the *CLN3*-off sample still seems to show some residual band retardation compared to the de-phosphorylated sample signifying a level of phosphorylation still remains. Taken with the Cdc28 inhibition and kinase assay results, this implies that the Cdc28-Cln3 kinase complex is responsible in part for Lrg1 phosphorylation.

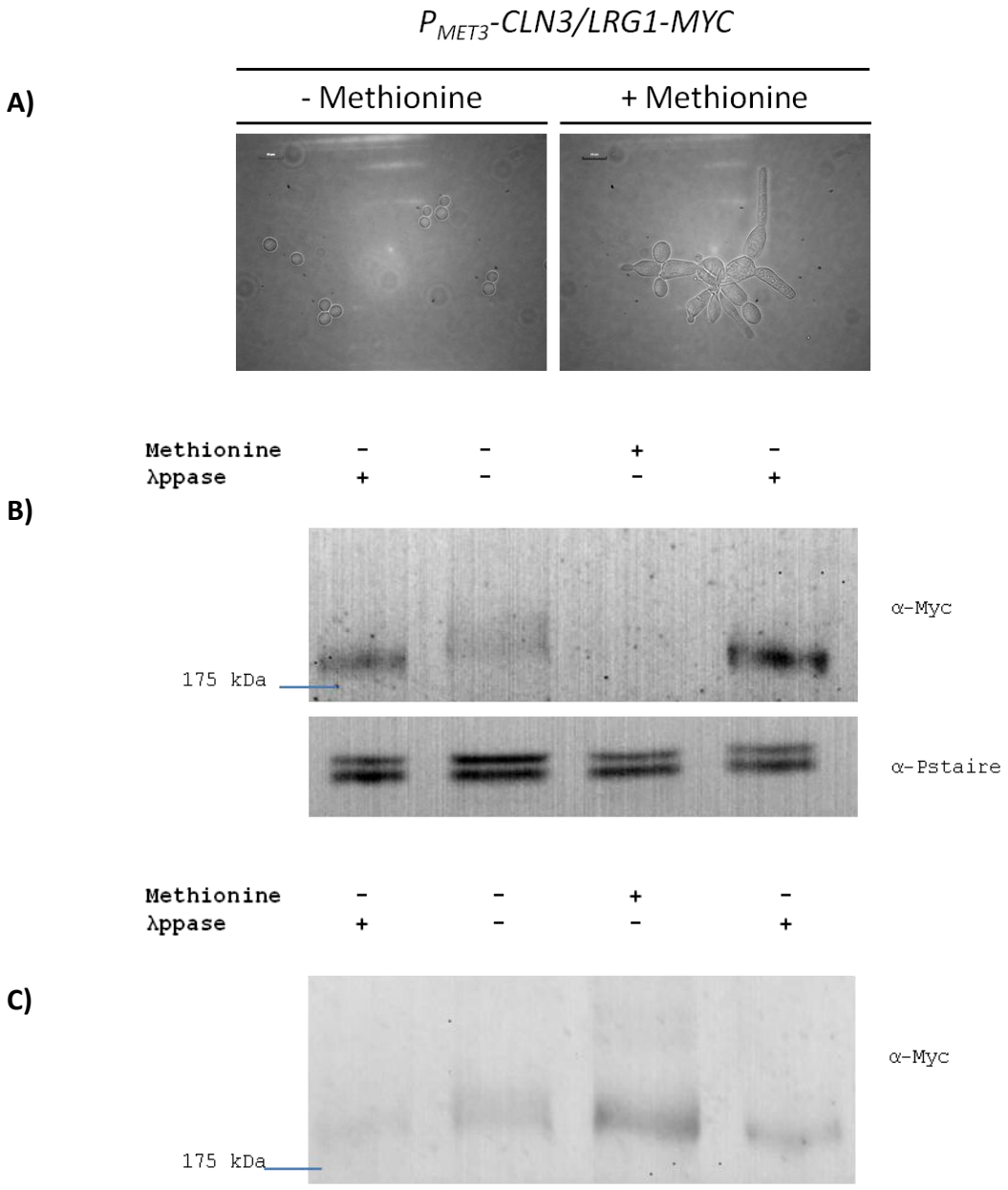

Figure 4.13 ***C. albicans*** **Lrg1 is less abundant and less phosphorylated upon depletion of the G1 cyclin Cln3**

A) Images of P_{MET3}-*CLN3/LRG1-MYC* grown under yeast inducing conditions both with and without methionine. Scale bar represents 10 µm.

(B) A P_{MET3}-*CLN3/LRG1-MYC* strain was grown for three hours in yeast-inducing conditions in both the presence and absence of methionine to either induce or repress expression of the G1 cyclin Cln3. Protein lysates were then extracted from cells before 30 µg was run on SDS-PAGE and treated to an anti-MYC western blot. An identical gel probed with anti-PSTAIRE antibody was also run as a loading control.

(C) The protein lysates from (B) were re-run, increasing the levels of the repressed sample by a factor of 4 to allow for the reduced amount of Lrg1-Myc present.

4.3.10 The mitotic cyclins Clb2 and Clb4 are not responsible for the phosphorylation of *C. albicans* Lrg1

The role of the mitotic cyclins Clb4 and Clb2 in phosphorylation of Lrg1 was assessed in a similar manner to that of Cln3. The P_{MET3}-*CLB2/LRG1-MYC* and P_{MET3}-*CLB4/LRG1-MYC* strains were re-inoculated into methionine plus or methionine minus media to induce yeast. After two hours, repression was confirmed by visualisation of the correct phenotype, seen as inviable cell with pointed, elongated projections upon depletion of Clb2 and viable pseudohyphae upon Clb4 depletion (figure 4.14a) (Bensen et al., 2005). Cells were then treated to total cell lysate extraction, SDS-PAGE and western blot (figure 4.14b) The first thing to note is that the phosphatase treated sample has run slower than the fast migrating Lrg1-Myc band, indicating that the phosphatase treatment has not worked correctly. Secondly, in contrast to the *CLN3* repression and Cdc28 inhibition, the protein levels of Lrg1-Myc remain the same when *CLB2* and *CLB4* are repressed. The phosphorylation state of Lrg1 also remains the same in repressed samples, showing two different bands indicating different phospho-forms of the protein that are also present in the control samples where the cyclins are being expressed. It can be concluded that neither of the mitotic cyclins Clb4 or Clb2 take part in the Cdc28 mediated phosphorylation of *C. albicans* Lrg1

4.3.11 The *lrg1ΔΔ/LRG1-MYC* strain shows a wild-type phenotype

To ensure that the Lrg1-Myc protein in *the lrg1ΔΔ/LRG1-MYC* re-integrated strain is functional, it was grown for 3 hours as yeast along with the *LRG1-MYC* strain, in which the promoter is native, and treated to a protein extraction, SDS-PAGE and western blot with anti-MYC antibody. An anti-PSTAIRE western blot was also performed as a loading control. As can be seen in figure 4.145a, the PSTAIRE blot shows that the samples from both strains have been equally loaded with cell lysate. In the anti-MYC blot, there is more signal from the *lrg1ΔΔ/LRG1-MYC* sample than the *LRG1-MYC* sample indicating more Lrg1 protein present. This increase in protein levels is most probably due to the fact that in the *LRG1-MYC* strain, only half of the total Lrg1 protein levels will be MYC tagged because a wild-type copy of the gene is still present, whereas in *lrg1ΔΔ/LRG1-MYC* strain, the total amount of Lrg1 is MYC tagged.

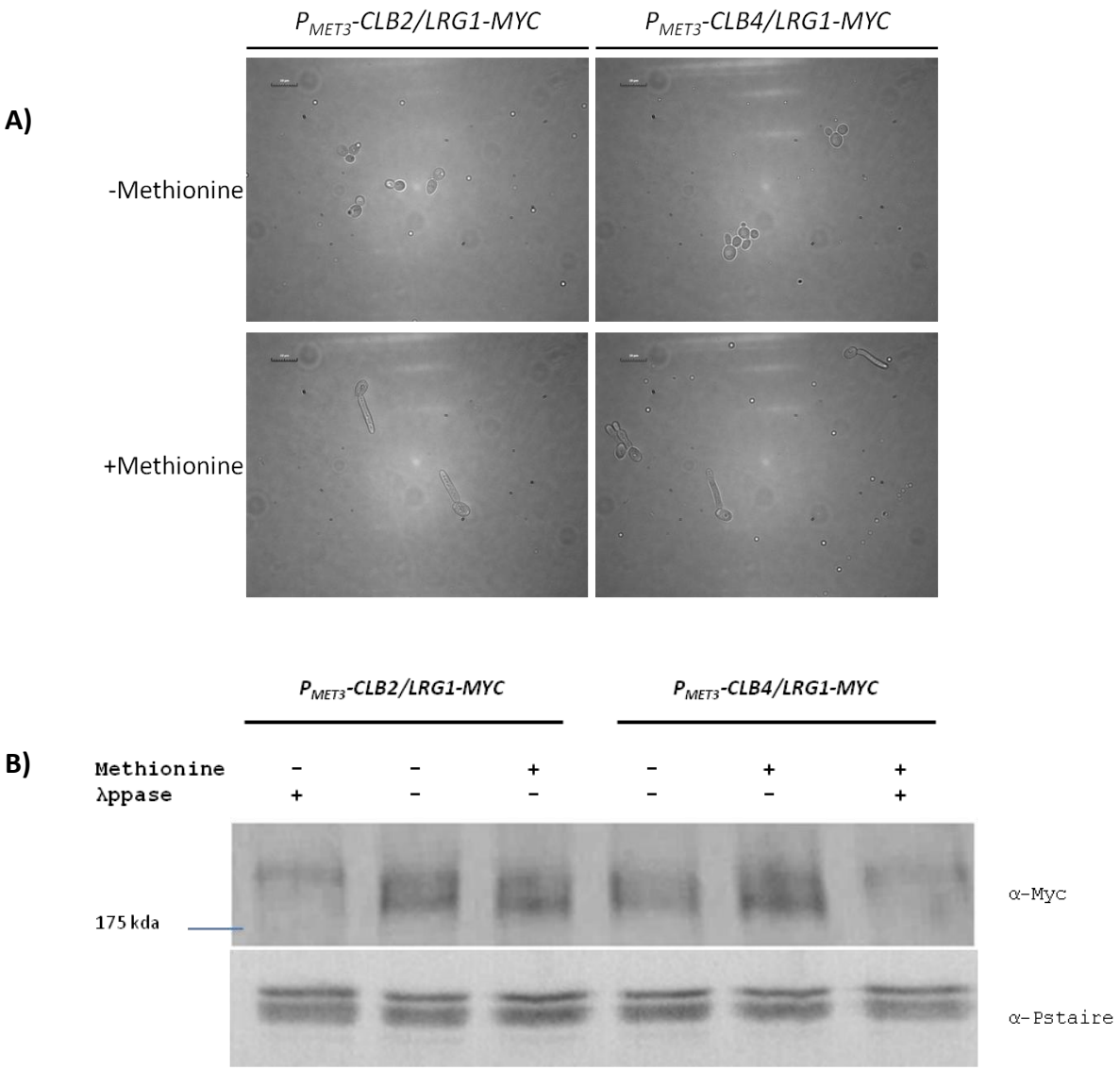

<u>Figure 4.14</u> *C. albicans* Lrg1 shows no change in phosphorylation upon depletion of the G2 cyclins Clb2 and Clb4

The P_{MET3}-*CLB2/LRG1-MYC* and P_{MET3}-*CLB4/LRG1-MYC* strains were each grown in both the presence and absence of methionine to either induce or repress the expression of Clb2 or Clb4 in yeast inducing conditions for 2 hours. After confirmation of correct phenotype via microscopy (A), cell protein was extracted and 30 µg run on SDS-PAGE followed by anti-MYC western blot (B). An identical gel was also run and probed with anti-PSTAIRE anti-bodies to serve as a loading control. Scale bar is 5 µm

A)

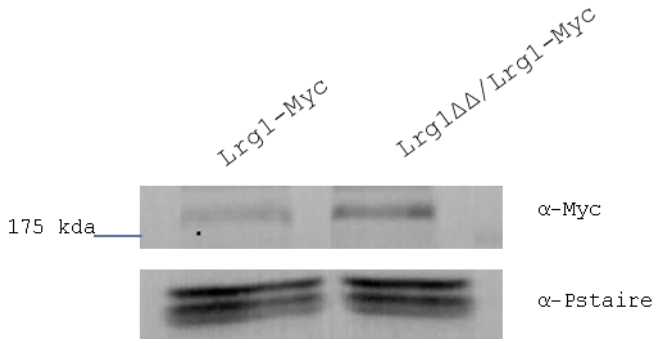
Lrg1-Myc
Lrg1ΔΔ/Lrg1-Myc
175 kda
α-Myc
α-Pstaire

B)

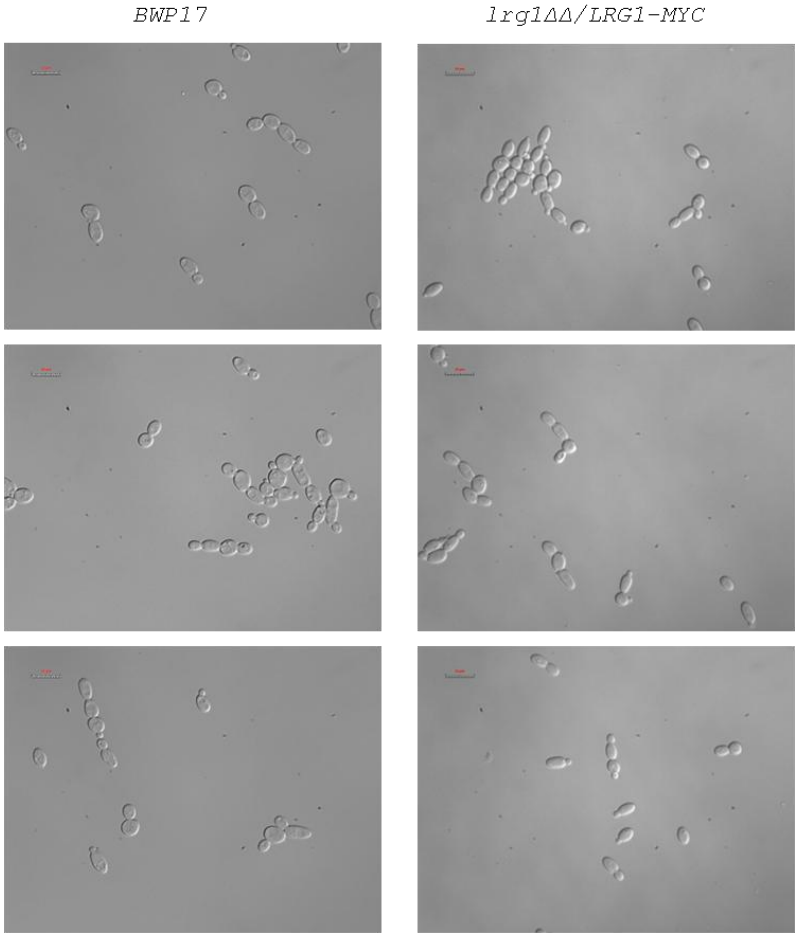
BWP17
lrg1ΔΔ/LRG1-MYC

C)

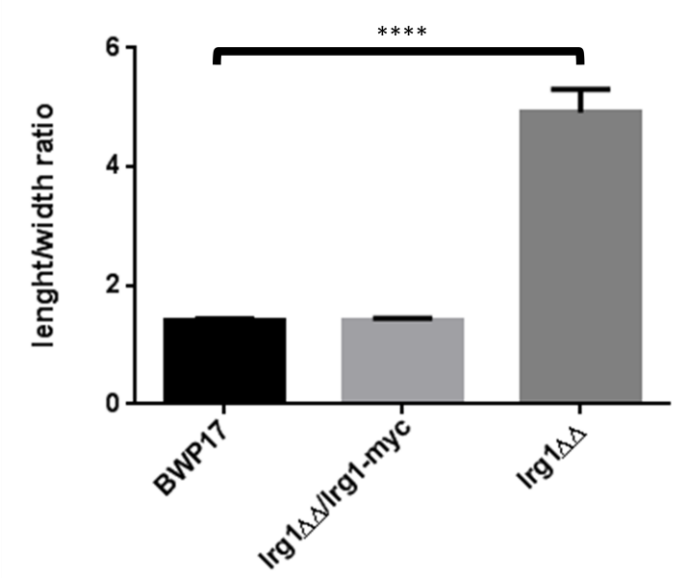
****
lenght/width ratio
6
4
2
0
BWP17
lrg1ΔΔ/lrg1-myc
lrg1ΔΔ

<u>Figure 4.15</u> Re-integration of *LRG1-MYC* into its native locus via the p*CIP10-LRG1-MYC-URA* plasmid restores wild-type levels of protein and complements the *lrg1ΔΔ* phenotype

A) The *LRG1-MYC* and *lrg1ΔΔ/LRG1-MYC* strains were grown in yeast-inducing conditions for 3 hours before total cell protein was extracted and 30 µg run on SDS-PAGE followed by both anti-MYC and anti-PSTAIRE western blot as a loading control.
B) The wild-type *BWP17* strain and the re-integrated *lrg1ΔΔ/LRG1-MYC* strain were grown for 3 hours in conditions to induce the yeast morphology, before they were fixed with formaldehyde and then visualised with a DIC light microscope.
C) Images taken in (B) were analysed with ImageJ software to measure the length/width ratios of cells of the two strains. The mean ratio of 100 cells is shown with the error bars representing the standard error of the mean (SEM). An unpaired t-test was performed on the data using GraphPad which found no significant difference between the two strains. The *BWP17* and *lrg1ΔΔ* strains are statistically different to a confidence interval of 0.0001.

As the protein levels of the re-integrated *LRG1* seem to be similar to the wild-type strain, the *lrg1ΔΔ/LRG1-MYC* was grown under yeast-inducing conditions along with the *BWP17* control strain, before formaldehyde fixing and visualisation via a DIC microscope. The images of the two strains are shown in figure 4.15b. The images show that the strain with *LRG1* re-integrated into its own native locus has morphology similar to that of the control strain and no longer displays the phenotype of an *LRG1* deletion. To confirm this, length to width ratios of 100 cells of *lrg1ΔΔ/LRG1-MYC* were compared to that of *BWP17* (figure 4.15c). The results show that *BWP17* has an average length: width ratio of 1.411 with a standard error of +/- 0.031, whilst the re-integrated strain as a mean ratio of 1.423 +/- 0.031. Using an unpaired t-test test reveals no significant difference between the two. It can be concluded then reintegration of *LRG1-MYC* via homologous recombination of the linearised plasmid restores normal growth phenotype and wild-type levels of Lrg1.

4.3.12 Mutation of *LRG1* in the Cdc28 full phosphorylation consensus sites

To investigate if *C. albicans* Cdc28 phosphorylates the four full phosphorylation consensus site in the N-terminus of Lrg1, the codon for each of the putative critical residues was mutated in the *pCIP10-LRG1-MYC-URA* plasmid using site directed mutagenesis. The codons for each of the four residues -T7, S65, T273 and S319- were mutated to the codon for non-phosphorylatable alanine (figure 4.16b), sequenced in full to ensure no other mutations had been introduced and transformed into the *lrg1ΔΔ* strain as above. In the same manner, the two serine residues were also mutated to aspartic acid and the two threonine residues to glutamic acid (figure 4.16a), which mimic constant phosphorylation at these sites but retain the size of the side chain of the replaced residues. The mutated plasmids were then transformed into the *lrg1ΔΔ* strain as shown in figure 4.4, resulting in *lrg1ΔΔ/LRG1(4A$_{CDC28}$)-MYC* and *lrg1ΔΔ/LRG1(2E2D$_{CDC28}$)-MYC* strains.

4.3.13 The phenotypic effects of the Lrg1(4A$_{CDC28}$) and Lrg1(4E$_{CDC28}$) mutations

The effects of the non-phosphorylatable and phosphomimetic mutations were analysed via growth of the *lrg1ΔΔ/LRG1(4A$_{CDC28}$)-MYC* and *lrg1ΔΔ/LRG1(2E2D$_{CDC28}$)-MYC* strains for 3 hours as yeast followed by visualisation under a light microscope. *BWP17* was also grown as a control strain. The images are shown in figure 4.17a. To analyse the phenotype of the different strains, the length to width ratios of 100 cells per strain was calculated and is represented in figure 4.17b. The length to width ratio of *BWP17* is 1.411, with a standard error of ± 0.031 with the *lrg1ΔΔ/LRG1(4A$_{CDC28}$)-MYC* strain having a slightly higher ratio of 1.430 ± 0.039. However the two ratios do not show any significant difference in an unpaired t-test, implying that the inability to phosphorylate Lrg1 at the four full Cdc28 consensus sites does not impair the protein function.

A)

```
caLrg1         1 MKHSFDTPQRGNSIHHSFGNPNASNTTRSTINIVESPDNRGSIIATTEPSSPPPPQQPLK
Lrg14E         1 MKHSFDEPQRGNSIHHSFGNPNASNTTRSTINIVESPDNRGSIIATTEPSSPPPPQQPLK
                 ****** **************************************************

caLrg1        61 DSGSSPRRKFNPFGHSRSHSHTSNNGKRLFYPVHHDGRYHNMNDQYPPISTVSQSMHPSS
Lrg14E        61 DSGSDPRRKFNPFGHSRSHSHTSNNGKRLFYPVHHDGRYHNMNDQYPPISTVSQSMHPSS
                 **** **************************************************

caLrg1       121 PVPSSPTPTPAPAPTTTSSSKPKREQSLRYYIPRDTPPQTPPMSQLPKPVGKSPQPNWTN
Lrg14E       121 PVPSSPTPTPAPAPTTTSSSKPKREQSLRYYIPRDTPPQTPPMSQLPKPVGKSPQPNWTN
                 ************************************************************

caLrg1       181 LIPPLPGKPQPSYNSPDSFQQQKQNKLIDTDDFNFGTEPIISSPESSSRQHPDPLSNQSN
Lrg14E       181 LIPPLPGKPQPSYNSPDSFQQQKQNKLIDTDDFNFGTEPIISSPESSSRQHPDPLSNQSN
                 ************************************************************

caLrg1       241 FNNNTINNYSNYRSSTRSGLDPSQRHSIAVSPTPEKQDSATQSTDTINTSSIRPVPSVYV
Lrg14E       241 FNNNTINNYSNYRSSTRSGLDPSQRHSIAVSPEPEKQDSATQSTDTINTSSIRPVPSVYV
                 ******************************** ************************

caLrg1       301 AGSSSSLPHKQQQQQEPSSPSKSERKPGRK
Lrg14E       301 AGSSSSLPHKQQQQQEPSDPSKSERKPGRK
                 ****************** ***********
```

B)

```
caLrg1         1 MKHSFDTPQRGNSIHHSFGNPNASNTTRSTINIVESPDNRGSIIATTEPSSPPPPQQPLK
Lrg14A         1 MKHSFDAPQRGNSIHHSFGNPNASNTTRSTINIVESPDNRGSIIATTEPSSPPPPQQPLK
                 ****** **************************************************

caLrg1        61 DSGSSPRRKFNPFGHSRSHSHTSNNGKRLFYPVHHDGRYHNMNDQYPPISTVSQSMHPSS
Lrg14A        61 DSGSAPRRKFNPFGHSRSHSHTSNNGKRLFYPVHHDGRYHNMNDQYPPISTVSQSMHPSS
                 **** **************************************************

caLrg1       121 PVPSSPTPTPAPAPTTTSSSKPKREQSLRYYIPRDTPPQTPPMSQLPKPVGKSPQPNWTN
Lrg14A       121 PVPSSPTPTPAPAPTTTSSSKPKREQSLRYYIPRDTPPQTPPMSQLPKPVGKSPQPNWTN
                 ************************************************************

caLrg1       181 LIPPLPGKPQPSYNSPDSFQQQKQNKLIDTDDFNFGTEPIISSPESSSRQHPDPLSNQSN
Lrg14A       181 LIPPLPGKPQPSYNSPDSFQQQKQNKLIDTDDFNFGTEPIISSPESSSRQHPDPLSNQSN
                 ************************************************************

caLrg1       241 FNNNTINNYSNYRSSTRSGLDPSQRHSIAVSPTPEKQDSATQSTDTINTSSIRPVPSVYV
Lrg14A       241 FNNNTINNYSNYRSSTRSGLDPSQRHSIAVSPAPEKQDSATQSTDTINTSSIRPVPSVYV
                 ******************************** ************************

caLrg1       301 AGSSSSLPHKQQQQQEPSSPSKSERKPGRK
Lrg14A       301 AGSSSSLPHKQQQQQEPSAPSKSERKPGRK
                 ****************** ***********
```

<u>Figure 4.16</u> Production of Lrg1(2E2D) and Lrg1(4A) phospho-mutants.

Site directed mutagenesis was carried out on the *pCIP10-LRG1-MYC-URA* plasmid to replace the serine/threonine residues of the Cdc28 full consensus sites to either phosphomimetic aspartic/glutamic acid (A) or non-phosphorylatable alanine (B). These plasmids were then linearised and transformed into the *lrg1ΔΔ* strain to give rise to the *lrg1ΔΔ/LRG1(4A$_{CDC28}$)-MYC* and *lrg1ΔΔ/LRG1(2E2D$_{CDC28}$)-MYC* strains.

The images of *lrg1ΔΔ/LRG1(2E2D$_{CDC28}$)-MYC* appear to show a similar phenotype to the *lrg1ΔΔ* strain, with cells that have an increase in polarisation and are elongated. The cells length: width ratio of 2.075 ± 0.078 confirms this increase in cell length, similar to, but not as severe as cells lacking Lrg1 entirely (4.916 ± 0.389).

In addition, using the equation for the volume of a prolate ellipsoid, average cellular volume was calculated for each strain. As depicted in figure 4.17c, the *lrg1ΔΔ/LRG1(2E2D$_{CDC28}$)-MYC* strain shows an increase in cellular volume, 94.88 ±4.6 μm^3 compared to 67.04 ±2.3 μm^3 in the wild-type cells. This is an increase of 1.4 times the volume of wild-type cells, similar to the increase seen in the length to width ratio, and is not surprising given the extra cell length shown in these cells. In contrast, the *lrg1ΔΔ/LRG1(4A$_{CDC28}$)-MYC* strain shows decreased cell volume (54.51 ±2. μm^3), a ratio of 0.8 times the volume of the wild-type strain. Perhaps this indicates that the cells have the same proportions as wild-type cells, but are slightly smaller. Both strains are significantly different to the wild-type strain in an unpaired t-test with p-values of 0.0001.

From these results two things can be deduced. First, as the Lrg1(2E2D$_{CDC28}$) mutant protein appears to possess a similar phenotype to that of the strain lacking the protein, it can be said that phosphorylation of Lrg1 by Cdc28 in *C. albicans* in these four full consensus sites effectively inhibits the action of the protein, either through its GAP activity on Rho1 or its localisation within the cell. Secondly, mutation of the four full Cdc28 consensus sites to non-phosphorylatable alanine has little effect on the cells, only decreasing their volume. This is a similar situation to when the N-terminal extension containing the sites is deleted. Taking these pieces of evidence together suggests that the N-terminal extension of *C. albicans* Lrg1 not seen in the homologous *S. cerevisiae* protein acts as a negative regulator of the protein rather than a positive one. That is the organism can grow happily without or being unable to phosphorylate the extension, but it can be modified in such a way as to inhibit the proteins function if required. Given that the lack of Lrg1 in *C. albicans* results in highly polarised growth could this extension have emerged to allow the organism to grow in the hyphal and pseudohyphal morphologies required for its virulence?

A)

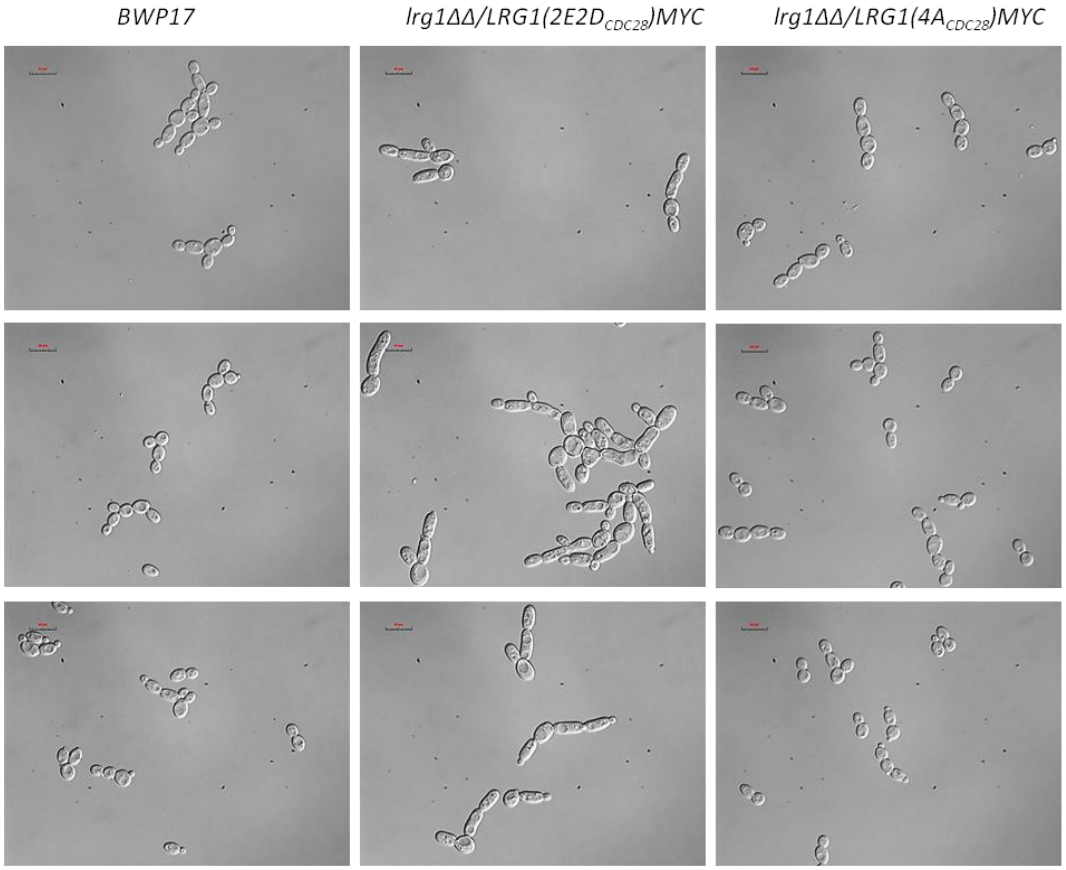
BWP17
lrg1ΔΔ/LRG1(2E2D$_{CDC28}$)MYC
lrg1ΔΔ/LRG1(4A$_{CDC28}$)MYC

B)

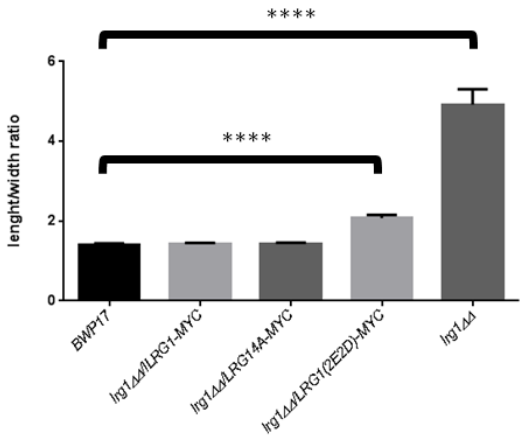
****
****
lenght/width ratio
0
2
4
6
BWP17
lrg1ΔΔ/LRG1-MYC
lrg1ΔΔ/LRG14A-MYC
lrg1ΔΔ/LRG1(2E2D)-MYC
lrg1ΔΔ

C)

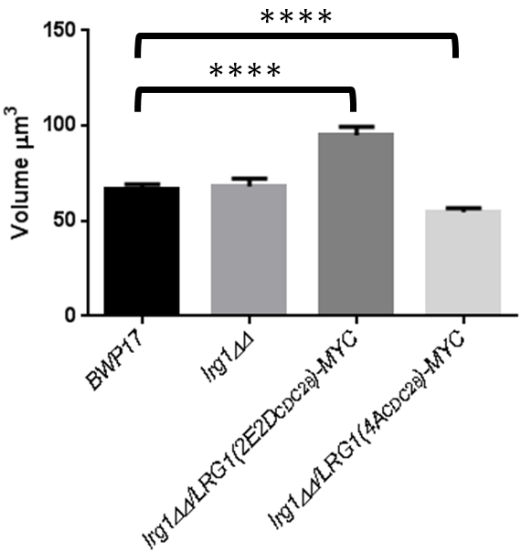
****
****
Volume µm^3
0
50
100
150
BWP17
lrg1ΔΔ
lrg1ΔΔ/LRG1(2E2DCDC28)-MYC
lrg1ΔΔ/LRG1(4ACDC28)-MYC

<u>Figure 4.17</u> The Lrg1(2E2D) mutant displays a similar phenotype to cells lacking Lrg1

A) The *lrg1ΔΔ/LRG1(4A$_{CDC28}$)-MYC* and *lrg1ΔΔ/LRG1(2E2D$_{CDC28}$)-MYC* strain were grown in conditions to induce the yeast morphology for 3 hours before cells were fixed with formaldehyde. The wild-type *BWP17* strain was also grown as control. Cells were then visualised via a Leica DIC light microscope.

B) ImageJ was used to measure the length/width ratios of cells imaged in (A). The average ratio for each strain is shown with its SEM along with that of the *lrg1ΔΔ* strain and *lrg1ΔΔ/LRG1-MYC.* An unpaired two-tailed t-test revealed that he *BWP17* and *lrg1ΔΔ/LRG1(2E2D$_{CDC28}$)-MYC* data were statically different to within a 0.0001 confidence interval. N=50

C) Average cell volume for each strain was calculated using the equation for the volume of a prolate ellipsoid: $V=4/3Pi*ab^2$. N=50

4.3.14 The phosphorylation state of the Lrg1 phospho-mutants

Due to the altered charge provided by phospho-mimetic or non-phosphorylatable mutations, mutated proteins should show differing mobility when run on SDS-PAGE. To investigate whether the Lrg1 phospho-mutants had an altered mobility, the *LRG1-MYC, lrg1ΔΔ/LRG1(2E2D$_{CDC28}$)-MYC* and *lrg1ΔΔ/LRG1(4A$_{CDC28}$)-MYC* strains were grown as yeast for three hours before total cell lysate was extracted and run on SDS-PAGE. A western blot was then performed and probed with anti-MYC antibodies. A sample of Lrg1-Myc was also treated with lambda phosphatase and run alongside as a control. An identical gel was run and probed with anti-PSTAIRE as a loading control. Results are shown in figure 4.18. The Lrg1(2E2D$_{CDC28}$)-MYC and Lrg1(4A$_{CDC28}$)-MYC proteins both show the same two bands as Lrg1-Myc, indicating that the mutations haven't had an effect on the mobility of either the non-phosphorylated or phosphorylated form of the proteins.

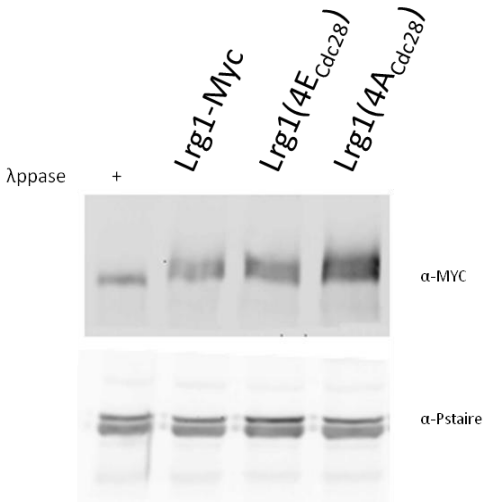

Figure 4.18 The Lrg1 (2E2D) and (4A) mutants do not have an altered mobility on SDS-PAGE

The *LRG1-MYC, lrg1ΔΔ/LRG1(2E2D$_{CDC28}$)-MYC* and *lrg1ΔΔ/LRG1(4A$_{CDC28}$)-MYC* strains were grown as yeast for 3 hours before their cell lysate was run on SDS-PAGE along with a phosphatase treated Lrg1-Myc sample. A western blot was then performed and then probed with anti-MYC antibodies. An identical gel was run and probed with anti-PSTAIRE antibodies as a loading control.

4.3.15 Growth of the Lrg1 phospho-mutants on Caspofungin

Due to the similar phenotype to cells lacking *LRG1* that the *lrg1ΔΔ/LRG1(2E2D)-MYC* strain shows, it was decided to analyse the phospho-mutant's growth on the antifungal drug caspofungin. Overnight cultures of *lrg1ΔΔ/LRG1(4A$_{CDC28}$)-MYC* and *lrg1ΔΔ/LRG1(2E2D $_{CDC28}$)-MYC* strains were sonicated briefly, adjusted to read the same absorbance at OD_{600}, diluted to $1x10^4$ and $1x10^6$ before being spotted onto plates containing an increasing concentration of caspofungin (figure 4.19). The *BWP17* and *lrg1ΔΔ* strains are also shown for comparison. The results show that cells growing with the Lrg1(2E2D$_{CDC28}$)-MYC protein are hyper-susceptible to all concentrations of the drug when compared to the wild-type cells. However, the phospho-mutant is seen to grow slightly better in the presence of caspofungin than the *lrg1ΔΔ* cells. This result confirms what is seen with the length: width ratios of the strains above: that the phospho-mimetic mutations result in a similar, but not as severe, phenotype to cells that lack *LRG1*. On the other hand, the strain with the Lrg1(4A$_{CDC28}$)-MYC protein shows an increase in growth on all concentrations of the drug when compared to the wild-type strain, indicating a resistance to caspofungin. Interestingly, although no

obvious phenotype is seen visually in these cells, the mutation of the Cdc28 sites to non-phosphorylatable alanine residues does result in caspofungin resistance.

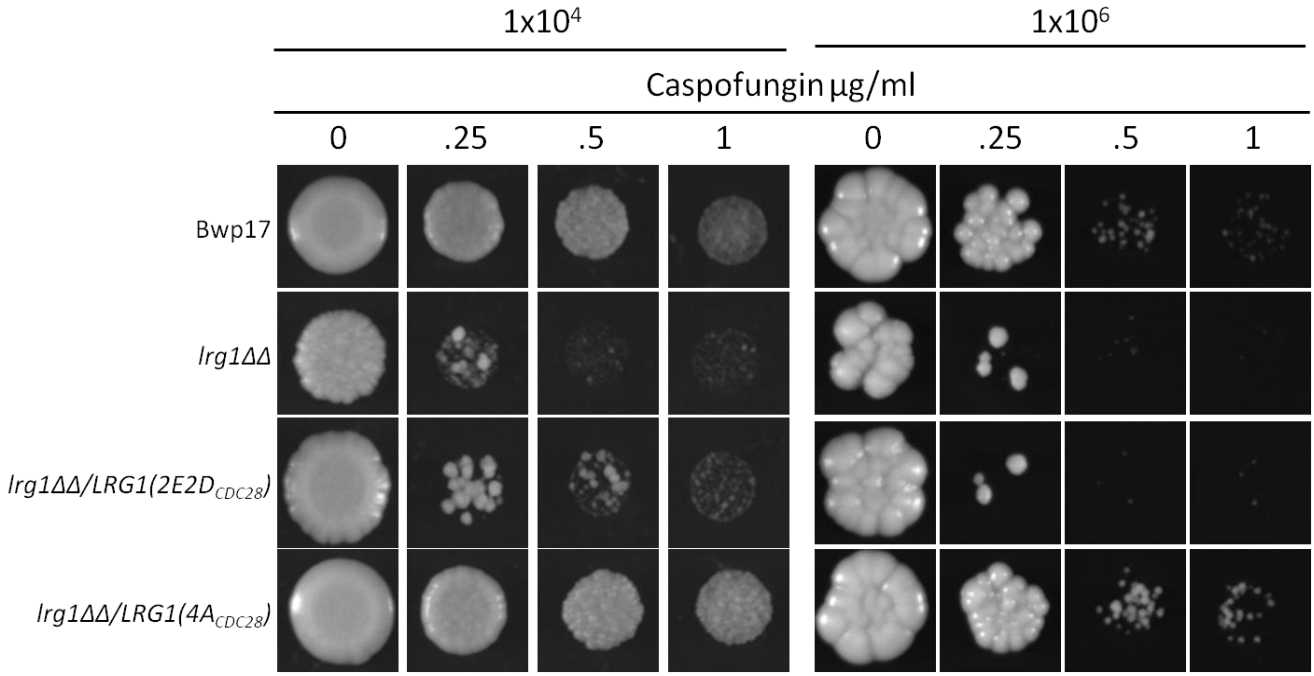

Figure 4.19 Phospho-mimetic mutations at the Cdc28 consensus sites within Lrg1 increase susceptibility to caspofungin

The two strains expressing Lrg1 with phosphomimetic or non-phosphorylatable mutations were grown in YPD overnight then sonicated briefly before adjustment to read the same absorbance at OD_{600}. The cells were then prepared to the indicated dilutions and spotted onto YPD plates containing increasing concentrations of caspofungin.

4.3.16 Mutagenesis of full and minimal Cdc28 sites within *Ca*Lrg1

This study has already shown that full Cdc28 consensus sites on the *C. albicans* Lrg1 protein can exert control over polarised growth within the cell. However, there are also 15 minimal Cdc28 phosphorylation sites in the protein, 12 of which are within the N-terminal extension. To investigate the role of these sites, the *pCIP10-LRG1(2E2D$_{CDC28}$)-MYC-URA* plasmid was mutated using multi-site directed mutagenesis to mutate the 15 remaining serine/threonine residues to either phospho-mimetic aspartic acid or glutamic acid, respectively. Due to time constraints, it was only possible to mutate 11 of the 15 minimal sites, resulting in the

plasmid containing the following mutations: (T7E, S65D, T273E, S319D,S36D,S50D,S120D,S125D,T127E,T129E,S173D,S195D,S271D,T503E,T1067E).

This plasmid was then transformed into the *lrg1ΔΔ* strain to produce *lrg1ΔΔ/LRG1(15E$_{CDC28}$)-MYC.* This strain was then induced to grow as yeast for 3 hours before ethanol fixation and visualisation with a Leica light microscope, shown in figure 4.20 (left panel). The *BWP17* strain was grown at the same time as a control. Surprisingly, the 15E mutant, which includes the four phosphomimetic full Cdc28 sites, does not show the same hyperpolarised, elongated cell phenotype that the *LRG1(2E2D$_{CDC28}$)-MYC* strain does. Instead, when the average length: width ratio of the *lrg1ΔΔ/LRG1(15E$_{CDC28}$)-MYC* cells are compared to the *BWP17* strain (figure 4.20, right panel), they are actually more spherical. The average *BWP17* cells length: width ratio is 1.21± .02 (SEM) whilst the average for cells with the Lrg1(15E$_{CDC28}$)-Myc protein is 1.08± .01. This indicates that the addition of the 11 phospho-mimetic mutations in minimal Cdc28 consensus sites has conversely led to a loss of polarisation in the cell and an increase in isotropic growth. Interestingly, when the average cellular volume of the mutant is calculated, it is larger to a significant difference than the wild-type (figure 4.20, bottom panel) due to the more spherical shape. Because of the opposite effects of the 2E2D and 15E mutants, it could be speculated that phosphorylation at these sites is used to control the protein in antagonistic ways.

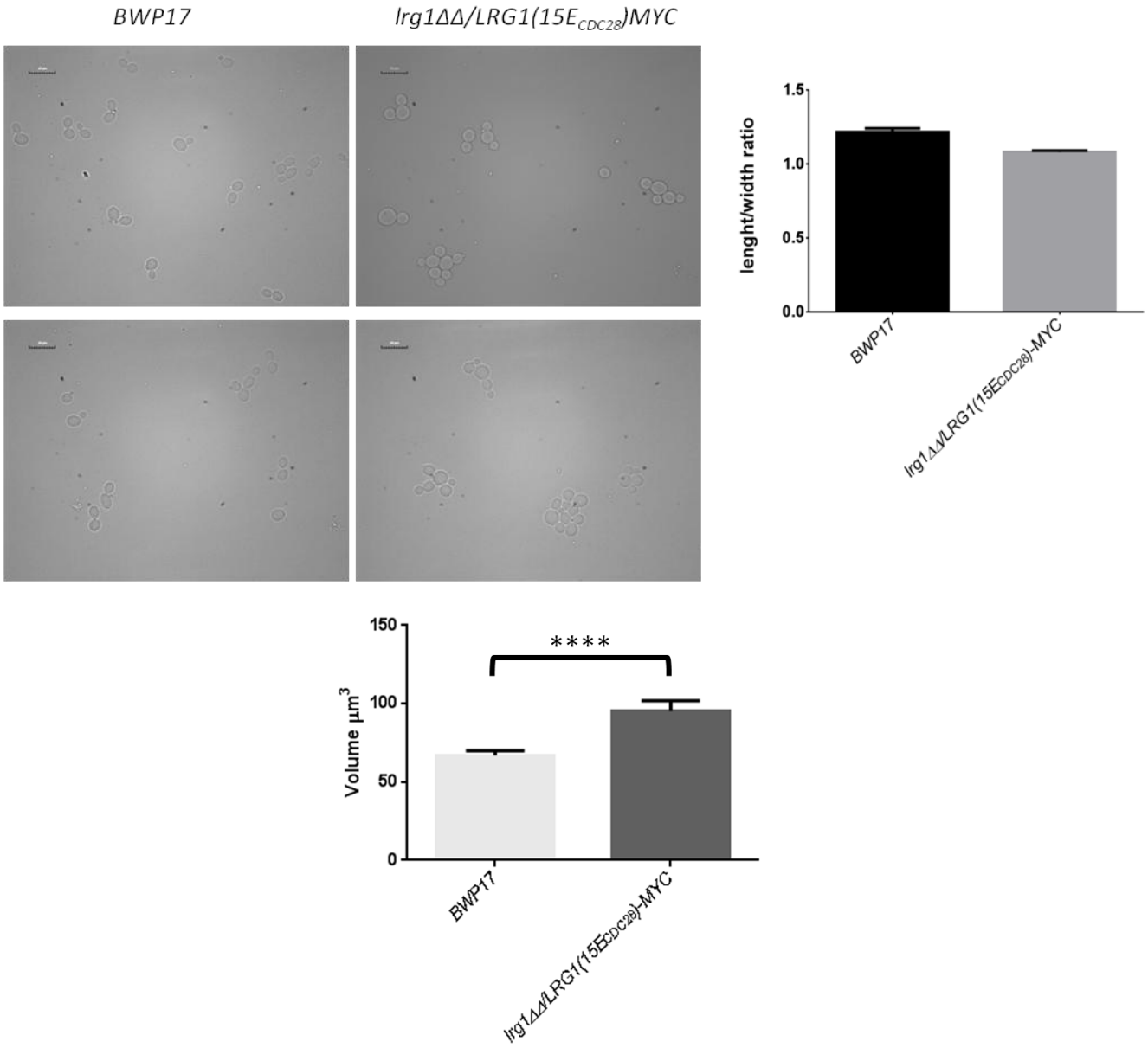

Figure 4.20 **The Lrg1(15E) mutant results in a loss of polarisation.**

Top Left: *BWP17* and *lrg1ΔΔ/LRG1(15E$_{CDC28}$)-MYC* were grown in conditions to induce the yeast morphology for 3 hours before cells were fixed with formaldehyde. Cells were then visualised with a Leica DIC light microscope.

Top Right: ImageJ was used to measure the length/width ratios of cells. The average ratio for each strain is shown with its SEM. An unpaired two-tailed t-test was performed on the *BWP17* and *lrg1ΔΔ/LRG1(15E$_{CDC28}$)-MYC* data and revealed that the sets were statistically different to within a 0.0001 confidence interval. N=60

Bottom: The average volumes of *BWP17* and *lrg1ΔΔ/LRG1(15E$_{CDC28}$)-MYC* strains were calculated using the formula shown in figure 4.17c. Error bars represent SEM. Values were found to be significantly different in an unpaired t-test with a p-value of 0.0001. N=60

4.3.17 Localisation of active Rho1 and phosphorylation of Lrg1 during the cell cycle in C*. albicans* yeast

In an attempt to link the phosphorylation state of *C. albicans* Lrg1 with the localisation of Rho1 in the cell during different stages of the cell cycle, an elutriation experiment was carried out on the *lrg1ΔΔ/LRG1-MYC/GFP-RID* strain. For this, exponentially growing cells are treated to centrifugation whilst an opposing force is applied via fluid flow, thus setting up a gradient of cells due to their size. Then, small G1 phase cells were collected from elutriation and re-inoculated into media to induce yeast phase growth. This method attempts to collect synchronised cells by size fractionation while keeping disturbance minimal. Every 20 minutes after re-inoculation, a sample of *lrg1ΔΔ/LRG1-MYC/GFP-RID* cells was taken and flash-frozen for later protein extraction, SDS-PAGE and western blot. A sample of live cells was taken to visualise GFP-RID on a DeltaVision fluorescence microscope and a sample of cells was fixed with ethanol. The fixed cells were later stained with DAPI to visualise the nucleus of cells via the DeltaVision microscope.

In order to deduce at which stage of the cell cycle the cells were in at each time point, the images of the fixed cells were used to count the number of cells that were mono- or bi-nucleate, whilst images of the live cells were used to determine whether cells had a small, medium or large bud. The images of live cells were also used to determine where, when it could be seen in cells, GFP-RID was localised at each time point. The cell-cycle, GFP-RID localisation and phosphorylation state of Lrg1 is shown in figure 4.21

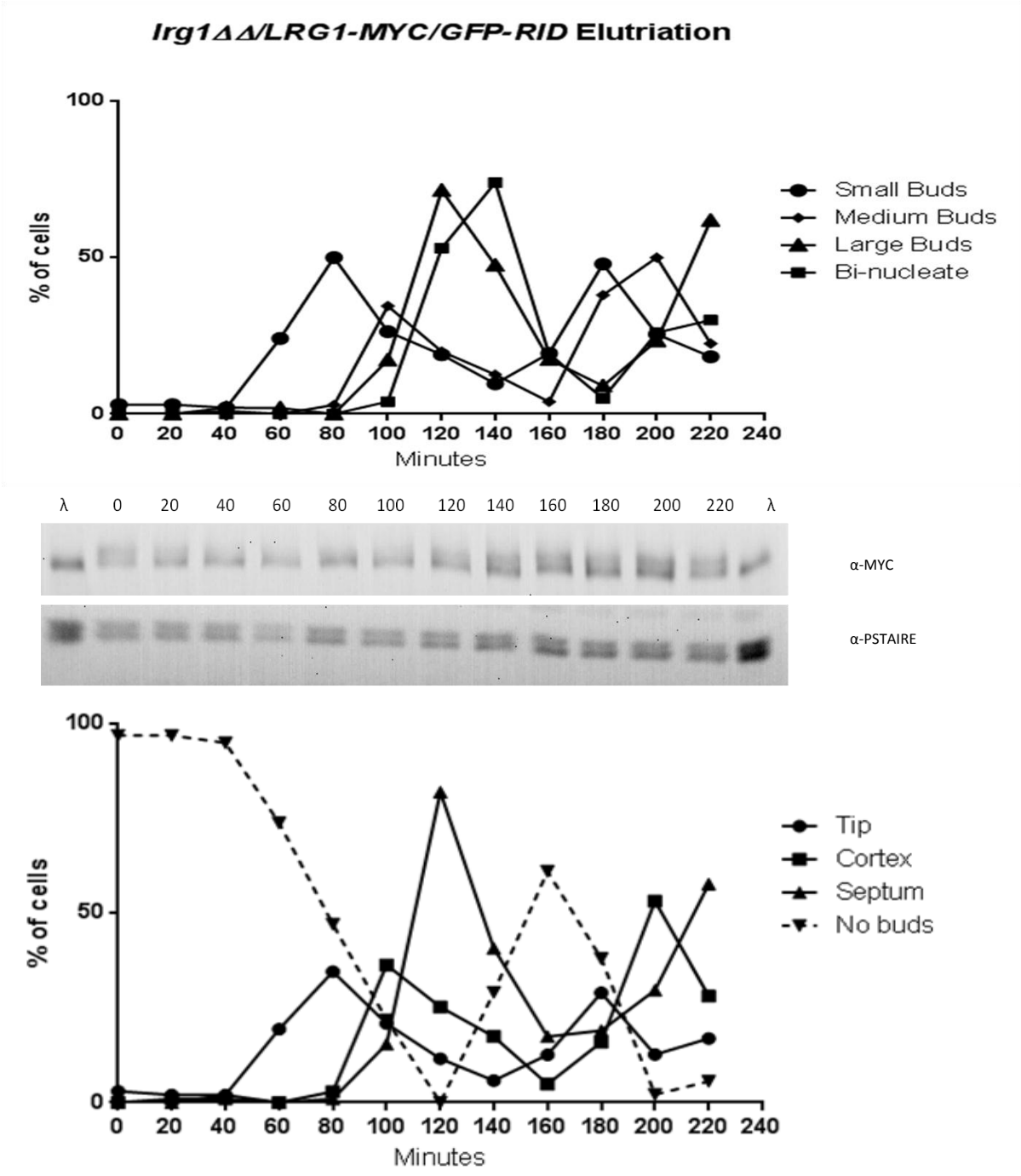

Figure 4.21 **Elutriation of the lrg1ΔΔ/*LRG1-MYC/GFP-RID* strain**

The *lrg1ΔΔ/LRG1-MYC/GFP-RID* strain was subjected to elutriation in order to obtain synchronised, small, early G1 phase cells. These G1 cells were then inoculated into fresh media and grown for 4 hours in yeast inducing conditions. Every 20 minutes 3 samples of culture were taken, one ethanol-fixed one flash-frozen and the last imaged instantly on a DeltaVision fluorescence microscope using the FITC filter.

A) The ethanol-fixed cells were later stained with DAPI, imaged on the DeltaVision fluorescence microscope and cells counted for small, medium or large buds and whether or not the cells were bi-nucleate.

B) Total cell lysate was extracted from the flash-frozen cells before 30 µg was run on SDS-PAGE, followed by an anti-MYC western blot to detect the Lrg1-Myc protein (top). An identical gel was run subjected to an anti-PSTAIRE western blot as a loading control (bottom).
C) The images taken of the live cells were used to count where GFP-RID could be seen in cells, whether it was localised at the bud tip, cortex or the septum.

Analysis of the cell cycle data (figure 4.21a) shows that buds start emerging from mother cells at around 50 minutes, corresponding to the G1/S phase transition, with a peak of small buds at 80 minutes. Medium size buds then peak at 100 minutes corresponding to a switch to isotropic growth during G2. A peak of large buds is then seen at 120 minutes along with an increase in the number of cells that are bi-nucleate, corresponding to the mitotic phase of the cycle. By 140 minutes the majority of cells are un-budded, indicating that they have gone through cytokinesis, and have started the next cell cycle. From 140-220 minutes, the synchrony of the cells is starting to fade, so data from these time points was disregarded.

The GFP-RID localisation data (figure 4.21c) shows that at 80 minutes, where the majority of cells have small buds, GFP-RID is localised mainly to the tips of buds, indicating that active Rho1 is present and this is where cell wall remodelling (polarised growth) is occurring. Then at 100 minutes, where medium buds are present, GFP-RID is re-localised to the cell cortex, indicating a change in the location of active Rho1 and the switch from polarised to isotropic growth. Then when cells are large and mitosis is occurring at 120 minutes, GFP-RID is now re-localised to the septum where polarised growth takes place before cell division. It can be concluded that during the cell cycle, active Rho1 first localises to the growing bud tip during late G1/M phase where growth is polarised, before re-localising to the cell cortex during isotropic growth during G2 and finally localising to the septum for another phase of polarised growth for cell division.

By growing a synchronised culture of *lrg1ΔΔ/LRG1-MYC/GFP-RID* cells, it is shown in figure 4.21b, that during the early G1 phase of *C. albicans* cell cycle the Lrg1 protein remains phosphorylated from the previous cell cycle. Lrg1 is then de-phosphorylated before active Rho1 localises to the emerging daughter bud at the G1/S phase transition and remains that way during polarised growth of the bud tip and isotropic growth during G2. During M phase

of the cell cycle, Lrg1 is again phosphorylated during which time, active Rho1 is re-localised to the cell septum for another period of polarised growth required to produce the β-1,3-glucan for the secondary septum to form either side of the primary septum and cell division to occur. At first glance, this would seem counter intuitive when taken with the fact that phosphomimetic mutations in the four full Cdc28 consensus sites produces longer cells, as the protein isn't phosphorylated during growth of the tip. However, the protein is phosphorylated during the highly polarised growth phase at the septum, so perhaps mutation of the protein at the Cdc28 sites results in increased activity in Rho1, wherever it is located, in other words, resulting in a complete loss of Rho1 regulation?

4.3.18 Lrg1(2E2D$_{CDC28}$) causes mis-localisation of active Rho1

To examine the result of the Lrg1 phosphomimetic mutations on active Rho1, the *GFP-RID* and *lrg1ΔΔ/LRG1(2E2D$_{CDC28}$)-MYC/GFP-RID* strains were grown in yeast-inducing conditions for 3 hours before visualisation on a DeltaVision fluorescence microscope. Images are shown in figure 4.22. The images show that in the presence of Lrg1(2E2D$_{CDC28}$), GFP-RID can still be seen to localise to the tip, cortex or septum of cells like the control strain. However, as mentioned previously, the mutant cells have a larger length/width ratio which is also observed in this data-set. Analysis of the cells was carried out so that the lengths of cells were measured where GFP-RID could be seen at the tip, cortex or septum. Results are shown in figure 4.22 (centre-left panel). As reported earlier, the average length and SEM of wild-type cells with active Rho1 at the tip, cortex and septum is 2.249± .214, 3.228± .158, and 4.165± .163 respectively. The corresponding data for the *lrg1ΔΔ* strain is 8.383± 1.496, 4.707± .694 and 6.278± .497 respectively. The mutant strain expressing the Lrg1(2E2D$_{CDC28}$) proteins shows similar values to that of the strain lacking a copy of *LRG1.* Cells with active Rho1 at the bud tip have an average length of 8.797± 1.098, where it can be seen at the cortex the average length is 5.627± .551 and at the septum 6.674± 0.579. A two-tailed T-test reveals that there is a statistical difference between the wild-type cells and those with the Lrg1(2E2D$_{CDC28}$) mutant protein within a confidence interval of 0.01 where GFP-RID is at the septum and 0.0001 where it is at the tip or cortex. As with the *lrg1ΔΔ* strain discussed earlier, the average of *lrg1ΔΔ/LRG1(2E2D $_{CDC28}$)-MYC/GFP-RID* cells where active Rho1 is at the tip is much higher than the average where it is at either the cortex or septum. Most

probably this effect is because some cells are present that are totally locked in the highly polarised state where the growth machinery doesn't relocate from the tip and the cells become extremely long. Whereas the cells that have active Rho1 relocated to the cortex and septum are still longer than the wild-type, but don't have an overall average as large as those with the protein locked at the tip. This is confirmed when the standard deviation (SD) of the data sets is analysed (figure 4.22, centre-right panel). The *lrg1ΔΔ/LRG1(2E2D$_{CDC28}$)-MYC/GFP-RID* strain has SD figures of 4.660, 2.915 and 3.379 for active Rho1 at the tip, cortex and septum respectively, compared to 0.910, 0.839 and 0.672 for the control strain. This shows that not only does the Lrg1(2E2D $_{CDC28}$) mutant have a larger range of cell lengths but also that the cell length where active Rho1 is located at the tip is more variable than when the mutant displays it at the cell cortex or septum, confirming the above suggestion. Furthermore, as with the cells lacking *LRG1* analysed earlier, 20% of those expressing the phosphomimetic 2E2D Lrg1 show GFP-RID at both the tip and septum concurrently, compared to 1% of cells in the wild type strain and 0% in the strain expressing the Lrg1(4A$_{CDC28}$) protein (figure 4.22, bottom panel), indicating an incomplete localisation of the polarisation machinery as well as a delay.

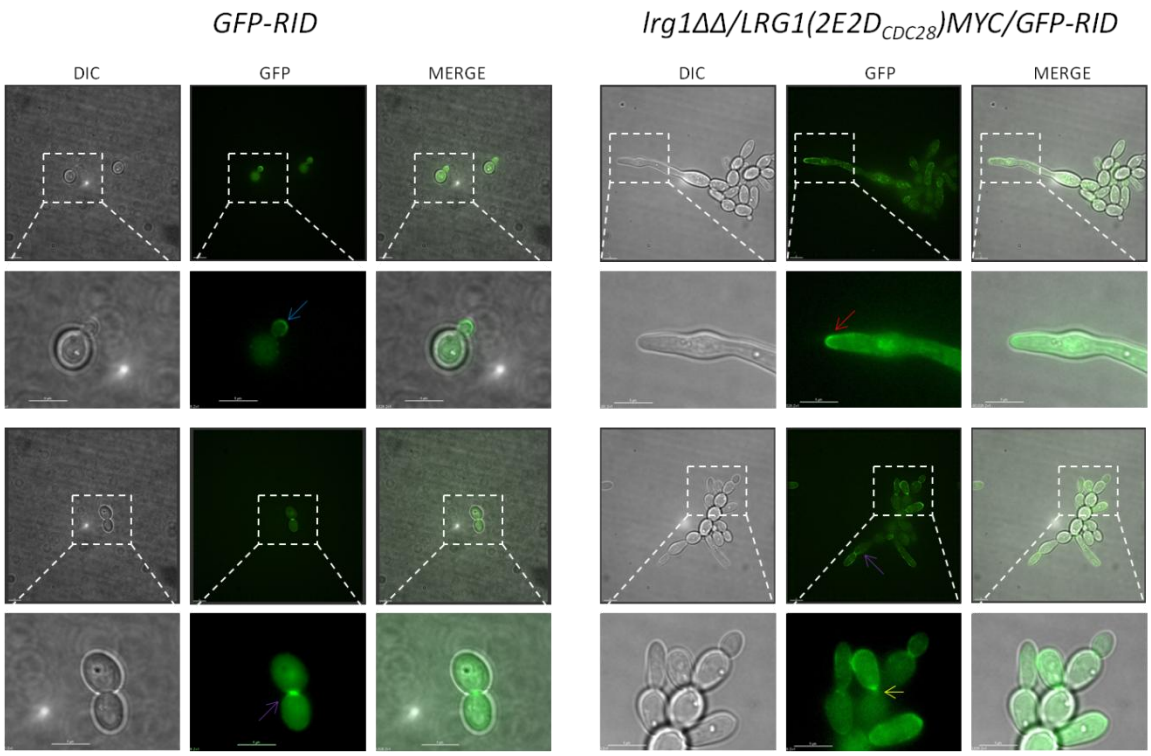
GFP-RID
lrg1ΔΔ/LRG1(2E2D$_{CDC28}$)MYC/GFP-RID
DIC
GFP
MERGE
DIC
GFP
MERGE

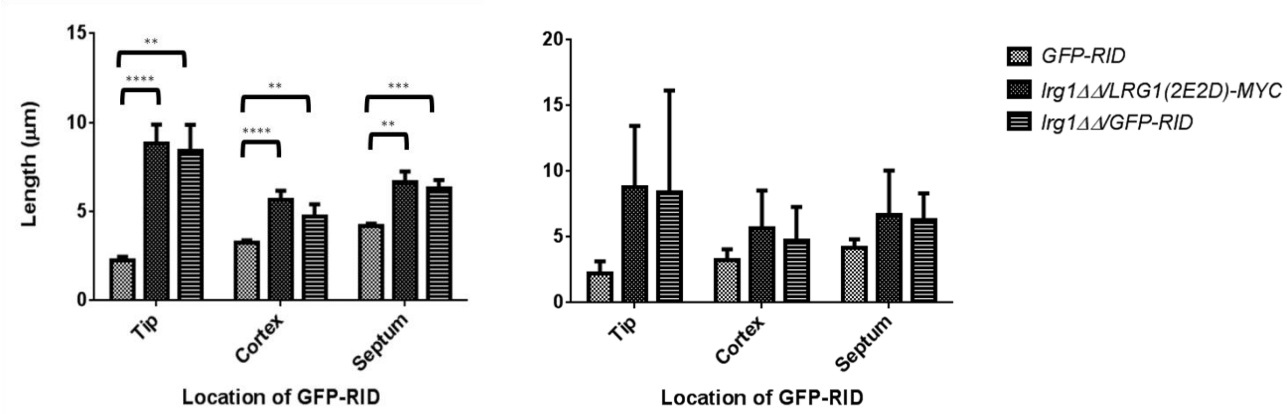
Length (µm)
15
10
5
0
**
****
**
****
***
**
Tip
Cortex
Septum
Location of GFP-RID
20
15
10
5
0
Tip
Cortex
Septum
Location of GFP-RID
GFP-RID
lrg1ΔΔ/LRG1(2E2D)-MYC
lrg1ΔΔ/GFP-RID

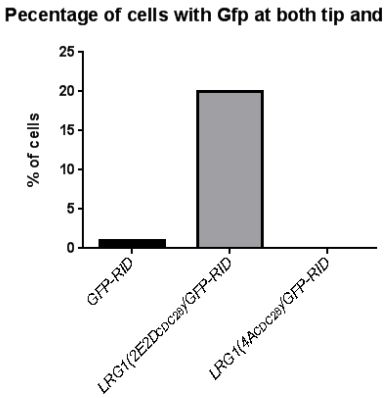
Pecentage of cells with Gfp at both tip and septum
% of cells
25
20
15
10
5
0
GFP-RID
LRG1(2E2DCDC28)/GFP-RID
LRG1(4ACDC28)/GFP-RID

Figure 4.22 Re-localisation of GFP-RID is delayed in the *LRG1(2E2D)-MYC/GFP-RID* strain

Top: The *GFP-RID* and *lrg1ΔΔ/LRG1(2E2D* $_{CDC28}$*)-MYC/GFP-RID* strains were grown for 3 hours in yeast inducing conditions on microscopy agar pads, before visualisation on a DeltaVision fluorescence microscope using the FITC filter. Blue arrows show cells with GFP-RID at the tip only, purple arrows show GFP-RID at the septum only and yellow arrows show GFP-RID at the tip and septum simultaneously. The red arrow shows a cell where GFP-RID has become locked at the end of a long cell. The scale bar represents 5 µm.

Middle left: The images of each strain were used to determine the average length (plus SEM) of cells when GFP-RID could be seen at the bud tip, cortex or septum. The data from the *lrg1ΔΔ* strain is also shown for comparison. N=45 for each strain, 15 cells per GFP-RID location.

Middle right: Displays the same data as the middle left panel but with the standard deviation of the data shown.

Bottom: Cells were analysed to see what proportion contained GFP-RID at both the tip and septum concurrently. N=50

**= statistically different with a confidence interval of ≤ 0.01

***= ≤ 0.001

****= ≤ 0.0001

4.3.19 Lrg1 phospho-mutants modify the activity as well as the localisation of active Rho1

In order to assess the effects of the phospho-mutations in Lrg1 on the activity of Rho1, the intensity of fluorescence emitted from of *lrg1ΔΔ/LRG1(2E2D* $_{CDC28}$*)-MYC/GFP-RID* and *lrg1ΔΔ/LRG1(4A* $_{CDC28}$*)-MYC/GFP-RID* was analysed along with the wild-type, *GFP-RID* strain. Cells were grown under yeast inducing conditions for three hours before being visualised on a DeltaVision fluorescence microscope. The cell wall of each bud was then traced and the fluorescence emitted from GFP-RID detected was projected onto the length of the bud from the tip to the bud neck, as described in chapter 3. First, each cell plot was used to calculate an average cellular level of GFP-RID, and therefore Rho1 activity for each strain, which is depicted in figure 4.23 (left panel) in arbitrary units of fluorescence intensity. The average cellular level of active Rho1 in the wild-type strain is 284.7± 2.038 (SEM), whereas in the

strain expressing Lrg1(2E2D$_{CDC28}$) this figure is 335.5± 6.730, which is statistically different in an un-paired t-test to a confidence level of 0.0001. This indicates that the phosphomimetic mutations of the Cdc28 consensus sites within Lrg1 result in an increased activity in Rho1. In contrast, the average cellular level of active Rho1 in the *lrg1ΔΔ/LRG1(4A* $_{CDC28}$*)-MYC/GFP-RID* strain is 225± 6.167, which is also statistically different to the wild-type cells. Therefore, the non-phosphorylatable mutations have the opposite effect to the phosphomimetic mutations and decrease the activity of Rho1.

Next, cells from each strain were categorised depending whether their highest level of fluorescence was at the tip, cell cortex or the site of septum formation and an average fluorescence reading for each location calculated, shown in figure 4.23 (right panel). When the majority of GFP-RID is located at any of the three locations, the same pattern of active Rho1 is observed; Lrg1(2E2D$_{CDC28}$) causes an increase in activity when compared to wild type and Lrg1(4A$_{CDC28}$) causes a decrease in activity. Furthermore, these results are shown to be significantly different to the wild-type at both the tip and cortex locations. However, the *2E2D* and *4A* strains show a statistical difference to each other but not to the wild-type strain when GFP-RID is present at the septum.

From the above results, it can be concluded that phosphorylation of *C. albicans* Lrg1 by Cdc28 inhibits the proteins negative regulatory effect on Rho1.

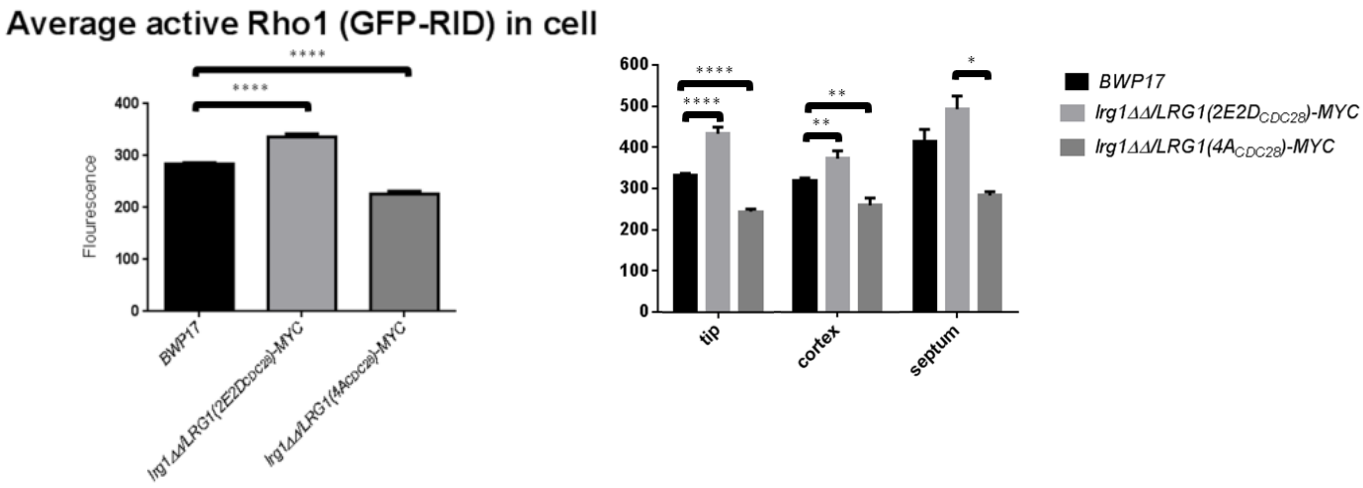

<u>Figure 4.23</u> The Lrg1 (2E2D) and (4A) mutants alter the activity of Rho1 in *C. albicans*

Left: *lrg1ΔΔ/LRG1(2E2D $_{CDC28}$)-MYC/GFP-RID, lrg1ΔΔ/LRG1(4A $_{CDC28}$)-MYC/GFP-RID* and *GFP-RID (BWP17)* strains were grown for three hours in yeast inducing conditions before being visualised on a DeltaVision fluorescence microscope. Images were used to project the fluorescence emitted from the cell wall of the bud onto its length. Average cellular fluorescence intensity was then calculated for each strain and an unpaired t-test performed on the results. The confidence interval is 0.0001. N=45
Right: Cells were categorised according to the location of their highest intensity reading of either the tip, cell cortex of site of septum formation. Average readings for each category for each strain were then calculated and an unpaired t-test performed. Four stars equals a confidence level of 0.0001, two stars equals 0.01 and one star equals 0.05. N=15 cells per GFP-RID location.

4.4 Discussion

4.4.1 The N-terminal extension in *C. albicans* Lrg1 contains multiple phosphorylation motifs

In the previous chapter, it was shown that the *C. albicans* Lrg1 protein has an N-terminal extension that is not present in the *S. cerevisiae* ortholog. In this chapter, it was discovered that this N-terminal extension contained four full and fifteen minimal consensus sites for potential phosphorylation by the master cell-cycle regulator Cdc28. It has been reported that Cdc28 targets often contain clustered consensus motifs (Moses et al., 2007). Given that this study has shown that deletion of *LRG1* results in hyper-polarised, elongated cells and that Cdc28 is highly involved in producing the extended periods of polarised growth required for hyphal growth, it seems that the N-terminal domain of Lrg1 is a target for regulation by Cdc28 phosphorylation at these consensus motifs.

It was shown that during yeast growth, full length Lrg1 displays a slow migrating band when run on SDS-PAGE compared to a phosphatase-treated sample, indicating that the protein is phosphorylated. However, when the N-terminal region of *Ca*Lrg1 is deleted, this slower migrating band disappears, indicating that this is the site of phosphorylation on the protein. On the other hand, it was shown in chapter 3 that deletion of the N-terminus did not have any phenotypic effect on the cells, even if the phosphorylation state of the protein is changed. Perhaps the phosphorylation of the N-terminus negatively regulates Lrg1, but lack of the extension does not have any deleterious effects because the protein is still there to perform its cellular role. Another hypothesis may be that another form of Lrg1 regulation exists for instance its expression or degradation.

4.4.2 C. albicans Lrg1 is a target for phosphorylation by the cell cycle regulator Cdc28

To provide further evidence that Lrg1 is phosphorylated by Cdc28, this study used a number of approaches. Firstly, it was shown that the phosphorylation state of Lrg1 is altered when the Cdc28 kinase is inhibited by 1NM-PP1. However, instead of being less phosphorylated as expected, Lrg1 actually became hyperphosphorylated, possibly indicating that lack of Cdc28 phosphorylation causes phosphorylation elsewhere on the protein by a different kinase?

This result also doesn't provide evidence for direct phosphorylation via Cdc28. Hence, a kinase assay was performed with purified *Ca*Cdc28 and the bacterially expressed N-terminal region of *C. albicans* Lrg1. The kinase assay showed that Cdc28 could directly phosphorylate the N-terminal region of Lrg1. Furthermore, the lower level of phosphorylation seen on a fragment of Lrg1 with its four full Cdc28 consensus sites mutated to non-phosphorylatable alanine proves that the kinase does act on these sites as speculated above.
This study also revealed at what point during the cell cycle that Cdc28 acted upon Lrg1. Analysing the phosphorylation state of Lrg1 in different cyclin mutants revealed that the protein loses its phosphorylation when expression of the G1 cyclin *CLN3* is repressed suggesting that Cdc28-Cln3 phosphorylates Lrg1 during this stage of the cell cycle. Interestingly, repression of *CLN3* results a hyper-polarised elongated cells as a terminal phenotype. This observation was confirmed using elutriation to obtain synchronised cells based on their size. This experiment showed that phosphorylation of Lrg1 was present before a bud tip emerged from cells, but disappeared at the G1/S transition. The data gained from elutriated cells also revealed that the phosphorylation of Lrg1 returned during M phase; however the phosphorylation state of the protein was not altered when expression of either of the mitotic cyclins (*CLB2* or *CLB4*) was inhibited.

4.4.3 Phosphorylation of Lrg1 by Cdc28 causes changes in polarised growth and the activity of Rho1

The evidence presented above provides evidence that Cdc28 phosphorylates Lrg1 in *C. albicans*, but they do nothing to address the cellular role of this phosphorylation. The physiological role of phosphorylation can be deduced by replacement of key consensus residues with non-phosphorylatable alanine or phospho-mimetic glutamic/aspartic acid. The key residues in the four full Cdc28 consensus sites of Lrg1 were mutated this way in C. *albicans*.
The phospho-mimetic mutations in Lrg1 had 4 main effects:

1. Rho1 show delayed, incomplete or failed re-localisation from the bud tip to the cortex and site of septum formation.
2. Highly polarised cells which possess a larger volume.
3. Increased activity of Rho1 at all three sites of growth.

4. Increased sensitivity to caspofungin.

In contrast, the effects of the Lrg1 non-phosphorylatable mutant are not as severe:

1. A decrease in activity of Rho1 at all three sites of growth.
2. Resistance to the action of caspofungin
3. Decreased average cell volume.

The effect of the Lrg1(2E2D$_{CDC28}$) mutant produces a similar phenotype to that of the strain lacking any copy of *LRG1*, albeit not as severe. This suggests that phosphorylation of Lrg1 at the Cdc28 full consensus sites negatively regulates the protein. The fact that the Lrg1(4A$_{CDC28}$) protein has opposite effects on the activity of Rho1 and sensitivity to caspofungin would also suggest this. However, the absence of any deleterious effect suggests that in the absence of phosphorylation, Lrg1 behaves normally, similar to what was found in Chapter 3 with the Lrg1 N-terminal truncation.

The results of the Lrg1 phospho-mutants growth on caspofungin is of great significance. As discussed in Chapter 3, one would expect cells with a higher activity of Rho1 and therefore β-1,3-glucan synthase to build a resistance to the drug. However, similar to the *lrg1ΔΔ* strain, the Lrg1(2E2D$_{CDC28}$) mutant protein causes increased sensitivity to caspofungin. Could this be due to an increased number of targets that are present in the cell? Fascinatingly, mutation of the full Cdc28 consensus sites to non-phosphorylatable alanine results in an increased resistance to caspofungin, providing an interesting area of further drug research.

4.4.4 Model of Cdc28 action on Lrg1 in *C. albicans*

Taking the above pieces of evidence together has led to the proposal for a model of the action of Cdc28 phosphorylation on Lrg1, depicted in figure 4.24 and the role of this phosphorylation in the cell cycle (figure 4.25). The model proposes that in the absence of phosphorylation of the Lrg1's N-terminal domain by Cdc28, the LIM and RhoGAP domains of the protein remain accessible. This results in Rho1-GTP being hydrolysed to Rho1-GDP, decreasing Rho1 and hence β-1,3,glucan synthase activity. Conversely, phosphorylation of Lrg1 at the four full Cdc28 sites results in a change in conformation where the N-terminal extension inhibits binding of the LIM and RhoGAP domains to Rho1. This results in two things: 1) Regulation of Rho1 and hence the glucan synthase is lost and hence their activity

increases and 2) Control of Rho1 localisation is lost. This phosphorylation occurs at the M/G2 transition of the cell cycle to lock Rho1 at the site of septum formation, producing the large amounts of glucan to be laid down for the secondary septum. Upon lifting of this phosphorylation, Rho1 is free to localise to the cell cortex to produce isotropic growth. Presumably, although we have been unable to identify it, this phosphorylation also occurs from late G1 to G2 phase to lock Rho1 at the growing bud tip as suggested by the phenotype of the phospho-mimetic Lrg1 mutant.

There are however, problems with this model, most importantly, the phospho-mimetic mutations of Cdc28 consensus sites results in elongated cells, but phosphorylation of Lrg1 has been shown to take place in the M/G1 phase of the cell cycle and disappear before a bud emerges and Rho1 is localised to its tip. Conceivably, this phosphorylation in M-phase could be for the highly polarised growth required to form the secondary septum. Surely then, one would expect Rho1 to be instead locked at the septum in the phospho-mimetic mutant. However, perhaps Lrg1 is only partly responsible for Rho1 re-localisation, so that it can be distributed elsewhere by other means which are temporally slower in the absence of Lrg1 control, giving the hyper-active glucan synthase a longer time to extrude glucan into the cell wall, resulting in the increased polarisation. The fact that the Lrg1(15E) mutant- which contains mutations in the four full sites and 11 additional Cdc28 minimal sites- reverses the polarised nature of the 2E2D mutation, proves that Lrg1 itself is under more complex regulation than just the four Cdc28 consensus motifs. Or perhaps the phosphorylation/de-phosphorylation occurring on Lrg1 when polarised growth is occurring at the bud tip is too fast to detect with the method used in this study.

One would assume that the model of phosphorylation above allows Rho1 to become locked at the tips of hyphae and provide the continuous periods of polarised growth needed during this growth morphology. However, hyphal growth is not impaired when the N-terminal extension of Lrg1, that is phosphorylated, is deleted. In contrast, when both copies of *LRG1* are deleted hyphal growth is still impaired, as shown in Chapter 3. Again this provides further evidence that there is a complex regulation of this process.

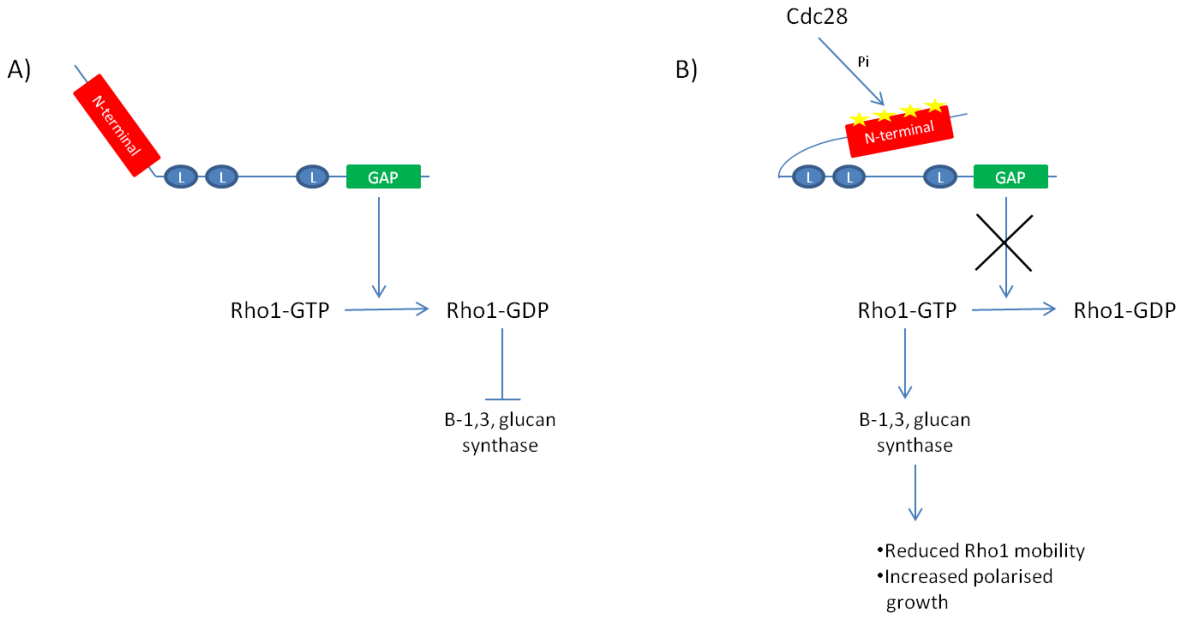

<u>Figure 4.24</u> Model of Lrg1 phosphorylation by Cdc28 in *C. albicans*

A) Without any phosphorylation of the N-terminal domain by Cdc28, Lrg1 is available to catalyse the reaction of Rho1-GTP to Rho1-GDP, inhibiting the glucan synthase.

B) Phosphorylation (yellow stars) of Lrg1 by Cdc28 in the N-terminal domain causes a conformational change in the protein, preventing the Rho-GAP domain from accessing Rho1. This allows Rho1 to remain active and the glucan synthase activity also increases. This lack of Rho1 regulation causes a lack in Rho1 mobility throughout the cell. Therefore glucan is extruded into the cell wall for a longer amount of time, resulting in an increase in polarised growth. This action possibly takes place during the M/G1 phase of the cell cycle in order to provide the highly polarised growth needed to form the secondary septum.

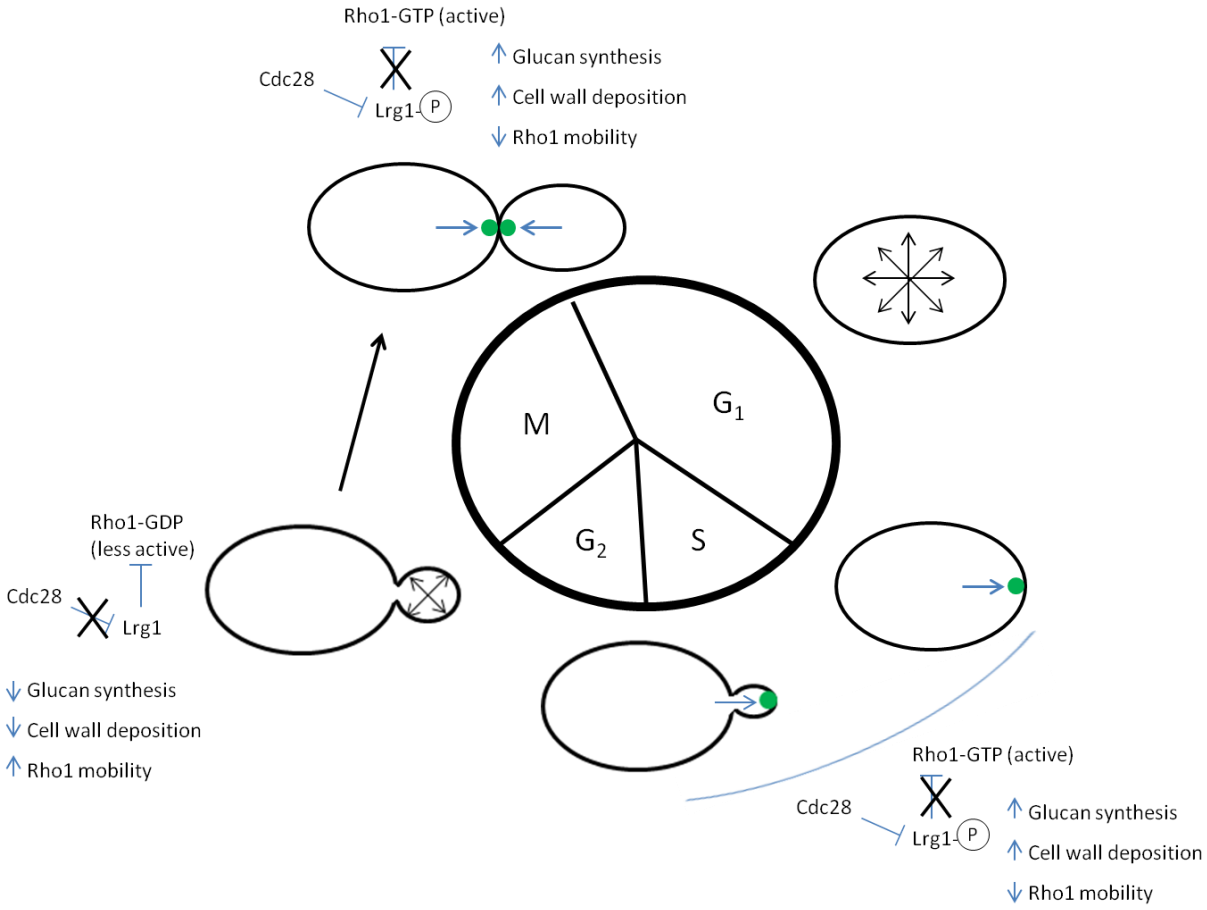

<u>Figure 4.25</u> The consequences of Cdc28 phosphorylation of Lrg1 on the cell cycle

Using the data presented in this study has led to the following proposal of the effects of Cdc28 action on Lrg1 during the cell cycle. Cdc28 phosphorylates Lrg1 at the M/G2 transition. This inhibits the negative regulation of Lrg1 on Rho1 (green), increasing its activity along with that of the β-1,3-glucan synthase. The phosphorylation also locks Rho1 at the site of septum formation. These two consequences cause the increase in deposition of glucan required for the secondary septum. Once this phosphorylation is lifted, Rho1 re-localises to the cell cortex for a period of isotropic growth. Phosphorylation of Lrg1 takes place again from late G1 to the G2 phase of the cycle, producing polarised growth at the growing bud tip. Again once this regulation is lifted, Rho1 re-localises to the cell cortex for a period of isotropic growth in G2.

5 Phospho-regulation of Lrg1 by Cbk1

5.1 Introduction

5.1.2 The Cbk1 kinase

The *C. albicans* Cbk1 (cell wall biosynthesis kinase) protein is a member of the NDR (nuclear dbf2-related) kinase group (a sub-class of AGC protein kinases) which is highly conserved amongst many organisms (Hergovich et al., 2006). The kinase phosphorylates either serine or threonine residues and has been shown to have a high affinity for sites that contain a histidine residue at the minus 5 position to Ser/Thr, followed by any amino acid and then either arginine or lysine at -3 or -2. This consensus site for Cbk1 phosphorylation is abbreviated to HX(K/R)(K/R)S/T (Mazanka et al., 2008). All NDR kinases are activated via phosphorylation at two sites along the length of the protein. A serine/threonine residue in the C-terminal hydrophobic domain is phosphorylated often by a Ste-20-like kinase whilst a conserved serine/threonine residue in the activation domain of the protein is auto-phosphorylated. Members of this kinase family are known to be involved in cellular processes such as such as morphological changes, proliferation, apoptosis and mitotic exit and are reviewed fully in (Hergovich et al., 2006). For example, Cbk1 in *S. cerevisiae* is required for shmoo formation, the Cbk1 homologs in *N. crassa* (Cot1) and *A. nidulans* (CotA) are both required for hyphal formation and the *S. pombe* homolog (Orb6) deletion mutant results in round cells (Shi et al., 2008; Verde et al., 1998; Yarden et al., 1992). In *N. crassa* it has also been shown that *COT1* and *LRG1* interact genetically (Vogt and Seiler, 2008b).

5.1.3 Cbk1 and the RAM network in *S. cerevisiae*

The yeast RAM (regulation of Ace2 transcription factor and polarised morphogenesis) network is well studied in *Saccharomyces cerevisiae* and is known to be comprised of at least 6 essential proteins with varying functions. Mob2 forms a complex with Cbk1 and is required for both activation and localisation of the kinase (Weiss et al., 2002). Kic1, a Ste20-like kinase acts upstream of Cbk1 and probably activates it via phosphorylation of its C-

terminus (see above). Hym1 interacts with Cbk1 and Kic1 and is important for localisation of the complex, whilst Pag1 is a large scaffold protein that may aid the action of Kic1. The final member Sog2 has an unknown function (Nelson et al., 2003).

As its name alludes, the RAM network has two main roles. The first is its responsibility for maintaining polarised growth. Although no direct link between the RAM network and polarised growth has been deduced, Cbk1 and Mob2 have been shown to localise to the two sites of highly polarised growth: the bud tip during bud enlargement and then the mother/bud neck during mitosis (Weiss et al., 2002). All other members of the RAM network have also been shown to localise to sites of polarised growth and mutants of any of the components form spherical cells with wider bud necks and an increase in aborted mating projections, indicating a loss of cell polarisation (Nelson et al., 2003).

The second role of the RAM network is to ensure that the Ace2 transcription factor is localised to the daughter nucleus at the correct time. Ace 2 is responsible for the transcription of the chitinases and glucanases (septum degradation enzymes SDE's) that will eventually degrade the septum formed between the mother and daughter cells, allowing them to separate (Colman-Lerner et al., 2001). It is for this reason that mutations in the RAM network result in cell-separation defects. During mitosis, both Cbk1 and Ace2 are inhibited by Cdc28 phosphorylation, until, during late anaphase/telophase, the mitotic exit network (MEN) is triggered, which leads to the release of Cdc14 from the nucleus (Brace et al., 2011). Cdc14 then de-phosphorylates Cbk1 at its Cdc28 consensus sites. This de-phosphorylation activates the Cbk1-Mob2 complex and allows transport of Ace2 to the daughter nucleus. Ace2 is then phosphorylated at its nuclear export sequence by Cbk1 which ensures it remains in the daughter nucleus and transcribes the genes for cell separation (Jansen et al., 2006). This process ensures that septum degradation takes place after mitosis has completed.

5.1.4 The *C. albicans* RAM network

The function of the RAM network in *Candida albicans* is less well studied. A study by Song et al, 2008, sought to explore the role of the RAM network in polarised and hyphal growth in the organism. They found that each of the *C. albicans* orthologs of the *S. cerevisiae* proteins were also essential for RAM network function. Mutants resulted in more spherical cells that

had a cell lysis defect, indicating both a loss of polarity and a cell wall defect. The phenotype of a *cbk1ΔΔ* mutant is depicted in figure 5.1. The mutants also formed large aggregates of cells due to a failing in cell separation. Perhaps most interestingly though was the failure of the RAM network mutants to form hyphae under any laboratory conditions and many genes required for hyphal growth were dependent on a functional RAM network (Song et al., 2008).

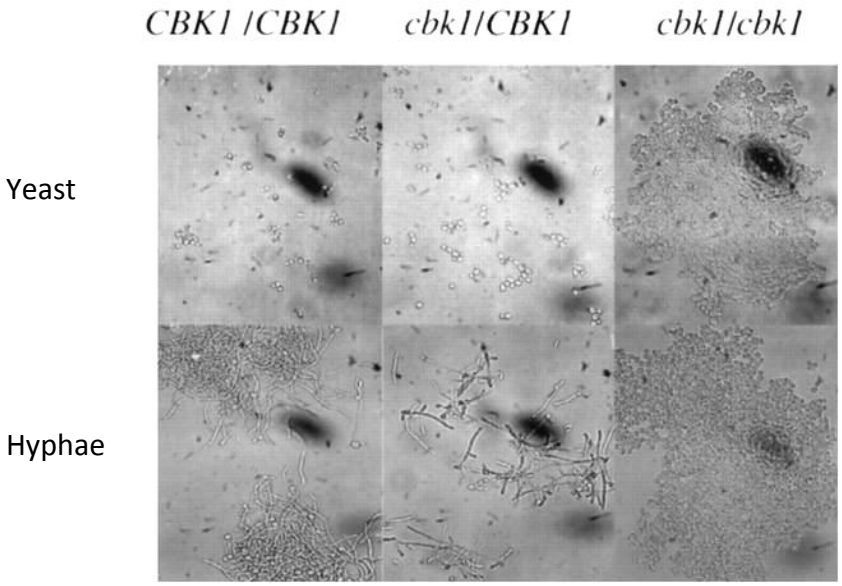

Image taken from: (McNemar and Fonzi, 2002).

Figure 5.1 Loss of *C. albicans CBK1* results in loss of polarisation and a cell separation defect.

Loss of any members of the *C. albicans* RAM network results in a cell separation defect and a loss of polarity resulting in an inability to grow as hyphae. A wild-type strain, *CBK1/cbk1Δ* heterozygote and a *cbk1ΔΔ* strain are shown above growing as both yeast (top) and hyphae (bottom).

5.1.5 The RAM network and Cdc28 in *C. albicans*

It has recently become apparent that in *C. albicans,* the RAM network and Cdc28 play similar or antagonistic roles in a number of ways. During hyphal growth, Cdc28-Hgc1 phosphorylates the Sep7 septin, which in turn inhibits the Cdc14 phosphatase from locating at the septin ring. This inhibition results in Cbk1 remaining phosphorylated at its inhibiting

Cdc28 consensus sites. Cbk1 is then unable to licence Ace2 to the daughter nucleus to transcribe the SDE's and hence hyphal cells remain attached (Gonzalez-Novo et al., 2008). Cdc28-Hgc1 also down regulates the SDE's via phosphorylation of Efg1 (Wang et al., 2009). Cdc28 also directly interacts with the RAM network during hyphal growth. The kinase phosphorylates Cbk1's partner Mob2 upon hyphal induction. This phosphorylation is necessary for correct hyphal growth and maintenance of the polarisome components at the hyphal tip (Gutierrez-Escribano et al., 2011). This suggests that Cbk1 is being controlled by the Cdc28 kinase. There is evidence that Cbk1, Cdc28 and the mechanism of polarised growth in *C. albicans* are all linked.

5.1.6 Aims of this chapter

Given that this study has shown that Cdc28 regulates the activity of Lrg1 to bring about polarised growth, and it has been shown that Cdc28 and Cbk1 work together to bring about hyphal growth (discussed above), this chapter aims to address whether Cbk1 plays a regulatory role on the Lrg1 protein in *C. albicans.* The evidence presented addresses the potential phosphorylation of Lrg1 by the Cbk1 kinase. Also using evidence presented in chapter 4, the possible physiological role resulting from Cbk1 action on Lrg1 is discussed.

5.2 Strain construction

5.2.1 Construction of an *LRG1-MYC/cbk1ΔΔ* strain

In order to assess the relationship between *C. albicans* Lrg1 and Cbk1 *in vivo,* a strain with *LRG1* epitope tagged with *MYC* and lacking any copy of *CBK1* was needed. The Phosphorylation state of Lrg1 in this strain can then be compared to that in a strain possessing *CBK1*. The *LRG1-MYC* strain produced in chapter 4 was used as a base strain. The first copy of *CBK1* was deleted in a similar way to the *LRG1* deletion strain in chapter 3. A PCR cassette was created with a *HIS1* selectable marker flanked by homologous sequences to the regions 5' and 3' of *C. albicans CBK1,* shown in figure 5.2 (top).

Recombination with the *C. albicans* genome results in replacement of the *CBK1* gene with the selectable marker and acquirement of histidine prototrophy. Correct integration was confirmed via PCR (figure 5.2, bottom).

Due to the extremely sick nature of a *cbk1ΔΔ* strain, it was not possible to delete the second copy of *CBK1* in the same way as above. Instead a PCR-based method was used to create larger regions of identity either side of the selectable marker (Derbise et al., 2003). The *ARG4* marker was first amplified as shown above and purified. The 500 bp either side of the *CaLRG1* gene, including the regions of identity on the selectable marker fragment, were then amplified from *C. albicans* genomic DNA and purified. The selectable marker, 5' and 3' fragments were used in another PCR reaction from which amplification results in one DNA fragment with the two regions of 500 bp identity fused either side of the selectable marker. The whole process is shown in figure 5.3a. Correct replacement of the second copy of *CBK1* was confirmed using diagnostic PCR (figure 5.3b). Lack of *CBK1* was confirmed via a negative result using internal primers in a PCR reaction (figure 5.3b) and visualisation of the *cbk1ΔΔ* phenotype. The resulting strain was named *LRG1-MYC/cbk1ΔΔ*.

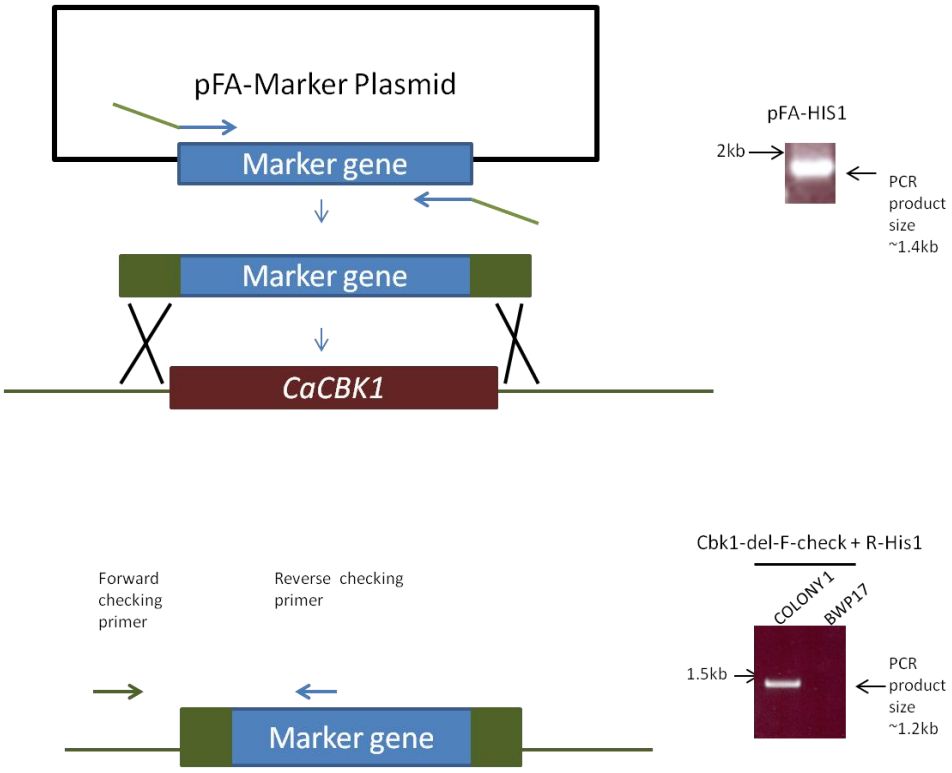

<u>Figure 5.2</u> Deletion of the first copy of *CaCBK1*

Cbk1-del-F and *cbk1-del-R* primers were used to amplify a *HIS1* cassette with 5' identity to the area upstream of *CaCBK1* and 3' identit to a region downstream of it (TOP). Integration results in deletion of *CBK1* and replacement with *HIS1*. Correct insertion was selected for by growth on media lacking histidine and diagnostic PCR with a forward primer upstream of *CBK1* and a reverse primer in the *HIS1* gene (BOTTOM).

A)

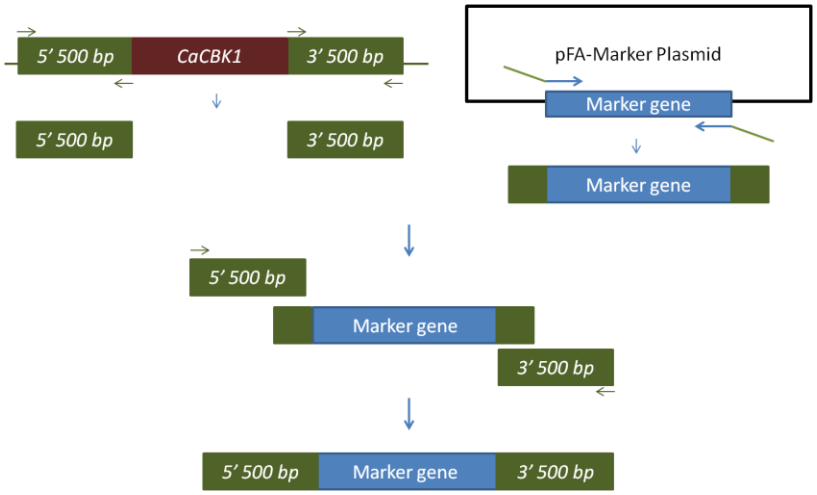

B)

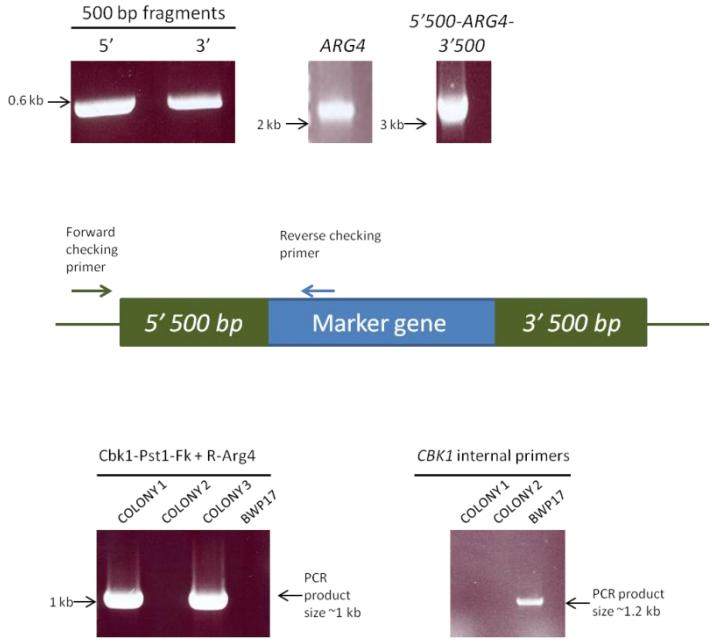

<u>Figure 5.3</u> Producing a *cbk1ΔΔ* strain via multi-step PCR

The second copy of *CBK1* was deleted in the following way.

A) The 500 bp regions either side of *C. albicans CBK1* were amplified from gDNA and purified. Cbk1 S1 and S3 primers were used for the *5'* fragment S2 and S4 for the *3'* fragment. These 500 bp fragments were used in a PCR reaction along with the *ARG* deletion cassette produced from the pFa-ARG4 plasmid, produced as shown in figure 5.2 The reaction used primers at the 5' end of 5'500 bp (Cbk1-S3) and at the 3' end of 3'500 bp (Cbk1-S4). The overlap on the fragments produced an end product with the *ARG4* gene flanked by 500 bp regions of identity.

B) Correct integration into the genome was confirmed via diagnostic PCR with a forward primer upstream of the 5' 500 bp region and a reverse primer in the *ARG4* marker. Internal *CBK1* primers were also used in PCR to ensure no other copy of the gene existed elsewhere in the genome.

5.3 Results

5.3.1 *C. albicans* Lrg1 contains consensus sites for the kinase Cbk1

As mentioned earlier, the Cbk1 kinase phosphorylates serine or threonine residues at the consensus site HX(K/R)(K/R)S/T, (Mazanka et al., 2008). Regan, 2010, performed a search of the *Candida albicans* proteome using a pattern match tool which searched for peptides that contained any of the possible permutations of the consensus sequence. Lrg1 was identified as having 4 possible Cbk1 consensus sites, with the 6th highest number of sites over the whole proteome (Regan, H., University of Sheffield, unpublished). The four sites are serine 80, threonine 623, serine 1009 and threonine 1059 and are shown in figure 5.4 (top panel). Further analysis of the four identified sites reveals that the S80 residue lies inside the protein's N-terminal extension, T623 is located in between the two LIM protein-protein interaction domains, whilst S1009 and T1059 are found just before the GTPase-activation domain. Figure 5.4 (bottom panel) also shows the free energy prediction of Lrg1 from chapter 3 and shows that all four consensus sites are present in regions of disorder suggesting that they are open to phosphorylation and possibly required for regulation of the protein.

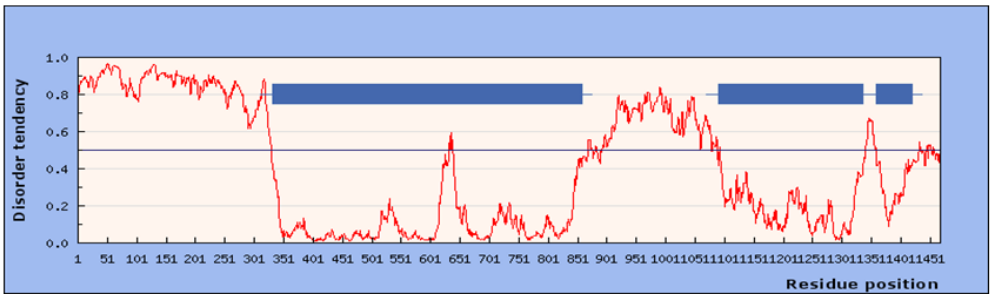


```
   1  MKHSFDTPQR GNSIHHSFGN PNASNTTRST INIVESPDNR GSIIATTEPS
  51  SPPPPQQPLK DSGSSPRFKF NPFGHSRSHS HTSNNGKRLF YPVHHDGRYH
 101  NMNDQYPPIS TVSQSMHPSS PVPSSPTPTP APAPTTTSSS KPKREQSLRY
 151  YIPRDTPPQT PPMSQLPKPV GKSPQPNWTN LIPPLPGKPQ PSYNSPDSFQ
 201  QQKQNKLIDT DDFNFGTEPI ISSPESSSRQ HPDPLSNQSN FNNNTINNYS
 251  NYRSSTRSGL DPSQRHSIAV SPTPEKQDSA TQSTDTINTS SIRPVPSVYV
 301  AGSSSSLPHK QQQQQEPSSP SKSERKPGRK KSRKVCAKCG LEITSQFVRA
 351  LNNAYHVDCF TCHECGKQCS AKFFPYEITN EQDGTKTQVA LCEYDYFKKL
 401  DLICYVCNSA LRGPYITALG NKYHLEHFRC NVCQRVFESD ESYYEHDNNI
 451  YCHFHYSKLY ASHCEGCQSS IVKQFVELFR GGRNQHWHPE CYMVHKFWNV
 501  CITPDSVGLQ KLFDLPDDVL NGLKLVKDDN ESHISVDSAM LMSIEQQIEQ
 551  VVLKCWVTLS GYEEITAKCI SDMLLCACTG NKFNGIVVTG KLVLNVEVLF
 601  NALDYVILMC KSSHELLHKK FGTPPNKDDS ESSSTEEEYF QMLKKEPRNI
 651  TGKIMSYLAI LRKSDHIAKS GSLSAELLSV ITGCAHYLKL LIRLGLYNAL
 701  KLNRLYGTTN AIEKFLQLTS EHEAISLLAG DSKTQLSLIN SKLTIPASST
 751  DACSSCAKSI EKSCLKLDNN RWHVRCFVCS LCKRTIPSIE ASETKFDVIH
 801  QSIVCRECPC EHFDTGFHLV SDLSQLIYLL KIALFRSRSV MKVDLTKVPR
 851  SYLSDSQSDT DTVDVAQDNY SQTLNDVTSL RSKRQSQKLS KSIKKKARKS
 901  IIVEAPEADK ARKEDIKTHP LGMKSSGVGT NDTSRSSGIN DETTIADELN
 951  DLSFDSQTSK QQGSRKTSSA SQLSYNPGGD ENLSVTRKSL KIRDEPQRQT
1001  TNTHLDRTSD LLKNEKSLTL DDIPRIVAAE QAREQRPNAF KHHNSLYQRQ
1051  TAPHRLKATG HTSTVITPTG VLDNILNTSQ PHPEEPVAVR KQKYYSELTK
1101  DEHFIIRHIA VEALSHISKS YSNKEELLSL IQTKKQPTFW DKFKFGGGDG
1151  KKDKVMAVFG VDLQVLTKKY GIDSDLGVGP SKLRIPIVVD DIIAALRQKD
1201  MSVEGIFRLN GNIKKLRELT EQINKNPLKS PDFSIQNAVQ LAALMKKWLR
1251  ELPNPLLTFG LYDMWVSSQR QVNPVLRKRV LQLTYCMLPR SHRNLVEVLL
1301  YFFSWVASFS EIDEETGSKM DIHNLATVIA PNILISKQSS NSSSGNSSNS
1351  GTNNSDSQQA SGDNYFLAIE VVNQLIEQHE EFSIIPSDIL EFYEKCGFDK
1401  FDSTKKEITT RDVMIKIDKE LKEKPDYFDN FELKNPTGSL TSQEVKRNSV
1451  SRIESKIQNR ELNGISER*
```

<u>Figure 5.4</u> ***C. albicans*** **Lrg1 contains multiple consensus sites for the Cbk1 kinase**

Top: Regan, 2010, identified CaLrg1 as having 4 Cbk1 phosphorylation consensus sites (BLUE) via a protein pattern search of the *C. albicans* proteome. This was the 6th highest number of sites seen in any protein. Further analysis revealed that one of these sites is located in the N-terminal extension discussed in Chapter 3 (yellow), another is located in between the two LIM domains of the protein (grey) and the last two are located just before the GTPase activating domain (green).

Bottom: The free energy plot of *Ca*Lrg1 reveals that all four sites are located in regions of disorder.

5.3.2 The Lrg1 N-terminal extension is a substrate for Cbk1 *in vitro*

In order to investigate whether *C. albicans* Lrg1 is a substrate for the Cbk1 kinase, an *in vitro* kinase assay was carried out on the purified recombinant GST-Lrg1(NT) fragment discussed in chapter 4. A strain which contained Cbk1 epitope tagged with MYC at its C-terminus (*CBK1-MYC*) (Caballero-Lima, D. University of Sheffield) was used in an anti-MYC immunoprecipitation (IP) to purify the active kinase which was then incubated with GST-Lrg1(NT) in the kinase assay. As a positive control, the fragment was also incubated with purified Cdc28-MYC, whilst the fragment was incubated with an anti-MYC IP of a *BWP17* wild-type lysate as a negative control. Instead of using an antibody to detect the subsequent phosphorylation, the kinase and fragment were incubated with radioactive γ-labelled ^{32}P-ATP as performed in (Jansen et al., 2006). The results are shown in figure 5.5. The sample with both the Lrg1 N-terminal fragment and Cbk1 shows a band at the expected size for the fragment, indicating that Cbk1 has phosphorylated the peptide. However, this signal isn't as intense as the lane with the Cdc28 kinase. This is due to the presence of only one of the four Cbk1 consensus sites being present in the N-terminal fragment, compared to 17 Cdc28 sites. The lane with the IP of the *BWP17* lysate does not show any signal from the Lrg1 fragment, showing that there were no contaminants from the pull-down that and that the signal detected is specific to the target kinases.

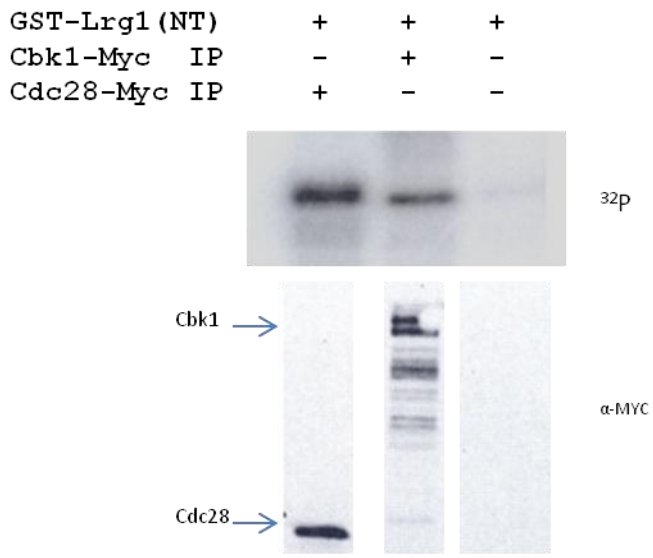

Figure 5.5 Cbk1 phosphorylates Lrg1 *in vitro*

The GST-Lrg1 N-terminal fragment produced in Chapter 4 was incubated with purified Cbk1-Myc and ^{32}P-labelled ATP in a kinase assay. The fragment was also incubated with purified Cdc28 as a positive control, and an anti-Myc IP of a wild-type *BWP17* lysate as a negative control. After the reaction, phosphorylation of Lrg1 was detected by autoradiography.

5.3.3 *C. albicans* is differentially phosphorylated in a *cbk1ΔΔ* background

Using the *LRG1-MYC* and *LRG1-MYC/cbk1ΔΔ* strains, the *in vivo* phosphorylation state of *C. albicans* both in the presence and absence of the Cbk1 kinase was investigated. Overnight cultures of the two strains were re-inoculated into both yeast and hyphal inducing conditions and grown for a period of 120 and 90 minutes, respectively. Cultures were then treated to a protein extraction, SDS-PAGE and anti-MYC western blot. A sample of *LRG1-MYC* protein extract was also subjected to phosphatase treatment and run alongside the above samples. Results are shown in figure 5.6. In the yeast samples, it can be seen that at 0 minutes, there is two separate bands of Lrg1-Myc in the strain possessing *CBK1,* corresponding to the different phospho-forms of the protein seen earlier. However, in the sample lacking *CBK1,* these two bands collapse into one, indicating that the protein fails to be phosphorylated. However, in the 120 minute yeast sample, this loss of the slower migrating band is less severe in the *cbk1ΔΔ* strain. Two clear bands do still exist, but the slower migrating band is not as high on the gel as the slow migrating band in the strain possessing the Cbk1 protein. This would suggest that the protein is failing to be

phosphorylated by Cbk1, but is maybe still being phosphorylated by another kinase. The samples from the hyphal cells also show that in the strain lacking *CBK1,* only one band of Lrg1-Myc is seen which is fast migrating, compared to two separate bands in the wild-type strain. It can be concluded that Cbk1 does phosphorylate Lrg1 *in vivo* at stationary phase, yeast and hyphal morphologies. Although Lrg1 is also phosphorylated by a different kinase during yeast growth, most probably by Cdc28 due to the results seen in chapter 4.

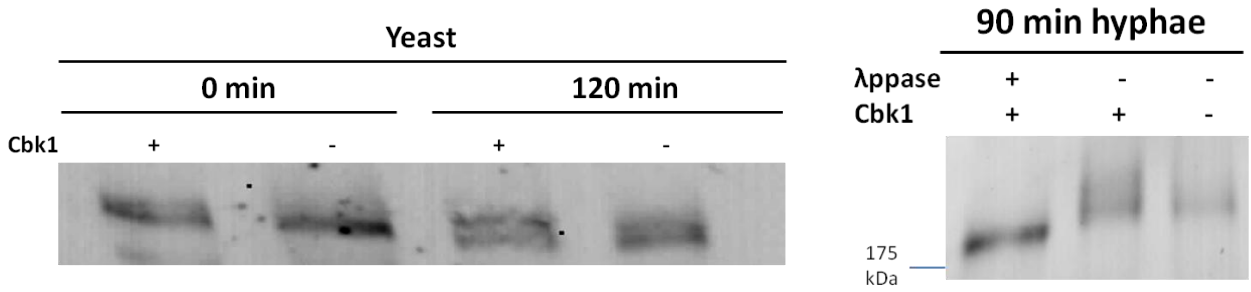

Figure 5.6 Lrg1 is differentially phosphorylated in a *cbk1ΔΔ* background
Stationary phase overnight cultures of the *LRG1-MYC* and *LRG1-MYC/cbk1ΔΔ* strains were re-inoculated into both yeast and hyphal inducing conditions and grown for the time indicated. Total protein lysate was then extracted from these cells along with the stationary phase culture before being subjected to SDS-PAGE, and anti-MYC western blot.

5.3.4 Mutagenesis of the Cbk1 consensus phosphorylation sites in *C. albicans* Lrg1

In order to investigate the physiological role of Lrg1 phosphorylation by Cbk1, the *pCIP10-LRG1-MYC-URA* plasmid was used to mutate the Cbk1 consensus sites on *LRG1*. The serine residues at positions 80 and 1009 were mutated to aspartic acid and the threonine residues at positions 623 and 1059 were mutated to glutamic acid on the same plasmid. Aspartic and glutamic acid mimic the charge of a constant phosphorylated residue whilst retaining the size and shape of amino acids they substituted. On a separate plasmid, all four residues were also mutated to alanine, which is incapable of being phosphorylated. The mutated residues are shown in figure 5.7. After mutagenesis, the full length of *LRG1* and its promoter

in the two plasmids were sequenced to ensure no other mutations had been introduced. The plasmids were then linearised and transformed into the *lrg1ΔΔ* strain, before confirmation of integration and expression of Lrg1-Myc via PCR and anti-Myc western blot respectively as shown in chapter 4. The two strains created were *lrg1ΔΔ/LRG1(4A$_{CBK1}$)-MYC* and *lrg1ΔΔ/LRG1(2E2D$_{CBK1}$)-MYC*

<u>Figure 5.7</u> Mutagenesis of Cbk1 consensus sites within *C. albicans* Lrg1

The p*CIP10-LRG1-MYC-URA* was used in site directed mutagenesis in order to mutate the key phosphorylatable residue in the Cbk1 consensus sites within *Ca*Lrg1.

Top: For phospho-mimetic mutations, Serine 80 and 1009 were mutated to aspartic acid (D) whilst threonine 623 and 1059 were mutated to glutamic acid (E).

Bottom: All four residues were mutated to non-phosphorylatable alanine (A).

The two resulting plasmids were then sequenced in full.

5.3.5 Analysis of the Lrg1 phospho-mutants in the Cbk1 consensus sites

In order to investigate the cellular phenotypes resulting from mutation of the Cbk1 consensus sites in *C. albicans* Lrg1, overnight cultures of the *lrg1ΔΔ/LRG1(4A$_{CBK1}$)-MYC* and *lrg1ΔΔ/LRG1(2E2D$_{CBK1}$)-MYC* strains were re-inoculated into yeast-inducing media and grown for 3 hours. The *lrg1ΔΔ/LRG1-MYC* and *BWP17* strains were also grown in the same way to act as controls. Cells were then fixed with ethanol and visualised under a Leica DIC light microscope. Images of the visualised cells are shown in figure 5.8 (top). On first inspection, it can be seen that cells expressing the Lrg1(2E2D$_{CBK1}$)-Myc phospho-mimetic protein appear to be growing in a more polarised, elongated fashion than the control strain that has wild-type Lrg1-Myc. This phenotype is reminiscent of cells both lacking a copy of *LRG1* and cells containing a copy of Lrg1 with its Cdc28 consensus sites also mutated to mimic phosphorylation. On the other hand, the cells expressing the mutated Lrg1 with non-phosphorylatable alanine at the Cbk1 consensus sites- Lrg1(4A$_{CBK1}$)-Myc- show only a minor elongation of cells. In order to properly assess the phenotype of the strains with mutated Cbk1 consensus sites, the average length to width ratio of the fixed cells was calculated. As can be seen in figure 5.8 (bottom left), the *BWP17* and *lrg1ΔΔ/LRG1-MYC* strains have an average (± SEM) length: width ratio of 1.411± 0.031 and 1.423± 0.031 respectively, with no significant difference detected between them in am unpaired t-test. As suspected, the *lrg1ΔΔ/LRG1(4A$_{CBK1}$)-MYC* cells have a slightly higher ratio of 1.555± 0.039, indicating more elongated, polarised cells. However, the t-test shows no significant difference between these cells and the control strain, demonstrating that mutation of the Cbk1 consensus sites in Lrg1 to non-phosphorylatable alanine does not cause any noticeable effects to cell growth. On the other hand, the length: width ratio of cells expressing the Lrg1(2E2D$_{CBK1}$)-Myc protein is 2.205± 0.180, significantly different to the control strains, indicating that the increase of polarisation seen in this strain is a defined phenotype caused by the mutated Cbk1 consensus sites mimicking phosphorylation. Interestingly, this strain shows a lower ratio than the strain lacking Lrg1 (4.916± 0.389) and the results from the two strains show a significant difference in an unpaired t-test. This indicates that although the strain lacking *LRG1* and the strain expressing the Lrg1(2E2D$_{CBK1}$)-Myc protein show a similar phenotype, with highly polarised elongated cells, the mutations in the Cbk1 sites are less severe and could be considered a separate phenotype to that of the *lrg1ΔΔ* strain. This is a similar

situation to that of the Lrg1(2E2D$_{CDC28}$)-Myc protein discussed earlier and in fact the length to width ratios of cells with mutations in the Cbk1 sites show no significant difference to cells with mutations in the Cdc28 sites.

The cells were then analysed to calculate an average cell volume for the two phospho-mutants strains, shown in figure 5.8 (bottom right). The strain expressing the Lrg1(2E2D$_{CBK1}$)-Myc protein have higher average cell volume than the wild type strain, whilst the Lrg1(4A$_{CBK1}$)-Myc protein causes as lower cellular volume than the wild-type. These differences are seen to be significantly different using an unpaired t-test. This is a similar pattern seen with the Lrg1 phospho-mutants in the Cdc28 consensus motifs. In fact the non-phosphorylatable mutants in the Cbk1 and Cdc28 sites show no significant difference in their average volumes. However, the phosphomimetic mutant in the Cbk1 sites shows a significantly higher average volume (118.7 μm^3 ± 7.42) compared to the phosphomimetic mutations in the four Cdc28 consensus sites (94.88 μm^3 ± 4.60).

5.3.6 The *lrg1ΔΔ/LRG1(4A$_{CBK1}$)-MYC* strain grows as hyphae

Due to the increased polarised growth seen in cells expressing Lrg1(2E2D$_{CBK1}$), and the inability of *cbk1ΔΔ* to form hyphae, one could speculate that phosphorylation of Lrg1 by Cbk1 is required for hyphal growth. If this was true, it would follow that *lrg1ΔΔ/LRG1(4A$_{CBK1}$)-MYC* would also be unable to form hyphae. To test this hypothesis *lrg1ΔΔ/LRG1(4A$_{CBK1}$)-MYC* was induced to form hyphae on agar microscope slides and then visualised every 30 minutes. Results are shown in figure 5.9. The images show that the cells with the non-phosphorylatable mutations in Lrg1 grow normal hyphae, contrary to the hypothesis above. Perhaps unsurprisingly, this indicates that the action of Cbk1 on Lrg1 is not the only mechanism for polarised growth that Cbk1 controls.

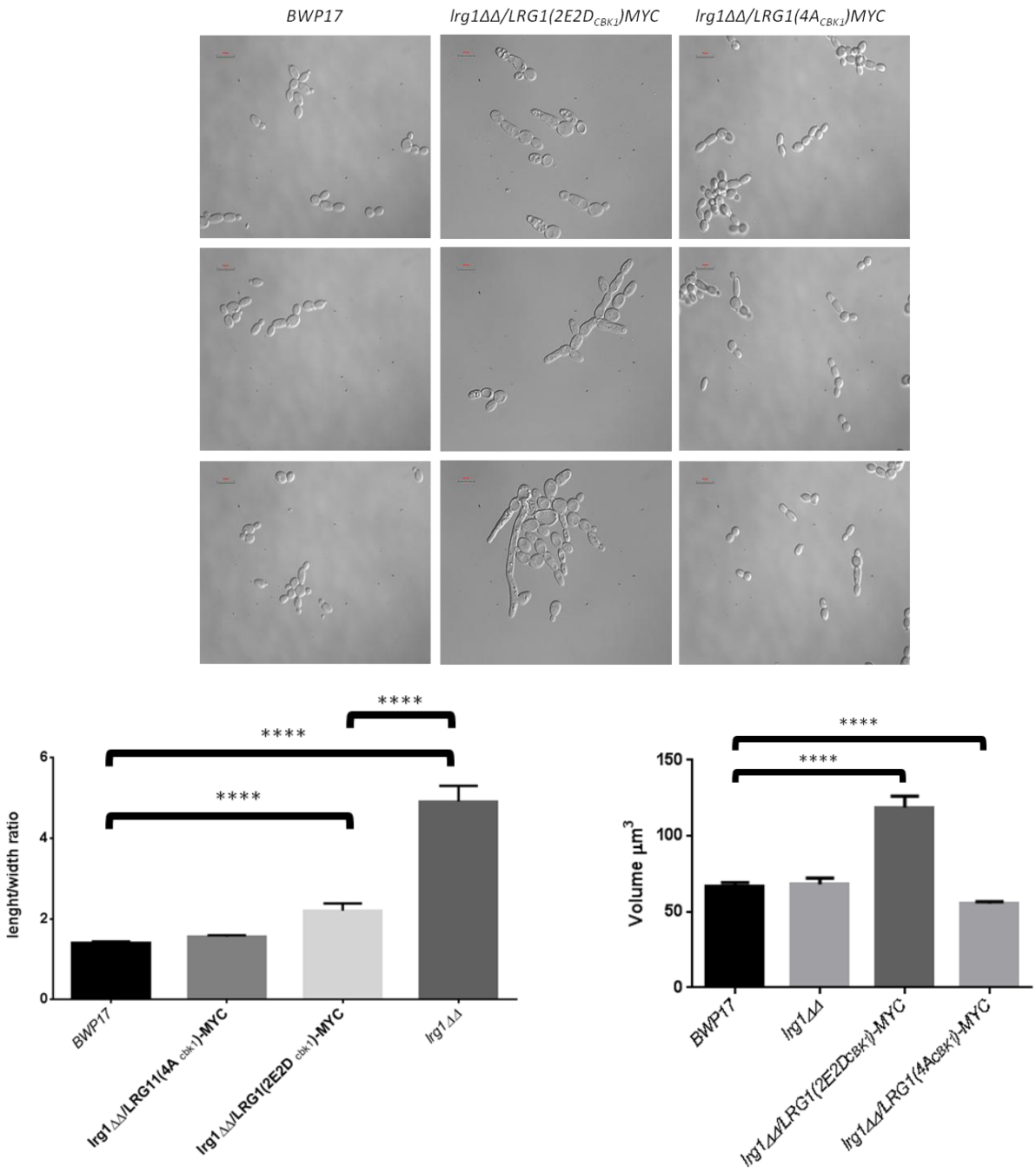

<u>Figure 5.8</u> Phospho-mimetic mutations of Cbk1 consensus sites within Lrg1 result in an increase in polarisation

Top: the *BWP17, lrg1ΔΔ/LRG1(4A$_{CBK1}$)-MYC* and *lrg1ΔΔ/LRG1(2E2D$_{CBK1}$)-MYC* strains were grown under yeast inducing conditions for 3 hours before ethanol fixation and visualisation on a Leica DIC light microscope.

Bottom left: Images were used to calculate the average length: width ratios of cells from each strain. The average length: width ratio of the *lrg1ΔΔ* strain is also shown. Four stars show the results are significantly different in an unpaired T-test with a p-value of 0.0001.

Bottom right: Average cell lengths were calculated using the formulae for a prolate ellipsoid: $V=4/3Pi*ab^2$. N=50

lrg1ΔΔ/Lrg1(4A$_{CBK1}$)-MYC

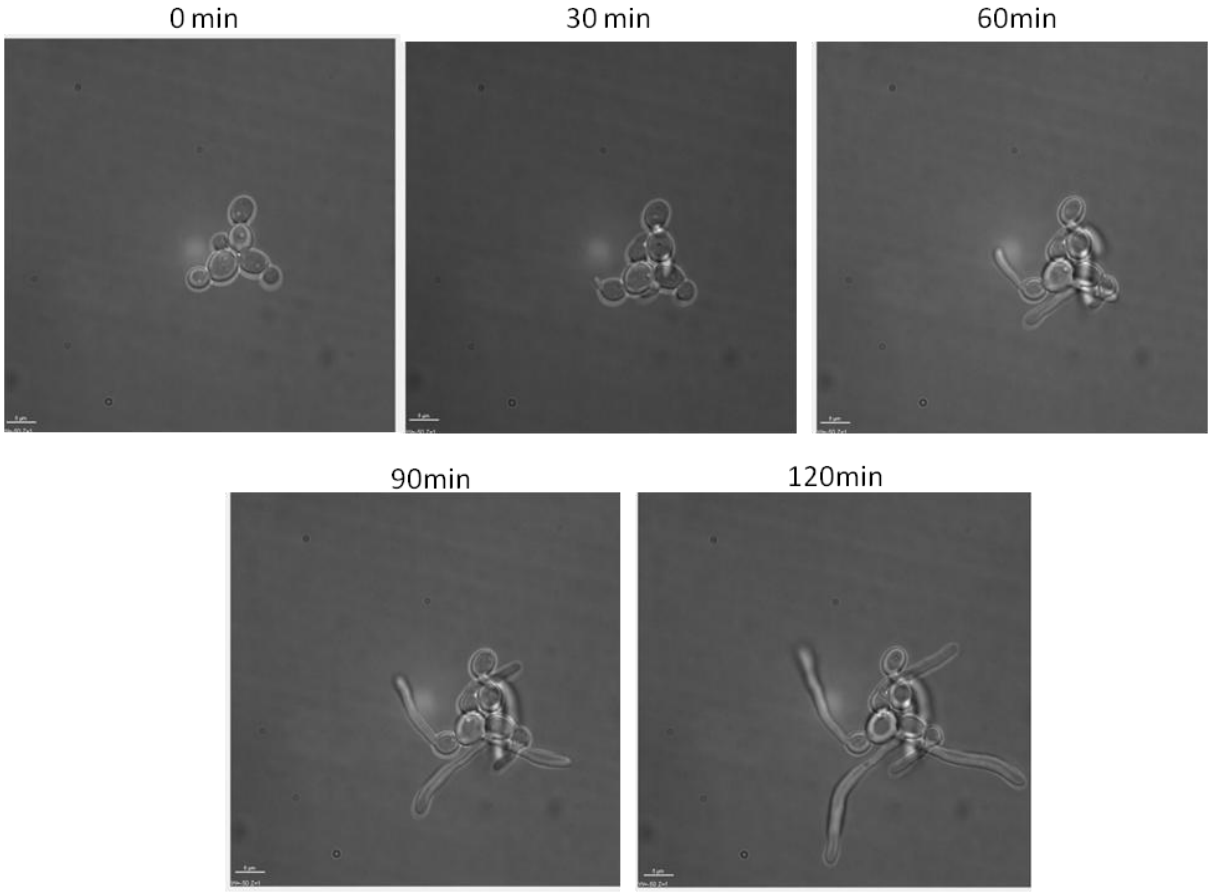

Figure 5.9 ***lrg1ΔΔ/LRG1(4A$_{CBK1}$)-MYC*** **shows normal hyphal growth**
The *lrg1ΔΔ/LRG1(4A$_{CBK1}$)-MYC* strain was induced to form hyphae on agar microscopy pads and then visualised every 30 minutes using a Delta Vision Spectris 4.0 microscope with Softworx^{TM} 3.2.2 software (Applied Precision Instruments).

5.3.7 Phosphorylation of Cbk1 consensus sites within *Ca*Lrg1 results in altered sensitivity to caspofungin

In order to assess the effect of echinocandins on the phospho-mimetic and non phosphorylatable mutants, *lrg1ΔΔ/LRG1(4A$_{CBK1}$)-MYC* and *lrg1ΔΔ/LRG1(2E2D$_{CBK1}$)-MYC,* were grown overnight in YPD media, sonicated briefly to break clumps of cells and adjusted to read the same absorbance at OD_{600}. Cultures were then diluted to $1x10^4$ and $1x10^6$ and plated on increasing concentrations of caspofungin. The results can be seen in figure 5.10 along with *BWP17*, *lrg1ΔΔ,* and Cdc28 site phospho-mutants for comparison. The cells with

the Lrg1(2E2D$_{CBK1}$) protein, appear to be almost completely growth inhibited at the lowest concentration of the drug, more so than even the strain lacking *LRG1*. However, inhibition of growth is lower at the higher drug concentrations and to a level similar to both *lrg1ΔΔ* and *lrg1ΔΔ/LRG1(2E2D$_{CDC28}$)-MYC,* this seems counterintuitive but is probably due to the well observed phenomenon of paradoxical growth, where higher levels of drug seem to inhibit growth less than lower levels. (Rueda et al., 2014)**.** On the other hand, growth of the strain with the Lrg1(4A$_{CBK1}$) protein, shows an increased resistance to caspofungin compared to the strain lacking *LRG1,* the one that contains the Lrg1(2E2D$_{CBK1}$) protein and even the wild-type strain. These results echo those seen in the phospho-mimetic and non-phosphorylatable mutants of the Cdc28 consensus sites which are shown for comparison and provides evidence that the phenotypes of the phospho-mutants in the Cdc28 and Cbk1 consensus sites are not only similar when observed visually via length: width ratios, but also have a similarity in terms of a molecular underpinning.

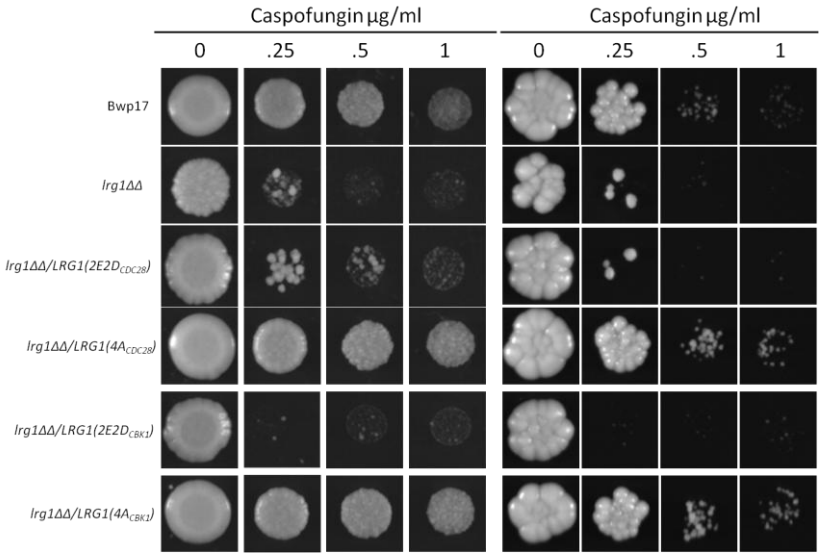

<u>Figure 5.10</u> Lrg1 Phospho-mutants of Cbk1 consensus sites have altered sensitivity to caspofungin

The *lrg1ΔΔ/LRG1(4A$_{CBK1}$)-MYC* and *lrg1ΔΔ/LRG1(2E2D$_{CBK1}$)-MYC* strains were grown in overnight cultures to stationary phase before brief sonication and adjustment to read the same absorbance at OD_{600}. Cultures were then diluted to $1x10^4$ and $1x10^6$ before being spotted onto YPD agar plus increasing concentrations of caspofungin. The *BWP17*, *lrg1ΔΔ* and phospho-mutant strains from chapter 3 are shown for comparison.

5.4 Discussion

5.4.1 C. albicans Lrg1 is a target for the Cbk1 kinase

In chapter 4, it was shown that Lrg1 is negatively regulated by phosphorylation at four Cdc28 consensus motifs in its N-terminal extension. This negative regulation causes an increase in polarised growth.

This chapter identified that one of the four Cbk1 consensus motifs previously identified, is also located in the N-terminal extension whilst the other 3 are located in regions of disorder next to the proteins LIM and RhoGAP domains. This and the fact that Cbk1 and Cdc28 are both implicated in *C. albicans* morphogenesis made Lrg1 a strong candidate for being targeted by Cbk1.

This study showed that the N-terminal domain of Lrg1 is able to be phosphorylated by the Cbk1 kinase *in vitro.* We also showed that the phosphorylation pattern of Lrg1 *in vivo* is altered in cells lacking any copy of *CBK1*. During growth in hyphal-inducing conditions, the phosphorylation of Lrg1 appears to disappear completely in cells lacking Lrg1. This loss of phosphorylation is also seen in stationary phase cells. In contrast, after cells are grown in yeast-inducing conditions for two hours, some residual phosphorylation is still seen on Lrg1 in cells that lack Cbk1. This could be due to the action of Cdc28 on Lrg1 described in chapter 4.

5.4.2 Phosphorylation of Lrg1 by Cbk1 results in an increase in polarised growth.

To investigate the physiological role of Cbk1 phosphorylation upon Lrg1, two Lrg1 phospho-mutants were created. The key residues in the Cbk1 consensus motifs were mutated to either phospho-mimetic or non-phosphorylatable amino acids. The Lrg1(2E2D$_{CBK1}$) mutant causes cells to grow in a more elongated, polarised fashion, similar to the result obtained with the Lrg1(2E2D$_{CDC28}$) mutant seen in chapter 4. Also similar to the mutant Cdc28 sites, cells expressing Lrg1(2E2D$_{CBK1}$) have an increased sensitivity to caspofungin, although this protein seems to cause a greater inhibition of growth than mutation in the Cdc28 sites. Due to time constraints, the consequences of the phospho-mimetic mutation on Rho1 were not investigated. However, due to the similar phenotypes seen in the two phospho-mimetic

strains, it could be inferred that phosphorylation of Lrg1 by Cbk1 also has the same effects on the localisation and activity of Rho1 as phosphorylation by Cdc28 observed earlier. Mutation of the four Cbk1 consensus motifs to non-phosphorylatable alanine also showed similar characteristics to the strains carrying mutations in the Cdc28 consensus sites. Cells did not show a change in their length or level of polarisation, but they did show a decreased average cell volume. The Lrg1($4A_{cbk1}$) mutant also cause increased resistance to caspofungin.

5.4.3 Model of Cbk1 Phosphorylation upon Lrg1

The data discussed above leads to a model of the physiological role of phosphorylation on Lrg1 by Cbk1 as shown in figure 5.11.

Phosphorylation of Lrg1 by Cbk1 at its four consensus motifs results in increased polarised growth in the cells. Unlike in the results with the Cdc28 phosphorylation, we do not have as yet any data to suggest a molecular mechanism behind this regulation. However, due to the similar phenotypes of cells expressing Lrg1($2E2D_{CBK1}$) to cells lacking *LRG1* or containing mutations in Cdc28 consensus sites, it can be speculated that the phosphorylation by Cbk1 leads to negative regulation of Lrg1. This negative regulation then presumably lifts the negative regulation upon Rho1 activity and possibly alters its mobility, producing polarised growth for longer periods of time, as seen in Chapter 3.

The phosphorylation of Lrg1 and subsequent increase in polarised growth by Cbk1 could be required for hyphal growth. The fact that Lrg1 is phosphorylated by Cbk1 during hyphal growth and lack of *CBK1* results in the inability to produce hyphae supports this. However, one would then expect the *lrg1ΔΔ/LRG1(*$4A_{CBK1}$*)* mutant to be unable to grow as hyphae, which has been shown above to be untrue. Perhaps this is because of redundant processes that Cbk1 controls during hyphal growth. Either way it is obvious that control of Lrg1 by Cbk1 phosphorylation plays a part in polarised growth.

Given the discussion in Chapter 4 on the possible role of Cdc28 on Lrg1 during formation of the secondary septum, could the action of Cbk1 on Lrg1 also be involved in this process. Due to the role that Cbk1 is involved plays in the processes behind degradation of the septum for cytokinesis, maybe it also has a role in the formation of it.

The resistance of the *lrg1ΔΔ/LRG1(4A$_{CBK1}$)* strain to caspofungin is also counter-intuitive to what one would expect, as was seen the non-phosphorylatable Cdc28 motifs. This also suggests that phosphorylation by Cbk1 has the same result on Rho1 and the glucan synthase as phosphorylation by Cdc28: producing a higher number of targets for the drug to attack.

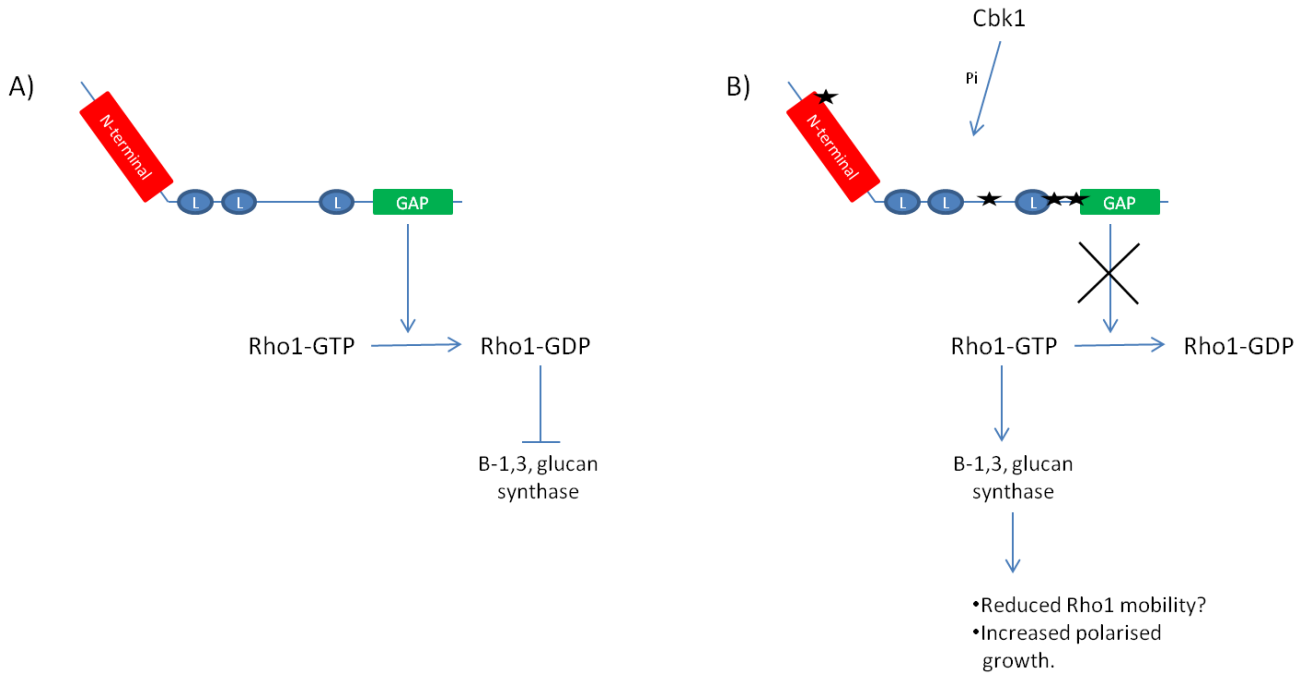

Figure 5.11 Model of Cbk1 phosphorylation on Lrg1 in *C. albicans*

A) Without any phosphorylation of the N-terminal domain by Cbk1, Lrg1 is available to catalyse the reaction of Rho1-GTP to Rho1-GDP, inhibiting the glucan synthase.

B) Phosphorylation (black stars) of Lrg1 by Cbk1 preventing the Rho-GAP domain from accessing Rho1. This allows Rho1 to remain active and the glucan synthase activity also increases. This lack of Rho1 regulation possibly causes a lack in Rho1 mobility throughout the cell. Therefore glucan is extruded into the cell wall for a longer amount of time, resulting in an increase in polarised growth.

6 General discussion

This study set out to try and characterise the putative *C. albicans* Lrg1 protein, its regulatory control and possible roles in morphogenesis. Initially it was found that *C. albicans* Lrg1 contained a 330 amino acid extension that is not seen in the *S. cerevisiae* homolog, indicating both a possible divergence in function and a possible regulatory domain on the protein. Interestingly though, deletion of this N-terminal extension appears to have no effect on cell growth.

The *LRG1* homolog in *S. cerevisiae* is responsible for efficient cell separation and deletion mutants possess increased invasive growth, but no cell aberrant elongation is seen (Svarovsky and Palecek, 2005). On the other hand, the N*. crassa* homolog is essential for hyphal tip extension (Vogt and Seiler, 2008b). In both organisms, Lrg1 is a negative regulator of the β-1, 3-glucan synthase through its action on Rho1. This study showed that similar to *N. crassa, Ca*Lrg1 localises to sites of cell wall growth, however in contrast, deletion of the protein in *C. albicans* results in an increase in polarised growth and invasiveness in the yeast morphology, whilst there is little effect on the growth of hyphae. This increase in polarised growth is associated with an increase in the activity of Rho1 as visualised via a fluorescent Rho1-GTP binding reporter. The advantages of this reporter were that the activity of Rho1 could be assessed as well as the cellular location and unlike *in vitro* GTPase assays, Rho1 activity was gauged under physiological conditions. However, one must be careful due to the reporter effectively acting as a competitor of Rho1 targets. Along with an increase in activity, during growth as yeast, Rho1 also shows a delayed or incomplete re-localisation from the growing tip to the site of septation. This distribution defect and increase in activity leads to the hypothesis that Lrg1 controls the switch from polarised growth at the growing tip, to isotropic growth at the cell cortex and then back to polarised growth at the site of septation through its action on Rho1. Indeed there is a suggestion that in *S. cerevisiae,* although Cdc42 is responsible for setting up early polarisation in the cell, it is Rho1 that is responsible for maintaining polarised growth (Cabib et al., 1998; Zhang et al., 2001).

Further analysis of the *C. albicans* Lrg1 N-terminal extension revealed sixteen potential Cdc28 phosphorylation motifs-four full and twelve minimal-plus three more minimal motifs were identified elsewhere in the protein. It is becoming more apparent that post-

translational modifications such as phosphorylation play an important role in protein regulation (Leach and Brown, 2012). Here, it was shown that the N-terminal extension of *Ca*Lrg1 is subjected to phosphorylation during yeast growth. Cdc28 was shown as being able to phosphorylate Lrg1 *in vitro* and Lrg1 phosphorylation was altered upon inhibition of Cdc28, pointing to this kinase as being responsible for the modification. Analysis of the phosphorylation state of Lrg1 in various cyclin mutants and in synchronised cells suggested that Cdc28 acts with its cyclin Cln3 to phosphorylate Lrg1 during late mitosis and early G1. In *S. cerevisiae* there is evidence for Cdc28 phosphorylating the Rho1 GEF Tus1 in late G1/S phase, priming Rho1 for activation for bud emergence (Kono et al., 2008). Perhaps phosphorylation of Lrg1 by Cdc28 operates antagonistically at this time?

The physiological role of Lrg1 phosphorylation by Cdc28 was investigated by producing mutants in which the four full Cdc28 motifs were altered to either mimic phosphorylation or be non-phosphorylatable. The phospho-mimetic mutant shows a similar phenotype to the *lrg1ΔΔ* mutant. Cells are elongated and highly polarised; Rho1 activity is increased and also shows a defect in re-localisation from the bud-tip. This indicates that Cdc28 phosphorylation upon Lrg1 negatively regulates the protein. This is then consistent with the observation that phosphorylation occurs in late M, early G1 phase so that Rho1 is available for the highly polarised growth needed for the secondary septum and cell division. Although it is strange that both the phosphomimetic and deletion mutants fail to separate.

One would then expect that the non-phosphorylatable mutant would show the opposite phenotype. This is observed in terms of a lowered Rho1 activity level. However, visually the 4A mutant is morphologically indistinguishable from wild-type cells other than a slightly reduced volume. This is a similar situation to when the N-terminal extension was deleted, further indicating that phosphorylation is inhibitory, and suggesting that Lrg1 lacking regulation in the N-terminus behaves normally.

The phospho-mutant results led to the proposal of a model in which phosphorylation of Lrg1 at the four full Cdc28 motifs causes the N-terminal domain to inhibit the binding and GAP activity of the protein, which increases the activity of Rho1, but decreases its mobility leading to an increase in polarised growth. However, the results gained from the Lrg1($15E_{CDC28}$) mutant, which seems to reverse the phenotype of phosphomimetic mutants in the four full Cdc28 motifs, appears to indicate that the regulation of Lrg1 is more complex than the model describes and requires further investigation. It is plausible though, that

Cdc28 and the cell cycle are linked to Rho1, a controller of polarity, through its regulator Lrg1.

C. albicans Lrg1 had previously been identified as having multiple Cbk1 phosphorylation motifs (Regan, H. PhD thesis University of Sheffield). Also, in *N. crassa*, *LRG1* is genetically linked to the *CBK1* homolog *COT1*. This study showed that in *C. albicans,* Lrg1 is capable of being phosphorylated *in vitro* by Cbk1. In addition Lrg1 lost phosphorylation in both yeast and hyphal morphologies when *CBK1* was absent. To explore this further, as with the Cdc28 motifs, phospho-mimetic and non-phosphorylatable mutants of the Cbk1 phosphorylation motifs were produced.

The phospho-mimetic mutant showed the same phenotype as the Lrg1(2E2D$_{CDC28}$) mutant, with highly polarised, elongated cells, further suggesting that phosphorylation of Lrg1 negatively regulates the protein. This increase in polarised growth caused by phosphorylation may also explain why *cbk1ΔΔ* cells are unable to form hyphae, which requires extended periods of polarised growth (McNemar and Fonzi, 2002). If this were true, the non-phosphorylatable mutant should be defective in hyphal growth. However this is not the case and the Lrg1(4A$_{CDC28}$) mutant is efficient in hyphal growth, possibly indicating that Cbk1 brings about polarised growth by other mechanisms. Conversely, it would be also be interesting to create a *cbk1ΔΔ/lrg1ΔΔ* strain, which would reveal whether the increase in polarised growth caused by loss of *LRG1* could overcome the lack of polarised growth observed in *cbk1ΔΔ.* Much like the Lrg1(4A$_{CDC28}$) and N-terminal deletion mutants, the Lrg1(4A$_{CBK1}$) mutant shows little effect on growth, again indicating that non-phosphorylated form of the protein is not defective. Similarly, would a Lrg1(2E2D$_{CDC28}$2E2D$_{CBK1}$) mutant produce the same phenotype as the *lrg1ΔΔ* strain.

Due to time constraints, and difficulty in strain construction, it was not possible to assess the activity of Rho1 in the Cbk1 motif mutants. However, due to the similar phenotypes of the mutants to those in the Cdc28 consensus motifs, one could hypothesise that the Lrg1(2E2D$_{CBK1}$) phosphomimetic mutant showed an increase in Rho1 activity whilst the non-phosphorylatable mutant has the opposite effect. Further investigation into the phosphatase that is responsible for the de-phosphorylation of both the Cbk1 and Cdc28 consensus motifs may also provide insights into the proteins regulation. The joint action of Cbk1 and Cdc28 phosphorylation on Lrg1 is shown in figure 6.1.

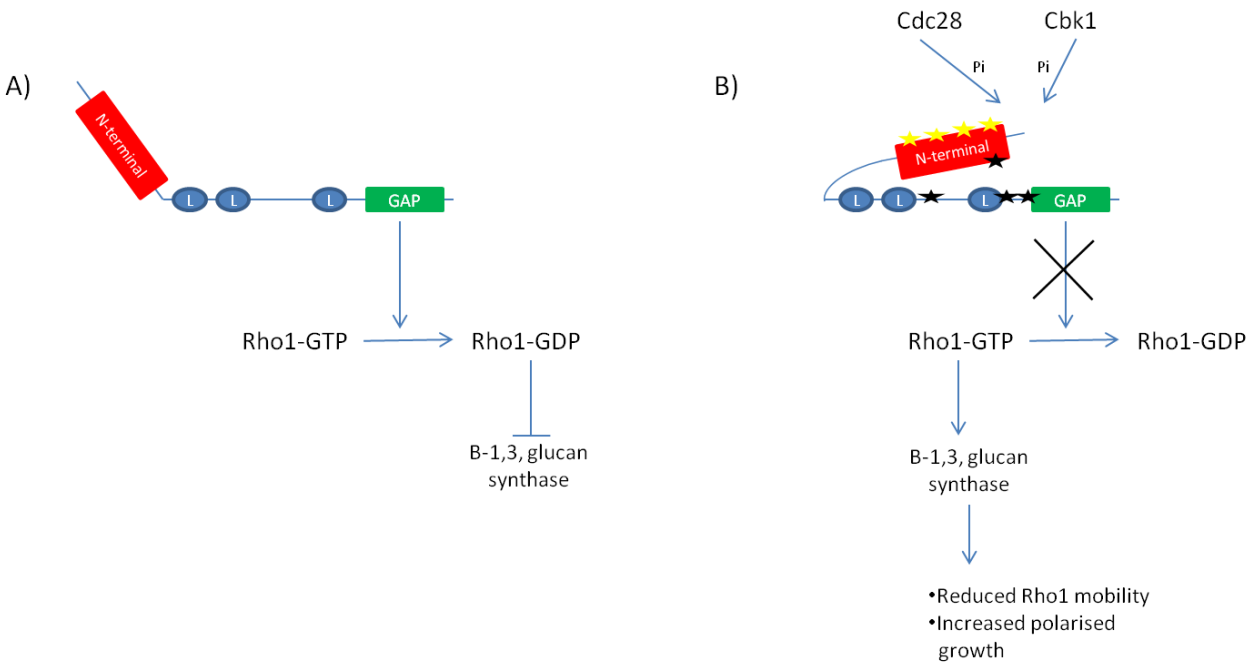

<u>Figure 6.1</u> The joint action of Cdc28 and Cbk1 phosphorylation on Lrg1 brings about polarised growth

A) In the absence of phosphorylation of Lrg1, the proteins GAP domain acts on Rho1, converting it from its GTP-bound, active form to its GDP-bound inactive form. This action also decreases the activity of the β-1,3-glucan synthase.

B) Phosphorylation of Lrg1 by Cdc28 (yellow stars) and/or Cbk1 (black stars) results in the inhibition of the negative regulation Lrg1 exerts on Rho1. The Rho1 protein remains GTP-bound, increasing the activity of the glucan synthase. The active form of Rho1 also has a reduced mobility which, coupled with the increased glucan production, results in an increase in polarised growth at either the bud tip or site of septation.

The echinocandin class of drugs are a major defence in the treatment of *C. albicans* (Pea, 2013). The drug targets the β-1,3-glucan synthase, inhibiting cell wall synthesis (Perlin, 2007) and as such mutants in the synthase genes are a huge source of resistance (Beyda et al., 2012). If Lrg1 negatively regulates the β-1,3-glucan synthase through its action on Rho1, it would be expected that deletion of *LRG1* would cause increased resistance to this class of drugs. Indeed, this is has been shown in *N. crassa (Vogt and Seiler, 2008b).* However, the *lrg1ΔΔ, lrg1Δ/LRG1(2E2D$_{CDC28}$)* and *lrg1Δ/LRG1(42E2D$_{CBK1}$)* strains, of which the former two show increased Rho1 activity, exhibit an increased sensitivity to caspofungin. Conversely, the *lrg1Δ/LRG1(4A$_{CDC28}$)* which shows a decreased Rho1 activity, and *lrg1Δ/LRG1(4A$_{CBK1}$)* both show a resistance to the drug not seen in the wild-type strain. This is the opposite result to what was expected. As alluded to in the text, perhaps the increase in Rho1 is producing an increased number of active glucan synthase molecules for the drug to attack. Or maybe Lrg1 is also controlling targets of Rho1 other than the glucan synthases, which has been reported in other fungi (Lorberg et al., 2001b) causing other defects of the cell wall that are shown when exposed to caspofungin. Either way, this study has shown that Lrg1 is an important protein for further study in relation to the echinocandins and also demonstrates that studying the basic molecular biology of *C. albicans* can provide real world benefits.

In conclusion, this study has shown that the GTPase activating protein Lrg1 is responsible for controlling polarised growth in *C. albicans.* Through its negative action on Rho1, Lrg1 controls the switch from polarised growth at the bud tip of yeast to isotropic growth at the cell cortex before a return again to polarised growth at the site of septum formation. The protein shows an evolutionary diversion from that of other fungi, with an N-terminal extension that plays a role in the regulation of the protein. Lrg1 itself is negatively regulated by the concerted action of both Cdc28 in the N-terminal extension and Cbk1. Phosphorylation by Cdc28 links growth of the daughter bud to the cell cycle, whilst regulation by Cbk1 may provide an insight into the mechanisms behind the highly polarised nature of hyphal growth. We have also shown that phosphorylation of Lrg1 results in hypersensitivity to caspofungin, providing a point for further drug research.

List of figures

Chapter1

Chapter 3

List of Tables

References

Adams, A.E., Johnson, D.I., Longnecker, R.M., Sloat, B.F., and Pringle, J.R. (1990). CDC42 and CDC43, two additional genes involved in budding and the establishment of cell polarity in the yeast Saccharomyces cerevisiae. The Journal of cell biology *111*, 131-142.

Adams, A.E., and Pringle, J.R. (1984). Relationship of actin and tubulin distribution to bud growth in wild-type and morphogenetic-mutant Saccharomyces cerevisiae. The Journal of cell biology *98*, 934-945.

Alberts, A.S. (2001). Identification of a carboxyl-terminal diaphanous-related formin homology protein autoregulatory domain. The Journal of biological chemistry *276*, 2824-2830.

Alberts, A.S., Bouquin, N., Johnston, L.H., and Treisman, R. (1998). Analysis of RhoA-binding proteins reveals an interaction domain conserved in heterotrimeric G protein beta subunits and the yeast response regulator protein Skn7. The Journal of biological chemistry *273*, 8616-8622.

Baetz, K., Moffat, J., Haynes, J., Chang, M., and Andrews, B. (2001). Transcriptional coregulation by the cell integrity mitogen-activated protein kinase Slt2 and the cell cycle regulator Swi4. Mol Cell Biol *21*, 6515-6528.

Bartnicki-Garcia, S., Hergert, F., and Gierz, G. (1989). Computer simulation of fungal morphogenesis and the mathematical basis for hyphal (tip) growth. Protoplasma *153*, 46-57.

Bassilana, M., and Arkowitz, R.A. (2006). Rac1 and Cdc42 have different roles in Candida albicans development. Eukaryot Cell *5*, 321-329.

Bassilana, M., Hopkins, J., and Arkowitz, R.A. (2005). Regulation of the Cdc42/Cdc24 GTPase module during Candida albicans hyphal growth. Eukaryot Cell *4*, 588-603.

Beauvais, A., Drake, R., Ng, K., Diaquin, M., and Latge, J.P. (1993). Characterization of the 1,3-beta-glucan synthase of Aspergillus fumigatus. J Gen Microbiol *139*, 3071-3078.

Becksague, C.M., and Jarvis, W.R. (1993). Secular Trends In The Epidemiology Of Nosocomial Fungal-Infections In The United-States, 1980-1990. J Infect Dis *167*, 1247-1251.

Bennett, R.J., and Johnson, A.D. (2003). Completion of a parasexual cycle in Candida albicans by induced chromosome loss in tetraploid strains. The EMBO journal *22*, 2505-2515.

Bensen, E.S., Clemente-Blanco, A., Finley, K.R., Correa-Bordes, J., and Berman, J. (2005). The mitotic cyclins Clb2p and Clb4p affect morphogenesis in Candida albicans. Mol Biol Cell *16*, 3387-3400.

Berman, J., and Sudbery, P.E. (2002). Candida albicans: A molecular revolution built on lessons from budding yeast. Nature Reviews Genetics *3*, 918-930.

Beyda, N.D., Lewis, R.E., and Garey, K.W. (2012). Echinocandin resistance in Candida species: mechanisms of reduced susceptibility and therapeutic approaches. The Annals of pharmacotherapy *46*, 1086-1096.

Bishop, A., Lane, R., Beniston, R., Chapa-y-Lazo, B., Smythe, C., and Sudbery, P. (2010). Hyphal growth in Candida albicans requires the phosphorylation of Sec2 by the Cdc28-Ccn1/Hgc1 kinase. The EMBO journal *29*, 2930-2942.

Bishop, A.C., Ubersax, J.A., Petsch, D.T., Matheos, D.P., Gray, N.S., Blethrow, J., Shimizu, E., Tsien, J.Z., Schultz, P.G., Rose, M.D.*, et al.* (2000). A chemical switch for inhibitor-sensitive alleles of any protein kinase. Nature *407*, 395-401.

Biswas, S., Van Dijck, P., and Datta, A. (2007). Environmental sensing and signal transduction pathways regulating morphopathogenic determinants of Candida albicans. Microbiology and molecular biology reviews : MMBR *71*, 348-376.

Blankenship, J.R., Fanning, S., Hamaker, J.J., and Mitchell, A.P. (2010). An extensive circuitry for cell wall regulation in Candida albicans. PLoS pathogens *6*, e1000752.

Booher, R.N., Deshaies, R.J., and Kirschner, M.W. (1993). Properties of Saccharomyces cerevisiae wee1 and its differential regulation of p34CDC28 in response to G1 and G2 cyclins. The EMBO journal *12*, 3417-3426.

Bosco, E.E., Mulloy, J.C., and Zheng, Y. (2009). Rac1 GTPase: a "Rac" of all trades. Cell Mol Life Sci *66*, 370-374.

Boyd, C., Hughes, T., Pypaert, M., and Novick, P. (2004). Vesicles carry most exocyst subunits to exocytic sites marked by the remaining two subunits, Sec3p and Exo70p. The Journal of cell biology *167*, 889-901.

Brace, J., Hsu, J., and Weiss, E.L. (2011). Mitotic exit control of the Saccharomyces cerevisiae Ndr/LATS kinase Cbk1 regulates daughter cell separation after cytokinesis. Mol Cell Biol *31*, 721-735.

Brown, J.L., Bussey, H., and Stewart, R.C. (1994). Yeast Skn7p functions in a eukaryotic two-component regulatory pathway. The EMBO journal *13*, 5186-5194.

Buttery, S.M., Yoshida, S., and Pellman, D. (2007). Yeast formins Bni1 and Bnr1 utilize different modes of cortical interaction during the assembly of actin cables. Mol Biol Cell *18*, 1826-1838.

Caballero-Lima, D., Kaneva, I.N., Watton, S.P., Sudbery, P.E., and Craven, C.J. (2013). The spatial distribution of the exocyst and actin cortical patches is sufficient to organize hyphal tip growth. Eukaryot Cell *12*, 998-1008.

Caballero-Lima, D., and Sudbery, P.E. (2014). In Candida albicans, phosphorylation of Exo84 by Cdk1-Hgc1 is necessary for efficient hyphal extension. Mol Biol Cell *25*, 1097-1110.

Cabib, E., Drgonova, J., and Drgon, T. (1998). Role of small G proteins in yeast cell polarization and wall biosynthesis. Annu Rev Biochem *67*, 307-333.

Care, R.S., Trevethick, J., Binley, K.M., and Sudbery, P.E. (1999). The MET3 promoter: a new tool for Candida albicans molecular genetics. Mol Microbiol *34*, 792-798.

Chaffin, W.L. (2008). Candida albicans cell wall proteins. Microbiology and molecular biology reviews : MMBR *72*, 495-544.

Chang, F., and Herskowitz, I. (1990). Identification of a gene necessary for cell cycle arrest by a negative growth factor of yeast: FAR1 is an inhibitor of a G1 cyclin, CLN2. Cell *63*, 999-1011.

Chapa y Lazo, B., Bates, S., and Sudbery, P. (2005). The G1 cyclin Cln3 regulates morphogenesis in Candida albicans. Eukaryot Cell *4*, 90-94.

Chen, W., Lim, H.H., and Lim, L. (1993). The CDC42 homologue from Caenorhabditis elegans. Complementation of yeast mutation. The Journal of biological chemistry *268*, 13280-13285.

Colman-Lerner, A., Chin, T.E., and Brent, R. (2001). Yeast Cbk1 and Mob2 activate daughter-specific genetic programs to induce asymmetric cell fates. Cell *107*, 739-750.

Corvest, V., Bogliolo, S., Follette, P., Arkowitz, R.A., and Bassilana, M. (2013). Spatiotemporal regulation of Rho1 and Cdc42 activity during Candida albicans filamentous growth. Mol Microbiol *89*, 626-648.

Court, H., and Sudbery, P. (2007). Regulation of Cdc42 GTPase activity in the formation of hyphae in Candida albicans. Mol Biol Cell *18*, 265-281.

Crampin, H., Finley, K., Gerami-Nejad, M., Court, H., Gale, C., Berman, J., and Sudbery, P. (2005). Candida albicans hyphae have a Spitzenkorper that is distinct from the polarisome found in yeast and pseudohyphae. Journal of cell science *118*, 2935-2947.

Cvrckova, F., and Nasmyth, K. (1993). Yeast G1 cyclins CLN1 and CLN2 and a GAP-like protein have a role in bud formation. The EMBO journal *12*, 5277-5286.

Dahmann, C., Diffley, J.F., and Nasmyth, K.A. (1995). S-phase-promoting cyclin-dependent kinases prevent re-replication by inhibiting the transition of replication origins to a pre-replicative state. Curr Biol *5*, 1257-1269.

Dawid, I.B., Breen, J.J., and Toyama, R. (1998). LIM domains: multiple roles as adapters and functional modifiers in protein interactions. Trends Genet *14*, 156-162.

Derbise, A., Lesic, B., Dacheux, D., Ghigo, J.M., and Carniel, E. (2003). A rapid and simple method for inactivating chromosomal genes in Yersinia. FEMS Immunol Med Microbiol *38*, 113-116.

Dieterich, C., Schandar, M., Noll, M., Johannes, F.J., Brunner, H., Graeve, T., and Rupp, S. (2002). In vitro reconstructed human epithelia reveal contributions of Candida albicans EFG1 and CPH1 to adhesion and invasion. Microbiology-(UK) *148*, 497-506.

Dinkel, H., Van Roey, K., Michael, S., Davey, N.E., Weatheritt, R.J., Born, D., Speck, T., Kruger, D., Grebnev, G., Kuban, M.*, et al.* (2014). The eukaryotic linear motif resource ELM: 10 years and counting. Nucleic Acids Res *42*, 7.

Dirick, L., Bohm, T., and Nasmyth, K. (1995). Roles and regulation of Cln-Cdc28 kinases at the start of the cell cycle of Saccharomyces cerevisiae. The EMBO journal *14*, 4803-4813.

Donaldson, A.D., Raghuraman, M.K., Friedman, K.L., Cross, F.R., Brewer, B.J., and Fangman, W.L. (1998). CLB5-dependent activation of late replication origins in S. cerevisiae. Molecular cell *2*, 173-182.

Dosztanyi, Z., Csizmok, V., Tompa, P., and Simon, I. (2005). IUPred: web server for the prediction of intrinsically unstructured regions of proteins based on estimated energy content. Bioinformatics *21*, 3433-3434.

Duret, L., Gasteiger, E., and Perriere, G. (1996). LALNVIEW: a graphical viewer for pairwise sequence alignments. Computer applications in the biosciences : CABIOS *12*, 507-510.

Dvorsky, R., Blumenstein, L., Vetter, I.R., and Ahmadian, M.R. (2004). Structural insights into the interaction of ROCKI with the switch regions of RhoA. Journal Of Biological Chemistry *279*, 7098-7104.

Eitzen, G., Thorngren, N., and Wickner, W. (2001). Rho1p and Cdc42p act after Ypt7p to regulate vacuole docking. The EMBO journal *20*, 5650-5656.

Enserink, J.M., and Kolodner, R.D. (2010). An overview of Cdk1-controlled targets and processes. Cell Div *5*, 11.

Evangelista, M., Blundell, K., Longtine, M.S., Chow, C.J., Adames, N., Pringle, J.R., Peter, M., and Boone, C. (1997). Bni1p, a yeast formin linking cdc42p and the actin cytoskeleton during polarized morphogenesis. Science *276*, 118-122.

Finger, F.P., Hughes, T.E., and Novick, P. (1998). Sec3p is a spatial landmark for polarized secretion in budding yeast. Cell *92*, 559-571.

Fitch, P.G., Gammie, A.E., Lee, D.J., de Candal, V.B., and Rose, M.D. (2004). Lrg1p Is a Rho1 GTPase-activating protein required for efficient cell fusion in yeast. Genetics *168*, 733-746.

Fujisawa, K., Fujita, A., Ishizaki, T., Saito, Y., and Narumiya, S. (1996). Identification of the Rho-binding domain of p160(ROCK), a Rho-associated coiled-coil containing protein kinase. Journal Of Biological Chemistry *271*, 23022-23028.

Fujiwara, T., Tanaka, K., Mino, A., Kikyo, M., Takahashi, K., Shimizu, K., and Takai, Y. (1998). Rho1p-Bni1p-Spa2p interactions: implication in localization of Bni1p at the bud site and regulation of the actin cytoskeleton in Saccharomyces cerevisiae. Mol Biol Cell *9*, 1221-1233.

Gola, S., Martin, R., Walther, A., Dunkler, A., and Wendland, J. (2003). New modules for PCR-based gene targeting in Candida albicans: rapid and efficient gene targeting using 100 bp of flanking homology region. Yeast *20*, 1339-1347.

Gonzalez-Novo, A., Correa-Bordes, J., Labrador, L., Sanchez, M., Vazquez de Aldana, C.R., and Jimenez, J. (2008). Sep7 is essential to modify septin ring dynamics and inhibit cell separation during Candida albicans hyphal growth. Mol Biol Cell *19*, 1509-1518.

Goud, B., Salminen, A., Walworth, N.C., and Novick, P.J. (1988). A GTP-binding protein required for secretion rapidly associates with secretory vesicles and the plasma membrane in yeast. Cell *53*, 753-768.

Gow, N.A., and Hube, B. (2012). Importance of the Candida albicans cell wall during commensalism and infection. Curr Opin Microbiol *15*, 406-412.

Gow, N.A.R., Brown, A.J.P., and Odds, F.C. (2002). Fungal morphogenesis and host invasion. Curr Opin Microbiol *5*, 366-371.

Guo, W., Tamanoi, F., and Novick, P. (2001). Spatial regulation of the exocyst complex by Rho1 GTPase. Nature cell biology *3*, 353-360.

Gutierrez-Escribano, P., Gonzalez-Novo, A., Suarez, M.B., Li, C.R., Wang, Y., de Aldana, C.R., and Correa-Bordes, J. (2011). CDK-dependent phosphorylation of Mob2 is essential for hyphal development in Candida albicans. Mol Biol Cell *22*, 2458-2469.

Haase, S.B., Winey, M., and Reed, S.I. (2001). Multi-step control of spindle pole body duplication by cyclin-dependent kinase. Nature cell biology *3*, 38-42.

Hartwell, L.H. (1974). Saccharomyces cerevisiae cell cycle. Bacteriological reviews *38*, 164-198.

Hartwell, L.H., Mortimer, R.K., Culotti, J., and Culotti, M. (1973). Genetic Control of the Cell Division Cycle in Yeast: V. Genetic Analysis of cdc Mutants. Genetics *74*, 267-286.

Harvey, S.L., and Kellogg, D.R. (2003). Conservation of mechanisms controlling entry into mitosis: budding yeast wee1 delays entry into mitosis and is required for cell size control. Curr Biol *13*, 264-275.

Hausauer, D.L., Gerami-Nejad, M., Kistler-Anderson, C., and Gale, C.A. (2005). Hyphal guidance and invasive growth in Candida albicans require the Ras-like GTPase Rsr1p and its GTPase-activating protein Bud2p. Eukaryot Cell *4*, 1273-1286.

Hazan, I., Sepulveda-Becerra, M., and Liu, H.P. (2002). Hyphal elongation is regulated independently of cell cycle in Candida albicans. Molecular Biology Of The Cell *13*, 134-145.

Heckman, D.S., Geiser, D.M., Eidell, B.R., Stauffer, R.L., Kardos, N.L., and Hedges, S.B. (2001). Molecular evidence for the early colonization of land by fungi and plants. Science *293*, 1129-1133.

Henchoz, S., Chi, Y., Catarin, B., Herskowitz, I., Deshaies, R.J., and Peter, M. (1997). Phosphorylation- and ubiquitin-dependent degradation of the cyclin-dependent kinase inhibitor Far1p in budding yeast. Genes & development *11*, 3046-3060.

Hergovich, A., Stegert, M.R., Schmitz, D., and Hemmings, B.A. (2006). NDR kinases regulate essential cell processes from yeast to humans. Nature Reviews Molecular Cell Biology *7*, 253-264.

Hickman, M.A., Zeng, G., Forche, A., Hirakawa, M.P., Abbey, D., Harrison, B.D., Wang, Y.M., Su, C.H., Bennett, R.J., Wang, Y.*, et al.* (2013). The 'obligate diploid' Candida albicans forms mating-competent haploids. Nature *494*, 55-59.

Hope, H., Bogliolo, S., Arkowitz, R.A., and Bassilana, M. (2008). Activation of Rac1 by the guanine nucleotide exchange factor Dck1 is required for invasive filamentous growth in the pathogen Candida albicans. Mol Biol Cell *19*, 3638-3651.

Hope, H., Schmauch, C., Arkowitz, R.A., and Bassilana, M. (2010). The Candida albicans ELMO homologue functions together with Rac1 and Dck1, upstream of the MAP Kinase Cek1, in invasive filamentous growth. Mol Microbiol *76*, 1572-1590.

Huang, D., Friesen, H., and Andrews, B. (2007). Pho85, a multifunctional cyclin-dependent protein kinase in budding yeast. Mol Microbiol *66*, 303-314.

Huang, X., and Miller, W. (1991). A time-efficient, linear-space local similarity algorithm. Advances in Applied Mathematics *12*, 337-357.

Hull, C.M., and Johnson, A.D. (1999). Identification of a mating type-like locus in the asexual pathogenic yeast Candida albicans. Science *285*, 1271-1275.

Igual, J.C., Johnson, A.L., and Johnston, L.H. (1996). Coordinated regulation of gene expression by the cell cycle transcription factor Swi4 and the protein kinase C MAP kinase pathway for yeast cell integrity. The EMBO journal *15*, 5001-5013.

Imamura, H., Tanaka, K., Hihara, T., Umikawa, M., Kamei, T., Takahashi, K., Sasaki, T., and Takai, Y. (1997). Bni1p and Bnr1p: downstream targets of the Rho family small G-proteins which interact with profilin and regulate actin cytoskeleton in Saccharomyces cerevisiae. The EMBO journal *16*, 2745-2755.

Jansen, J.M., Barry, M.F., Yoo, C.K., and Weiss, E.L. (2006). Phosphoregulation of Cbk1 is critical for RAM network control of transcription and morphogenesis. Journal Of Cell Biology *175*, 755-766.

Johnson, D.I., and Pringle, J.R. (1990). Molecular characterization of CDC42, a Saccharomyces cerevisiae gene involved in the development of cell polarity. The Journal of cell biology *111*, 143-152.

Jones, L.A., and Sudbery, P.E. (2010). Spitzenkorper, exocyst, and polarisome components in Candida albicans hyphae show different patterns of localization and have distinct dynamic properties. Eukaryot Cell *9*, 1455-1465.

Jung, U.S., and Levin, D.E. (1999). Genome-wide analysis of gene expression regulated by the yeast cell wall integrity signalling pathway. Mol Microbiol *34*, 1049-1057.

Jung, U.S., Sobering, A.K., Romeo, M.J., and Levin, D.E. (2002). Regulation of the yeast Rlm1 transcription factor by the Mpk1 cell wall integrity MAP kinase. Mol Microbiol *46*, 781-789.

Kadosh, D., and Johnson, A.D. (2005). Induction of the Candida albicans filamentous growth program by relief of transcriptional repression: a genome-wide analysis. Mol Biol Cell *16*, 2903-2912.

Kaldis, P., Sutton, A., and Solomon, M.J. (1996). The Cdk-activating kinase (CAK) from budding yeast. Cell *86*, 553-564.

Kamada, Y., Jung, U.S., Piotrowski, J., and Levin, D.E. (1995). The protein kinase C-activated MAP kinase pathway of Saccharomyces cerevisiae mediates a novel aspect of the heat shock response. Genes & development *9*, 1559-1571.

Keaton, M.A., and Lew, D.J. (2006). Eavesdropping on the cytoskeleton: progress and controversy in the yeast morphogenesis checkpoint. Curr Opin Microbiol *9*, 540-546.

Ketela, T., Green, R., and Bussey, H. (1999). Saccharomyces cerevisiae mid2p is a potential cell wall stress sensor and upstream activator of the PKC1-MPK1 cell integrity pathway. J Bacteriol *181*, 3330-3340.

Kim, K.Y., and Levin, D.E. (2011). Mpk1 MAPK association with the Paf1 complex blocks Sen1-mediated premature transcription termination. Cell *144*, 745-756.

Kim, K.Y., Truman, A.W., and Levin, D.E. (2008). Yeast Mpk1 mitogen-activated protein kinase activates transcription through Swi4/Swi6 by a noncatalytic mechanism that requires upstream signal. Mol Cell Biol *28*, 2579-2589.

Kimura, K., Tsuji, T., Takada, Y., Miki, T., and Narumiya, S. (2000). Accumulation of GTP-bound RhoA during cytokinesis and a critical role of ECT2 in this accumulation. Journal Of Biological Chemistry *275*, 17233-17236.

Klis, F.M., Boorsma, A., and De Groot, P.W. (2006). Cell wall construction in Saccharomyces cerevisiae. Yeast *23*, 185-202.

Knaus, M., Pelli-Gulli, M.P., van Drogen, F., Springer, S., Jaquenoud, M., and Peter, M. (2007). Phosphorylation of Bem2p and Bem3p may contribute to local activation of Cdc42p at bud emergence. The EMBO journal *26*, 4501-4513.

Kohno, H., Tanaka, K., Mino, A., Umikawa, M., Imamura, H., Fujiwara, T., Fujita, Y., Hotta, K., Qadota, H., Watanabe, T.*, et al.* (1996). Bni1p implicated in cytoskeletal control is a putative target of Rho1p small GTP binding protein in Saccharomyces cerevisiae. The EMBO journal *15*, 6060-6068.

Kollar, R., Reinhold, B.B., Petrakova, E., Yeh, H.J., Ashwell, G., Drgonova, J., Kapteyn, J.C., Klis, F.M., and Cabib, E. (1997). Architecture of the yeast cell wall. Beta(1-->6)-glucan interconnects mannoprotein, beta(1-->)3-glucan, and chitin. The Journal of biological chemistry *272*, 17762-17775.

Kono, K., Nogami, S., Abe, M., Nishizawa, M., Morishita, S., Pellman, D., and Ohya, Y. (2008). G1/S cyclin-dependent kinase regulates small GTPase Rho1p through phosphorylation of RhoGEF Tus1p in Saccharomyces cerevisiae. Mol Biol Cell *19*, 1763-1771.

Kopecka, M., and Kreger, D.R. (1986). Assembly of microfibrils in vivo and in vitro from (1----3)-beta-D-glucan synthesized by protoplasts of Saccharomyces cerevisiae. Archives of microbiology *143*, 387-395.

Kurat, C.F., Wolinski, H., Petschnigg, J., Kaluarachchi, S., Andrews, B., Natter, K., and Kohlwein, S.D. (2009). Cdk1/Cdc28-dependent activation of the major triacylglycerol lipase Tgl4 in yeast links lipolysis to cell-cycle progression. Molecular cell *33*, 53-63.

La Valle, R., and Wittenberg, C. (2001). A role for the Swe1 checkpoint kinase during filamentous growth of Saccharomyces cerevisiae. Genetics *158*, 549-562.

Lagorce, A., Hauser, N.C., Labourdette, D., Rodriguez, C., Martin-Yken, H., Arroyo, J., Hoheisel, J.D., and Francois, J. (2003). Genome-wide analysis of the response to cell wall mutations in the yeast Saccharomyces cerevisiae. The Journal of biological chemistry *278*, 20345-20357.

Lavoie, H., Sellam, A., Askew, C., Nantel, A., and Whiteway, M. (2008). A toolbox for epitope-tagging and genome-wide location analysis in Candida albicans. Bmc Genomics *9*, 1471-2164.

Leach, M.D., and Brown, A.J. (2012). Posttranslational modifications of proteins in the pathobiology of medically relevant fungi. Eukaryot Cell *11*, 98-108.

Lesage, G., and Bussey, H. (2006). Cell wall assembly in Saccharomyces cerevisiae. Microbiology and molecular biology reviews : MMBR *70*, 317-343.

Levin, D.E. (2011). Regulation of cell wall biogenesis in Saccharomyces cerevisiae: the cell wall integrity signaling pathway. Genetics *189*, 1145-1175.

Levin, D.E., and Bartlett-Heubusch, E. (1992). Mutants in the S. cerevisiae PKC1 gene display a cell cycle-specific osmotic stability defect. The Journal of cell biology *116*, 1221-1229.

Lew, D.J., and Reed, S.I. (1993). Morphogenesis in the yeast cell cycle: regulation by Cdc28 and cyclins. The Journal of cell biology *120*, 1305-1320.

Li, C.R., Lee, R.T., Wang, Y.M., Zheng, X.D., and Wang, Y. (2007). Candida albicans hyphal morphogenesis occurs in Sec3p-independent and Sec3p-dependent phases separated by septin ring formation. Journal of cell science *120*, 1898-1907.

Li, S., Ault, A., Malone, C.L., Raitt, D., Dean, S., Johnston, L.H., Deschenes, R.J., and Fassler, J.S. (1998). The yeast histidine protein kinase, Sln1p, mediates phosphotransfer to two response regulators, Ssk1p and Skn7p. The EMBO journal *17*, 6952-6962.

Lo, H.J., Kohler, J.R., DiDomenico, B., Loebenberg, D., Cacciapuoti, A., and Fink, G.R. (1997). Nonfilamentous C-albicans mutants are avirulent. Cell *90*, 939-949.

Lockhart, S.R., Pujol, C., Daniels, K.J., Miller, M.G., Johnson, A.D., Pfaller, M.A., and Soll, D.R. (2002a). In Candida albicans, white-opaque switchers are homozygous for mating type. Genetics *162*, 737-745.

Lockhart, S.R., Pujol, C., Daniels, K.J., Miller, M.G., Johnson, A.D., Pfaller, M.A., and Soll, D.R. (2002b). In Candida albicans, white-opaque switchers are homozygous for mating type. Genetics *162*, 737-745.

Loeb, J.D., Sepulveda-Becerra, M., Hazan, I., and Liu, H. (1999). A G1 cyclin is necessary for maintenance of filamentous growth in Candida albicans. Mol Cell Biol *19*, 4019-4027.

Lorberg, A., Schmitz, H.P., Jacoby, J.J., and Heinisch, J.J. (2001a). Lrg1p functions as a putative GTPase-activating protein in the Pkc1p-mediated cell integrity pathway in Saccharomyces cerevisiae. Molecular genetics and genomics : MGG *266*, 514-526.

Lorberg, A., Schmitz, H.P., Jacoby, J.J., and Heinisch, J.J. (2001b). Lrg1p functions as a putative GTPase-activating protein in the Pkc1p-mediated cell integrity pathway in Saccharomyces cerevisiae. Molecular Genetics And Genomics *266*, 514-526.

Luo, G., Zhang, J., Luca, F.C., and Guo, W. (2013). Mitotic phosphorylation of Exo84 disrupts exocyst assembly and arrests cell growth. The Journal of cell biology *202*, 97-111.

Madden, K., and Snyder, M. (1998). Cell polarity and morphogenesis in budding yeast. Annual review of microbiology *52*, 687-744.

Mahlert, M., Leveleki, L., Hlubek, A., Sandrock, B., and Bolker, M. (2006). Rac1 and Cdc42 regulate hyphal growth and cytokinesis in the dimorphic fungus Ustilago maydis. Mol Microbiol *59*, 567-578.

Manning, B.D., Padmanabha, R., and Snyder, M. (1997). The Rho-GEF Rom2p localizes to sites of polarized cell growth and participates in cytoskeletal functions in Saccharomyces cerevisiae. Mol Biol Cell *8*, 1829-1844.

Marchler-Bauer, A., Zheng, C., Chitsaz, F., Derbyshire, M.K., Geer, L.Y., Geer, R.C., Gonzales, N.R., Gwadz, M., Hurwitz, D.I., Lanczycki, C.J.*, et al.* (2013). CDD: conserved domains and protein three-dimensional structure. Nucleic Acids Res *41*, D348-352.

Martin, H., Rodriguez-Pachon, J.M., Ruiz, C., Nombela, C., and Molina, M. (2000). Regulatory mechanisms for modulation of signaling through the cell integrity Slt2-mediated pathway in Saccharomyces cerevisiae. The Journal of biological chemistry *275*, 1511-1519.

Mazanka, E., Alexander, J., Yeh, B.J., Charoenpong, P., Lowery, D.M., Yaffe, M., and Weiss, E.L. (2008). The NDR/LATS family kinase Cbk1 directly controls transcriptional asymmetry. Plos Biology *6*, 1778-1790.

Mazur, P., Morin, N., Baginsky, W., el-Sherbeini, M., Clemas, J.A., Nielsen, J.B., and Foor, F. (1995). Differential expression and function of two homologous subunits of yeast 1,3-beta-D-glucan synthase. Mol Cell Biol *15*, 5671-5681.

McCusker, D., Denison, C., Anderson, S., Egelhofer, T.A., Yates, J.R., 3rd, Gygi, S.P., and Kellogg, D.R. (2007). Cdk1 coordinates cell-surface growth with the cell cycle. Nature cell biology *9*, 506-515.

McNemar, M.D., and Fonzi, W.A. (2002). Conserved serine/threonine kinase encoded by CBK1 regulates expression of several hypha-associated transcripts and genes encoding cell wall proteins in Candida albicans. J Bacteriol *184*, 2058-2061.

Meinhart, A., Kamenski, T., Hoeppner, S., Baumli, S., and Cramer, P. (2005). A structural perspective of CTD function. Genes & development *19*, 1401-1415.

Miller, M.G., and Johnson, A.D. (2002). White-opaque switching in Candida albicans is controlled by mating-type locus homeodomain proteins and allows efficient mating. Cell *110*, 293-302.

Morschhauser, J., Michel, S., and Staib, P. (1999). Sequential gene disruption in Candida albicans by FLP-mediated site-specific recombination. Mol Microbiol *32*, 547-556.

Moseley, J.B., and Goode, B.L. (2006). The yeast actin cytoskeleton: from cellular function to biochemical mechanism. Microbiology and molecular biology reviews : MMBR *70*, 605-645.

Moses, A.M., Heriche, J.K., and Durbin, R. (2007). Clustering of phosphorylation site recognition motifs can be exploited to predict the targets of cyclin-dependent kinase. Genome Biol *8*, R23.

Muller, L., Xu, G., Wells, R., Hollenberg, C.P., and Piepersberg, W. (1994). LRG1 is expressed during sporulation in Saccharomyces cerevisiae and contains motifs similar to LIM and rho/racGAP domains. Nucleic Acids Res *22*, 3151-3154.

Nelson, B., Kurischko, C., Horecka, J., Mody, M., Nair, P., Pratt, L., Hughes, T., Boone, C., and Luca, F. (2003). RAM: a conserved signaling network that regulates Ace2p transcription factor and polarized morphogenesis. Yeast *20*, S63-S63.

Nern, A., and Arkowitz, R.A. (2000). Nucleocytoplasmic shuttling of the Cdc42p exchange factor Cdc24p. The Journal of cell biology *148*, 1115-1122.

Nigg, E.A. (1993). Cellular substrates of p34-c-dc2 and its companion cyclin-dependent kinases. Trends in Cell Biology *3*, 296-301.

Nonaka, H., Tanaka, K., Hirano, H., Fujiwara, T., Kohno, H., Umikawa, M., Mino, A., and Takai, Y. (1995a). A Downstream Target of Rho1 Small Gtp-Binding Protein Is Pkc1, a Homolog of Protein-Kinase-C, Which Leads to Activation of the Map Kinase Cascade in Saccharomyces-Cerevisiae. Embo Journal *14*, 5931-5938.

Nonaka, H., Tanaka, K., Hirano, H., Fujiwara, T., Kohno, H., Umikawa, M., Mino, A., and Takai, Y. (1995b). A downstream target of RHO1 small GTP-binding protein is PKC1, a homolog of protein kinase C, which leads to activation of the MAP kinase cascade in Saccharomyces cerevisiae. The EMBO journal *14*, 5931-5938.

Nugroho, T.T., and Mendenhall, M.D. (1994). An inhibitor of yeast cyclin-dependent protein kinase plays an important role in ensuring the genomic integrity of daughter cells. Mol Cell Biol *14*, 3320-3328.

Oh, Y., and Bi, E. (2011). Septin structure and function in yeast and beyond. Trends Cell Biol *21*, 141-148.

Ohama, T., Suzuki, T., Mori, M., Osawa, S., Ueda, T., Watanabe, K., and Nakase, T. (1993). Nonuniversal Decoding Of The Leucine Codon Cug In Several Candida Species. Nucleic Acids Research *21*, 4039-4045.

Ortiz, D., Medkova, M., Walch-Solimena, C., and Novick, P. (2002). Ypt32 recruits the Sec4p guanine nucleotide exchange factor, Sec2p, to secretory vesicles; evidence for a Rab cascade in yeast. The Journal of cell biology *157*, 1005-1015.

Ozaki-Kuroda, K., Yamamoto, Y., Nohara, H., Kinoshita, M., Fujiwara, T., Irie, K., and Takai, Y. (2001). Dynamic localization and function of Bni1p at the sites of directed growth in Saccharomyces cerevisiae. Mol Cell Biol *21*, 827-839.

Ozaki, K., Tanaka, K., Imamura, H., Hihara, T., Kameyama, T., Nonaka, H., Hirano, H., Matsuura, Y., and Takai, Y. (1996). Rom1p and Rom2p are GDP/GTP exchange proteins (GEPs) for the Rho1p small GTP binding protein in Saccharomyces cerevisiae. The EMBO journal *15*, 2196-2207.

Paravicini, G., Cooper, M., Friedli, L., Smith, D.J., Carpentier, J.L., Klig, L.S., and Payton, M.A. (1992). The osmotic integrity of the yeast cell requires a functional PKC1 gene product. Mol Cell Biol *12*, 4896-4905.

Park, H.O., and Bi, E. (2007). Central roles of small GTPases in the development of cell polarity in yeast and beyond. Microbiology and molecular biology reviews : MMBR *71*, 48-96.

Pea, F. (2013). Current pharmacological concepts for wise use of echinocandins in the treatment of Candida infections in septic critically ill patients. Expert Rev Anti Infect Ther *11*, 989-997.

Perlin, D.S. (2007). Resistance to echinocandin-class antifungal drugs. Drug resistance updates : reviews and commentaries in antimicrobial and anticancer chemotherapy *10*, 121-130.

Peter, M., and Herskowitz, I. (1994). Direct inhibition of the yeast cyclin-dependent kinase Cdc28-Cln by Far1. Science *265*, 1228-1231.

Philip, B., and Levin, D.E. (2001). Wsc1 and Mid2 are cell surface sensors for cell wall integrity signaling that act through Rom2, a guanine nucleotide exchange factor for Rho1. Mol Cell Biol *21*, 271-280.

Pruyne, D., and Bretscher, A. (2000). Polarization of cell growth in yeast. I. Establishment and maintenance of polarity states. Journal of cell science *113 (Pt 3)*, 365-375.

Pruyne, D.W., Schott, D.H., and Bretscher, A. (1998). Tropomyosin-containing actin cables direct the Myo2p-dependent polarized delivery of secretory vesicles in budding yeast. The Journal of cell biology *143*, 1931-1945.

Pulver, R., Heisel, T., Gonia, S., Robins, R., Norton, J., Haynes, P., and Gale, C.A. (2013). Rsr1 focuses Cdc42 activity at hyphal tips and promotes maintenance of hyphal development in Candida albicans. Eukaryot Cell *12*, 482-495.

Qadota, H., Python, C.P., Inoue, S.B., Arisawa, M., Anraku, Y., Zheng, Y., Watanabe, T., Levin, D.E., and Ohya, Y. (1996). Identification of yeast Rho1p GTPase as a regulatory subunit of 1,3-beta-glucan synthase. Science *272*, 279-281.

Ram, A.F., Brekelmans, S.S., Oehlen, L.J., and Klis, F.M. (1995). Identification of two cell cycle regulated genes affecting the beta 1,3-glucan content of cell walls in Saccharomyces cerevisiae. FEBS letters *358*, 165-170.

Richardson, H., Lew, D.J., Henze, M., Sugimoto, K., and Reed, S.I. (1992). Cyclin-B homologs in Saccharomyces cerevisiae function in S phase and in G2. Genes & development *6*, 2021-2034.

Richman, T.J., Toenjes, K.A., Morales, S.E., Cole, K.C., Wasserman, B.T., Taylor, C.M., Koster, J.A., Whelihan, M.F., and Johnson, D.I. (2004). Analysis of cell-cycle specific localization of the Rdi1p RhoGDI and the structural determinants required for Cdc42p membrane localization and clustering at sites of polarized growth. Curr Genet *45*, 339-349.

Roberts, C.J., Nelson, B., Marton, M.J., Stoughton, R., Meyer, M.R., Bennett, H.A., He, Y.D., Dai, H., Walker, W.L., Hughes, T.R*., et al.* (2000). Signaling and circuitry of multiple MAPK pathways revealed by a matrix of global gene expression profiles. Science *287*, 873-880.

Ross, K.E., Kaldis, P., and Solomon, M.J. (2000). Activating phosphorylation of the Saccharomyces cerevisiae cyclin-dependent kinase, cdc28p, precedes cyclin binding. Mol Biol Cell *11*, 1597-1609.

Rothman, J.E. (1996). The protein machinery of vesicle budding and fusion. Protein science : a publication of the Protein Society *5*, 185-194.

Rudner, A.D., and Murray, A.W. (2000). Phosphorylation by Cdc28 activates the Cdc20-dependent activity of the anaphase-promoting complex. The Journal of cell biology *149*, 1377-1390.

Rueda, C., Cuenca-Estrella, M., and Zaragoza, O. (2014). Paradoxical growth of Candida albicans in the presence of caspofungin is associated with multiple cell wall rearrangements and decreased virulence. Antimicrobial agents and chemotherapy *58*, 1071-1083.

Russell, P., Moreno, S., and Reed, S.I. (1989). Conservation of mitotic controls in fission and budding yeasts. Cell *57*, 295-303.

Sagot, I., Klee, S.K., and Pellman, D. (2002a). Yeast formins regulate cell polarity by controlling the assembly of actin cables. Nature cell biology *4*, 42-50.

Sagot, I., Rodal, A.A., Moseley, J., Goode, B.L., and Pellman, D. (2002b). An actin nucleation mechanism mediated by Bni1 and profilin. Nature cell biology *4*, 626-631.

Schaub, Y., Dunkler, A., Walther, A., and Wendland, J. (2006). New pFA-cassettes for PCR-based gene manipulation in Candida albicans. J Basic Microbiol *46*, 416-429.

Schindelin, J., Arganda-Carreras, I., Frise, E., Kaynig, V., Longair, M., Pietzsch, T., Preibisch, S., Rueden, C., Saalfeld, S., Schmid, B*., et al.* (2012). Fiji: an open-source platform for biological-image analysis. Nature methods *9*, 676-682.

Schmelzle, T., Helliwell, S.B., and Hall, M.N. (2002). Yeast protein kinases and the RHO1 exchange factor TUS1 are novel components of the cell integrity pathway in yeast. Mol Cell Biol *22*, 1329-1339.

Schmidt, A., Schmelzle, T., and Hall, M.N. (2002). The RHO1-GAPs SAC7, BEM2 and BAG7 control distinct RHO1 functions in Saccharomyces cerevisiae. Mol Microbiol *45*, 1433-1441.

Schott, D.H., Collins, R.N., and Bretscher, A. (2002). Secretory vesicle transport velocity in living cells depends on the myosin-V lever arm length. The Journal of cell biology *156*, 35-39.

Schwob, E., Bohm, T., Mendenhall, M.D., and Nasmyth, K. (1994). The B-type cyclin kinase inhibitor p40SIC1 controls the G1 to S transition in S. cerevisiae. Cell *79*, 233-244.

Shi, J., Chen, W., Liu, Q., Chen, S., Hu, H., Turner, G., and Lu, L. (2008). Depletion of the MobB and CotA complex in Aspergillus nidulans causes defects in polarity maintenance that can be suppressed by the environment stress. Fungal genetics and biology : FG & B *45*, 1570-1581.

Sinha, I., Wang, Y.M., Philp, R., Li, C.R., Yap, W.H., and Wang, Y. (2007). Cyclin-dependent kinases control septin phosphorylation in Candida albicans hyphal development. Dev Cell *13*, 421-432.

Slutsky, B., Staebell, M., Anderson, J., Risen, L., Pfaller, M., and Soll, D.R. (1987). "White-opaque transition": a second high-frequency switching system in Candida albicans. J Bacteriol *169*, 189-197.

Song, Y., Cheon, S.A., Lee, K.E., Lee, S.Y., Lee, B.K., Oh, D.B., Kang, H.A., and Kim, J.Y. (2008). Role of the RAM Network in Cell Polarity and Hyphal Morphogenesis in Candida albicans. Molecular Biology Of The Cell *19*, 5456-5477.

Songyang, Z., Blechner, S., Hoagland, N., Hoekstra, M.F., Piwnica-Worms, H., and Cantley, L.C. (1994). Use of an oriented peptide library to determine the optimal substrates of protein kinases. Curr Biol *4*, 973-982.

Sonneborn, A., Bockmuhl, D.P., Gerads, M., Kurpanek, K., Sanglard, D., and Ernst, J.F. (2000). Protein kinase A encoded by TPK2 regulates dimorphism of Candida albicans. Mol Microbiol *35*, 386-396.

Sopko, R., Huang, D., Smith, J.C., Figeys, D., and Andrews, B.J. (2007). Activation of the Cdc42p GTPase by cyclin-dependent protein kinases in budding yeast. The EMBO journal *26*, 4487-4500.

Spellman, P.T., Sherlock, G., Zhang, M.Q., Iyer, V.R., Anders, K., Eisen, M.B., Brown, P.O., Botstein, D., and Futcher, B. (1998). Comprehensive identification of cell cycle-regulated genes of the yeast Saccharomyces cerevisiae by microarray hybridization. Mol Biol Cell *9*, 3273-3297.

Stegert, M.R., Hergovich, A., Tamaskovic, R., Bichsel, S.J., and Hemmings, B.A. (2005). Regulation of NDR protein kinase by hydrophobic motif phosphorylation mediated by the mammalian Ste20-like kinase MST3. Molecular And Cellular Biology *25*, 11019-11029.

Stothard, P. (2000). The sequence manipulation suite: JavaScript programs for analyzing and formatting protein and DNA sequences. Biotechniques *28*.

Stynen, B., Van Dijck, P., and Tournu, H. (2010). A CUG codon adapted two-hybrid system for the pathogenic fungus Candida albicans. Nucleic Acids Research *38*.

Su, Z., Osborne, M.J., Xu, P., Xu, X., Li, Y., and Ni, F. (2005). A bivalent dissectional analysis of the high-affinity interactions between Cdc42 and the Cdc42/Rac interactive binding domains of signaling kinases in Candida albicans. Biochemistry-Us *44*, 16461-16474.

Sudbery, P. (2007). Morphogenesis of a human fungal pathogen requires septin phosphorylation. Dev Cell *13*, 315-316.

Sudbery, P. (2008). Regulation of polarised growth in fungi Biology Reviews *22*, 44-45.

Sudbery, P., Gow, N., and Berman, J. (2004). The distinct morphogenic states of Candida albicans. Trends Microbiol *12*, 317-324.

Sudbery, P.E. (2001). The germ tubes of Candida albicans hyphae and pseudohyphae show different patterns of septin ring localization. Mol Microbiol *41*, 19-31.

Sudbery, P.E. (2011). Growth of Candida albicans hyphae. Nature reviews Microbiology *9*, 737-748.

Svarovsky, M.J., and Palecek, S.P. (2005). Disruption of LRG1 inhibits mother-daughter separation in Saccharomyces cerevisiae. Yeast *22*, 1117-1132.

Tamaskovic, R., Bichsel, S.J., Rogniaux, H., Stegert, M.R., and Hemmings, B.A. (2003). Mechanism of Ca2+-mediated regulation of NDR protein kinase through autophosphorylation and phosphorylation by an upstream kinase. Journal Of Biological Chemistry *278*, 6710-6718.

Taylor, J.W., Geiser, D.M., Burt, A., and Koufopanou, V. (1999). The evolutionary biology and population genetics underlying fungal strain typing. Clin Microbiol Rev *12*, 126-+.

Teh, E.M., Chai, C.C., and Yeong, F.M. (2009). Retention of Chs2p in the ER requires N-terminal CDK1-phosphorylation sites. Cell Cycle *8*, 2964-2974.

TerBush, D.R., Maurice, T., Roth, D., and Novick, P. (1996). The Exocyst is a multiprotein complex required for exocytosis in Saccharomyces cerevisiae. The EMBO journal *15*, 6483-6494.

Tong, Z., Gao, X.D., Howell, A.S., Bose, I., Lew, D.J., and Bi, E. (2007). Adjacent positioning of cellular structures enabled by a Cdc42 GTPase-activating protein-mediated zone of inhibition. The Journal of cell biology *179*, 1375-1384.

Utsugi, T., Minemura, M., Hirata, A., Abe, M., Watanabe, D., and Ohya, Y. (2002). Movement of yeast 1,3-beta-glucan synthase is essential for uniform cell wall synthesis. Genes to cells : devoted to molecular & cellular mechanisms *7*, 1-9.

Valdivia, R.H., Baggott, D., Chuang, J.S., and Schekman, R.W. (2002). The yeast clathrin adaptor protein complex 1 is required for the efficient retention of a subset of late Golgi membrane proteins. Dev Cell *2*, 283-294.

Vallim, M.A., Nichols, C.B., Fernandes, L., Cramer, K.L., and Alspaugh, J.A. (2005). A Rac homolog functions downstream of Ras1 to control hyphal differentiation and high-temperature growth in the pathogenic fungus Cryptococcus neoformans. Eukaryot Cell *4*, 1066-1078.

van Drogen, F., and Peter, M. (2002). Spa2p functions as a scaffold-like protein to recruit the Mpk1p MAP kinase module to sites of polarized growth. Curr Biol *12*, 1698-1703.

Vauchelles, R., Stalder, D., Botton, T., Arkowitz, R.A., and Bassilana, M. (2010). Rac1 dynamics in the human opportunistic fungal pathogen Candida albicans. Plos One *5*, 0015400.

Verde, F., Wiley, D.J., and Nurse, P. (1998). Fission yeast orb6, a ser/thr protein kinase related to mammalian rho kinase and myotonic dystrophy kinase, is required for maintenance of cell polarity and coordinates cell morphogenesis with the cell cycle. Proc Natl Acad Sci U S A *95*, 7526-7531.

Virag, A., and Harris, S.D. (2006). The Spitzenkorper: a molecular perspective. Mycological research *110*, 4-13.

Virag, A., Lee, M.P., Si, H., and Harris, S.D. (2007). Regulation of hyphal morphogenesis by cdc42 and rac1 homologues in Aspergillus nidulans. Mol Microbiol *66*, 1579-1596.

Vogt, N., and Seiler, S. (2008a). The RHO1-specific GTPase-activating protein LRG1 regulates polar tip growth in parallel to Ndr kinase signaling in Neurospora. Mol Biol Cell *19*, 4554-4569.

Vogt, N., and Seiler, S. (2008b). The RHO1-specific GTPase-activating Protein LRG1 Regulates Polar Tip Growth in Parallel to Ndr Kinase Signaling in Neurospora. Molecular Biology Of The Cell *19*, 4554-4569.

Walch-Solimena, C., Collins, R.N., and Novick, P.J. (1997). Sec2p mediates nucleotide exchange on Sec4p and is involved in polarized delivery of post-Golgi vesicles. The Journal of cell biology *137*, 1495-1509.

Wang, A., Raniga, P.P., Lane, S., Lu, Y., and Liu, H.P. (2009). Hyphal Chain Formation in Candida albicans: Cdc28-Hgc1 Phosphorylation of Efg1 Represses Cell Separation Genes. Molecular And Cellular Biology *29*, 4406-4416.

Wang, Y. (2009). CDKs and the yeast-hyphal decision. Curr Opin Microbiol *12*, 644-649.

Warenda, A.J., and Konopka, J.B. (2002). Septin function in Candida albicans morphogenesis. Mol Biol Cell *13*, 2732-2746.

Watanabe, D., Abe, M., and Ohya, Y. (2001). Yeast Lrg1p acts as a specialized RhoGAP regulating 1,3-beta-glucan synthesis. Yeast *18*, 943-951.

Wegener, A.D., and Jones, L.R. (1984). Phosphorylation-induced mobility shift in phospholamban in sodium dodecyl sulfate-polyacrylamide gels. Evidence for a protein structure consisting of multiple identical phosphorylatable subunits. The Journal of biological chemistry *259*, 1834-1841.

Weiss, E.L., Kurischko, C., Zhang, C., Shokat, K., Drubin, D.G., and Luca, F.C. (2002). The Saccharomyces cerevisiae Mob2p-Cbk1p kinase complex promotes polarized growth and acts with the mitotic exit network to facilitate daughter cell-specific localization of Ace2p transcription factor. Journal Of Cell Biology *158*, 885-900.

Williams, K.E., and Cyert, M.S. (2001). The eukaryotic response regulator Skn7p regulates calcineurin signaling through stabilization of Crz1p. The EMBO journal *20*, 3473-3483.

Wilson, R.B., Davis, D., and Mitchell, A.P. (1999). Rapid hypothesis testing with Candida albicans through gene disruption with short homology regions. J Bacteriol *181*, 1868-1874.

Winter, D., Podtelejnikov, A.V., Mann, M., and Li, R. (1997). The complex containing actin-related proteins Arp2 and Arp3 is required for the motility and integrity of yeast actin patches. Curr Biol *7*, 519-529.

Wisplinghoff, H., Bischoff, T., Tallent, M., Seifert, H., Wenzel, R.P., and Edmond, M.B. (2004). Nosocomial bloodstream infections in US hospitals: analysis of 24,179 cases from a prospective nationwide surveillance study. (vol 39, pg 309, 2004). Clinical Infectious Diseases *39*, 1093-1093.

Wu, H., and Brennwald, P. (2010). The function of two Rho family GTPases is determined by distinct patterns of cell surface localization. Mol Cell Biol *30*, 5207-5217.

Yamochi, W., Tanaka, K., Nonaka, H., Maeda, A., Musha, T., and Takai, Y. (1994). Growth site localization of Rho1 small GTP-binding protein and its involvement in bud formation in Saccharomyces cerevisiae. The Journal of cell biology *125*, 1077-1093.

Yarden, O., Plamann, M., Ebbole, D.J., and Yanofsky, C. (1992). cot-1, a gene required for hyphal elongation in Neurospora crassa, encodes a protein kinase. The EMBO journal *11*, 2159-2166.

Yoshida, S., Kono, K., Lowery, D.M., Bartolini, S., Yaffe, M.B., Ohya, Y., and Pellman, D. (2006). Polo-like kinase Cdc5 controls the local activation of Rho1 to promote cytokinesis. Science *313*, 108-111.

Young, M.E., Cooper, J.A., and Bridgman, P.C. (2004). Yeast actin patches are networks of branched actin filaments. The Journal of cell biology *166*, 629-635.

Zhang, X., Bi, E., Novick, P., Du, L., Kozminski, K.G., Lipschutz, J.H., and Guo, W. (2001). Cdc42 interacts with the exocyst and regulates polarized secretion. The Journal of biological chemistry *276*, 46745-46750.

Zhang, X., Orlando, K., He, B., Xi, F., Zhang, J., Zajac, A., and Guo, W. (2008). Membrane association and functional regulation of Sec3 by phospholipids and Cdc42. The Journal of cell biology *180*, 145-158.

Zhao, C., Jung, U.S., Garrett-Engele, P., Roe, T., Cyert, M.S., and Levin, D.E. (1998). Temperature-induced expression of yeast FKS2 is under the dual control of protein kinase C and calcineurin. Mol Cell Biol *18*, 1013-1022.

Zheng, X., and Wang, Y. (2004). Hgc1, a novel hypha-specific G1 cyclin-related protein regulates Candida albicans hyphal morphogenesis. The EMBO journal *23*, 1845-1856.

Zheng, X.D., Lee, R.T.H., Wang, Y.M., Lin, Q.S., and Wang, Y. (2007). Phosphorylation of Rga2, a Cdc42 GAP, by CDK/Hgc1 is crucial for Candida albicans hyphal growth. Embo Journal *26*, 3760-3769.

Zheng, Y., Cerione, R., and Bender, A. (1994). Control of the yeast bud-site assembly GTPase Cdc42. Catalysis of guanine nucleotide exchange by Cdc24 and stimulation of GTPase activity by Bem3. The Journal of biological chemistry *269*, 2369-2372.

Zheng, Y., Hart, M.J., Shinjo, K., Evans, T., Bender, A., and Cerione, R.A. (1993). Biochemical comparisons of the Saccharomyces cerevisiae Bem2 and Bem3 proteins. Delineation of a limit Cdc42 GTPase-activating protein domain. The Journal of biological chemistry *268*, 24629-24634.

Zigmond, S.H., Evangelista, M., Boone, C., Yang, C., Dar, A.C., Sicheri, F., Forkey, J., and Pring, M. (2003). Formin leaky cap allows elongation in the presence of tight capping proteins. Curr Biol *13*, 1820-1823.

Ziman, M., Chuang, J.S., and Schekman, R.W. (1996). Chs1p and Chs3p, two proteins involved in chitin synthesis, populate a compartment of the Saccharomyces cerevisiae endocytic pathway. Mol Biol Cell *7*, 1909-1919.